Challenges to Skeletal Muscle During Advancing Age: A Translational Approach

by

Andrew Christian D'Lugos

A Dissertation Presented in Partial Fulfillment
of the Requirements for the Degree
Doctor of Philosophy

Approved May 2018 by the
Graduate Supervisory Committee:

Jared M. Dickinson, Chair
Matthew P. Buman
Glenn A. Gaesser
Matthew J. Huentelman
Christos S. Katsanos

ARIZONA STATE UNIVERSITY

August 2018

ABSTRACT

The purpose of this dissertation was 1) to develop noninvasive strategies to assess skeletal muscle size, architecture, and composition in young and old adults (study #1) and 2) evaluate the impact of chemotherapeutic treatment on skeletal muscle satellite cells and capillaries (study #2). For study #1 ultrasound images were obtained from the quadriceps muscles of young (8 m, 8 f) and older (7 m, 5 f) participants on two occasions, separated by 5-15 days. Images were collected while the participants were both standing and supine, and were analyzed for muscle thickness, pennation angle, and echogenicity. In addition, test-retest reliability and ICCs were evaluated for each posture and when imaging sites remained marked or were re-measured from visit #1 to visit #2. Generally, in both younger and older adults muscle thickness was greater and echogenicity was lower in the anterior quadriceps when images were collected standing versus supine. Maintaining the imaging site between visits did not influence test re-test reliability for either age group. Older adults exhibited smaller muscle thickness, lower pennation angle and increased echogenicity. Further, variability for the use of ultrasound to determine muscle thickness and pennation angle was greater in older versus younger adults. Findings from study #1 highlight several methodological considerations for US-based assessment of skeletal muscle characteristics that should be considered for improving reproducibility and generalizability of US to assess skeletal muscle characteristics and function across the aging spectrum. This is particularly relevant given the emerging use of ultrasound to assess skeletal muscle characteristics in healthy and clinical populations. In the second study, ovariectomized female Sprague-Dawley rats were randomized to receive three bi-weekly intraperitoneal injections of the chemotherapeutic drug, Doxorubicin (DOX) (4mg/kg; cumulative dose 12mg/kg) or vehicle (VEH; saline). Animals were euthanized 5d following the last injection, and the soleus (SOL) and extensor digitorum longus (EDL) muscles were dissected and prepared for immunohistochemical and RT-qPCR analyses. Relative to VEH, cross-sectional area (CSA) of the SOL and EDL muscle fibers were 26% and 33% smaller, respectively, in DOX animals ($P<0.05$). In the SOL satellite cell and capillary densities were 39% and 35% lower, respectively, in DOX animals ($P<0.05$), whereas in the EDL satellite cell and capillary densities were unaffected by DOX administration ($P>0.05$). In the SOL MYF5 mRNA expression was

increased in DOX animals (P<0.05), while in the EDL MGF mRNA expression was reduced in DOX animals (P<0.05). Chronic DOX administration is associated with reduced fiber size in multiple skeletal muscles, however DOX appears to impact the satellite cell and capillary densities in a muscle-specific manner. These findings from study #2 highlight that therapeutic targets to protect skeletal muscle from DOX may vary across muscles. Collectively, these findings 1) improve the ability to examine muscle size and function in younger and older adults, and 2) identify promising therapeutic targets to protect skeletal muscle from the harmful effects of chemotherapy treatment.

DEDICATION

I dedicate this dissertation to my best friend and fiancé, Jess. While the countless hours in the lab led to less time spent together, her support for my goals never wavered. Through her encouragement and love she helped me through the toughest times and shared with me the good times. It has truly been an adventure.

ACKNOWLEDGEMENT

I would first like to thank all of the staff, especially Theresa Jorgensen, Ginger Hook, and Veronica Zamora, that unbeknownst to most, are vital to the research enterprises at ASU and imperative to my accomplishments. I would also like to thank all of the research participants who volunteered for studies that extend beyond this dissertation; without your generosity and trust none of this would be possible. Thank you to the many student volunteers who were integral to the progress I've made and the good times I've had at ASU. To my close friends and past mentors, thank you for the continued support and everlasting channel of bad scientific banter; I hope to share an office again someday.

My appreciation for my mentor, Jared Dickinson, is difficult to capture in words. Jared has always set the best example, whether in the lab or at home with his family. I hope to adopt the same humility and respect for others that Jared has shown during my time with him. Conversations over morning coffee; it's the little things that leave the biggest impact. To Glenn Gaesser, I sincerely enjoyed the "stories from the Monark" episodes several times each week. Glenn's meticulous perspective on the scientific landscape showed me what it means to truly discern fact from fallacy. Thank you to Matt Huentelman for your refreshing enthusiasm and perspective in addressing the traditional questions of our field of exercise physiology with unique, innovative approaches. To Matt Buman, Christos Katsanos, and Sid Angadi, thank you for both broadening and refining my scientific abilities, each through your own specific teachings.

TABLES OF CONTENTS

CHAPTER Page

LIST OF TABLES vii

LIST OF FIGURES xi

1 INTRODUCTION 1

Aims and Hypotheses 3

2 REVIEW OF LITERATURE 5

Introduction 5

Skeletal Muscle Structure, Function, and Adaptation 5

Whole Muscle 5

General Skeletal Muscle Structure 5

Whole Skeletal Muscle Function 6

Skeletal Muscle Fiber 7

Skeletal Muscle Fiber Structure 7

Skeletal Muscle Fiber Function 7

Skeletal Muscle Fiber Types 8

Skeletal Muscle Adaptation 9

General Overview 9

Signaling 10

Transcription 10

Translation 11

Summary 11

Ultrasonography and Muscle Architecture 11

History of Ultrasound Imaging 11

Muscle Thickness 13

Pennation Angle and Fascicle Length 25

Echogenicity 40

Reliability of Ultrasound-Derived Muscle Architecture Measurements 45

CHAPTER Page

Doxorubicin and Skeletal Muscle 52

Overview of Doxorubicin 52

Impact of Doxorubicin on Skeletal Muscle Function 52

Impact of Doxorubicin on Skeletal Muscle Size 58

Impact of Doxorubicin in Human Cancer Patients 64

Divergent Exercise: High-Intensity Interval Exercise vs. Moderate-Intensity Exercise 65

General Overview 65

Acute Skeletal Muscle Responses 66

Chronic Skeletal Muscle Adaptations 71

3 SKELETAL MUSCLE ARCHITECTURE ACROSS THE AGING SPECTRUM: A COMPARISON OF ULTRASOUND TECHNIQUES AND AN ASSESSMENT OF RELIABILITY 75

Introduction 76

Materials and Methods 79

Participants 79

Study Design 79

Skeletal Muscle Ultrasound Imaging 80

Participant Posture During Imaging 81

Influence of Identifying Imaging Sites 81

Muscle Function Testing 81

Dual-Energy X-Ray Absorptiometry (DXA Scan) 82

Ultrasound Image Analysis 82

Statistical Analysis 83

Results 85

Subjects 85

CHAPTER Page

Measurement of Skeletal Muscle Parameters 85

Influence of Posture on Skeletal Muscle Parameters 85

Reproducibility of Skeletal Muscle Measurements 86

Test-retest Reliability of Skeletal Muscle Measurements 87

Relationship Between Skeletal Muscle Measurements and Muscle Function 88

Discussion 90

Influence of Posture 90

Reliability of Skeletal Muscle US 91

Relationship to Muscle Function 93

Conclusions 94

4 REDUCED SATELLITE CELL AND CAPILLARY ABUNDANCE IN RAT SKELETAL MUSCLE FOLLOWING CHRONIC DOXORUBICIN ADMINISTRATION 139

Introduction 140

Methods 142

Study Design 142

Immunohistochemistry 142

Image Acquisition and Analysis 143

RNA Extraction and Semiquantitative Real-Time PCR 144

Statistical Analysis 144

Results 146

Muscle Fiber CSA 146

Satellite Cell and Myonuclei Content 146

Capillary Content 146

Myogenic Gene Expression 147

Discussion 148

5 CONCLUSION 158

CHAPTER Page

REFERENCES 161

APPENDIX

A ULTRASOUND STUDY CONSENT FORM 184

B ULTRASOUND IMAGE COLLECTION PROTOCOL 192

C ULTRASOUND IMAGE ANALYSES PROTOCOL – THICKNESS 195

D ULTRASOUND IMAGE ANALYSES PROTOCOL – PENNATION ANGLE 198

E ULTRASOUND IMAGE ANALYSES PROTOCOL – ECHOGENICITY 201

F SKELETAL MUSCLE RNA ISOLATION 204

G DETERMINATION OF RNA CONCENTRATION – BIOTEK TAKE 3 PLATE 207

H DNASE TREATMENT OF ISOLATED RNA 209

I CDNA SYNTHESIS 211

J PRIMER DESIGN 214

K PRIMER TESTING AND OPTIMIZATION 217

L DNA AGAROSE GEL PROTOCOL 224

M PCR ANALYSIS PROTOCOL 224

N SKELETAL MUSCLE IMMUNOHISTOCHEMICAL ANALYSES – CSA AND FIBER TYPE 228

O SKELETAL MUSCLE IMMUNOHISTOCHEMICAL ANALYSES – SATELLITE CELLS AND MYONUCLEI 231

P SKELETAL MUSCLE IMMUNOHISTOCHEMICAL ANALYSES – CAPILLARY DENSITY 235

LIST OF TABLES

Table Page

2-1 Summary of Ultrasound-Derived Muscle Thickness Measurements in the Quadriceps: Relationship to Muscle Function and Changes with Exercise Training 16

2-2 Summary of Ultrasound-Based Pennation Angle and Fascicle Length Measurements in the Quadriceps. 30

2-3 Summary of Ultrasound-Based Echogenicity Measurements in the Quadriceps 42

2-4 Summary of Ultrasound-based Quadriceps Muscle Architecture Measurements with Reported Reliability 47

2-5 Summary of the Impact of Anthracyclines on Skeletal Muscle Function 55

2-6 Summary of the Impact of Anthracyclines on Skeletal Muscle Size 61

2-7 Summary of Acute Skeletal Muscle Response: HIIE vs MOD 69

2-8 Summary of Chronic Skeletal Muscle Adaptations: HIIT vs MOD 73

3-1 Subject Characteristics 96

3-2 Muscle Thickness at A1 97

3-3 Muscle Thickness at A2 97

3-4 Muscle Thickness at L1 98

3-5 Muscle Thickness at L2 98

3-6 Muscle Thickness at L3 98

3-7 Pennation Angle 99

3-8 Echogenicity at A1 100

3-9 Echogenicity at A2 100

3-10 Echogenicity at L1 101

3-11 Echogenicity at L2 101

3-12 Echogenicity at L3 101

3-13 Test-Retest Intraclass Correlation Coefficients for Anterior Muscle Thickness 102

3-14 Test-Retest Intraclass Correlation Coefficients for Anterior Muscle Thickness in Young 103

Table Page

3-15 Test-Retest Intraclass Correlation Coefficients for Anterior Muscle Thickness in Old ... 103

3-16 Test-Retest Intraclass Correlation Coefficients for Lateral Muscle Thickness 104

3-17 Test-Retest Intraclass Correlation Coefficients for Lateral Muscle Thickness in Young 105

3-18 Test-Retest Intraclass Correlation Coefficients for Later Muscle Thickness in Old..... 105

3-19 Test-Retest Intraclass Correlation Coefficients for Pennation Angle..... 106

3-20 Test-Retest Intraclass Correlation Coefficients for Pennation Angle Young 106

3-21 Test-Retest Intraclass Correlation Coefficients for Pennation Angle Old 106

3-22 Test-Retest Intraclass Correlation Coefficients for Echogenicity..... 107

3-23 Test-Retest Intraclass Correlation Coefficients for Echogenicity in Young 108

3-24 Test-Retest Intraclass Correlation Coefficients for Echogenicity in Old 108

3-25 Muscle Thickness for A1 Rectus Femoris..... 109

3-26 Muscle Thickness for A1 Vastus Intermedius 109

3-27 Muscle Thickness for A1 RF+VI..... 110

3-28 Muscle Thickness for A2 Rectus Femoris..... 110

3-29 Muscle Thickness for A2 Vastus Intermedius 111

3-30 Muscle Thickness for A2 RF+VI..... 111

3-31 Muscle Thickness for L1 Vastus Lateralis..... 112

3-32 Muscle Thickness for L1 Vastus Intermedius 112

3-33 Muscle Thickness for L1 VL+VI..... 113

3-34 Muscle Thickness for L2 Vastus Lateralis..... 113

3-35 Muscle Thickness for L2 Vastus Intermedius 114

3-36 Muscle Thickness for L2 VL+VI..... 114

3-37 Muscle Thickness for L3 Vastus Lateralis..... 115

3-38 Muscle Thickness for L3 Vastus Intermedius 115

3-39 Muscle Thickness for L3 VL+VI..... 116

3-40 Pennation Angle L1 Vastus Lateralis 117

3-41 Pennation Angle L1 Vastus Intermedius 117

Table Page

3-42 Pennation Angle L2 Vastus Lateralis 118
3-43 Pennation Angle L2 Vastus Intermedius 118
3-44 Pennation Angle L3 Vastus Lateralis 119
3-45 Echogenicity for A1 Rectus Femoris 120
3-46 Echogenicity for A1 Vastus Intermedius 120
3-47 Echogenicity for A2 Rectus Femoris 121
3-48 Echogenicity for A2 Vastus Intermedius 121
3-49 Echogenicity for L1 Vastus Lateralis 122
3-50 Echogenicity for L1 Vastus Intermedius 122
3-51 Echogenicity for L2 Vastus Lateralis 123
3-52 Echogenicity for L2 Vastus Intermedius 123
3-53 Echogenicity for L3 Vastus Lateralis 124
3-54 Echogenicity for L3 Vastus Intermedius 124
3-55 Best Single Site Predictors of Peak Isometric Torque of the Quadriceps 125
3-56 Stepwise Linear Regression Predicting Peak Isometric Torque of the Quadriceps 125
3-57 Mixed Model Results for Posture in Muscle Thickness- Anterior Sites 126
3-58 Mixed Model Results for Posture in Muscle Thickness- Lateral Sites 126
3-59 Mixed Model Results for Posture in Pennation Angle- Lateral Sites 127
3-60 Mixed Model Results for Posture in Echogenicity- Anterior Sites 128
3-61 Mixed Model Results for Posture in Echogenicity- Lateral Sites 128
3-62 Mixed Model Results for Absolute Reliability in Muscle Thickness- Anterior Sites 129
3-63 Mixed Model Results for Absolute Reliability in Muscle Thickness- Lateral Sites 129
3-64 Mixed Model Results for Relative Reliability in Muscle Thickness- Anterior Sites 130
3-65 Mixed Model Results for Relatively Reliability in Muscle Thickness- Lateral Sites 130
3-66 Mixed Model Results for Absolute Reliability in Pennation Angle- Lateral Sites 131
3-67 Mixed Model Results for Relative Reliability in Pennation Angle- Lateral Sites 131
3-68 Mixed Model Results for Absolute Reliability in Echogenicity- Anterior Sites 132

Table Page

3-69 Mixed Model Results for Absolute Reliability in Echogenicity- Lateral Sites 132

3-70 Mixed Model Results for Relative Reliability in Echogenicity- Anterior Sites 133

3-71 Mixed Model Results for Relative Reliability in Echogenicity- Lateral Sites 133

4-1 Primer Sequences Used for Real-Time PCR..... 152

4-2 Soleus and Extensor Digitorum Longus Muscle mRNA Analyses for Markers of Myogenic Activity 153

LIST OF FIGURES

Figure Page

2-1 Conceptual Schematic Depicting the Series of Events from Leading to Alterations in Cellular Protein 9

2-2 B-Mode Ultrasound Image in the Longitudinal Plane of the Lateral Quadriceps 12

2-3 B-mode US Image of the Vastus Lateralis (VL) and Lateral Vastus Intermedius (VI) 25

2-4 Simplified Schematic of Possible Combinations of MT, PA, and FL Responses Following Chronic Exercise Training 27

3-1 Longitudinal Plane Ultrasound Scan of the Vastus Lateralis (VL) and Lateral Aspect of the Vastus Intermedius (VI) 80

3-2 Skeletal Muscle Thickness of the Anterior Quadriceps Measured while Standing and Supine 134

3-3 Skeletal Muscle Thickness of the Lateral Quadriceps Measured while Standing and Supine 135

3-4 Skeletal Muscle Pennation Angle of the Lateral Quadriceps Measured while Standing and Supine 136

3-5 Skeletal Muscle Echogenicity of the Anterior Quadriceps Measured while Standing and Supine 137

3-6 Skeletal Muscle Echogenicity of the Lateral Quadriceps Measured while Standing and Supine 138

4-1 The Effect of Chronic Doxorubicin Administration on Muscle Fiber Cross-Sectional Area (CSA) 154

4-2 Representative Immunohistochemical Image of Satellite Cell Detection in the Soleus and Extensor Digitorum Longus 155

4-3 The Effect of Chronic Doxorubicin Administration on Satellite Cell and Myonuclei Densities 156

4-4 The Effect of Chronic Doxorubicin Administration on Capillary Density 157

CHAPTER ONE

INTRODUCTION

Skeletal muscle is a highly plastic tissue, demonstrating remarkable adaptation and remodeling in response to a variety of stimuli, particularly exercise (46) and nutrition (255). For example, it is well understood that exercise training can alter the size and metabolic profile of skeletal muscle (43), producing a muscle phenotype that is better able to perform an exercise or movement. While the plasticity of skeletal muscle is relatively well preserved throughout the aging process, a gradual deterioration of cellular structure and function can occur in skeletal muscle, particularly in response to aging and disease (43, 118). In particular, aging is associated with a progressive decline in skeletal muscle size and function (60, 141), termed sarcopenia, that has detrimental effects on the quality of life in elderly populations. Further, medications that are often used in elderly populations can also impact skeletal muscle function. For instance, common over-the-counter analgesics have been shown to interfere with adaptations of skeletal muscle to exercise (246), while chemotherapeutic agents can have toxic effects on skeletal muscle (94). In particular, these unfavorable adaptations occurring in skeletal muscle not only impair movement, but also affect overall metabolic health as skeletal muscle serves as an amino acid reservoir, provides substrate for other tissues, and delivers substrate during malnutrition, starvation, and injury (153).

Skeletal muscle adaptation is regulated through an intricate array of molecular events that ultimately lead to the accumulation of specific proteins in the muscle fibers (72). For example, changes in transcriptional activity and the rate of translation dictate which specific proteins are produced, and consequently, which unique functional changes will manifest in skeletal muscle. In addition, skeletal muscle satellite cells have also been identified to serve an essential role in skeletal muscle growth and regeneration. Consequently, identifying the specific molecular mechanisms regulating the unique adaptation of skeletal muscle to various stimuli, and how these mechanisms impact the size and function of skeletal muscle, provides a platform to 1) establish important therapeutic targets for intervention during unfavorable muscle adaptations, and 2) identify overlap between these targets and those stimulated by various therapeutic strategies. This

dissertation is comprised of two independent projects aimed at addressing challenges to skeletal muscle in advancing age.

The purpose of the first project is to directly assess the reliability of two predominate methodologies for ultrasound-based examination of quadriceps muscle size, architecture, and composition in young and old individuals. The emergence of ultrasonography has allowed clinicians and researchers to detect changes in whole muscle characteristics, include fiber pennation angle and muscle composition (67, 139). Along with muscle size, these variables largely dictate the functional capacity of a muscle (140, 173). Ultrasound has been valuable in demonstrating age-related impairments in pennation angle (167, 236) and muscle composition (17, 236, 247). However, the current body of literature lacks consensus on a standardized method to assess skeletal muscle characteristics, with two primary methodologies being practiced (4, 25). The underlying difference in each protocol involves the posture of the subject during image acquisition, where the subject is either standing (4) or lying supine (25). Each postural approach has its own unique advantages, especially when the patient population may be limited in their ability to assume one posture over the other. For example, patients with congestive heart failure are reluctant to lay supine due to the increased incidences of dyspnea and pulmonary edema (178), while individuals who are bed-ridden may be unable to stand. To our knowledge, differences in the measures of skeletal muscle characteristics and the test-retest reliability of each distinct postural approach to ultrasound have not been investigated. The goal of this study is to better understand the reliability and variability of different ultrasound protocols and techniques to examine whole skeletal muscle characteristics and how they relate to muscle function. This information is necessary to improve the ability of ultrasound to identify individuals at risk for skeletal muscle decline and evaluate the progress of therapies aimed at improving skeletal muscle.

The purpose of the second project is to determine the impact of a common chemotherapeutic drug on the satellite cell and capillary content in multiple skeletal muscles. In addition to aging, disease and associated treatments can accelerate reductions in muscle quality. For instance, cancer survivors comprise a growing portion of the elderly population (55). However, while cancer treatments have become more effective, some are accompanied with negative side

effects leading to skeletal atrophy (27, 32) and dysfunction (33, 91, 111). The common chemotherapeutic drug Doxorubicin (DOX) is associated with many negative side effects in skeletal muscle including muscle atrophy (27, 32) and dysfunction (33, 91, 111, 122), however the cellular mechanisms responsible are still unclear. Unfortunately, this knowledge gap impedes our ability to develop effective therapies to protect skeletal muscle from DOX. In this regard, satellite cells are a population of resident stem cells that govern the regenerative program in skeletal muscle (230). In addition, these cells engage in unique crosstalk with neighboring capillaries to facilitate myogenic and angiogenic processes (6, 45), both of which are critical to skeletal muscle health. The impact of DOX on skeletal muscle satellite cells and capillaries is still unclear, thus, there remains a need to explore the impact of DOX administration on satellite cells and capillary contents in skeletal muscle. The goal of this study is to more precisely characterize the impact of DOX on the populations of vital cells within skeletal muscle. This information is critical to identify therapeutic targets for the development of strategies aimed at mitigating the deleterious off-target effects of DOX in skeletal muscle.

I. AIMS AND HYPOTHESES

Through the studies described here, this dissertation will address distinct aspects of the age-related challenges (i.e. sarcopenia, drug side-effects) to skeletal muscle while traversing the translational spectrum.

Study 1 Aim: Directly assess the influence of posture on ultrasound based measures of skeletal muscle and determine the test-retest reliability of each distinct postural approach to skeletal muscle ultrasound in a cohort of young and older males and females.

Study 1 Hypothesis: We hypothesize that measures of whole skeletal muscle characteristics will differ between each postural approach to ultrasound and that aging will be associated with lower test-retest reliability for ultrasound measured of skeletal muscle characteristics.

Study 2 Aim:	Determine the impact of chronic DOX administration on satellite cell and capillary populations in multiple skeletal muscles.
Study 2 Hypothesis:	We hypothesize that DOX administration will be associated with lower satellite cell and capillary content in multiple skeletal muscles.

CHAPTER TWO

REVIEW OF LITERATURE

I. INTRODUCTION

The contents of this literature review are focused on skeletal muscle physiology/biology during advancing age. Attention is given to discuss relevant topics ranging from the specific molecular processes occurring within skeletal muscle cells to whole muscle characteristics. Further, this Dissertation includes research that spans the clinical translational spectrum from basic animal research to applied human studies. Consequently, this literature review includes relevant literature from both animal and human-subject studies. Specific topics related to the subsequent chapters are also highlighted within this literature review, in particular: the impacts of drug treatment, exercise, and aging on various processes in skeletal muscle vital to healthy aging; methodological approaches to assess *in-vivo* characteristics of whole muscle, with a focus on ultrasonographic imaging; and cellular processes within skeletal muscle, examined through whole-transcriptome RNA sequencing.

II. SKELETAL MUSCLE STRUCTURE, FUNCTION, AND ADAPTATION

Skeletal muscle is a highly organized and complex tissue that comprises approximately 40% of total body weight and contains 50-75% of all body proteins. While skeletal muscle significantly contributes to multiple bodily functions, arguably a primary function of skeletal muscle is the conversion of chemical energy into mechanical work to generate force and power, maintain posture, and produce movement (76).

A. Whole Skeletal Muscle

1. General Skeletal Muscle Structure

Each whole skeletal muscle is enclosed by connective tissue called the epimysium. Within each whole skeletal muscle are multiple fasciculi, which contain bundles of muscle fibers (the cell of muscle tissue), blood vessels, and nerves that are enclosed by connective tissue called the

perimysium. Each individual muscle fiber within the fasciculi is enclosed by connective tissue called endomysium. Thus, the endomysium is what separates each muscle fiber. Together, the epimysium, perimysium, and endomysium extend beyond the belly of the muscle to form the tendon or aponeurosis which anchors to the periosteum of bone or connective tissue of another muscle, respectively. The connective tissue networks within skeletal muscle plays an important role in structure maintenance and the transmission of force from the muscle to the bone during contraction (133).

2. Whole Skeletal Muscle Function

Muscle architecture is a major determinant of whole muscle contractile function (39). Pioneered by the studies of Gans and Bock (83) and Gans and De Vries (84), measurements of muscle architecture commonly include pennation angle, fiber (or fascicle) length, and physiological cross-sectional area as these characteristics impact whole muscle function (see below). Pennation angle is defined as the angle to which the fiber (or fascicle) runs relative to the force-generating axis of the muscle, and typically ranges from 0° to 30° (140). The degree and direction of pennation varies between and sometimes within skeletal muscles, where muscles with greater pennation angle tend to contract slower but produce more force (143). Pennation allows for “fiber packing” or the inclusion of more fibers in parallel within a muscle, contributing to the overall force producing capacity (142).

Muscles with larger pennation angles also tend to have shorter fascicle (or fiber) lengths. Even the most longitudinally oriented muscles (or muscles with lowest pennation angles) have fibers that extend only about 60% of the muscle length (140). Fascicle length is directly related to contractile velocity, which is vital for the production of muscle power (rate of force generation over time) (140). Together, fascicle length and pennation angle, along with muscle mass and density, allow for the calculation of a muscle’s physiological cross-sectional area (pCSA). The pCSA represents the theoretical sum of the cross-sectional area of all muscle fibers within a muscle (143),

and is the only architectural parameter that is directly proportional to the maximal tetanic force produced by a muscle (194).

B. Skeletal Muscle Fiber

1. Skeletal Muscle Fiber Structure

In addition to whole muscle architecture, the function of a muscle also depends on function of the cells (muscle fibers) that comprise it. A skeletal muscle is composed of anywhere from several hundred to over a million individual muscle fibers (69). On average, the cross-sectional area of muscle fibers in adult humans ranges from 2000-7500 μm^2 (35). Each muscle fiber is encased in two separate membranes, the basement membrane and plasma membrane, or sarcolemma which constitutes the endomysium. The basement membrane is a composed of glycogen proteins and collagen networks and is freely permeable to proteins and metabolites (35). The plasma membrane is selective in what ions and substrates cross it, and it plays an active role in transmitting action potentials that facilitate a muscle contraction.

Within the skeletal muscle fiber are approximately 2000 myofibrils, each approximately 1-2 μm^2 in area (150). Within each myofibril, the contractile units of skeletal muscle, known as sarcomeres, are arranged in series. The striated appearance of myofibrils stems from the regional density of thick and thin filaments with the sarcomeres. The thin filaments are anchored to a z-disc, which borders the ends of each sarcomere, called the I band. Thin filaments are comprised of the proteins actin, troponin and tropomyosin. Thick filaments are largely comprised of myosin heavy chain (MHC) and myosin light chain proteins. The interaction between the thick and thin filaments within sarcomeres are the mechanical bases of all muscle contractions.

2. Skeletal Muscle Fiber Function

The theory that explains the contractile function of a muscle fiber, termed the sliding filament theory, was first proposed in 1954 by two independent labs (120, 121). Upon the excitation of a motor unit by an alpha motor neuron, an action potential along the sarcolemma of the muscle fiber, triggering the Dihydropyridine receptors to open ryanodine receptors, which engages the

release of calcium into the cytosol of the fiber. Calcium binds to troponin within the thin filament, which shifts the position of tropomyosin, exposing a myosin binding site on actin. A cross-bridge forms when the MHC protein binds to actin and performs a power stroke, sliding the thick and thin filaments relative to one another. This action ultimately pulls the z-discs towards the midline of the sarcomere, resulting in sarcomere shortening. Adenosine triphosphate (ATP) then binds to the myosin head, where it is hydrolyzed, resulting in the detachment of the existing cross-bridge and recurrence of this cycle. The number of actin-myosin cross-bridges largely dictates the magnitude of force produced by a sarcomere (76). Joint movement is realized once the generated force is transmitted from the z-discs of the sarcomeres in series to the myotendinous junction and tendon, eventually reaching bone (76).

3. Skeletal Muscle Fiber Types

Skeletal muscle is comprised of different types of muscle fibers. These muscle fiber types are differentiated by the MHC isoform expressed within the myosin head, which largely dictates each fiber's contractile characteristics (202). In human adult skeletal muscle, three distinct MHC isoforms exist, MHC I, MHC IIa, MHC IIx (225). Comparatively, in other mammals such as rodents, four distinct MHC isoforms exist, MHC I, MHC IIa, MHC IIb, MHC IIx (26). "Hybrid" fibers are skeletal muscle fibers that contain two or more MHC isoforms (262, 263), whereas a fiber that contains only one MHC isoform is referred to as a "pure" fiber.

Pure MHC IIa and MHC IIx fibers are able to produce slightly more isometric force compared to pure MHC I fibers (29, 30, 259, 260). On the other hand, fiber excursion (contractile velocity) of MHC IIa and IIx fibers is much greater compared to MHC I fibers (29, 245), which is directly related to the rate at which the specific MHC isoform hydrolyzes ATP (16). MHC IIa and MHC IIx fibers are capable of generating five to six times more power than MHC I fibers (30, 245, 260), which is largely the result of their greater contractile velocity (as compared to their slight differences in force generating abilities).

C. Skeletal Muscle Adaptation

1. General Overview

Skeletal muscle possesses significant plasticity. It is capable of modifying its functional and metabolic properties in response to repeated and chronic disruptions in homeostasis. The ability

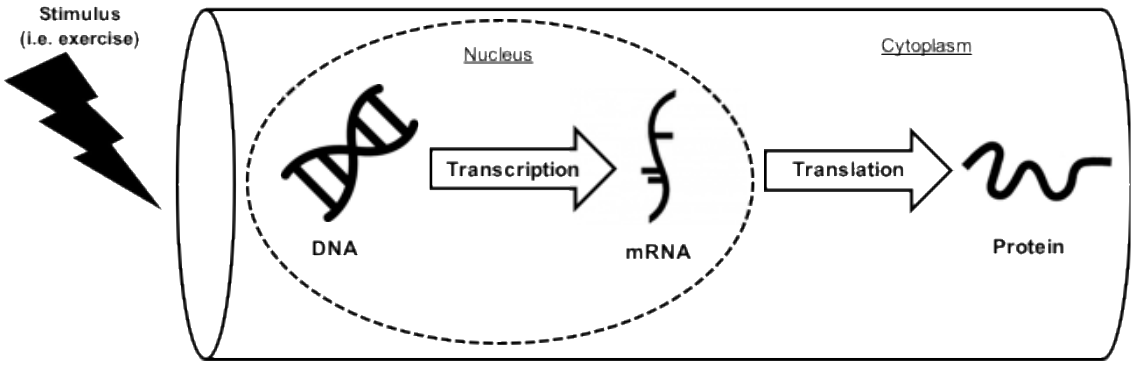


Figure 2-1. Conceptual schematic depicting the series of molecular events from leading to alterations in cellular protein. A stimulus (i.e. exercise) is placed upon the muscle cell, perturbing it from homeostasis. Cellular signaling events then cue the transcription of specific mRNA in the nucleus. These mRNA are then transported to the cytoplasm, bound by a ribosome, and translated into functional proteins.

for muscle to adapt is the consequence of a series of molecular events that ultimately lead to the accumulation of specific proteins. For instance, during exercise, contractions trigger transient surges in the quantity of messenger RNA (mRNA) that occur 3 to 24 hours following the exercise bout, depending on the specific mRNA and exercise modality (23, 264). This increase in mRNA is coupled with an increase in the rate of protein synthesis (translation), which can remain elevated for 48-72 hours following acute exercise (160, 190). Thus, in general the directional changes in the quantity of specific mRNA are in synchrony with the directional change of a particular protein (28). Therefore, repeated exercise stimuli repeatedly increase mRNA quantity eventually resulting in measureable alterations in protein content and function. Collectively, long-term changes in skeletal muscle morphology and function are the product of the cumulative effects of each acute, intermittent exercise stimulus. The molecular events regulating skeletal muscle adaptation are discussed below.

2. Cellular Signaling

The conversion of a stimulus (i.e., muscle contraction, change in physiological state) into the molecular events altering skeletal muscle phenotype is largely accomplished through the activation of a variety of complex cellular signaling pathways (72). These signaling pathways are comprised of networks of molecules (largely proteins) that coordinate to control one or more cellular functions, such as the transcription of new mRNA or translation of mRNA into protein. While specific signaling pathways within skeletal muscle are beyond the scope of this review, activators of skeletal muscle signaling include mechanotransduction, ATP turn-over, production of reactive oxygen species, redox balance, and others (64). Overall, signaling events represent the initial regulator of transcriptional and translational activity during muscle adaptation. For a review of specific signaling pathways that have a role in regulating the response of skeletal muscle to exercise, see these reveiws (41, 47, 207).

3. Transcription

Gene expression, known as transcription, is the process through which the genetic material of DNA is read and interpreted. Thus, transcription is often thought of as the “blueprint” or “intention” for eventual adjustments in protein composition (31). The end result of transcription is the formation of an RNA molecule that contains a specific sequence of nucleotides. The sequence of nucleotides in a RNA molecule is dictated by the sequence of nucleotides in the gene found in DNA. This process is initiated when the cell is signaled to produce more of a protein or enzyme. When stimulated, RNA polymerase reads a particular sequence of DNA (gene), specified by one or more transcription factors, and generates a complimentary single stranded RNA within the nucleus (208) (Fig. 2-1). Once the RNA polymerase encounters the terminator region of the gene, the formation of the RNA molecule is complete and it is exported into the cytosol where post-transcriptional modification such as alternative splicing, where exon sequences are rearranged to encode distinct proteins from a single mRNA (208). Consequently, “gene expression” most often refers to changes in the abundance of a particular mRNA molecule.

4. Translation

Three versions of RNA exist: tRNA, rRNA, and mRNA. The RNA that provides the nucleotide sequence to form specific proteins is the mRNA. Once the mRNA is transported into the cytoplasm, it is bound by a ribosome that translates the specific base sequences of the mRNA into a specific sequence of amino acids to form a protein/polypeptide (Fig. 2-1). Following translation, the amino acid sequences typically undergoes post-translation modification enabling its proper function (208). Together, the translation of mRNA into new, functioning proteins is often referred to as protein synthesis. Skeletal muscle protein synthesis is a vital response following exercise and has been shown to persist for up to 48 hours following an exercise bout (190).

5. Summary

Collectively, the aforementioned molecular processes (cellular signaling, transcription, translation) are repeatedly and synchronously activated following each acute exercise session. Over time, the repeated stimulate of these molecular events ultimately leads produces alterations in cellular makeup (protein abundance) and function of skeletal muscle (72).

III. ULTRASONOGRAPHY AND MUSCLE ARCHITECTURE

A. History of Ultrasound Imaging

The technological foundation of ultrasound imaging dates back to 1880, when Jacques and Pierre Curie discovered the piezoelectric effect of quartz crystals (49-51). This discovery demonstrated the ability of quartz crystals to produce outward traveling sound waves when an electric current is applied. Subsequently these sound waves are able to generate an electric signal when they reverberate off an object and return to the crystals. Interestingly, the practical application of this discovery was popularized between World War I and World War II. During this period, reflectoscopes were developed as underwater “microphones”, utilizing the piezoelectric effect as a means of echolocation to detect submarines and identify damage on the hulls of ships (196). Subsequently, this technology was adapted and employed as a medical device in 1942 by Dr. Karl

Dussik in an attempt to visualize brain tumors (62). Today, modern ultrasound devices still utilize the piezoelectric effect with quartz crystals encapsulated in digital handheld probes paired to computers for real-time imaging feedback.

The first reported use of ultrasound for musculoskeletal diagnostics was in 1958, when Donald and colleagues utilized ultrasound imaging to differentiate between cystic and solid masses in the abdomen (61). As technology improved, brightness mode (B-mode) ultrasound became capable of revealing differences in the echogenicity (brightness) of different tissues, which was considered to be associated with articular and periarticular injuries and diseases. With current ultrasound technology, anatomical compartments such as bone, muscle, connective tissue, and fat are easily distinguishable (Fig. 2-2).

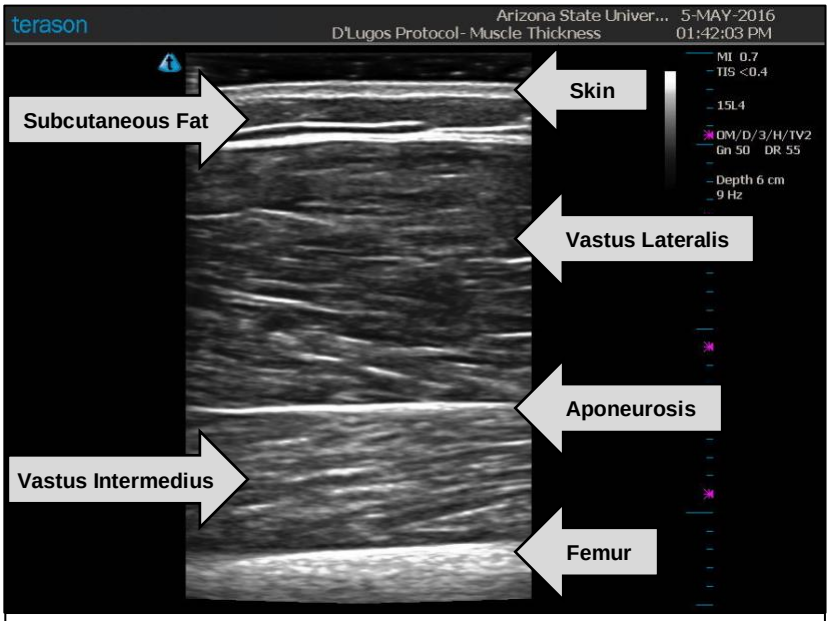


Figure 2-2. B-mode ultrasound image in the longitudinal plane of the lateral quadriceps. Differences in echogenicity (brightness) allow for clear differentiation of several tissue compartments including skin, fat, muscle, connective tissue, and bone.

A single two-dimensional image of skeletal muscle can provide valuable insight into a skeletal muscle's phenotype through the ability to quantify and measure muscle thickness (MT), pennation angle (PA) and fascicle length (FL). Similarly, a muscle's composition can also be assessed through the measure of echogenicity (EG). These variables are routinely coupled with functional assessments of the muscle(s) and may serve as predictors of muscle strength and

function (5, 205, 270). The following sections address the use of ultrasound imaging (US) in the measurement of skeletal muscle size, architecture, and composition. Given the focus of this dissertation on imaging of only the quadriceps femoris (*see Chapter 3*), this review will focus on the quadriceps femoris muscle group, comprised of the *vastus lateralis* (VL), *rectus femoris* (RF), *vastus intermedius* (VI), and *vastus medialis* (VM). Please note that US has also been applied to the study of other skeletal muscle groups (67, 191).

B. Muscle Thickness

Skeletal muscle thickness (MT) is defined as the perpendicular distance between the two-fascia surrounding a muscle. As an indicator of skeletal muscle mass, US-based muscle thickness measurements are strongly related to the cross-sectional area (CSA) of a muscle when measured via magnetic resonance imaging (MRI) (2). When compared with the manual measurement of quadriceps muscles from cadavers, US measurements of MT differed by only 0.03 cm, or 1% to 1.5% of the average adult quadriceps thickness (80). US-based MT assessments has since been accepted as a valid alternative to more invasive techniques (i.e., muscle biopsy) or expensive approaches, such as MRI, computed tomography (CT), or dual-energy x-ray absorptiometry (DXA) (195).

A disadvantage of US is the relatively limited imaging area compared to the aforementioned imaging technologies. The area of an US image is dictated by the size of the transducer (the probe that emits and receives sound) which is typically ~4 cm in length. Thus, a single longitudinal US image (Fig. 2) only depicts the MT in a ~4cm region of a particular anatomical region. Therefore, it is not uncommon to acquire images from multiple sites along the same muscle, which is important since heterogeneity of MT within each muscle of the quadriceps has been well documented with US (13, 24, 25, 66, 152). In the VL and RF, MT decreases from proximal to distal, whereas in the VM, MT increases distally (13, 25, 66). While the MT of the anterior aspect of the VI appears fairly uniform across the length of the leg (25), the lateral aspect of the VI appears to decrease from proximal to distal (13, 25). Given that MT varies within the quadriceps muscles, care must be taken to ensure measures are taken at the same site to allow for appropriate comparisons.

Alternatively, variability may be reduced if measures are taken at multiple sites along the quadriceps. Thus, the ability for US to quickly assess MT at multiple sites on multiple muscles provides the ability observe within- and between-muscle responses to stimuli such as exercise training.

Following a resistance training program, increases in the CSA of the quadriceps muscles also differ at distinct regions along each muscle (176). Indeed, varying degrees of hypertrophy within a muscle have been demonstrated using US measures of MT at different sites longitudinally along a muscle (24, 66, 152). Far more common is the use of US to assess changes in MT at a single location on one or multiple muscles of the quadriceps following a chronic exercise routine (10, 11, 20, 24, 66, 105, 152, 169, 199, 203, 214, 232, 237, 258, 267). Documented changes in quadriceps MT range from increases of 5% to 47% from pre- to post-training. All but one study (169) included a resistance exercise intervention, whereas Murach et al. (169) observed no change in MT of the VL following 12 weeks of run training. Increases in MT following exercise training vary slightly between the four muscles of the quadriceps; VL: 5-17%, RF: 7-47%, VI: 9-15%, and VM: 11-15%. Interestingly, while quadriceps MT is smaller in old versus young individuals (7, 236), the current body of literature indicates a similar degree of change in following training between young (< 50 yrs) and old (> 50 yrs) populations. Changes in MT following training in young are: VL: 5-17%, RF: 7-47%, VI: 10-14%, VM: ~14%, while changes in the MT of older populations are: VL: 8-15%, RF: 8-23%, VI: 9-15%, VM: 11-15% (Table 2-1).

Not only is MT examined as an indicator for hypertrophy, but also as a means to predict skeletal muscle function. Given the shared quadriceps tendon and functional role of the quadriceps muscles, the MT of the quadriceps muscles is commonly correlated to isolated actions of the knee joint such as isometric and isokinetic knee extension (KE). Several studies have demonstrated a moderate, positive relationship (r = 0.41 – 0.70) between the combined MT of several or all quadriceps muscles and peak KE force (3, 40, 78, 256, 261). Examining the relationship between the MT and peak KE force in a muscle specific manner reveals varying degrees of correlation amongst the four quadriceps muscles: VL: r = 0.54 – 0.84, RF: r = 0.19 – 0.88, VI: r = 0.42 – 0.82, VM: r = 0.39 – 0.92 (Table 2-1). Overall, the MT of each quadriceps muscle varies in its relation to

peak KE force. Furthermore, in the only study to directly compare between young (24 ± 4 yrs) and older (68 ± 5 yrs) participants, the relationships between the MT of each quadriceps muscle and peak KE were lower in old (236). The age-related reduction in the relationship between MT and KE force may indicate varying architectural or compositional differences that occur in skeletal muscle with advancing age, or differences in the ability of the tendon to transfer force (42). However, while the measurement of MT is effective in assessing muscle mass within and between muscles, US imaging enables other measurements capable of revealing architectural or compositional details of skeletal muscle.

Table 2-1 (pg. 16-24). Summary of ultrasound-derived muscle thickness measurements in the quadriceps: relationship to muscle function and changes with exercise training

Author, Year (Reference)	Age (yrs)	Muscle	Training		Correlation to Muscle Function
			Exercise	Outcome	
Freilich, 1995 (75)	18 - 50	Quad	-	-	Isomet. KE; Men: *r* = 0.55 Women: *r* = 0.56
Cadore, 2012 (40)	66 ± 5	VI	-	-	Isomet. KE: *r* = 0.42 Isokin. KE (60°/s): *r* = 0.53 Isokin. KE (180°/s): *r* = 0.51 Isokin. KE (360°/s): *r* = 0.52
		VM			Isomet. KE: *r* = 0.42 Isokin. KE (60°/s): *r* = 0.55 Isokin. KE (180°/s): *r* = 0.62 Isokin. KE (360°/s): *r* = 0.60
		Quad			Isomet. KE: *r* = 0.43 Isokin. KE (60°/s): *r* = 0.57 Isokin. KE (180°/s): *r* = 0.63 Isokin. KE (360°/s): *r* = 0.61
Fukumoto, 2012 (78)	70 ± 6	Quad	-	-	Isomet. KE: *r* = 0.47
Strasser, 2013 (236)	Y: 24 ± 4 O: 68 ± 5	VL	-	-	Isomet. KE; Y: *r* =0.838; O: *r* = 0.756
		VI			Y: *r* =0.918; O: *r* = 0.815
		VM			Y: *r* =0.920; O: *r* = 0.875
		RF			Y: *r* =0.880; O: *r* = 0.834
Wantanabe, 2013 (256)	74 ± 6	Quad	-	-	Isomet. KE: *r* = 0.411
Abe, 2014 (3)	52 – 82	Quad	-	-	Isomet. KE: *r* = 0.703

Table 2-1 (pg. 16-24). Summary of ultrasound-derived muscle thickness measurements in the quadriceps: relationship to muscle function and changes with exercise training

Author, Year (Reference)	Age (yrs)	Muscle	Training		Correlation to Muscle Function
			Exercise	Outcome	
Wilhelm, 2014 (261)	66 ± 5	Quad	-	-	1RM: r = 0.656 Isomet. KE: r = 0.620
Ando, 2014 (13)	22 ± 1	VL	-	-	(ns)
		VI (lateral)			(ns)
		VI (anterior)			Isomet. KE: r = 0.74
		VM			Isomet. KE: r = 0.39
		RF			Isomet. KE: r = 0.19
Tillquist, 2014 (242)	31 ± 8	Quad	-	-	
Lopez, 2017 (148)	66 ± 5	Quad	-	-	30sec Sit-to-stand: r = 0.51
Raj, 2017 (219)	68 ± 5	VL	-	-	Isomet. KE: r = 0.62 Isokin. KE (60°/s): r = 0.66 Isokin. KE (120°/s): r = 0.60 Isokin. KE (240°/s): r = 0.65 Isokin. KE (360°/s): r = 0.54
		RF+VI			Isomet. KE: r = 0.56 Isokin. KE (60°/s): r = 0.60 Isokin. KE (120°/s): r = 0.59 Isokin. KE (240°/s): r = 0.62 Isokin. KE (360°/s): r = 0.53

Table 2-1 (pg. 16-24). Summary of ultrasound-derived muscle thickness measurements in the quadriceps: relationship to muscle function and changes with exercise training

Author, Year (Reference)	Age (yrs)	Muscle	Training		Correlation to Muscle Function
			Exercise	Outcome	
Stock, 2017 (234)	12 ± 1	VL RF	-	-	VL: Sprint speed: r = -0.538 Agility: r = -0.555 Isomet KE: r = 0.422 RF: Jump height: r = 0.400 Sprint speed: r = -0.606 Peak velocity: r = 0.491 Agility: r = -0.646 Isomet. KE: r = 0.564
Blazevich, 2003 (24)	22 ± 2	VL (distal) VL (proximal) RF (distal) RF (proximal)	Weeks 1-4: 3 sets of 10 LP, DL, LE 2d/week Weeks 5-9: Squats (SQ) 2d/week or Front hack squat (FHS) 2d/week or sprint/jump (SJ) 4d/week	VL (distal): ↔ VL (proximal): ↑ 11% (SQ) ↑ 12% (FSH) RF (distal): ↔ RF (proximal): ↑ 8% (SQ) ↑ 11% (FSH) ↑ 12% (SJ)	-
Alegre, 2006 (11)	22 ± 2	VL	3-4 sets of 6-12 half squat @ 50-60%1RM 3d/week 13 weeks	↑ 7%	Squat 1RM: r = 0.52 – 0.54

Table 2-1 (pg. 16-24). Summary of ultrasound-derived muscle thickness measurements in the quadriceps: relationship to muscle function and changes with exercise training

Author, Year (Reference)	Age (yrs)	Muscle	Training		Correlation to Muscle Function
			Exercise	Outcome	
Suetta, 2008 (237)	60 – 86	VL	RT: KE and LP 3d/week 12 weeks ES: electrical stimulation for 1h @ 40Hz 3d/week 12 weeks SR: functional mobility exercises 3d/week 12 weeks	RT: ↑ 15% ES: ↔ SR: ↔	-
Reeves, 2009 (203)	74 ± 3	VL	RT: 2 sets of 10 @ 80% 5RM 3d/week 14 weeks Eccentric only RT (ECC): 2 sets of 10 @ 80% 5RM 3d/week 14 weeks	RT: ↔ ECC: ↔	-
Baroni, 2013 (20)	24 ± 3	VL RF	3-5 sets of 10 ECC isokin. KE @ 60°/s 2d/week 12 weeks	4 weeks: VL: ↑ 5% RF: ↑ 7% 8 weeks: VL: ↑ 7% RF: ↑ 10% 12 weeks: VL: ↑ 7% RF: ↑ 10%	-

Table 2-1 (pg. 16-24). Summary of ultrasound-derived muscle thickness measurements in the quadriceps: relationship to muscle function and changes with exercise training

Author, Year (Reference)	Age (yrs)	Muscle	Training		Correlation to Muscle Function
			Exercise	Outcome	
Guilhelm, 2013 (105)	20 ± 3	VL	ECC Isoload (IL): 3-5 sets of 8 KE @ 120% 1RM 20 sessions 9 weeks ECC Isokin. (IK): 3-5 sets of *n* reps (work-matched to IL) KE @ maximal effort 20 sessions 9 weeks	IL: ↑ 10% IK: ↔	-

Table 2-1 (pg. 16-24). Summary of ultrasound-derived muscle thickness measurements in the quadriceps: relationship to muscle function and changes with exercise training

Author, Year (Reference)	Age (yrs)	Muscle	Training		Correlation to Muscle Function
			Exercise	Outcome	
Ema, 2013 (66)	27 ± 2	VL (distal) VL (proximal) VI-Lateral (distal) VI-Lateral (proximal) VI-Medial (distal) VI-Medial (proximal) VM (distal) VM (proximal) RF (distal) RF (proximal)	5 sets of 8 KE @ 80% 1RM 12 weeks	VL (distal): ↑ 9% VL (proximal): ↑ 8% VI-Lateral (distal): ↔ VI-Lateral (proximal): ↔ VI-Medial (distal): ↑ 14% VI-Medial (proximal): ↑ 10% VM (distal): ↔ VM (proximal): ↑ 14% RF (distal): ↑ 22% RF (proximal): ↑ 16%	-

Table 2-1 (pg. 16-24). Summary of ultrasound-derived muscle thickness measurements in the quadriceps: relationship to muscle function and changes with exercise training

Author, Year (Reference)	Age (yrs)	Muscle	Training		Correlation to Muscle Function
			Exercise	Outcome	
Radaelli, 2013 (199)	60 – 74	VL VI VM RF	High volume (HV): 3 sets per RE or Low volume (LV): 1 set per RE 2d/week 13 weeks	HV: VL: ↑ 13% VI: ↑ 15% VM: ↑ 15% RF: ↑ 11% LV: VL: ↑ 8% VI: ↑ 9% VM: ↑ 11% RF: ↑ 8%	-
Scanlon, 2014 (214)	71 ± 7	VL RF	2-4 sets of 8-12 reps @ 70-85% 1RM 2d/week 6 weeks	VL: ↔ RF: ↔	-
Wells, 2014 (258)	20 ± 1	VL	Whole body progressive RE 4d/week 15 weeks	VL0 (lateral): ↔ VL5 (5cm medial): ↑ 10%	Squat 1RM: VL0: r = 0.561

Table 2-1 (pg. 16-24). Summary of ultrasound-derived muscle thickness measurements in the quadriceps: relationship to muscle function and changes with exercise training

Author, Year (Reference)	Age (yrs)	Muscle	Training		Correlation to Muscle Function
			Exercise	Outcome	
Alegre, 2014 (10)	19 ± 2	VL	3-4 sets of 5-7 isomet. KE @ either 50° KF (K50) or 90° KF (K90) 2-3d/week 8weeks	K50: VL25 (proximal): ↑ 6% VL50 (middle): ↑ 5% VL75 (distal): ↔ K90: VL25 (proximal): ↑ 9% VL50 (middle): ↑ 14% VL75 (distal): ↑ 9%	-
Matta, 2015 (152)	19 ± 1	RF (proximal, distal)	3 sets of 10-11 isotonic (TON) or isokinetic (IK, 60°/s) KE 2d/week 14 weeks	TON: Proximal: ↑ 14% Distal: ↑ 47% IK: Proximal: ↑ 11% Distal: ↑ 32%	-
Murach, 2015 (169)	20 ± 1	VL	Running 4d/week 12 weeks	↔	-

Table 2-1 (pg. 16-24). Summary of ultrasound-derived muscle thickness measurements in the quadriceps: relationship to muscle function and changes with exercise training

Author, Year (Reference)	Age (yrs)	Muscle	Training		Correlation to Muscle Function
			Exercise	Outcome	
Stansinaki, 2015 (232)	22 ± 2	VL	Whole body RE 3d/week 6 weeks	↑ 7-17%	-
Yoshiko, 2017 (267)	78 ± 8	RF	Progressive rehab. program (RE & AE) 12 months	6mo.: ↔ 12mo.: ↑ 23%	-

Quad, quadriceps; isomet, isometric; KE, knee extension; VI, vastus intermedius; VM, vastus medialis; isokin, isokinetic; Y, young; O, old; VL, vastus lateralis; RF, rectus femoris; RM, repetition maximum; LP, leg press; ns, not statistically significant; DL, dead lift; SQ, squat; FHS, front hack squat; SJ, sprint/jump training; RT, resistance training; ES, electrical stimulation; SR, standard rehabilitation; ECC, eccentric; IL, isoload training; IK, isokinetic training; HV, high volume; LV, low volume; RE, resistance exercise; KF, knee flexion; TON, isotonic training; ↔, $p > 0.05$; ↑ or ↓, $p < 0.05$.

C. Pennation Angle and Fascicle Length

The function of skeletal muscle is governed, in part, based on the orientation of muscle fibers within the muscle (142, 203). Ultrasound imaging is capable of noninvasively assessing two hallmark architectural features of skeletal muscle, pennation angle and fascicle length. Pennation angle (PA) is defined as the angle between the orientation of a fascicle (bundle of muscle fibers) and the attached tendon (axis of forge generation) (Fig. 2-3). The degree of PA is directly related to force producing capacity of a muscle (143). Fascicle length (FL) is, in theory, a measurement of muscle fiber length. However, due to the difficulty to measure muscle fiber length in practice, FL is often measured from B-mode US images such as Fig. 2-3 instead. Defined as the distance between the intersection of the axis of force generation (tendon) and fascicle and the intersection of the opposing aponeurosis and fascicle, FL is proportional to the contractile velocity of a muscle (140). Due to geometrical constraints, a muscle with greater PA typically has shorter FL, and vice versa. Thus, variability in PA and FL between muscles largely explains the unique functional roles of varying muscles (143), even those with similar cross-sectional areas.

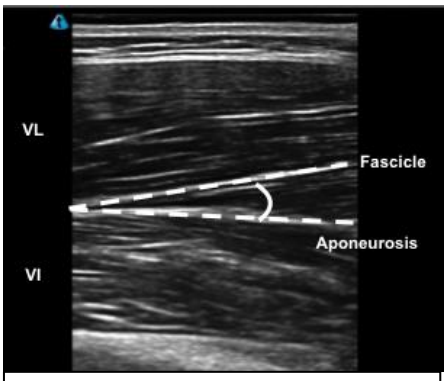


Figure 2-3. B-mode US image of the vastus lateralis (VL) and lateral vastus intermedius (VI). Pennation angle is measured as the angel between the fascicle and deep aponeurosis. Fascicle length is determined by extrapolating the superficial aponeurosis and fascicle to the right of the field of view until they intersect and measuring the distance from this intersection to the intersection with the deep aponeurosis.

Similar to MT, PA and FL not only vary across muscles, but also within muscles. Through US imaging, PA has been well documented to vary along different regions of all muscles of the quadriceps except the VI (24, 25, 66, 152, 157). In the VL and RF muscles, PA typically decreases from proximal to distal (24, 25, 66, 152), whereas in the VM, PA increases proximal to distal (25, 66). Although limited to one investigation, the PA of the VI appears somewhat constant along the length of the leg (25). The literature is limited regarding the heterogeneity of FL within each muscle of the quadriceps. Nonetheless, the simultaneous measurement of both PA and FL along multiple regions of a muscle can provide valuable insight into the functional characteristics of a muscle and how they are altered following various stimuli.

Exercise training is a powerful stimulus for skeletal muscle adaptation, and by assessing changes in PA and FL, one may better understand how a muscle is adapting following training. For instance, an increase in PA following training is likely the result of additional sarcomeres in parallel, or added contractile elements along the axis of force generation (172). This phenomenon of including more fibers along the force producing axis of a muscle is termed fiber packing (142). Conversely, the observation of increased FL following exercise training would infer that sarcomeres were added in series, resulting in greater contractile velocity (140). It is fairly common that PA and FL are measured simultaneously, however these variables often respond differently following chronic exercise training (Fig. 2-4).

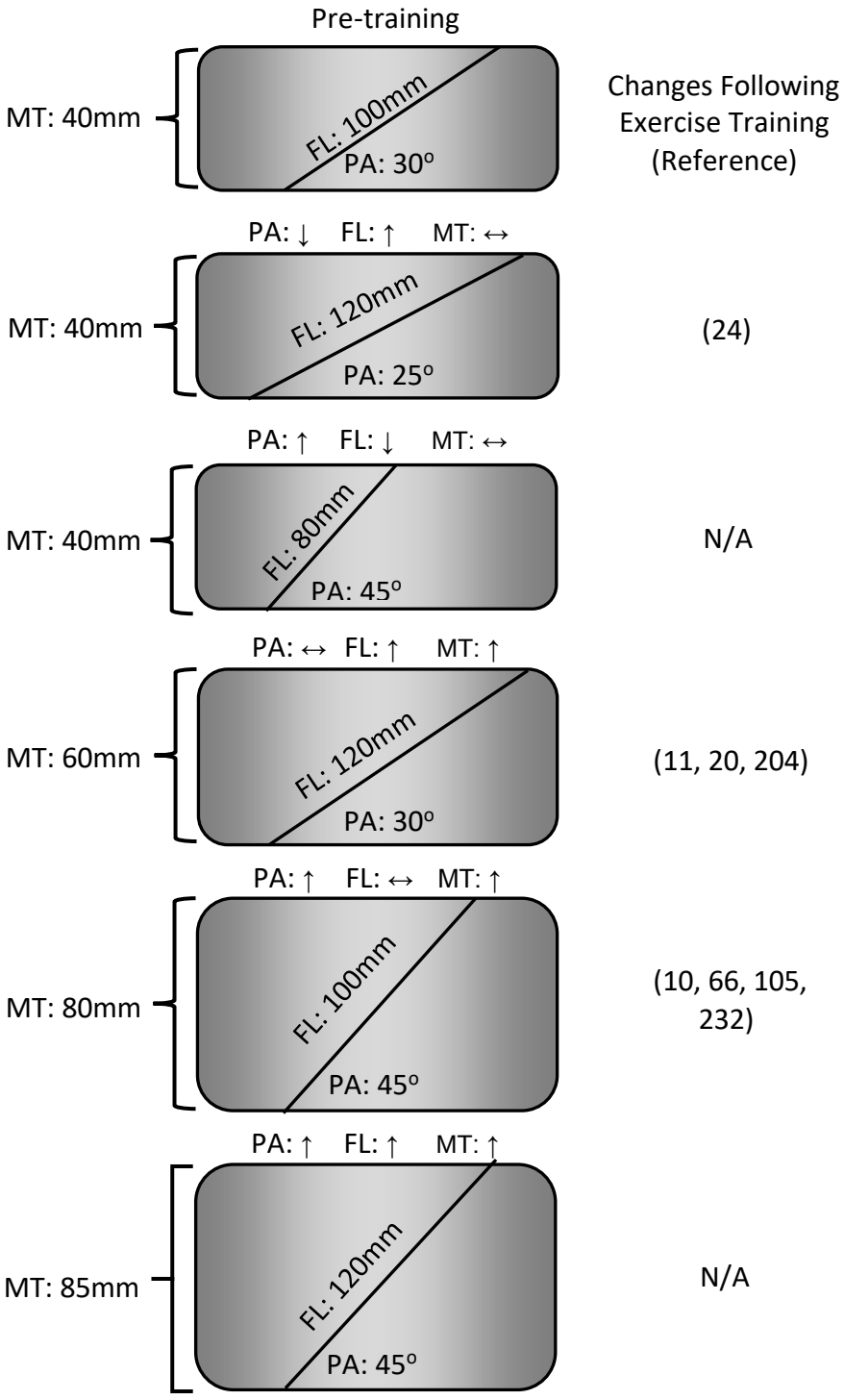


Figure 2-4. Simplified schematic of possible combinations of MT, PA, and FL responses following chronic exercise training. Numerical values and changes are not actual. MT, muscle thickness; PA, pennation angle; FL, fascicle length; N/A, no reference available.

Following an exercise training program, increases in quadricpes PA documented with US range from 4% following 12 weeks of knee extension resistance training (RT) (66) to 46% following 9 weeks of RT emphasizing squats (24). Changes in PA have been documented with a little as 5 weeks of knee extension training on a gravity-independent leg ergometer (220). All exercise training interventions included RT except for three studies, which included cycling (68), running (169), or functional mobility exercises (237). Functional mobility exercise was the only exercise training intervention to result in decreased PA (237), whereas cycling and running did not influence quadriceps PA (68, 169). Changes in PA also varied slightly between the muscles of the quadriceps. Increases in the PA of the VL ranged from 4% (66) to 36% following 14 weeks of RT (1), whereas changes in PA of the RF ranged from 13% (66) to 46% (24) both following 12 and 9 weeks of RT, respectively. Interestingly, changes in PA of the VI and VM following exercise training have only been documented in one study (66), where increases ranged from 6 – 12% in the VI and 4 – 7% in the VM following 12 weeks of RT.

Changes in FL following chronic exercise training range from increases of 2% following as little as 1.5 weeks of knee extension training on a gravity-independent leg ergometer (220), to 83% following 9 weeks of squat-focused RT (24). Changes in FL within each muscle of the quadriceps is limited to the VL and RF, as there are no documented changes in the FL of the VI or VM following exercise training. Increases in the FL of the VL range from 2 – 80% following 1.5 weeks of knee extension training (220) and 9 weeks of squat-focused RT (24), respectively. Changes in the FL of the RF range from 14% following 12 weeks of eccentric RT (20) to 83% following 9 weeks of squat-focused RT (24).

Accompanying the aging-induced decrease in quadriceps MT (7, 236) is a similar decrease in PA and FL (175), which may account for up to half of the age-related loss in maximal contractile force and velocity (174). However, while the body of literature is limited, it appears exercise is a viable means to increase PA and FL in the quadriceps muscles of older populations. Only four studies (203, 204, 214, 237) have employed US to assess changes in PA and FL of the quadriceps muscles following exercise training. Three studies report no changes in PA following 12 weeks of electrical stimulation (237), 6 weeks of RT (214), or 14 weeks of eccentric RT (203). Yet, two

investigations demonstrate 8% and 20% increases in PA following 12 weeks (237) and 14 weeks of RT (204), respectively. While 6 weeks of RT was sufficient to induces changes in FL of the VL or RF of older individuals (214), increases in VL FL have been noted following 14 weeks of traditional (204) and eccentric RT (203). Surprisingly, exercise-induced changes in the PA or FL of the VI or VM have not been demonstrated in older populations. Collectively, it does appear that exercise is capable of inducing positive adaptations in the skeletal muscle architecture of older adults.

Similar to US-based MT measurements, PA and FL are commonly assessed to predict muscle function. Several studies have demonstrated a positive, moderate relationship (r = 0.341 – 0.680) between PA and peak isometric KE torque (13, 219, 236). However, it appears that the PA of some, but not all of the quadriceps muscles exhibit this relationship with peak isometric KE. While Strasser et al. (236) demonstrated positive relationships between the PA of the VL , VI, and VM and peak isometric KE (r = 0.341, 0.680, 0.338; respectively), Ando and colleagues (13) showed that only the PA of the anterior VI was significantly correlated (r = 0.680) to peak isometric KE. Furthermore, an early study displayed no significant relationship between the PA of the VL or VI and peak isometric KE (209). Nonetheless, PA of the quadriceps has also been shown to be positively related to peak isometric squat (11) and 100m sprint performance (136). The relationship between FL and function of the quadriceps muscles has been less studied, with only one study demonstrating a significant relationship (r = -0.43) between FL of the VL and 100m sprint performance (136). In the only study to directly compare between young and old individuals, Strasser *et al.* (236) shows that only the PA of the VL, VI, and VM in the young are significantly related to peak isometric KE, whereas no significant relationships were revealed from the muscle architecture of the old. While it appears muscle architecture not only varies between muscles and age groups, so too does the relationship between muscle architecture and function. While more research examining muscle architecture in older populations is warranted, it is possible that quadriceps muscle function may be better predicted with a combination of US based measurements, including architecture, MT, and muscle composition.

Table 2-2 (pg. 30-39). Summary of Ultrasound-Based Pennation Angle and Fascicle Length Measurements in the Quadriceps.

Author, Year (Reference)	Age (yrs)	Muscle	Training		Correlation to Muscle Function
			Exercise	Outcome	
Kumagai, 2000 (136)	NA	VL	-	-	100m sprint; PA: r = 0.34 FL: r = -0.43
Strasser, 2013 (236)	Y: 24 ± 4 O: 68 ± 5	VL	-	-	Isomet. KE; PA: Y: r =0.341; O: r =0.322 (ns)
		VI			Y: r =0.680; O: r =0.306 (ns)
		VM			Y: r =0.338; O: r =0.253 (ns)
Ando, 2014 (13)	22 ± 1	VL	-	-	Isomet. KE; PA: r = 0.15 (ns) FL: ns
		VI (lateral)			PA: r = 0.68 (ns) FL: ns
		VI (anterior)			PA: r = 0.68 FL: ns
		VM			PA: r = 0.35 (ns) FL: ns
		RF			PA: r = 0.20 (ns) FL: ns

Table 2-2 (pg. 30-39). Summary of Ultrasound-Based Pennation Angle and Fascicle Length Measurements in the Quadriceps.

Author, Year (Reference)	Age (yrs)	Muscle	Training		Correlation to Muscle Function
			Exercise	Outcome	
Raj, 2017 (219)	68 ± 5	VL	-	-	PA: Isomet. KE: *r* = 0.36 Isokin. KE (60°/s): *r* = 0.31 (ns) Isokin. KE (120°/s): *r* = 0.26 (ns) Isokin. KE (240°/s): *r* = 0.31 (ns) Isokin. KE (360°/s): *r* = 0.28 (ns) FL: Isomet. KE: *r* = 0.04 (ns) Isokin. KE (60°/s): *r* = 0.13 (ns) Isokin. KE (120°/s): *r* = 0.11 (ns) Isokin. KE (240°/s): *r* = 0.09 (ns) Isokin. KE (360°/s): *r* = 0.00 (ns)
Rutherford, 1992 (209)	18 – 40	VL VI	4 sets of 6 KE @ 6RM 3d/week 12weeks	FA: ↔ FA: ↔	Isomet. KE: No relation.
Aagaard, 2001 (1)	27 ± 5	VL	4-5 sets of 4-12 Squats, LP, KE 2-3d/week 14weeks	PA: ↑ 36 ± 8%	-

Table 2-2 (pg. 30-39). Summary of Ultrasound-Based Pennation Angle and Fascicle Length Measurements in the Quadriceps.

Author, Year (Reference)	Age (yrs)	Muscle	Training		Correlation to Muscle Function
			Exercise	Outcome	
Blazevich, 2003 (24)	22 ± 2	VL (distal) VL (proximal) RF (distal) RF (proximal)	Weeks 1-4: 3 sets of 10 LP, DL, LE 2d/week Weeks 5-9: Squats (SQ) 2d/week or Front hack squat (FHS) 2d/week or sprint/jump (SJ) 4d/week	VL (distal) PA: ↔ FL: ↑ 80% w/ (SJ) VL (proximal) PA: ↓ 31% w/ (SJ) FL: ↑ 25% w/ (SJ) RF (distal) PA: ↑ 46% w/ (FHS) FL: ↑ 22% w/ (SQ) RF (proximal) PA: ↔ FL: ↑ 83% w/ (SQ); ↑ 39% w/ (SJ)	-
Reeves, 2004 (204)	74 ± 4	VL	2 sets of 10 KE and LP @ 60-80% 5RM 3d/week 14 weeks	PA: ↑ 8-10% FL: ↑ 28-35%	-
Alegre, 2006 (11)	22 ± 2	VL	3-4 sets of 6-12 half squat @ 50-60%1RM 3d/week 13 weeks	PA: ↔ FL: ↑ 10%	PA: Isometric squat: $r = 0.57$

Table 2-2 (pg. 30-39). Summary of Ultrasound-Based Pennation Angle and Fascicle Length Measurements in the Quadriceps.

Author, Year (Reference)	Age (yrs)	Muscle	Training		Correlation to Muscle Function
			Exercise	Outcome	
Seynnes, 2007 (220)	20 ± 2	VL	KE on gravity-independent flywheel ergometer 3d/week 5 weeks	1.5 weeks: PA: ↔ FL: ↑ 2% 3 weeks: PA: ↔ FL: ↑ 6% 5 weeks: PA: ↑ 8% FL: ↑ 10%	-
Suetta, 2008 (237)	60 – 86	VL	RT: KE and LP 3d/week 12 weeks ES: electrical stimulation for 1h @ 40Hz 3d/week 12 weeks SR: functional mobility exercises 3d/week 12 weeks	RT: PA: ↑ 22% ES: PA: ↔ SR: PA: ↓ 11%	Δ PA w/ RT: Δ Isokin. KE (60°/s): $r = 0.619$ Δ Isokin. KE (180°/s): $r = 0.530$

Table 2-2 (pg. 30-39). Summary of Ultrasound-Based Pennation Angle and Fascicle Length Measurements in the Quadriceps.

Author, Year (Reference)	Age (yrs)	Muscle	Training		Correlation to Muscle Function
			Exercise	Outcome	
Reeves, 2009 (203)	74 ± 3	VL	RT: 2 sets of 10 @ 80% 5RM 3d/week 14 weeks Eccentric only RT (ECC): 2 sets of 10 @ 80% 5RM 3d/week 14 weeks	RT: (previously reported: Reeves, 2004) ECC: PA: ↔ FL: ↑ 20%	-
Farup, 2012 (68)	23 ± 1	VL	END: 30-40min cycling or RT: 3-5 sets of 4-10 maximal reps 3d/week 10 weeks	END: PA: ↔ RT: PA: ↑ 23%	-
Baroni, 2013 (20)	24 ± 3	VL RF	3-5 sets of 10 ECC isokin. KE @ 60°/s 2d/week 12 weeks	4 weeks: VL PA: ↔ VL FL: ↑ 5% RF PA: ↔ RF FL: ↑ 6% 8 weeks: VL PA: ↔ VL FL: ↑ 17% RF PA: ↔ RF FL: ↑ 14% 12 weeks: VL PA: ↔ VL FL: ↑ 19% RF PA: ↔ RF FL: ↑ 17%	-

Table 2-2 (pg. 30-39). Summary of Ultrasound-Based Pennation Angle and Fascicle Length Measurements in the Quadriceps.

Author, Year (Reference)	Age (yrs)	Muscle	Training		Correlation to Muscle Function
			Exercise	Outcome	
Guilhelm, 2013 (105)	20 ± 3	VL	ECC Isoload (IL): 3-5 sets of 8 KE @ 120% 1RM 20 sessions 9 weeks ECC Isokin.: 3-5 sets of *n* reps (work-matched to IL) KE @ maximal effort 20 sessions 9 weeks	IL: PA: ↑ 11% FL: ↔ IK: PA: ↔ FL: ↔	-

Table 2-2 (pg. 30-39). Summary of Ultrasound-Based Pennation Angle and Fascicle Length Measurements in the Quadriceps.

Author, Year (Reference)	Age (yrs)	Muscle	Training		Correlation to Muscle Function
			Exercise	Outcome	
Ema, 2013 (66)	27 ± 2	VL (distal) VL (proximal) VI-Lateral (distal) VI-Lateral (proximal) VI-Medial (distal) VI-Medial (proximal) VM (distal) VM (proximal) RF (distal) RF (proximal)	5 sets of 8 KE @ 80% 1RM 12 weeks	PA: VL (distal): ↑ 4% VL (proximal): ↑ 11% VI-Lateral (distal): ↔ VI-Lateral (proximal): ↔ VI-Medial (distal): ↑ 12% VI-Medial (proximal): ↑ 6% VM (distal): ↑ 4% VM (proximal): ↑ 7% RF (distal): ↑ 19% RF (proximal): ↑ 13% FL: VL (distal): ↔ VL (proximal): ↔ VM (proximal): ↔ RF (proximal): ↔	-

Table 2-2 (pg. 30-39). Summary of Ultrasound-Based Pennation Angle and Fascicle Length Measurements in the Quadriceps.

Author, Year (Reference)	Age (yrs)	Muscle	Training		Correlation to Muscle Function
			Exercise	Outcome	
Scanlon, 2014 (214)	71 ± 7	VL RF	2-4 sets of 8-12 reps @ 70-85% 1RM 2d/week 6 weeks	PA: VL: ↔ RF: ↔ FL: VL: ↔ RF: ↔	-
Wells, 2014 (258)	20 ± 1	VL	Whole body progressive RE 4d/week 15 weeks	PA: VL0 (lateral): ↔ VL5 (5cm medial): ↔ FL: VL0 (lateral): ↑ 6% VL5 (5cm medial): ↔	-
Alegre, 2014 (10)	19 ± 2	VL	3-4 sets of 5-7 isomet. KE @ either 50° KF (K50) or 90° KF (K90) 2-3d/week 8weeks	PA: K50: ↔ K90: ↑ 12% FL: K50: ↔ K90: ↔	-

Table 2-2 (pg. 30-39). Summary of Ultrasound-Based Pennation Angle and Fascicle Length Measurements in the Quadriceps.

Author, Year (Reference)	Age (yrs)	Muscle	Training		Correlation to Muscle Function
			Exercise	Outcome	
McMahon, 2014 (156)	19 ± 3	VL (proximal, middle, distal)	Progressive RE of either longer length (LL, 40-90° KE) or shorter length (SL, 0-50° KE) 3d/week 8 weeks	PA: LL(proximal): ↑ 14% SL (proximal): ↑ 12% LL(middle): ↑ 6% SL (middle): ↑ 7% LL(distal): ↑ 7% SL (distal): ↑ 11% FL: LL(proximal): ↑ 27mm SL (proximal): ↑ 18mm LL(middle): ↑ 21mm SL (middle): ↑ 9mm LL(distal): ↑ 24mm SL (distal): ↑ 12mm	-
Franchi, 2014 (74)	25 ± 3	VL	4 sets of 8-10 concentric (CON) or eccentric (ECC) leg-press @ 80% 1RM 3d/week 10 weeks	PA: CON: ↑ 30% ECC: ↑ 5% FL: CON: ↑ 5% ECC: ↑ 12%	-

Table 2-2 (pg. 30-39). Summary of Ultrasound-Based Pennation Angle and Fascicle Length Measurements in the Quadriceps.

Author, Year (Reference)	Age (yrs)	Muscle	Training		Correlation to Muscle Function
			Exercise	Outcome	
Matta, 2015 (152)	19 ± 1	RF (proximal, distal)	3 sets of 10-11 isotonic (TON) or isokinetic (KIN, 60°/s) KE 2d/week 14 weeks	PA: TON Proximal: ↔ TON Distal: ↑ 20% KIN Proximal: ↔ KIN Distal: ↔	-
Murach, 2015 (169)	20 ± 1	VL	Running 4d/week 12 weeks	PA: ↔ FL: ↔	-
Stansinaki, 2015 (232)	22 ± 2	VL	Whole body RE 3d/week 6 weeks	PA: ↑ 20-26% FL: ↔	-

Quad, quadriceps; isomet, isometric; KE, knee extension; VI, vastus intermedius; VM, vastus medialis; isokin, isokinetic; Y, young; O, old; VL, vastus lateralis; RF, rectus femoris; RM, repetition maximum; LP, leg press; ns, not statistically significant; DL, dead lift; SQ, squat; FHS, front hack squat; SJ, sprint/jump training; RT, resistance training; ES, electrical stimulation; SR, standard rehabilitation; ECC, eccentric; IL, isoload training; IK, isokinetic training; HV, high volume; LV, low volume; RE, resistance exercise; KF, knee flexion; TON, isotonic training; ↔, $p > 0.05$; ↑ or ↓, $p < 0.05$

D. Echogenicity

B-mode US imaging enables the investigation of skeletal muscle mass and architecture from a single 2D image. However, what muscle mass and architecture fail to account for is the quality, or composition, of skeletal muscle. Echogenicity (EG) can be defined as the degree of sound reflection influenced by the acoustic impedance of tissues (191). In a 2D B-mode US image (Fig. 2-1), skeletal muscle has relatively low EG compared to the dense connective tissue of the aponeuroses and the border of the femur bone. The lower EG of skeletal muscle demonstrates that the impedance of sound through skeletal muscle is greater than that in connective tissue or bone. The early work of Heckmatt et al. (112) revealed that dystrophic and healthy muscles exhibited different levels of EG, indicating an alteration in the composition of dystrophic skeletal muscles. Since, EG has been correlated to the infiltration of fibrous (192) and adipose tissue (8, 269) into skeletal muscle. As more non-contractile tissue appears within skeletal muscle, the reflection of sound diminishes, and the EG increases. As a mean to assess intramuscular fat, primarily in the form of extramyocellular fat (between muscle fibers), US-based EG has been validated against the gold standard MRI (8, 269). However, while EG is limited in its ability distinguish between fibrous tissue and fat, it is a valid means to assess differences in skeletal muscle composition.

Similar to MT, PA, and FL, EG also appears to vary across the four muscles of the quadriceps. In both studies that have assessed EG in all quadriceps muscles the EG of the superficial quadriceps (VL, RF, VM) appear similar while the EG of the VI appears to be consistently lower (236, 261). However, rather than a true anatomical difference, this may be due to a limitation in US where deeper tissues appear less echoic (lower EG) due to an attenuation of the US beam (191).

Exercise training is known to alter the composition of skeletal muscle (99). Reductions in skeletal muscle EG, indicating reduced non-contractile tissue, following exercise training range from 9%, following 6 months of combined AE and RE (267), to 21%, following 13 weeks of RT (199). In the few studies that have examined muscle EG following exercise training (199, 214, 258, 267), none report EG to increase. The lack of increase in EG with exercise training indicates that

exercise training does not worsen muscle quality (i.e., resists infiltration of adipose and/or connective tissue into skeletal musce), when assessed via US.

It is well understood that aging is associated with a progressive decline in the quality of skeletal muscle (101, 163). Further, the replacement of muscle tissue with fibrous and fatty tissue has been implicated as a major contributor to reduced muscle quality with aging (114, 151, 271). Only one study (236) has directly compared skeletal muscle composition of young and old using US-based EG. Strasser et al. (236) reports that the EG of the VL, VI, VM, and RF are higher in old compared to young individuals, indicating a greater abundance of non-contractile tissue in the quadriceps of older individuals. Interestingly, three of the four exercise training studies that assessed muscle EG were conducted in older populations (Table 1-3). While six weeks of RT did not appear sufficient to change EG of the VL or RF, improvements in EG of the RF have been documented following as little as 13 weeks of RT (199). All exercise training studies include some form of RT, thus further research assessing the influence of AE training on muscle EG is warranted.

Skeletal muscle EG not only provides an indication as to muscle composition, but it has also been shown to relate to skeletal muscle function. EG of all quadriceps muscles are negatively correlated to peak isometric KE torque in both young [VL: r = -0.50, VI: r = -0.64, VM: r = -0.47, RF: r = -0.63 - -0.52; (234, 236)] and old [VL: r = -0.55, VI: r = -0.48, VM: r = -0.64, RF: r = -0.46 - -0.51; (40, 78, 256, 261)]. In addition, EG has also been shown to negatively correlate to more translatable functional tests such as the sit-to-stand (9, 148), 6-min walk (9), and jump height (234). Therefore, in addition to measure of MT, PA, and FL, EG serves as an additional US-based metric to predict muscle function.

Table 2-3 (pg.42-44). Summary of Ultrasound-Based Echogenicity Measurements in the Quadriceps.

Author, Year (Reference)	Age (yrs)	Muscle	Training		Correlation to Muscle Function
			Exercise	Outcome	
Cadore, 2012 (40)	66 ± 5	RF	-	-	Isomet. KE: *r* = -0.51 Isokin. KE (60°/s): *r* = -0.48 Isokin. KE (180°/s): *r* = -0.64 Isokin. KE (360°/s): *r* = -0.67
Fukumoto, 2012 (78)	70 ± 6	Quad	-	-	Isomet. KE: *r* = -0.33
Strasser, 2013 (236)	Y: 24 ± 4 O: 68 ± 5	VL	-	-	Isomet. KE; Y: *r* =-0.500; O: *r* =-0.272 (ns)
		VI			Y: *r* =-0.640; O: *r* =-0.339 (ns)
		VM			Y: *r* =-0.470; O: *r* =-0.100 (ns)
		RF			Y: *r* =-0.630; O: *r* = -0.301 (ns)
Wantanabe, 2013 (256)	74 ± 6	Quad	-	-	Isomet. KE: *r* = -0.333
Wilhelm, 2014 (261)	66 ± 5	VL	-	-	1RM: *r* = -0.562 Isomet. KE: *r* = -0.551
		VI			1RM: *r* = -0.501 Isomet. KE: *r* = -0.484
		VM			1RM: *r* = -0.656 Isomet. KE: *r* = -0.640
		RF			1RM: *r* = -0.498 Isomet. KE: *r* = -0.460

Table 2-3 (pg.42-44). Summary of Ultrasound-Based Echogenicity Measurements in the Quadriceps.

Author, Year (Reference)	Age (yrs)	Muscle	Training		Correlation to Muscle Function
			Exercise	Outcome	
Akima, 2017 (9)	M: 65 – 82 F: 65 – 88	VL RF	-	-	Sit-to-stand; M: *r* = 0.518; F: *r* = 0.168 (ns) 6-min walk; M: *r* = -0.519; F: *r* = 0.009 (ns) Sit-to-stand; M: *r* = 0.398; F: *r* = 0.511 6-min walk; M: *r* = -0.36 (ns); F: *r* = -0.16 (ns)
Lopez, 2017 (148)	66 ± 5	Quad	-	-	30sec Sit-to-stand: *r* = -0.56
Stock, 2017 (234)	12 ± 1	VL RF	-	-	VL: Jump height: *r* = -0.436 Peak velocity: *r* = -0.406 Sprint speed: *r* = 0.436 Agility: *r* = 0.359 RF: Jump height: *r* = -0.331 Sprint speed: *r* = 0.480 Agility: *r* = 0.540 Isomet. KE: *r* = -0.524
Radaelli, 2013 (199)	60 – 74	RF	High volume (HV): 3 sets per RE or Low volume (LV): 1 set per RE 2d/week 13 weeks	HV: RF: ↓ 21% LV: RF: ↓ 12%	-

Table 2-3 (pg.42-44). Summary of Ultrasound-Based Echogenicity Measurements in the Quadriceps.

Author, Year (Reference)	Age (yrs)	Muscle	Training		Correlation to Muscle Function
			Exercise	Outcome	
Scanlon, 2014 (214)	71 ± 7	VL RF	2-4 sets of 8-12 reps @ 70-85% 1RM 2d/week 6 weeks	VL: ↔ RF: ↔	-
Wells, 2014 (258)	20 ± 1	VL	Whole body progressive RE 4d/week 15 weeks	↔	-
Yoshiko, 2017 (267)	78 ± 8	RF	Progressive rehab. program (RE & AE) 12 months	6mo.: ↓ 9% 12mo.: ↔	-

Quad, quadriceps; isomet, isometric; KE, knee extension; VI, vastus intermedius; VM, vastus medialis; isokin, isokinetic; Y, young; O, old; VL, vastus lateralis; RF, rectus femoris; RM, repetition maximum; LP, leg press; ns, not statistically significant; DL, dead lift; SQ, squat; FHS, front hack squat; SJ, sprint/jump training; RT, resistance training; ES, electrical stimulation; SR, standard rehabilitation; ECC, eccentric; IL, isoload training; IK, isokinetic training; HV, high volume; LV, low volume; RE, resistance exercise; KF, knee flexion; TON, isotonic training; ↔, $p > 0.05$; ↑ or ↓, $p < 0.05$

E. Reliability of Ultrasound-Derived Muscle Architecture Measurements

Accuracy in skeletal muscle US is highly dependent on operator ability. As a testament to this point, US specialists such as diagnostic medical sonographers have become more prevalent in various health professions. Skeletal muscle US is commonly utilized in chronic studies to assess changes in skeletal muscle characteristics that reflect changes in muscle function. Therefore, establishing the test-retest reliability of skeletal muscle US is imperative for the ability to detect changes over serial measurements.

In the measurement of MT, common sources of variability include probe orientation relative to the skin and excessive force of the probe on the skin, causing deformations in the underlying tissues. While most studies restrict serial measurements to being made by the same sonographer, the inter-rate reliability of MT measures of the quadriceps appears to be good (ICCs: 0.73 – 0.99) (242). Perhaps more important, the test-retest reliability of US-obtained MT ranges from ICCs of 0.77 to ICCS of 0.90 (Table 2-4), and ICCs appear to be similar for measurements in all quadriceps muscles (25, 66, 236). In addition, test-retest reliability of MT measures appears to be similar regardless of if repeated measures are performed on the same day (4, 25, 164, 241, 242) or on different days (7, 13, 20, 66, 236). Measures of MT are predominantly assessed with subjects either standing (4) or supine (268). Of the few studies that have assessed the reliability of MT measurements while standing (4, 241), test-retest reliability appears to be similar to when MT measures are collected supine (Table 2-4). Lastly, the test-retest reliability of MT measures appears to be slightly lower in older individuals, when the reliability within young and old are directly compared (7, 236). This suggests that the ability to detect changes in MT of older adults may be impeded due to increased day-to-day variability. Overall, US appears to be a reliable means to assess MT of the quadriceps across various approaches (supine vs. standing) and ages (young vs. old).

Ultrasound measures of muscle architecture, including and PA and FL, are largely susceptible to sources of variability associated with US given relatively fine image detail (Fig. 2-3) required for such analyses. In addition, fascicles often extend past the visible field of view of an US image, limited by the width of the US transducer. This results in the extrapolation of FL based on

measurements of the MT and PA. Across all quadriceps muscles, the test-retest reliability of US measures of PA and FL range from 0.436 – 0.960 and 0.758 – 0.980, respectively (Table 2-4). While the reliability of FL measurements appear to be similar across all quadriceps (13, 25, 66), PA measurements in the VM appear less reliable compared to measures in the remaining quadriceps (236), which are similarly reliable (13, 25, 66). Concerning the two predominant approaches to skeletal muscle US, imaging when subjects stand versus lay supine, the reliability of PA and FL measurements have not been assessed when subjects were imaged standing. Studies are warranted to directly assess the influence of subject posture during imaging on the reliability of PA and FL measures of the quadriceps. Additionally, only one study (236) has examined the influence of age on the reliability of PA measures in the quadriceps. This study demonstrated lower reliability in the PA measurements of the VI and VM in old compared to young (236). To date, no studies have examined the reliability of FL measures in the quadriceps of older individuals. Collectively, the literature is limited concerning the reliability of PA and FL measurements collected in different subject postures and age groups.

Table 2-4 (pg.47-51). Summary of ultrasound-based quadriceps muscle architecture measurements with reported reliability

Author, Year (Reference)	Age (yrs)	Muscle	Subject Position	Type of Reliability	Reliability
			Muscle Thickness		
Abe, 1994 (4)	18 – 50	Quad	Stand	Test-retest	Mean Diff = -0.71 – 0.19 mm ICC = 0.97-0.99
Blazevich, 2006 (25)	M: 20 ± 3 F: 21 ± 3	VL, VI, VM, RF	Supine	Test-retest	Mean Diff = 0.74 – 0.97 mm ICC = 0.882 – 0.970
Moreau, 2009 (164)	12 ± 4	VL RF	Supine	Inter-rater	ICC = 0.99 ICC = 0.98
Thoirs, 2009 (241)	22 + 50	Quad	Supine Stand	Test-retest	ICC = 0.8 – 0.95 ICC = 0.79 – 0.94
Strasser, 2013 (236)	Y: 24 ± 4 O: 68 ± 5	VL VI VM RF	Supine	Test-retest	Y: ICC = 0.957 O: ICC = 0.852 Y: ICC = 0.978 O: ICC = 0.928 Y: ICC = 0.979 O: ICC = 0.949 Y: ICC = 0.972 O: ICC = 0.876
Agyapong-Badu, 2014 (7)	Y: 18 – 35 O: 65 – 90	Quad	Supine	Test-retest	Y: ICC = 0.78 – 0.95 MDC = 5.5 mm O: ICC = 0.77 – 0.94 MDC = 5.9 mm
Ando, 2014 (13)	22 ± 1	VL, VI, RF	Supine	Test-retest	ICC = 0.966

Table 2-4 (pg.47-51). Summary of ultrasound-based quadriceps muscle architecture measurements with reported reliability

Author, Year (Reference)	Age (yrs)	Muscle	Subject Position	Type of Reliability	Reliability
Tillquist, 2014 (242)	31 ± 8	Quad	Supine	Test-retest	ICC = 0.940 – 0.990 Mean Diff. = 3.30 mm
				Inter-rater	ICC = 0.730 – 0.990 Mean Diff. = -2.80 mm
Baroni, 2013 (20)	24 ± 3	VL RF	Supine	Test-retest	VL: ICC = 0.910 RF: ICC = 0.960
Ema, 2013 (66)	27 ± 2	VL (distal) VL (proximal) VI-Lateral (distal) VI-Lateral (proximal) VI-Medial (distal) VI-Medial (proximal) VM (distal) VM (proximal) RF (distal) RF (proximal)	Supine	Test-retest	VL (distal): ICC = 0.991 VL (proximal): ICC = 0.976 VI-Lateral (distal): ICC = 0.978 VI-Lateral (proximal): ICC = 0.979 VI-Medial (distal): ICC = 0.955 VI-Medial (proximal): ICC = 0.951 VM (proximal): ICC = 0.861 RF (distal): ICC = 0.984 RF (proximal): ICC = 0.985

Table 2-4 (pg.47-51). Summary of ultrasound-based quadriceps muscle architecture measurements with reported reliability

Author, Year (Reference)	Age (yrs)	Muscle	Subject Position	Type of Reliability	Reliability
Pennation Angle & Fascicle Length					
Blazevich, 2006 (25)	M: 20 ± 3 F: 21 ± 3	VL, VI, VM, RF	Supine	Test-retest	PA: Mean Diff. = 0.24 – 1.22° ICC = 0.899 – 0.991 FL: Mean Diff. = 10.2 – 19.4 mm ICC = 0.758 – 0.863
Moreau, 2009 (164)	12 ± 4	VL	Supine	Inter-rater	PA: ICC = 0.96 FL: ICC = 0.88
		RF			PA: ICC = 0.95 FL: ICC = 0.95
Strasser, 2013 (236)	Y: 24 ± 4 O: 68 ± 5	VL	Supine	Test-retest	Y: ICC = 0.530 O: ICC = 0.687
		VI			Y: ICC = 0.783 O: ICC = 0.741
		VM			Y: ICC = 0.436 O: ICC = 0.189
Ando, 2014 (13)	22 ± 1	VL, VI, RF	Supine	Test-retest	PA: ICC = 0.949 FL: ICC = 0.836
Baroni, 2013 (20)	24 ± 3	VL	Supine	Test-retest	PA: VL: ICC = 0.900 RF: ICC = 0.950
		RF			FL: VL: ICC = 0.910 RF: ICC = 0.950

Table 2-4 (pg.47-51). Summary of ultrasound-based quadriceps muscle architecture measurements with reported reliability

Author, Year (Reference)	Age (yrs)	Muscle	Subject Position	Type of Reliability	Reliability
Ema, 2013 (66)	27 ± 2	VL (distal) VL (proximal) VI-Lateral (distal) VI-Lateral (proximal) VI-Medial (distal) VI-Medial (proximal) VM (distal) VM (proximal) RF (distal) RF (proximal)	Supine	Test-retest	PA: VL (distal): ICC = 0.931 VL (proximal): ICC = 0.885 VI-Lateral (distal): ICC = 0.919 VI-Lateral (proximal): ICC = 0.943 VI-Medial (distal): ICC = 0.948 VI-Medial (proximal): ICC = 0.795 VM (distal): ICC = 0.940 VM (proximal): ICC = 0.945 RF (distal): ICC = 0.921 RF (proximal): ICC = 0.921 FL: VL (distal): ICC = 0.966 VL (proximal): ICC = 0.838 VM (proximal): ICC = 0.902 RF (proximal): ICC = 0.980

Table 2-4 (pg.47-51). Summary of ultrasound-based quadriceps muscle architecture measurements with reported reliability

Author, Year (Reference)	Age (yrs)	Muscle	Subject Position	Type of Reliability	Reliability
			Echogenicity		
Strasser, 2013 (236)	Y: 24 ± 4 O: 68 ± 5	VL	Supine	Test-retest	Y: ICC = 0.623 O: ICC = 0.297
		VI			Y: ICC = 0.650 O: ICC = 0.313
		VM			Y: ICC = 0.624 O: ICC = 0.209
		RF			Y: ICC = 0.571 O: ICC = 0.307
Young, 2015 (269)	20 – 64	RF	Supine	Test-retest	ICC = 0.91 CV = 3.3%
Varanoske, 2017 (252)	20 ± 2	VL	Supine	Test-retest	ICC = 0.718 SEM = 3.117 AU MD = 8.641 AU CV = 4.6%

MDC: minimal detectable change; Quad, quadriceps; isomet, isometric; KE, knee extension; VI, vastus intermedius; VM, vastus medialis; isokin, isokinetic; Y, young; O, old; VL, vastus lateralis; RF, rectus femoris; RM, repetition maximum; LP, leg press; ns, not statistically significant; DL, dead lift; SQ, squat; FHS, front hack squat; SJ, sprint/jump training; RT, resistance training; ES, electrical stimulation; SR, standard rehabilitation; ECC, eccentric; IL, isoload training; IK, isokinetic training; HV, high volume; LV, low volume; RE, resistance exercise; KF, knee flexion; TON, isotonic training.

IV. Doxorubicin and Skeletal Muscle

A. Overview of Doxorubicin

Anthracycline class chemotherapeutics, which were derived from *Streptomyces* bacteria, were originally discovered in the 1960s (34). Anthracyclines have been utilized clinically for over 50 years to aid in the treatment of many types of cancers, including leukemia, lymphoma, breast, and prostate (85). Danorubicin was the first anthracycline compound to be fully characterized and used in the treatment of leukemias (85). Soon thereafter, Doxorubicin (DOX) was developed (16) with a broader spectrum of applications and was considered one of the most effective chemotherapeutics (257). The anti-tumor effects of DOX vary, but include the inhibition of DNA replication by intercalating into DNA helixes and impairing topoisomerase II activity, and the generation of free radicals leading to DNA damage (211). Specifically, DOX enters cells through passive diffusion (224) whereupon it can displace nuclear proteins, bind to DNA, and result in conformational changes of the DNA structure (198). DOX also possesses a strong affinity for cardiolipin inside mitochondrial membranes, and when bound produces high amounts of reactive oxygen species (ROS) (233). Collectively, these processes culminate into the primary task of DOX, which is to seize tumor cell growth and replication.

While DOX, and anthracyclines as a whole, are widely regarded for their antitumor effects, their clinical utility is limited due to their negative side-effects in noncancerous tissues (94). Early reports of severe patient fatigue following DOX treatment (183) led to the revelation of DOX-induced cardiotoxicitiy [see reviews (238, 250)]. In fact, a recent review concluded that 47% of studies assessing patient fatigue during and following anthracycline-based chemotherapy report fatigue that is “disabling and effecting physical capabilities of the patient” (94). While DOX has been widely shown to impact other off-target tissues (44), this review is focused on the impact of DOX on skeletal muscle.

B. Impact of Doxorubicin on Skeletal Muscle Function

Individuals diagnosed with cancer experience general impairments in skeletal muscle function as a result of the disease (244). Cancer treatments, such as chemotherapy, are largely

believed to exacerbate functional impairments in the skeletal muscle of cancer patients. While the cardiotoxic effects of DOX have been known for some time (238, 250), the negative effects of DOX on peripheral tissues such as skeletal muscle has gained more recent attention. In particular, maximal oxygen consumption (VO_2peak) of breast cancer patients is reduced following DOX treatment despite no signs of impaired cardiac function (217). This suggests that DOX may result in direct impairments in skeletal muscle function.

Preclinical models within the last decade demonstrate the negative effects of DOX on skeletal muscle function (Table 2-5). The systemic administration of DOX, through intraperitoneal injection, has been shown to induce contractile dysfunction in muscles of varying fiber type profiles, ranging from the predominantly slow-twitch soleus (33, 91, 111, 122) to the mainly fast-twitch extensor digitorum longus (EDL) (33, 90, 111, 122, 251), and even the diaphragm of mixed fiber type (92, 161). Thus, the skeletal muscle fiber type profile does not appear to impact the myotoxic effects of DOX on contractile function.

A majority of the studies administer DOX through a single-bolus injection (33, 90-92, 111, 122, 161). Administration of DOX in doses as low as 10 mg/kg and 12.5 mg/kg appear to increase fatigue and impair maximal twitch force in the soleus, but not the EDL (122). Therefore, single-bolus injections have commonly been comprised of doses of at least 15 mg/kg. Interestingly, while DOX can accumulate in skeletal muscle for up to 24 hours following a dose of 15 mg/kg, functional impairments persist for up to 5 days following the injection (111). This suggests that DOX may induce structural damage to the contractile units within skeletal muscle that continue well after the tissue has been cleared of the drug.

Nissinen *et al.* (186) administered DOX in smaller (6 mg/kg), sequential doses (4 doses every 2 weeks) over a longer period of time, similar to its use clinically. While this study did not assess the contractile function of a single muscle, it did demonstrate that a chronic, clinically-relevant DOX regimen impairs running performance (186). However, whether the decrement in whole body functionality is caused by the most proximal dose to the exercise test or the cumulative effects of the DOX regimen is unknown. Future research is warranted to investigate the impact of chronic, clinically-relevant, low-dose DOX regimens on skeletal muscle function.

Several studies have attempted to mitigate the DOX-induced impairments in skeletal muscle with a variety of countermeasures (Table 2-4). Many of the myotoxic effects of DOX are thought to stem from the generation of ROS (57). Works from Gilliam *et al.* postulated that DOX-induced ROS generation are dependent on tumor necrosis factor (TNF) (90, 92). The authors have employed both a TNF receptor knockout mouse model (90) and an anti-TNF drug (Etanercept) (92) in preclinical models of DOX and both countermeasures have resulted in preserved specific force in the EDL and diaphragm, respectively. In addition, several studies have attempted to combat DOX-induced ROS through the administration of a targeted mitochondrial antioxidant (SS31) (161) or overexpression of the mitochondrial antioxidant, catalase (91). Both interventions were shown to be effective in mitigating DOX-induced impairments in skeletal muscle function (91, 161). These findings suggest that DOX-induced impairments in skeletal muscle function are ROS-mediated, and that ROS generation is a viable therapeutic strategy to preserve muscle function in the face of DOX. Given its resounding benefits for muscle function and robust capacity to stimulate antioxidants (217), exercise training represents a promising intervention to preserve muscle function following DOX treatment. To date, only one study has investigated the impact of exercise training on DOX-induced muscle dysfunction, in which rats completed resistance or aerobic training for 10 weeks prior to a single bolus of DOX (33). Aerobic exercise training reduced fatigue associated with DOX in the soleus and EDL, while resistance exercise training improved maximal twitch force in the soleus (33). Overall, exercise appears to be a viable strategy to preserve several aspects of muscle function following DOX treatment. However, future studies are needed to translate these findings into human cancer patients following DOX chemotherapy.

Table 2-5 (pg. 55-57). Summary of the Impact of Anthracyclines on Skeletal Muscle Function.

Author, Year (Reference)	Species	Drug Regimen	Muscle	Function	Intervention	
					Countermeasure	Outcome
Gilliam, 2009 (90)	Mouse	20 mg/kg; Single dose	EDL	↓ Abs. Force ↓ Sp. Force ↑ Fatigue	TNFR1 knockout	↑ Sp. Force ↑ Fatigue
van Norren, 2009 (251)	Mouse	50, 100, 175 µM; Incubation	EDL	50 µM: ↑ Relax. Time 100 µM: ↓ Max Twitch Force, ↑ Relax. Time 175 µM: ↓ Max Twitch Force, ↑ Relax. Time	-	-
Gilliam, 2011 (92)	Mouse	20 mg/kg; Single dose	Diaphragm	↓ Sp. Force	Etanercept (anti-TNF drug)	↑ Sp. Force
Hydock, 2011 (122)	Rat	DOX1: 10mg/kg DOX2: 12.5 mg/kg DOX3: 15mg/kg Single dose	SOL; EDL	SOL DOX1: ↑ Fatigue DOX2: ↓ Max Twitch Force, ↑ Fatigue DOX3: ↓ Max Twitch Force, ↑ Fatigue EDL DOX1: ↔ DOX2: ↔ DOX3: ↓ Max Twitch Force	-	-

Table 2-5 (pg. 55-57). Summary of the Impact of Anthracyclines on Skeletal Muscle Function.

Author, Year (Reference)	Species	Drug Regimen	Muscle	Function	Intervention	
					Countermeasure	Outcome
Hayward, 2013 (111)	Rat	15 mg/kg; Single dose	SOL; EDL	SOL 1 day Post: ↔ 3-day Post: ↓ Max Twitch Force, ↓ Rate force dev. 5-day Post: ↓ Max Twitch Force, ↑ Rate force dec. EDL 1 day Post: ↓ Max Twitch Force, ↓ Rate force dev., ↑ Rate force dec. 3-day Post: ↓ Max Twitch Force, ↓ Rate force dev., ↑ Rate force dec. 5-day Post: ↓ Max Twitch Force, ↓ Rate force dev., ↑ Rate force dec.	-	-
Min, 2015 (161)	Rat	20 mg/kg; Single dose	Diaphragm	↓ Sp. Force	SS31 (Mito.-targeted anti-oxidant); SJA (Calpain-inhibitor)	SS31: ↑ Sp. Force SJA: ↔ Sp. Force
Gilliam, 2016 (91)	Mouse	20 mg/kg; Single dose	SOL	↓ Max Twitch Force	Mito. Catalase Overexpression	↑ Max Twitch Force
Nissinen, 2016 (186)	Mouse	24 mg/kg; 4 x 6 mg/kg doses; 2 wks	SOL; GN; TA	↓ Running performance	sACVR2b-Fc (TGFβ activinin binding inhibitor)	↔ Running performance

Table 2-5 (pg. 55-57). Summary of the Impact of Anthracyclines on Skeletal Muscle Function.

Author, Year (Reference)	Species	Drug Regimen	Muscle	Function	Intervention	
					Countermeasure	Outcome
Bredahl, 2016 (33)	Rat	15 mg/kg; Single dose	SOL; EDL	SOL ↓ Max Twitch Force, ↓ Rate force dev., ↑ Rate force dec. EDL ↓ Max Twitch Force	Run: 30-60min/d, 5d/wk, 10wks prior to DOX RT: elevated food/water, 10wks prior to DOX	Run: ↓ fatigue (SOL, EDL) RT: ↑ Max Twitch Force (SOL)

EDL, extensor digitorum longus; Abs, absolute; TNFR1, tumor necrosis factor receptor 1; Relax, relaxation; TNF, tumor necrosis factor; DOX, doxorubicin; SOL, soleus; Sp, specific; Dev, development; Dec, decline; Mito, mitochondria; GN, gastrocnemius; TA, tibialis anterior; sACVR2b, soluble ligand binding domain of activinin receptor type IIb-Fc region; TGFβ, transforming growth factor beta; Run, run training; RT, resistance training; ↔, $p > 0.05$; ↑ or ↓, $p < 0.05$.

C. Impact of Doxorubicin on Skeletal Muscle Size

The risk of toxicity from chemotherapy treatments may be increased in cancer patients with reduced skeletal muscle mass (15), which is a vital concern considering the potentially comprised musculature due to cancer cachexia (243). Therefore, preserving skeletal muscle mass throughout chemotherapy is critical to reducing the risk of drug-induced dysfunction. Unfortunately, DOX has a direct, negative impact on skeletal muscle mass. When DOX is directly injected into skeletal muscle, as is done during myectomies to treat spasm, there is an abrupt (2 days) loss of muscle fibers (184). In addition, when C2C12 myotubes are incubated in physiologically-relevant concentrations of DOX (0.20 μM), myotube width is decreased (93). Therefore, DOX appears to diminish muscle cell size and number when directly administered.

Preclinical animal models have provided extensive evidence of the impact of systemic DOX administration on skeletal muscle size (Table 2-6). Whole muscle weights of the soleus, EDL, and gastrocnemius have been shown to be reduced following a single injection of DOX ranging from 4 mg/kg to 20 mg/kg (32, 90, 91, 223). Concerning potential fiber type-specific differences in DOX-induced muscle wasting, single-bolus administrations of DOX appear to reduce the cross-sectional area (CSA) of MHCI and MHCIIa fibers in the soleus (161), MHCI, MHCIIa, MHCIIb/x fibers in the plantaris (161), MHCIIb fibers in the tibialis anterior (32), and MHCI, MHCIIa, MHCIIb/x fibers in the diaphragm (161). Following a large, single-bolus administration of DOX, all muscle fiber types appear susceptible to DOX myotoxicity.

When DOX is administered in a clinically-relevant approach over smaller, sequential doses, whole muscle weights of the soleus (186), gastrocnemius (102, 186), and tibialis anterior (186) appear to be reduced. Chronic DOX regimens also appear to reduce CSA of MHCI and MHCIIa fibers in the soleus (58), MHCI, MHCIIb, MHCIIx fibers in the gastrocnemius (102), and all fiber types in the plantaris (186). Whether DOX-induced muscle wasting is a result of the last dose or of the cumulative dosage requires further investigation. Collectively, DOX, whether administered through a large, single-bolus or smaller, sequential doses, appears capable of reducing whole muscle weight and muscle fiber size in various skeletal muscles. While the literature is limited,

chemotherapy regimens containing DOX also appear to result in reduced CSA of MHCI and MHCIIa fibers in the soleus (159) and gastrocnemius (27) of cancer patients.

While the cellular mechanisms through which DOX may exert these deleterious effects on skeletal muscle remain to be fully understood, studies have demonstrated DOX-induced increases in the formation of ROS (91), inflammatory cytokines (90, 92), and proteolytic markers (130, 227) that may all contribute to skeletal muscle wasting. In addition, chronic DOX regimens have demonstrated that DOX may reduce protein synthesis (186), possibly through impaired mammalian target of rapamycin (mTOR) signaling (58), which would inevitably lead to muscle wasting. An interesting possibility that has been paid relatively little attention is the impact of DOX on skeletal muscle stem cells, termed satellite cells, that are largely important for maintaining skeletal muscle mass and regeneration (135). Exposure to DOX *in vitro* has been shown to interfere with myogenic processes associated with satellite cells, (137, 138), and to impair progression of myoblasts through the myogenic lineage (137, 179, 197). However, further research is needed to discern the impact of systemic DOX administration on satellite cells in relation to skeletal muscle mass.

Several studies have attempted to mitigate the DOX-induced impairments in skeletal muscle with a variety of countermeasures (Table 2-5). Interventions targeting the DOX-induced generation of ROS appear to be largely successful in preserving both whole muscle weight and muscle fiber CSA following DOX (90, 91, 93, 161, 223). Additionally, when muscle protein synthesis was sustained with a TGFβ activinin binding inhibitor (186), whole muscle weight of the soleus, gastrocnemius, and tibialis anterior, along with fiber CSA of the tibialis anterior were preserved following chronic DOX administration. The link between ROS and protein synthesis-mediated muscle wasting with DOX was bridged by Dickinson *et al.* who showed chronic DOX administration to increase the expression of the mTOR inhibitor, REDD1, which is responsive to oxidative stress (58). The same study also showed chronic high intensity treadmill running to limit REDD1 expression, preserving mTOR signaling and CSA of MHCI and MHCIIa fibers in the soleus (58). Recently, Mijwel *et al.* demonstrated that 16 weeks of aerobic training or resistance training, both supplemented with high-intensity interval training, was successful in preserving MHCI and MHCI and MHCIIa fiber CSA, respectively during DOX treatment (159). Future studies investigating the

precise dose of exercise (mode, intensity) and time of exercise relative to DOX treatment (before, during, after) are warranted.

Table 2-6 (pg. 61-63). Summary of the Impact of Anthracyclines on Skeletal Muscle Size.

Author, Year (Reference)	Species	Drug Regimen	Muscle	Size	Intervention	
					Countermeasure	Outcome
Bonifati, 2000 (27)	Human	1.4 mg/kg; Schedule unknown	GN	↓ MHCI diameter (2/5 patients) ↓ MHCII diameter (2/5 patients)	-	-
Gilliam, 2009 (90)	Mouse	20 mg/kg; Single dose	EDL	↓ EDL weight	TNFR1 knockout	↔ EDL weight
Gilliam, 2011 (93)	C2C12	0.20 µM; Incubation	Myotubes	↓ Myotube width	SS31 (Mito.-targeted anti-oxidant)	↑ Myotube width
Braun, 2014 (32)	Mouse	4 mg/kg; Single dose	GN; TA	GN: ↓ GN weight TA: ↓ MHCIIb fiber CSA	GR knockout	GN: ↑ GN weight TA: ↑ MHCIIb fiber CSA
Gouspillou, 2015 (102)	Mouse	40 mg/kg total; 4 x 10 mg/kg doses, 1d/3wks	GN	↓ GN weight ↓ MHCI, MHCIIx, MHCIIb CSA	-	-

Table 2-6 (pg. 61-63). Summary of the Impact of Anthracyclines on Skeletal Muscle Size.

Author, Year (Reference)	Species	Drug Regimen	Muscle	Size	Intervention	
					Countermeasure	Outcome
Min, 2015 (161)	Rat	20 mg/kg; Single dose	Diaphragm; SOL, PL	Diaphragm: ↓ MHCI, MHCIIa, MHCIIb/x CSA SOL: ↓ MHCI, MHCIIa CSA PL: ↓ MHCI, MHCIIa, MHCIIb/x CSA	SS31 (Mito.-targeted anti-oxidant); SJA (Calpain-inhibitor)	SS31: ↑ MHCI CSA (Dia., SOL); ↑ MHCIIa CSA (Dia., SOL); ↑ MHCIIb CSA (PL) SJA: ↑ MHCI CSA (Dia., SOL); ↑ MHCIIa CSA (SOL PL)
Gilliam, 2016 (91)	Mouse	20 mg/kg; Single dose	SOL	↓ SOL weight	Mito. Catalase Overexpression	↔ SOL weight
Nissinen, 2016 (186)	Mouse	24 mg/kg; 4 x 6 mg/kg doses per 2 wks	SOL, GN; TA	↔ SOL weight; ↓ GN weight; ↓ TA weight; ↓ TA fiber CSA	sACVR2b-Fc (TGFβ activinin binding inhibitor)	↑ SOL weight; ↑ GN weight; ↑ TA weight; ↑ TA fiber CSA

Table 2-6 (pg. 61-63). Summary of the Impact of Anthracyclines on Skeletal Muscle Size.

Author, Year (Reference)	Species	Drug Regimen	Muscle	Size	Intervention	
					Countermeasure	Outcome
Sin, 2016 (223)	Mouse (young & old)	18 mg/kg; Single dose	GN	Young: ↓ GN weight Old: ↓ GN weight	Resveratrol	Young: ↑ GN weight Old: ↑ GN weight
Dickinson, 2017 (58)	Rat	12 mg/kg total; 3 x 4 mg/kg doses per 2 wks	SOL	↓ MHCI fiber CSA; ↓ MHCIIa fiber CSA	Run: 30-40min/d, 5d/wk, 1wk prior to and during DOX	↑ MHCI fiber CSA; ↑ MHCIIa fiber CSA
Mijwel, 2018 (159)	Human	Anthracycline or Anthracycline + taxane therapy; Dosing schedule unknown	VL	↓ MHCI fiber CSA; ↓ MHCIIa fiber CSA	RT+HIIT: 70-80% 1RM + 3 x 3min intervals on cycle ergometer, 2d/wk, 16wks AT+HIIT: 20min cycling or elliptical or rower + 3 x 3min intervals on cycle ergometer, 2d/wk, 16wks	RT+HIIT: ↑ MHCI fiber CSA; ↑ MHCIIa fiber CSA AT+HIIT: ↑ MHCI fiber CSA

GN, gastrocnemius; MHC, myosin heavy chain; EDL, extensor digitorum longus; TNFR1, tumor necrosis factor receptor 1; TA, tibialis anterior; GR, Glucocorticoid receptor; PL, plantaris; Mito, mitochondria; sACVR2b, soluble ligand binding domain of activinin receptor type IIb-Fc region; TGFβ, transforming growth factor beta; Run, run training; DOX, doxorubicin; RT, resistance training; HIIT, high-intensity interval training; AT, aerobic training; ↔, $p > 0.05$; ↑ or ↓, $p < 0.05$.

D. Impact of Doxorubicin in Human Cancer Patients

While the most prominent side effect of DOX-based chemotherapy in cancer patients is the dose-dependent cardiotoxicity [see reviews (238, 250)], weakness and fatigue are commonly reported in patients following DOX treatment (94). In particular, 47% of patients receiving DOX report sever fatigue (94). In breast cancer patients, 4 doses of DOX resulted in impaired 12 min walk test and increased perceived ratings of fatigue (216). Perhaps more concerning are reports of muscle weakness and fatigue persisting 1-5 years following DOX treatment (65, 248, 253). More quantitative studies have shown reduced lower limb strength (159) and grip strength (235) from pre- to post-DOX treatment. Collectively, DOX treatment is associated with immediate reductions in muscular strength, that persist several years following treatment as perceived weakness and fatigue.

Less is known regarding the impact of DOX treatment on skeletal muscle mass in humans, likely due to the inability to isolate the impact of DOX amongst other consequences of cancer such as cachexia, malnutrition, and reduced physical activity. Several studies have documented reductions in MHCI and MHCIIa fiber CSA following the perfusion of DOX to a localized limb (27, 159) or the systemic administration of DOX (27, 159). Each of these investigations examined lower limb muscles including the gastrocnemius (27, 159) and vastus lateralis (27, 159), thus future research investigating the impact of DOX on muscle mass of other vital muscles such as the diaphragm or erector spinae are warranted.

Exercise training has garnered attention as a potential therapy to alleviate the deleterious effects of DOX in skeletal muscle. The benefits of exercise to attenuate DOX-induced toxicity is strongly supported by the array of preclinical studies discussed above. When aerobic or resistance exercise training was performed during DOX treatment, CSA of MHCI and both MHCI and MHCIIa fibers was preserved, respectively (159). Even if cancer patients are unable to exercise during treatment due to increased fatigue, it appears that cancer survivors are still able to experience the benefits of exercise training following chemotherapy (48). In addition to the benefits of exercise training in skeletal muscle following DOX treatment, a wealth of cognitive and behavioral benefits from exercise training during chemotherapy have been reviewed recently (81). More research is

warranted to identify the optimal type and amount of exercise and to define the best time for exercise training relative to DOX treatment.

V. Divergent Exercise: High-Intensity Interval Exercise vs. Moderate-Intensity Exercise

A. General Overview

Skeletal muscle is a highly plastic tissue that is capable of adapting to changing functional and energetic demands from a variety of stimuli. Exercise represents a unique stimulus to skeletal muscle and is known to facilitate changes to the contractile, structural and metabolic properties within the muscle fibers, as well as to the extracellular environment (e.g., capillaries, connective tissue). The specific adaptive responses within skeletal muscle are dependent, in part, on the type of exercise performed. Aerobic and resistance exercise represent opposing ends of the exercise continuum and thus a majority of the literature investigating divergent exercise responses have focused on these two modes. Specifically, it is well documented that resistance exercise generally results in morphological alterations which confer increases in muscle size and strength (19, 108), whereas aerobic exercise improves oxidative capacity and fatigue resistance through the accumulation of mitochondrial proteins (70, 165). The distinct adaptations to each exercise are defined by the cumulative effect of the acute molecular responses to each exercise bout. The timing of the acute post-exercise mRNA bursts that drive changes in the functional protein pool typically peaks 4 to 8 hrs following exercise, with some mRNA responsive up to 24 hrs later (264). Collectively, understanding the unique adaptation of skeletal muscle to specific forms of exercise, and the underlying molecular responses, is important in utilizing targeted exercise strategies as a means to improve skeletal muscle. The focus the following sections are to highlight acute responses and chronic adaptations of skeletal muscle to different forms of aerobic exercise, particularly, moderate intensity continuous exercise (MOD) and high intensity interval exercise (HIIE).

B. Acute Skeletal Muscle Responses

The acute molecular responses to traditional, moderate-intensity aerobic exercise have been well documented (46, 98, 116, 117). In particular, much attention has been given to the acute molecular responses governing mitochondrial biogenesis, a hallmark adaptation to aerobic exercise. The high ATP turnover associated with aerobic exercise is associated with the activation of two key signaling pathways that are understood to be central to mitochondrial biogenesis (64). Together, AMP-activated protein kinase (AMPK) and p38 mitogen-activated protein kinase (MAPK) phosphorylate and activate peroxisome proliferator activated receptor γ coactivator-1α (PGC-1α) (46). In turn, PGC-1α regulates the activity of various transcription factors associated with the transcription of the nuclear and mitochondrial genome, eventually leading to increased mitochondrial content and functional capacity (46). Through perturbations in cellular oxygenation, aerobic exercise has also been shown to elicit acute increases in markers associated with capillarization and oxygenation (64). Acute angiogenic markers upregulated by aerobic exercise include hypoxia-inducible factor 1α (HIF-1α) and vascular endothelial growth factor a (VEGFA), which together with PGC-1α, induce the transcription of genes associated with erythropoiesis and angiogenesis (64, 239). In addition, aerobic exercise has been shown to increase the transcription of a multitude of metabolic genes associated with the mobilization and metabolism of carbohydrate and fat (46, 264). Recently, we have highlighted the acute increase in the mRNA expression of estrogen-related γ (ERRγ; *ESRRG)* following aerobic exercise (59). Interestingly, *ESRRG* is associated with phenotypical changes typical of aerobic exercise training, including: improved mitochondrial function, greater oxidative capacity, increased vascularization, a reduced respiratory exchange ratio, and a shift from MHC II to MHC I fibers (82, 146, 177, 201). Therefore, acute increase in *ESRRG* may represent an important early adaptive response to aerobic exercise.

More recent efforts have aimed to achieve similar adaptations to traditional, moderate-intensity aerobic exercise (MOD) with a lower time commitment. Low-volume, high-intensity interval exercise (HIIE) has garnered recent attention as an effective alternative to higher-volume, lower-intensity aerobic exercise. Typically characterized by intermittent efforts of intense exercise, interspersed with periods of recovery, multiple variations of HIIE exist (Table 2-7). Interestingly,

common acute molecular responses in skeletal muscle to HIIE largely mimic those following MOD. A majority of the literature regarding the acute responses to HIIE have focused on markers associated with mitochondrial biogenesis. HIIE has commonly been observed to increase the activation of AMPK and MAPK (77, 87, 144, 158). In addition, the mRNA and protein abundances of PGC-1α, citrate synthase (CS), and cytochrome c oxidase (COX) appear to be acutely upregulated following HIIE (87, 144, 158). Aside from acute markers of mitochondrial adaptation, HIIE has also been shown to influence the activation of pathways associated with skeletal muscle insulin signaling (188) and angiogenesis (115, 239). While HIIE has been shown to acutely activate SCs (180), a response commonly associated with resistance exercise (229), signaling proteins commonly associated with myocellular growth do not appear to be activated (87), ate least in the initial 3 hrs following exercise. Collectively, HIIE appears to elicit similar acute skeletal muscle responses to MOD. However, all but one study (180) were conducted in young individuals, thus investigations of the acute molecular responses of skeletal muscle to HIIE in elderly and clinical populations are warranted.

Few studies have directly compared the acute skeletal muscle responses between HIIE and MOD (Table 2-7). Several studies have demonstrated greater activation of AMPK following HIIE versus MOD (103, 134). Granata *et al.* also reported that nuclear levels of PGC-1α protein were only increased following HIIE, whereas no increase was observed in response to MOD (103). Indeed, activation of PGC-1α appears to be intensity-dependent (63) which may suggest superior mitochondrial adaptations following chronic HIIE, compared to MOD. When examined in a fiber type-specific manner, activation of AMPK and MAPK in MHCII fibers was greater following HIIE compared to MOD (134), which may suggest intensity-dependent differences in fiber recruitment patterns between HIIE and MOD (113). Somewhat related is the finding of increased SC activation in older adults who performed HIIE, but not MOD (180). While Nederveen *et al.* (180) did not assess fiber type-specific SC activation, the differential response in SC activation may also be due to greater recruitment of MHCII fibers (113). HIIE also appears to result in a greater stimulation of insulin signaling, as indicated by greater increase in insulin receptor substrate 1 (IRS1) phosphorylation and larger reduction in the phosphorylation of Akt substrate of 160kDa (AS160)

(188). While HIIE appears to augment the acute responses of several molecular process, HIIE may blunt acute angiogenic processes. Hoier *et al.* (115) demonstrated lower interstitial VEGF protein and endothelial cell proliferation following HIIE compared to MOD which may suggest that there is an upper limit of exercise intensity to achieve maximal angiogenesis (95). Overall, studies directly comparing the acute skeletal muscle responses between HIIE and MOD suggest that HIIE may induce superior initial adaptations, primarily related to mitochondrial adaptation.

Table 2-7 (pg. 69-70). Summary of Acute Skeletal Muscle Response: HIIE vs MOD

Author, Year (Reference)	Participants	Muscle Biopsy	Exercise		Outcome
			Mode	Protocol	
Bartlett, 2012 (21)	Rec. Active; Young; 10m	VL; Rest, immed. post, 3h post	Run	MOD: 50min @ 70% VO_{2peak} HIIE: 6 x 3min @ 90% VO_{2peak} w/ 3min rest	BOTH: ↑ $AMPK^{Thr172}$, ↑ $p38MAPK^{Thr180/Tyr182}$ (immed. post); ↑ PGC1α mRNA, ↑ HSP72 mRNA (3h post)
Hoier, 2013 (115)	Trained; Young; 9m	VL; Rest, 1h post, 3h post	Cycle	MOD: 60min @ 62% VO_{2peak} HIIE: 24 x 1min @ 117% VO_{2peak} w/ 1.5min rest	BOTH: ↑ interstitial VEGF (MOD > HIIE); ↑ endothelial cell prolif. (MOD > HIIE) HIIE: ↑ VEGF mRNA (1h post), Timp1 mRNA (3h post)
Scribbans, 2014	Rec. Active; Young, 6m	VL; Rest, immed. post	Cycle	MOD: 30min @ 65% VO_{2peak} HIIE:8 x 20sec @ 170% VO_{2peak}, 1-sec rest	BOTH: ↑ ACC^{Ser79}
Kristensen, 2015 (134)	Rec. Active; Young; 9m	VL; Rest, immed. post	Cycle	MOD: 30min @ 70% VO_{2peak} HIIE: 6 x 90sec @ 95% VO_{2peak} w/ 2.5min rest	BOTH: ↑ ACC^{Ser221} (MHCI fibers) ↑ ACC^{Ser221} (MHCII fibers; MOD < HIIE) HIIE: ↑ $AMPK^{Thr172}$ (MHCII fibers)
Nederveen, 2015 (180)	Sed.; Old; 22m	VL; Rest, 24h post, 48h post	Cycle	MOD: 30min @ 55-60% VO_{2peak} HIIE: 10 x 1min @ 90-95% VO_{2peak} w/ 1min rest	HIIE: ↑ $MyoD^{+}$ SCs (24h post, 48h post)
Granata, 2017 (103)	Rec. Active; Young; 19m	VL; Rest, immed. post, 3h post	Cycle	MOD: 24min @ 63% W_{max} HIIE: 4 x 30sec @ Wingate w/ 4min rest	HIIE: ↑ nuclear $p53^{Ser15}$ (immed. post, 3h post); ↑ nuclear $p38\ MAPK^{Thr180/Tyr182}$ (immed. post), ↑ nuclear PGC1α protein (immed. post, 3h post)

Table 2-7 (pg. 69-70). Summary of Acute Skeletal Muscle Response: HIIE vs MOD

Author, Year (Reference)	Participants	Muscle Biopsy	Exercise		Outcome
			Mode	Protocol	
Parker, 2017 (188)	Rec. Active; Young; 6m, 2f	VL; Rest, immed. post, 3h post	Cycle	MOD: 30min @ 50% W_{max} HIIE: 5 x 4min @ 75% W_{max} w/ 1min rest SIE: 4 x 30sec Wingate w/ 4min rest	ALL: ↑ $IRS1^{Ser307}$ (immed. post; HIIE > MOD); ↑ $p38MAPK^{Thr180/Tyr182}$ (immed. post); ↓ Akt^{Ser473} (immed. post) HIIE & SIE: ↓ $AS160^{Ser588}$ (immed. post, HIIE > SIE) SIE: ↑ $NF\text{-}kBp65^{Ser536}$ (immed. post)

Rec; recreationally; m, male; f, female; VL, vastus lateralis; immed, immediately post exercise; MOD, moderate intensity exercise; HIIE, high-intensity interval exercise; AMPK, 5' adenosine monophosphate-activated protein kinase; p38MAPK, p38 mitogen-activated protein kinases; PGC1α; peroxisome proliferator-activated receptor gamma coactivator 1-alpha; HSP72, heat shock protein 72; prolif, proliferation; VEGF, vascular endothelial growth factor; Timp1, tissue inhibitor of metalloproteinase 1; ACC, acetyl-CoA carboxylase; MHC, myosin heavy chain; sed, sedentary; MyoD, myogenic differentiation factor 1; SC, satellite cells; p53, tumor protein 53; SIE, sprint interval exercise; IRS1, insulin receptor substrate 1; Akt, protein kinase B; AS160, Akt substrate of 160 kDa; NF-kB, nuclear factor kappa-light-chain-enhancer of activated B cells; ↑ or ↓, $p < 0.05$.

C. Chronic Skeletal Muscle Adaptations

Over the course of weeks or months, the cumulative effect of the acute skeletal muscle response to each exercise bout alters the skeletal muscle phenotype to meet new functional demands. The skeletal muscle adaptations to chronic aerobic exercise have been well documented (70, 110, 165). Traditional aerobic exercise training is characterized by periods of high volume, low to moderate intensity, continuous exercise, eliciting relatively minor mechanical strain on the skeletal muscle. Chronic aerobic exercise training results in morphological and metabolic adaptations to skeletal muscle. Increased mitochondrial abundance and oxidative capacity is a well-established adaptation to chronic aerobic exercise training (64), which ultimately leads to increased fatigue resistance (109). Similarly, chronic aerobic exercise is associated with increased substrate storage in the form of muscle glycogen (35) and intramuscular triglycerides (IMTG) (100). Substrate utilization is also altered following chronic aerobic exercise, where reliance on glycogen stores is reduced at a given submaximal workload and oxidation of IMTGs is increased (100, 215). Chronic aerobic exercise also results in a greater occurrence of MHCI muscle fibers (70, 166) and increases in skeletal muscle capillaries (110). Altogether, the hallmark adaptations to traditional aerobic exercise consist of improvements in mitochondrial capacity, oxygen and substrate delivery, and substrate storage and utilization, collectively contributing to an enhanced endurance capacity of skeletal muscle.

Low-volume, high-intensity interval training (HIIT) appears to induce similar skeletal muscle adaptations compared to traditional aerobic exercise training, albeit with a fraction of the exercise time. HIIT has been shown to result in increased PGC-1α protein (119, 145, 189, 213) and subsequent improvements in mitochondrial capacity, as indicated by increases in CS and COX activity (38, 119, 125, 145, 189). In fact, increased CS has been documented following as few as 7 sessions of HIIT (189). The mitochondrial adaptations are accompanied by alterations in substrate storage. Increases in both muscle glycogen stores (38) and IMTGs (221) have been reported following 2 weeks and 6 weeks of HIIT, respectively. Concerning substrate storage, HIIT has also been shown to improve insulin sensitivity (119, 221) and GLUT4 abundance (119, 221). Similar to traditional aerobic exercise training, HIIT also appears capable of inducing a shift in

muscle fiber type, toward a greater distribution of MHCI muscle fibers (218, 254). An area that warrants further research is the impact of HIIT on capillarization. Although several studies have reported increased skeletal muscle capillaries following HIIT (53), Hoier *et al.* showed no change (115). In addition, investigation of the acute skeletal muscle responses to HIIE may indicate blunted angiogenesis (95), which could lead to negligible changes in skeletal muscle capillarization following HIIT. Finally, HIIT has also been documented to increase muscle fiber cross-sectional area (CSA) (254), an adaptation that is less associated with aerobic exercise yet still possible (107).

Studies that have directly compared skeletal muscle adaptations following HIIT and traditional aerobic exercise training (MOD) largely indicate similar adaptations are attained following each respective training modality (Table 2-8). However, a majority of the literature investigating skeletal muscle adaptations to HIIT have focused on mitochondrial adaptations, which may differ between HIIT and MOD. While both training modalities are effective in improving mitochondrial capacity, several studies report greater increases in mitochondrial respiration (104, 218) and CS activity (149) following HIIT versus MOD. This may be a result of the higher exercise intensity associated with HIIT, as two of the studies demonstrating superior mitochondrial adaptations administered HIIT and MOD training protocols that were matched for total work (104, 149). However, each of these studies employed rather short training periods of 2 weeks (149) and 4 weeks (104). Therefore, it is also likely that MOD training may elicit similar adaptations when performed over a longer training period. Overall, HIIT appears to elicit similar skeletal muscle adaptations to tradition, high-volume, moderate-intensity aerobic exercise. The most obvious benefit to HIIT is the relatively minimal exercise time required, a common reason for poor exercise compliance (96). In addition to the array of benefits in skeletal muscle, HIIT has been well documented to induce a variety of positive adaptations to other tissues and physiological systems (128). HIIT also appears to be a viable exercise therapy for several clinical populations including those with obesity (18), COPD (254), cancer (159), and heart failure (14, 249). Future studies investigating the impact of HIIT on skeletal muscle growth, atrophy, and function are warranted, especially in aging and clinical populations.

Table 2-8 (pg. 73-74). Summary of Chronic Skeletal Muscle Adaptations: HIIT vs MOD

Author, Year (Reference)	Participants (n)	Exercise Training		Outcome
		Mode	Protocol	
Vogiatzis, 2005 (254)	COPD; Old; (HIIT: 10, MOD: 9)	Cycle; 3d/wk; 10 wks	MOD: 30min @ 60% W_{max} HIIT: 45 x 30sec @ 100% W_{max}, 30sec rest	BOTH: ↓ MHCIIb dist.; ↑ MHCI CSA; ↑ MHCIIa CSA; ↑ Cap.:fiber ratio MOD: ↓ PFK activity
Gibala, 2006 (86)	Rec. Active; Young; (HIIT: 8m, MOD: 8m)	Cycle; 3d/wk; 2 wks	MOD: 90-120min @ 65% VO_{2peak} HIIT: 4-6 x 30sec Wingate	BOTH: ↑ COX activity; ↑ COXII protein; ↑ COXIV protein; ↑ glycogen
Burgomaster, 2008 (37)	Rec. Active; Young; (HIIT: 5m, 5f; MOD: 5m, 5f)	Cycle; 5d/wk; 6 wks	MOD: 40-60min @ 65% VO_{2peak} HIIT: 4-6 x 30sec Wingate, 4.5min rest	BOTH: ↑ CS activity; ↑ β-HAD activity; ↑ PGC1α protein
Daussin, 2008 (53)	Sed.; Young; (7m, 4f)	Cycle; 3d/wk; 8 wks	MOD: 20-35min @ 61% W_{max} HIIT: 4-7 x 1min @ 90% W_{max}, 4min rest (work matched)	BOTH: ↑ Cap. density HIIT: ↑ Mito. Resp.
Shepherd, 2012 (221)	Sed.; Young; (16m)	Cycle; MOD: 5d/wk; HIIT: 3d/wk; 6 wks	MOD: 40-60min @ 65% VO_{2peak} HIIT: 4-6 x 30sec Wingate, 4.5min rest	BOTH: ↑ IMTG; ↑ PLIN2 protien ↑ PLIN5 protien
Scribbans, 2014 (218)	Rec. Active; Young; (HIIT: 10, MOD: 9)	Cycle; 4d/wk; 6 wks	MOD: 30min @ 65% VO_{2peak} HIIT: 8 x 20sec @ 170% VO_{2peak}, 10sec rest	BOTH: ↑ MHCI dist.; ↓ MHCIIa/x dist.; ↑ SDH activity (all FT); ↑ Cap. density; ↑ GPD activity (MHCI) HIIT: ↑ GPD activity (MHCIIa)
Joanisse, 2015 (126)	Rec. Active; Young; (HIIT: 10, MOD: 9)	Cycle; 4d/wk; 6 wks	MOD: 30min @ 65% VO_{2peak} HIIT: 8 x 20sec @ 170% VO_{2peak}, 10sec rest	BOTH: ↑ active SCs; ↑ diff. SCs; ↑ terminally diff. SCs
Baekkerud, 2016 (18)	Overweight/Obese; Middle aged; (4HIIT: 5m, 7f; 1HIIT: 3m, 6f; MOD: 4m, 5f)	Run; 3d/wk; 6 wks	MOD: 45min @ 70% HR_{max} 1HIIT: 10 x 1min @ 90% HR_{max}, 1min rest 4HIIT: 4 x 4min @ 89-95% HR_{max}, 3min rest	ALL: ↑ CS activity

Table 2-8 (pg. 73-74). Summary of Chronic Skeletal Muscle Adaptations: HIIT vs MOD

Author, Year (Reference)	Participants (n)	Exercise Training		Outcome
		Mode	Protocol	
Granata, 2016 (104)	Rec. Active; Young; (HIIT: 11m, SIT: 9m, MOD: 9m)	Cycle; 3d/wk; 4 wks	MOD: 20-36min @ 65% W_{max} HIIT: 4-7 x 4min @ 90% W_{max}, 2min rest SIT: 4-10 x 30sec Wingate, 4min rest	SIT: ↑ Mito. resp.; ↑ PGC1α protein; ↑ p53 protein; ↑ PHF20 protein
Gillen, 2016 (89)	Sed.; Young; (HIIT: 9m, MOD: 10m)	Cycle; 3d/wk; 12 wks	MOD: 45min @ 70% HR_{max} HIIT: 3 x 20sec Wingate, 2min rest	BOTH: ↑ CS activity; ↑ ETC complexes
MacInnis, 2017 (149)	Rec. Active; Young; (10m)	Single-leg Cycle; 3d/wk; 2 wks	MOD: 30min @ 50% W_{max} HIIT: 4 x 5min @ 65% W_{max}, 2.5min rest	BOTH: ↑ COX IV protein; ↑ NDUFA9 protein; ↑ MFN2 protein HIIT: ↑ CS activity

COPD, chronic obstructive pulmonary disease; HIIT, high-intensity interval training; MOD, moderate intensity aerobic training; W_{max}, maximal wattage; MHC, myosin heavy chain; Cap, capillary; PFK, phosphofructokinase; m, male; f, female; VO_{2peak}, maximal oxygen consumption; COX, cytochrome c oxidase; PGC1α; peroxisome proliferator-activated receptor gamma coactivator 1-alpha; Mito, mitochondria; Resp, respiration; Sed, sedentary; IMTG, intramuscular triglyceride; PLIN2, perilipin 2; PLIN5, perilipin 5; SDH, succinate dehydrogenase; GPD, α-glycerophosphate dehydrogenase; SC, satellite cell; diff, differentiated; HR_{max}, maximal heart rate; CS, citrate synthase; p53, tumor protein 53; PHF20, plant homeodomain finger-containing protein 20; ETC, electron transport chain; NDUFA9, NADH:ubiquinone oxidoreductase subunit A9; MFN2, mitofusion 2; ↑ or ↓, $p < 0.05$.

CHAPTER 3

SKELETAL MUSCLE ARCHITECTURE ACROSS THE AGING SPECTRUM: A COMPARISON OF ULTRASOUND TECHNIQUES AND AN ASSESSMENT OF RELIABILITY

Andrew C. D'Lugos, Nathan J. Skotak, Jacquelyn J. Faris, Nicholas T. Thomas, Corey Mazo, Theresa M. Jorgensen, Matthew P. Buman, and Jared M. Dickinson

School of Nutrition and Health Promotion, Healthy Lifestyles Research Center, Exercise Science and Health Promotion, Arizona State University, Phoenix, AZ, USA

INTRODUCTION

Skeletal muscle plays a fundamental role in an array of physiological processes that are imperative to the ability to perform both metabolic and physical functions. With respect to contractile characteristics, the functional performance of skeletal muscle is largely dictated by muscle fiber type profile (myosin heavy chain isoform) (272) and its architectural characteristics, such as fiber pennation angle (PA) and physiological cross-sectional area (pCSA) (143, 172). Additionally, the composition of skeletal muscle (i.e. the presence of non-contractile tissues within muscle) may have implications for proper functioning of contractile (114, 270) and metabolic (240) processes in skeletal muscle. Consequently, feasible strategies to accurately evaluate skeletal muscle architecture and composition could provide valuable insights for assessing and/or improving muscle function in the setting of both muscle performance and disease.

Until recently, magnetic resonance imaging (MRI) has served as the gold-standard measurement for skeletal muscle architecture and composition. However, the utility of MRI is restricted by high costs, limited availability, and the necessity to position patients in a fixed prone or supine position. The emergence of real-time ultrasonography (US) has allowed for the examination of *in vivo* characteristics of skeletal muscle. Further, US presents minimal to no risk to the patient/subject, and it is extremely portable which provides access to a variety of populations, from bed-confined to ambulatory. In addition, US is an accurate and reliable means to measure muscle PA (139) and composition, the latter of which is indicated by the echogenicity (EG) or brightness of a tissue on US (192, 269). Since its emergence, US has also been accepted as a valid means of assessing age-induced changes in muscle size (17, 195, 236), PA (167, 236), and muscle composition (17, 236, 247). However, the current body of literature lacks consensus on a standardized method of assessment. This lack of standardization in skeletal muscle US is important, as it impedes the generalizability of findings across investigation.

Currently, two predominate approaches to measure skeletal muscle characteristics with US are utilized. For one of these approaches images are captured while the patient is standing, whereas during the other approach images are captured while the patient is supine [for examples, see following reviews (5, 67)]. Each postural approach has its own unique advantages, especially

when the patient population may be limited in their ability to assume one posture over the other. For example, patients with congestive heart failure are reluctant to lay supine due to the increased incidences of dyspnea and pulmonary edema (178), while individuals who are bed-ridden may be unable to stand. To our knowledge only one study (241) has directly compared US-based measures of skeletal muscle acquired both supine and standing. Thoirs and colleagues (241) acquired repeat measurements of muscle thickness (MT) in young to middle-aged adults while standing and supine, demonstrating smaller absolute MT measurements when imaged supine versus standing. However, to what extent posture may influence other US-based measurements, such as PA and EG, and whether this impact occurs at different anatomical sites along the quadriceps have yet to be determined. These methodological considerations are important when identifying changes in US-derived skeletal muscle characteristics that may indicate changes in a muscle's functional capacity.

Given the relatively high reliance on operator ability with US, an important consideration for accurate measurements of muscle characteristics is the test-retest reliability of the measure. When utilizing skeletal muscle US, anatomical imaging sites are identified relative to bony landmarks (i.e. greater trochanter of femur, lateral condyle of knee). Considering the architecture and size of a muscle, particularly the quadriceps (25), changes along its length, variations in imaging site identification may introduce variability in US measurements. While a common strategy, particularly in exercise training studies, is to maintain a constant imaging site over time by marking the skin, a thorough assessment of the impact of variability in imaging site identification on the test-retest reliability of skeletal muscle US has yet to be examined. Similarly, imaging posture has been shown to influence reliability (241), however the direct assessment of US reliability between postural approaches has also yet to be investigated.

The purpose of this study was to determine 1) the influence of posture on US determined measures and 2) the test-retest reliability of distinct skeletal muscle US approaches (posture and imaging site identification) in a cohort of young and older males and females. Moreover, it is very well understood that advancing age is associated with changes to the size, architecture, and composition of skeletal muscle (56, 175, 236). Therefore, a secondary purpose of this study was

to determine how aging may influence differences between postures and the test-retest reliability of skeletal muscle US measures. Identifying the reliability of various approaches to skeletal muscle US is critical to increasing the ability to accurately assess changes in skeletal muscle characteristics in a variety of populations. Ultimately the objective of the current study is to improve the ability, through skeletal muscle US, identify individuals at risk for skeletal muscle decline and evaluate the progress of therapies aimed at improving skeletal muscle function.

MATERIALS AND METHODS

Participants

Thirty healthy men and women from the greater Phoenix, AZ metropolitan area volunteered for this study. All subjects were considered recreationally active (performing ≤ 2 exercise sessions per week), but not engaged in a regularly scheduled exercise-training program. Screening was performed using an online survey (Qualtrics®), as well as a Physical Activity Readiness Questionnaire (PAR-Q). Subjects were eligible for inclusion if they were between 18 and 35 (young) or between 60 and 85 (old) yrs of age, and had a body mass index (BMI) ≤ 30 kg/m^2 (non-obese) for the young and ≤ 32 kg/m^2 for the old. Exclusion criteria included any acute or chronic illness, including but not limited to cardiac disease, uncontrolled hypertension, diabetes, or other metabolic disorders, arthritis of the knees or hips, a history of neuromuscular problems, lower limb injuries impeding function, or pregnancy. All subjects provided written informed consent prior to participation. Two subjects failed to complete the study due to reasons unrelated to the study and thus 28 subjects completed all aspects of the study (Table 3-1). All procedures were approved by the Institutional Review Board of Arizona State University, which is in compliance with the Declaration of Helsinki as revised in 1983.

Study Design

Subjects were studied on two separate occasions, separated by 6 ± 3 days. Both visits were identical except that during the first visit subject completed screening questionnaires and during the second visit subjects received a dual-energy x-ray absorptiometry (DXA) scan. Subjects were instructed to abstain from any heavy or unaccustomed physical activity for 48 h prior to each visit. During each visit, height and weight were recorded, ultrasound images of the quadriceps muscles of both legs were completed in both a supine and standing position, and the peak isometric torque of the quadriceps of each leg was assessed using an isokinetic dynamometer. US data collected from visit #1 was used to assess the influence of posture on US determined skeletal muscle characteristics, while US data collected from visit #1 and visit #2 was used to assess test-retest reliability.

Skeletal Muscle Ultrasound Imaging

In vivo skeletal muscle architecture of the *vastus lateralis* (VL), *rectus femoris* (RF), and *vastus intermedius* (VI) were examined with two-dimensional (2D) brightness mode (B-mode) ultrasonography (Terason 3300, Teratech, Burlington, MA) using a 4.5 cm linear array transducer (4-15MHz) (Fig. 3-1). A preset for skeletal muscle imaging was used to obtain all images with setting of the focal zones, gain, and frequency held constant across all subjects. Due to changes in muscle architecture and along the length of the leg, multiple imaging sites across the quadriceps were employed, as previously described (25). All imaging sites for a given leg were based on bony landmarks of the femur. Imaging sites on the lateral quadriceps were performed at 56% (L1), 39% (L2), and 22% (L3) of the distance from the lateral condyle of the knee to the head of the greater trochanter. Imaging sites on the anterior quadriceps were identified at 56% (A1) and 39% (A2) of this distance. Imaging sites were denoted on the skin with permanent marker by an "X" corresponding to the midline of the transducer. The transducer was coated in water-soluble gel to aid acoustic transmission and eliminate deformation of the skin and underlying tissues and oriented perpendicular to the skin to collect longitudinal images at each imaging site. Longitudinal images of the VL and lateral VI (VI_L) were collected at sites L1, L2, and L3, while longitudinal images of the RF anterior VI (VI_A) were collected at sites A1 and A2.

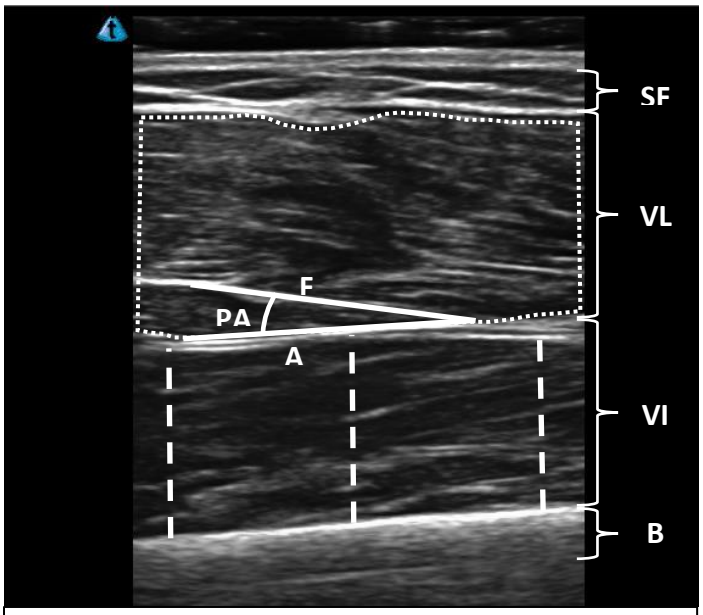


Fig 3-1. Longitudinal plane ultrasound scan of the vastus lateralis (VL) and lateral aspect of the vastus intermedius (VI). Pennation angle (PA, solid lines) was measured as the insertion angle of a fascicle (F) into the axis of force generation (A). Muscle thickness (dashed lines) was measured as the distance between the superior and deep muscle borders [i.e. deep aponeurosis and superficial border of femur (B)] at 3 locations, corresponding to 10%, 50%, and 90% of the field of view width. Echogenicity (dotted line) was measured be tracing a region of interest within a muscle, avoiding connective tissue and subcutaneous fat (SF).

Imaging sites were identical for images collected during the supine and standing postures (described below).

Participant posture during imaging.

To determine the influence of posture on the test-retest reliability of MT, PA, and EG measurements, US images of the quadriceps of both legs were acquired, as described above, while the participant rested supine and standing. Each participant was randomly assigned to begin the ultrasound imaging in either the supine or standing posture, switching to the opposite posture immediately after collection of US measures in the first posture. This order was replicated for a given subject during the first and second visit, however, the posture order was counterbalanced between young and old participants. Prior to imaging, subjects rested in each posture for 20 mins to allow for any potential intramuscular fluid shifts to subside (22). In the supine posture (SUP), participants were laid on a medical examination bed with the hip flexion and rotation standardized using a custom-built positioning unit and a towel-roll placed under the knee to achieve natural knee flexion of approximately 10°. In the standing position (STAND), subjects stood on a cushioned mat without footwear and during imaging, transferred their body weight onto the opposite leg from that which was being imaged to avoid contraction-induced changes in muscle architecture (79).

Influence of identifying imaging sites.

To determine the day-to-day variability of US-determined muscle characteristics, one leg of each participant was randomly assigned to have the “marked” imaging sites kept constant until the next visit (marked leg, M) while the imaging sites on the opposite leg were removed during the first visit (unmarked leg, UM). Subjects were provided a surgical skin marker and instructed to maintain the five imaging sites only on the marked leg between the first and second visit. During the second visit, the sites on the marked leg were verified using measurements from the first visit while the imaging sites on the unmarked leg were reestablished as detailed above.

Muscle function testing.

To identify the relationship between US measurements of the quadriceps acquired in both postures and the function of the quadriceps muscles, we assessed the peak isometric torque of the knee extensors. Following ultrasound imaging, subjects completed a 5-min warm-up on a cycle

ergometer (Model 828, Monark, Varberg, Sweden) at approximately 60 watts. Subjects were then fitted to the isokinetic dynamometer (HUMAC Norm, CSMi, Stoughton, MA) to assess their peak isometric unilateral knee extension torque for each leg. The subjects performed three, 5-second maximal isometric unilateral knee extensions at 60° knee flexion, separated by 30 s of rest. Each leg was tested in a randomized order on both visits. The highest isometric knee extension torque across both visits was recorded to represent the peak muscle function of each leg.

Dual-energy X-Ray Absorptiometry (DXA Scan).

During the second visit, subjects underwent a whole-body DXA scan. Prior to the scan, subjects were instructed to void their bladder after which they rested supine for 20 mins to allow fluids to subside.

Ultrasound image analysis.

Ultrasound images were transferred as uncompressed *.tiff* files to a designated computer (iMac, Apple, Cupertino, CA, USA) for the analysis of muscle thickness, pennation angle, and echogenicity (Fig. 3-1). Image analysis was carried out using publicly available software (ImageJ, National Institutes of Health, USA). For the analysis of muscle thickness, ImageJ was first calibrated using the visible depth scale on each image. Muscle thickness (MT) of the VL and RF was measured as the perpendicular distance between the border of subcutaneous fat and muscle to the deep aponeurosis. In the VI, MT was measured as the perpendicular distance between the superficial aponeurosis and the superficial border of the femur. At each site, combined MT of the two visible muscles (VL+VI, RF+VI) was also examined, measured as the perpendicular distance between the subcutaneous fat and muscle border to the superficial border of the femur. To account for changes in MT across the field of view (FOV) in each image, MT measurements were made at three locations across the FOV, corresponding to 10%, 50%, and 90% from left to right (based on width of FOV). Measurements at the three locations across the FOV were averaged into one composite MT measurement for a given muscle and imaging site.

Pennation angle (PA) was measured by tracing the angle of insertion of a visible fascicle border into the aponeurosis corresponding to axis of force generation (VL: deep aponeurosis; VI: superficial aponeurosis) (Fig. 3-1). In a given image, one to three PA's were measured, based on

the visibility of clear fascicular borders, and averaged to yield one PA measurement for a given muscle and image site. Due to the parallel orientation of fascicles to the aponeurosis in the RF (236), PA was not assessed in this muscle.

Echogenicity (EI) of the VL, RF, and VI was assessed using the gray-scale analysis function in ImageJ. First, images were converted to 8-bit grayscale in ImageJ, where EG resulted in a value ranging between 0 (black) to 255 (white). The EG of each muscle was assessed by tracing a region of interest in each muscle, carefully avoiding any surrounding bone or connective tissue. Special attention was paid to ensure the ultrasound unit settings of frequency, gain, and focal zone were kept constant across all subjects and visits.

Statistical Analysis

All statistical analyses were performed using SPSS statistical software (v.24, IBM, Tokyo, Japan). For comparison of subject characteristics, independent *t*-tests were employed. To assess the impact of age, sex, and posture on the skeletal muscle architecture measurements, a linear mixed-model with fixed effects for age, sex, and posture was carried out only on measurements from the first visit. To assess the test-retest reliability of all skeletal muscle architecture measurements, change scores for the absolute [visit 2 value – visit 1 value] and relative [(visit 2 value – visit 1 value) ÷ visit 1 value]*100 differences were first calculated. Next, a linear mixed model with fixed effects for sex, age, posture, and marking, and interactions among all terms was carried out on the absolute and relative test-retest differences. A Bonferroni correction was employed in all mixed model comparisons. Supplement pairwise analyses were used to discern differences in reliability between the four groups (age x sex), within the posture, leg, and leg x posture interactions. In addition, the agreement between ultrasound measurements made on each visit was determined within posture, marking, sex, and age using a 2-way random effects, single rater, absolute agreement intraclass correlation coefficient (ICC) analysis.

To examine which skeletal muscle architecture measurements best predict peak muscle function (peak isometric torque), a stepwise linear regression analysis (enter: $P \leq 0.05$; remove: $P \geq 0.10$) was performed using MT, PA, and EG measurement averaged across the two visits for a

given subject and the highest peak isometric torque for each leg across visits. Significance for all analyses was set *a priori* at $P < 0.05$. All data are expressed as mean±SE unless noted otherwise.

RESULTS

Subjects

Subject characteristics are displayed in table 3-1. Height and weight were similar between young and old ($P > 0.05$), but were greater in males versus females (163 ± 7 cm, 60 ± 9 kg) ($P < 0.001$). Body mass index (BMI) was greater ($P < 0.001$) in old females compared to young females, whereas BMI was similar between young and old males ($P > 0.05$). DXA-derived body fat percentage and fat mass were greater in old compared to young ($P < 0.001$). Lean mass was similar between young and old (P = 0.94), but was greater in males versus females ($P < 0.001$). Peak isometric torque (PIT) of the quadriceps was greater in young compared to old ($P < 0.016$) and in males versus females ($P < 0.001$).

Measurement of Skeletal Muscle Parameters

The influence of sex and age on US determined muscle characteristics were determined using measurements of MT, PA, and EG collected during the first visit (Tables 3-2 to 3-12). Quadriceps MT was lower in old compared to young in 12 of the 15 measurements (Tables 3-2 to 3-6), whereas PA was lower in old versus young in all 5 measurements (Table 3-7). In addition, the EG of the quadriceps was higher in old versus young in 7 of the 10 measurements (Tables 3-8 to 3-12). Females exhibited smaller MT compared to males in 9 of the 15 measurements, 7 of which occurred along the lateral quadriceps (Tables 3-4 to 3-6). Females exhibited lower PA than males in 2 of the 5 measurements (Table 3-7). Quadriceps EG was higher in females versus males in all 10 measurements (Tables 3-8 to 3-12).

Influence of Posture on Skeletal Muscle Parameters

Postural differences in the measurements of MT, PA, and EG are visually displayed in figures 3-2 to 3-6. In addition, *P*-values for all main effects and interactions with posture are displayed in tables 3-57 to 3-61. All pairwise comparisons and values for MT, PA, and EG obtained in the standing and supine positions are displayed in tables 3-2 to 3-12.

Posture during imaging largely affected the MT of the anterior quadriceps, where all 6 anterior MT measurements were larger when measured standing versus supine (Fig. 3-2, Tables 3-2 to 3-3). Conversely, MT of the VL at L1 was significantly smaller when measured standing

versus supine (Fig. 3-3, Table 3-4). Posture similarly influenced MT measurements in the young and old in all anterior measurements. However, the influence of posture on VL MT at L1 only occurred in young (Fig. 3-3, Table 3-4). Measurements of PA were minimally influenced by posture (Fig. 3-4, Table 3-7). An effect of posture on PA was only observed in young, in the measurement of VL PA at L2, where PA was lower when measured standing versus supine (Fig. 3-4, Table 3-7). Echogenicity measurements of the anterior quadriceps were lower when measured standing versus supine (Fig. 3-5, Tables 3-8 to 3-9). Along the lateral quadriceps, EG of the VI at L1 and L3 was lower when measured standing versus supine only in old (Fig. 3-6, Tables 3-10 to 3-12). The influence of posture on MT, PA, and EG did not differ between females and males.

Reproducibility of Skeletal Muscle Measurements

The absolute agreements between skeletal muscle measurements from the first and second visit are presented in tables 3-13 to 3-24. Intraclass correlation coefficients (ICCs) for MT across all groups ranged between 0.496 to 0.932 standing and 0.568 to 0.974 supine (Table 3-13, 3-16). In addition, the marked leg resulted in higher ICCs in 5 of the 15 MT measurements when standing and in 12 of the 15 MT measurements when supine. Measurements of MT when standing yielded ICCs ranging between 0.298 to 0.955 in young (Tables 3-14, 3-17) and -0.018 to 0.955 in old (Tables 3-15, 3-18). When MT was measured supine, ICCs ranged between 0.239 to 0.972 in young and 0.545 to 0.971 in old. In young, the marked leg resulted in higher ICCs in 11 of the 15 MT measurements when standing and 13 of the 15 MT measurements when supine. In the old, the marked leg yielded higher ICCs in 6 of the 15 MT measurements when standing and 7 of the 15 MT measurements when supine.

Reproducibility of PA across all groups ranged between ICCs of 0.310 to 0.721 standing and 0.143 to 0.822 supine (Table 3-19 to 3-20). In addition, the marked leg resulted in higher ICCs in 2 of the 5 PA measurements when standing and in 4 of the 5 PA measurements when supine. Measurements of PA when standing yielded ICCs ranging between -0.806 to 0.749 in young (Table 3-20) and -0.560 to 0.929 in old (Table 3-21). When PA was measured supine, ICCs ranged between -0.414 to 0.854 in young (Table 3-20) and -0.960 to 0.653 in old (Table 3-21). In young, the marked leg resulted in higher ICCs in 2 of the 5 PA measurements when standing and in 3 of

the 5 PA measurements when supine. In the old, the marked leg yielded higher ICCs in 2 of the 5 PA measurements when standing and in 4 of the 5 PA measurements when supine.

Measurements of EG across all groups yielded ICCs between 0.265 to 0.751 standing and 0.533 to 0.858 supine (Tables 3-22 to 3-24). In addition, the marked leg resulted in higher ICCs in 2 of the 10 EG measurements when standing and in 5 of the 10 EG measurements when supine. Measurements of EG when standing yielded ICCs ranging between 0.226 to 0.824 in young (Table 3-23) and -0.193 to 0.799 in old (Table 3-24). When EG was measured supine, ICCs ranged between 0.497 to 0.846 in young (Table 3-23) and 0.111 to 0.830 in old (Table 3-24). In young, the marked leg resulted in higher ICCs in 4 of the 10 EG measurements when standing and in 6 of the 10 EG measurements when supine. In the old, the marked leg yielded higher ICCs in 5 of the 10 EG measurements when standing and in 7 of the 10 EG measurements when supine.

Test-Retest Reliability of Skeletal Muscle Measurements

P-values for all main effects and interactions with marking are displayed in tables 3-62 to 3-71. All pairwise comparisons and day-to-day differences (absolute and relative) for MT, PA, and EG obtained in the standing and supine positions are displayed in tables 3-25 to 3-54.

The day-to-day differences in MT measurements were not different between postures in young. However, in old 6 of the 15 MT measurements resulted in greater day-to-day differences (6 absolute, 3 relative) when measurements were made standing compared to supine (Tables 3-25 to 3-29). In young day-to-day differences in MT were greater in the unmarked versus the marked leg in 6 of the 15 measurements, 2 when measured standing (1 absolute, 1 relative) and 4 when supine (4 absolute, 4 relative). In old, day-to-day differences in MT were greater in the unmarked versus the marked leg at 2 of the 15 measurements, 1 when measured standing (absolute) and 1 when supine (absolute). Conversely, day-to-day differences in MT of old were greater in the marked, versus the unmarked leg at 7 of the 15 measurements, 6 when measured standing (5 absolute, 4 relative) and 1 when measured supine (relative).

The day-to-day differences in PA (Tables 3-40 to 3-44) of young at 2 of the 5 measurements were lower (1 absolute, 2 relative) when standing versus supine, while supine resulted in lower day-to-day differences at 1 of the 5 measurements (relative). In old, 2 of the 5 PA

measurements resulted in lower day-to-day differences (1 absolute, 1 relative) when standing versus supine. In young, day-to-day differences in PA were greater in the marked versus the unmarked leg at 1 of the 5 measurements (1 absolute, 1 relative). In old, the day-to-day differences in PA were not influenced by leg marking.

The day-to-day difference in EG measurements was not different between postures in young. However, in old, 2 of the 10 EG measurements resulted in greater day-to-day differences (relative) when standing versus supine (Tables 3-45 to 3-54). In young, day-to-day differences in EG were greater in the unmarked versus the marked leg at 1 of the 10 measurements when measured standing (relative). In old, day-to-day differences in EG were greater in the unmarked versus the marked leg at 2 of the 10 measurements, both when measured standing (absolute). Conversely, day-to-day differences in EG of old were greater in the marked versus the unmarked leg at 1 of the 10 measurements when measured standing (relative).

Relationship Between Skeletal Muscle Measurements and Muscle Function

To determine which US-derived skeletal muscle measurements best predict PIT of the quadriceps, stepwise linear regressions were performed. The best single-site predictors for young, old, and all subjects are displayed in table 3-55. Across all subjects, PIT was best predicted by the MT of the VI_L at L2 when measured supine (R^2 = 0.791, β = 56.5) and the MT of the VL+VI at L1 when measured standing (R^2 = 0.686, β = 32.9). In young, PIT was best predicted by the MT of the $VL+VI_L$ at L2 when measured supine (R^2 = 0.620, β = 44.7) and the MT of the VI_L at L2 when measured standing (R^2 = 0.876, β =66.0). In old, PIT was best predicted by the EG of the VI_L at L1 when measured supine (R^2 = 0.827, β = -1.60) and the EG of the VI_L at L3 when measured standing (R^2 = 0.996, β =1.20).

The best combination of US measurements to predict PIT for young, old, and all subjects are displayed in table 3-56. Across all subjects, PIT was best predicted by a single MT measurement of the lateral quadriceps when measured supine (R^2 = 0.791) and a combination of three MT measurements at the anterior and lateral quadriceps when measured standing (R^2 = 0.854). In the young, PIT was best predicted by a combination MT and EG measurements of the anterior and lateral quadriceps when measured supine (R^2 = 0.969) and a single MT measurement

of the lateral quadriceps when measured standing (R^2 = 0.876). In the old, PIT was best predicted by a single MT and EG measurement of the lateral quadriceps when measured supine (R^2 = 0.966) and a single MT and EG measurement of the lateral quadriceps when measured when measured standing (R^2 = 1.00).

DISCUSSION

The current study sought to directly compare distinct methodological approaches to capturing US images for the measurement of quadriceps skeletal muscle MT, PA, and EG in young and old individuals. Several key findings resulted from this study. First, subject posture during US imaging influenced US-determined measurements only in the anterior quadriceps, where standing produced higher MT and lower EG values compared to supine. Second, reliability of MT measured while subjects were standing was lower compared to when measured supine. In contrast, we did not detect a systematic influence subject posture on the test-retest reliability for measures of PA, or EG in either age group. Third, while strategies to identify anatomical imaging sites did not influence reliability for any US measures, older age was associated with lower test-retest reliability for measures of MT and PA. Collectively, these results highlight several methodological considerations for US-based assessment of skeletal muscle characteristics that should be considered for improving reproducibility and generalizability of US to assess skeletal muscle characteristics or function.

Influence of Posture

Current strategies for skeletal muscle US include obtaining images from subjects in either the standing or supine position. However, it is understood that posture can influence fluid distribution throughout the body, and in particular, fluid accumulation in the interstitium of the lower legs is greater when standing compared to lying supine (155). Indeed, posture-induced fluid shifts cause noticeable changes in lower limb morphology when assessed with computerize tomography (CT) (22) and DXA (54). Consequently, US measurements of skeletal muscle may be influenced by the posture in which the subject is imaged. Therefore, a primary goal of this study was to examine whether collecting images while standing or supine influenced US-determined measures of MT, EG, and PA. In the current study, measurements collected while standing demonstrated greater MT in the anterior quadriceps than those collected in the supine position, whereas MT of the lateral quadriceps was not influenced by subject posture. Our findings are consistent with a previous study that measured the composite MT of the RF and VI_A, demonstrating greater MT when standing vs supine (241). Further, the larger MT of the anterior quadriceps while standing was

accompanied by lower EG at the same anatomical sites. Fluid accumulation in soft tissue negatively impacts EG (123), indicating that differences in MT between postures are likely due to the accumulation of fluid in the anterior quadriceps while standing. Despite lower EG of the VI_L in old when standing, which may be due to greater extracellular water content in elderly (73), age did not influence the impact of posture on measures of MT. Further, in the current study, subjects rested for 15 mins after changing postures prior to capturing US images for the first leg being measured. The influence of posture on measures of MT and EG was no different in the first or second leg that were measured following postural changes, indicating that the 15 mins allocated for fluid shifts to subside was sufficient. Collectively, these data suggest that subject posture is an important methodological consideration when utilizing skeletal muscle US, especially when examining the anterior quadriceps, and that 15 minutes of rest are warranted prior to capturing US images for assessment of (anterior) quadriceps characteristics.

In contrast to MT and EG, measurements of PA were not influenced by posture. Compared to the supine position, the weight-bearing nature of standing affords the subject the possibility of contracting the quadriceps. The PA of a muscle is dynamic from a passive to contracted state (79), and thus subjects were instructed to relax the measured leg by distributing their body weight onto the contralateral limb. The absence of a postural effect on PA suggests that this approach is effective in avoiding contraction-induced changes in PA when skeletal muscle US is performed standing.

Reliability of Skeletal Muscle US

Compared to imaging modalities such as MRI and DXA, the user dependence of US in characterizing skeletal muscle is significant. Therefore, establishing reliable measurement approaches is vital to accurately assess changes in skeletal muscle characteristics over serial measurements. The current study aimed to assess differences in the reliability of US measures of MT, PA, and EG between standing and supine in young and old individuals. We demonstrate that the reproducibility of MT measurements across all muscles is slightly lower when standing (ICCs: 0.541 – 0.932) compared to supine (ICCs: 0.773 – 0.974). Muscle thickness of the distal VL (site L3) exhibited the lowest reproducibility between visits in both postures, likely due to the proximity

of the imaging site to the musculotendinous junction. When excluding this measurement, our results are in accordance with previous studies of quadriceps MT while standing (241) and supine (66, 236, 241). The diminished reliability in standing versus supine may be due to difficulty in maintaining consistent probe orientation on the skin, as the subjects' legs are relatively more mobile compared to when supine. Further, independent of posture the reliability of MT measurements was generally lower in older individuals. An interesting finding was that age appeared to preferentially impact the relative (%) day-to-day difference in MT more so than the absolute (cm) difference. The influence of age revealed in the relative day-to-day differences may simply be the result of smaller MT measurements in the muscles of older compared to young. These findings indicate that detecting changes in quadriceps MT of older adults over time may be more difficult due to lower day-to-day reliability compared to young.

Measurements of quadriceps PA resulted in low to good reproducibility, according to the Fleiss ICC classification (222), while reproducibility of EG measurements ranged from moderate to good. These findings are in agreement with the only other study to assess the reliability of PA and EG measurements in the quadriceps of young and old (236). Overall, the reliability of PA and EG measures were largely similar between postures and age groups. Our results concerning the reproducibility of PA are lower compared to previous investigation assessing test-retest reliability within the same visit (13, 25, 164). In addition to the longer time period between visits in the current study (~ 1 week), our results may be explained by our imaging approach. In the current study, imaging was performed with the goal of collecting a single image suitable for measurements of MT, PA, and EG. Thus, special care was taken to not compress the tissue with the transducer for the assessment of MT, and to not adjust image contrast settings necessary to accurately assess EG. While this approach is time efficient, it may cause difficulty in visualizing fascicular border, especially in deep muscles. Thus, it is conceivable that the reproducibility of PA measurements may be improved if US operators are able to apply force to the tissue and alter image contrast to better visualize fascicular borders. To the best of our knowledge, the current study is the first to directly compare the influence of subject posture on the reliability of US measures of PA and EG. These findings suggest that although the reproducibility of EG and PA measurements is generally

lower than that of MT, reliability of EG and PA does not appear to be influenced by the posture in which they are measured.

Given the characteristics of skeletal muscle vary across the length of a muscle (), an important consideration for using US to assess skeletal muscle is the proper identification of anatomical imaging site. Therefore, it is important that images are captured at the same anatomical site for both cross-sectional and longitudinal comparison. To the best of our knowledge, a thorough assessment of the impact of imaging site identification on the reliability of skeletal muscle US has yet to be examined. Therefore, we sought to determine to what extent the reliability of skeletal muscle US measures differs when maintaining constant, marked imaging sites across two visits compared to reacquiring imaging sites based on measurements from bony landmarks. In the current study, we observed no systematic benefit of maintaining constant, marked imaging sites from one visit to the next for the reliability of MT, PA, or EG in either posture. Specifically, the reliability of only five of the thirty distinct US measurements collected each visit exhibited a benefit of maintaining marked imaging sites, all of which were measurements of MT or PA of the lateral quadriceps of the young age group. Maintaining a marked imaging site is often used in longitudinal study designs assessing changes in skeletal muscle characteristics, such as exercise training studies in which images are collected before and after exercise training (11, 20, 105, 199, 204, 237). However, our findings suggest that reacquiring anatomical imaging sites based on measures from bony landmarks does not reduce reliability, and thus is a suitable alternative to maintaining a marked imaging site. Collectively, as long as imaging sites are established relative to bony landmarks, as detailed in the current study, maintaining a marked imaging site may not be necessary for future studies or clinical diagnostics with serial measures aimed at assessing changes in skeletal muscle characteristics.

Relationship to Muscle Function

Skeletal muscle US can be utilized to assess changes in skeletal muscle characteristics that may indicate improvements or decrements in muscle function. Indeed, US-derived measurements of quadriceps MT [see review: (5)], PA (13, 219, 236), and EG (40, 78, 256, 261) are routinely associated with the peak functional capacity of the quadriceps in young and old

populations. However, given US images are commonly captured in either the supine and standing position, there remains a need to identify how the posture in which the images are collected influences how US can be used to examine changes in muscle function. Specifically, does the posture in which the images are collected impact which imaging site or which muscle characteristics will best predict function? In the current study, function of the quadriceps was assessed by peak isometric torque (PIT) of the knee extensors, which negates any influence of fiber-type or fiber length (140). As expected, PIT was 21% lower in old age group, compared to the young. Interestingly, subject posture had no influence on the relationship between US-determined characteristics of skeletal muscle and measures and PIT. Further, following stepwise regression analysis PA was not identified as a significant predictor of PIT in either age group or posture, which is consistent with previous work by Strasser *et al*. (236). On the other hand, MT of the VI_L and $VL+VI_L$ were the best single site predictors of PIT when measured supine and standing, respectively, in the young. This finding is in agreement with previous reports indicating VI MT is significant predictor of PIT (13, 236). In the old age group, EG of the VI_L was the best single predictor of PIT when supine and standing. Lopez *et al.* (148) recently demonstrated EG of the quadriceps as the best single predictor of a 30-sec sit-to-stand test in older adults, which together with the findings of the current study, suggest skeletal muscle composition may be more relevant to function than muscle mass (MT) in older adults. Interestingly, within young and old, US measurements of the lateral quadriceps, in particular the VI_L, were more predictive of muscle function. Collectively, given that US measures in the lateral quadriceps do not appear to be influenced by posture and also serve as shared predictors of muscle function between young and old, our findings suggest that the lateral compartment of the quadriceps may be the optimal region to assess for functionally relevant changes in skeletal muscle.

Conclusions

The results from the current study highlight sources of variability associated the use of US to examine skeletal muscle characteristics. The goal of this study was to thoroughly assess various US-based strategies for the measurement of MT, PA, and EG in young and old adults. Overall, our findings suggest that US measurements of the lateral quadriceps are ideal for assessing functional

changes in skeletal muscle, particularly given their collective relationship with muscle function and resistance to posture in both young and old. However, older age was associated with generally lower reliability which may impede the ability to accurately detect changes in the skeletal muscle of older adults. Future studies are warranted to identify the reliability of skeletal muscle US measures in clinical populations. The findings from this study can be used to improve reproducibility and generalizability across and within scientific investigations. This is particularly relevant given the emerging use of US to assess skeletal muscle characteristics in healthy and clinical populations.

Table 3-1. Subject Characteristics

Group (n)	Age (yrs)	Height (cm)	Weight (kg)	BMI (kg/m^2)	Body Fat (%)	Body Fat (kg)	Lean Mass (kg)	Peak Isometric Torque (Nm)
YM (8)	26 ± 4^{A}	178 ± 7^{a}	75 ± 8^{a}	24 ± 2^{a}	18 ± 1^{Aa}	12 ± 1^{A}	58 ± 7^{a}	224 ± 69^{a}
YF (8)	25 ± 4^{B}	166 ± 5^{Ba}	57 ± 6^{a}	21 ± 2^{Ba}	24 ± 3^{Ba}	13 ± 2^{B}	42 ± 3^{a}	157 ± 39^{Ba}
OM (7)	70 ± 7^{A}	177 ± 6^{b}	82 ± 12^{b}	26 ± 5	28 ± 9^{A}	23 ± 10^{A}	56 ± 6^{b}	182 ± 43^{b}
OF (5)	69 ± 8^{B}	158 ± 6^{Bb}	65 ± 11^{b}	26 ± 3^{B}	36 ± 5^{B}	23 ± 7^{B}	34 ± 5^{b}	112 ± 21^{Bb}
Y (8f, 8m)	26 ± 4^{A}	172 ± 9	66 ± 12	22 ± 2^{A}	21 ± 4^{A}	13 ± 2^{A}	49 ± 10	194 ± 66^{A}
O (5f, 7m)	70 ± 7^{A}	170 ± 11	75 ± 15	26 ± 3^{A}	32 ± 8^{A}	23 ± 8^{A}	49 ± 10	153 ± 50^{A}
M (15)	47 ± 23	178 ± 7^{a}	78 ± 11^{a}	25 ± 3	24 ± 9	18 ± 9	56 ± 6^{a}	205 ± 61^{a}
F (13)	42 ± 23	163 ± 7^{a}	60 ± 9^{a}	23 ± 3	29 ± 7	17 ± 7	41 ± 4^{a}	138 ± 39^{a}

Data are mean ± SD. Capital letters = age effect; Lower case letters = sex effect; Same letters denote differences within effect. Significance set at $p < 0.05$. BMI, body mass index; Y, young; O, old; M, male; F, female.

Table 3-2. Muscle Thickness at A1

Group	RF		VI		RF + VI	
	Stand**	Supine**	Stand**	Supine**	Stand**	Supine**
YM	2.38±0.11	2.04±0.11[a]	2.48±0.12[A]	1.81±0.11	4.97±0.19	3.94±0.19
YF	2.28±0.11	1.72±0.11[a]	2.47±0.12[B]	1.73±0.11	4.90±0.19[A]	3.57±0.19
OM	2.38±0.13	1.74±0.12	2.10±0.13[A]	1.55±1.12	4.69±0.20	3.42±0.20
OF	2.15±0.16	1.63±0.16	1.97±0.17[B]	1.41±0.16	4.16±0.25[A]	2.99±0.24
Y	2.33±0.08	1.88±0.08	2.47±0.08[A]	1.77±0.08[B]	4.93±0.14[A]	3.76±0.13[B]
O	2.26±0.10	1.68±0.10	2.03±0.11[A]	1.47±0.10[B]	4.44±0.16[A]	3.20±0.16[B]
M	2.38±0.09[a]	1.89±0.08	2.28±0.09	1.68±0.08	4.83±0.14	3.68±0.14
F	2.21±0.10[a]	1.67±0.10	2.22±0.10	1.57±0.10	4.55±0.16	3.27±0.14

Data are mean±SE. **Posture effect present in all comparisons; *Posture effect in pairwise comparisons; Capital letters = age effect; Lower case letters = sex effect; Same letters or symbols denote differences within effect.

Table 3-3. Muscle Thickness at A2

Group	RF		VI		RF + VI	
	Stand	Supine	Stand**	Supine**	Stand**	Supine**
YM	1.58±0.10[A]	1.37±0.10	2.22±0.13	1.51±0.13	3.96±0.20	3.01±0.20
YF	1.72±0.10*	1.20±0.10*	2.40±0.13[A]	1.56±0.13[A]	4.22±0.20[A]	2.91±0.20[A]
OM	1.88±0.11*[A]	1.23±0.11*	1.85±0.14	1.34±0.14	3.89±0.22	2.67±0.22
OF	1.89±0.14*	1.05±0.13*	1.65±0.18[A]	1.06±0.14[A]	3.55±0.26[A]	2.23±0.26[A]
Y	1.65±0.07*[A]	1.28±0.07*	2.30±0.09[A]	1.54±0.09[B]	4.09±0.14	2.96±0.14[A]
O	1.89±0.09*[A]	1.13±0.09*	1.75±0.11[A]	1.20±0.11[B]	3.73±0.17	2.44±0.17[A]
M	1.73±0.08*	1.30±0.08*	2.03±0.10	1.42±0.10	3.92±0.15	2.84±0.15
F	1.81±0.09*	1.12±0.08*	2.02±0.11	1.31±0.10	3.89±0.16	2.56±0.16

Data are mean±SE. **Posture effect present in all comparisons; *Posture effect in pairwise comparisons; Capital letters = age effect; Same letters or symbols denote differences within effect.

Table 3-4. Muscle Thickness at L1

Group	VL		VI		VL + VI	
	Stand	Supine	Stand	Supine	Stand	Supine
YM	2.56±0.09^{Aa}	2.78±0.09^{Ab}	1.88±1.11	2.02±0.11^{A}	4.53±0.19^{Aa}	4.90±0.19^{Ab}
YF	1.91±0.09^{Ba}	2.12±0.09^{Bb}	1.75±0.11^{A}	1.76±1.11^{B}	3.78±0.19^{Ba}	4.00±0.19^{Bb}
OM	1.77±0.10^{A}	1.95±0.10^{A}	1.62±0.13	1.45±0.12^{A}	3.59±0.20^{A}	3.50±0.50^{A}
OF	1.52±0.12^{B}	1.70±0.12^{B}	1.28±0.15^{A}	1.17±0.15^{B}	3.05±0.24^{B}	2.93±0.24^{B}
Y	2.24±0.07^{*A}	2.45±0.07^{*B}	1.82±0.08^{A}	1.89±0.08^{B}	4.16±0.14^{A}	4.45±0.14^{B}
O	1.65±0.08^{A}	1.83±0.08^{B}	1.45±0.10^{A}	1.30±0.10^{B}	3.32±0.16^{A}	3.21±0.16^{B}
M	2.17±0.07^{*a}	2.36±0.07^{*b}	1.75±0.09	1.74±0.08^{a}	4.06±0.14^{a}	4.20±0.14^{b}
F	1.71±0.08^{a}	1.91±0.08^{b}	1.52±0.09	1.45±0.09^{a}	3.42±0.15^{a}	3.46±0.15^{b}

Data are mean±SE. *Posture effect in pairwise comparisons; Capital letters = age effect; Lower case letters = sex effect; Same letters or symbols denote differences within effect.

Table 3-5. Muscle Thickness at L2

Group	VL		VI		VL + VI	
	Stand	Supine	Stand	Supine	Stand	Supine
YM	2.47±0.09^{Aa}	2.68±0.09^{Aa}	1.83±0.13^{A}	1.76±0.13^{A}	4.41±0.18^{Aa}	4.56±1.18^{Aa}
YF	1.97±0.09^{*Ba}	2.24±0.09^{*Ba}	1.69±0.13^{B}	1.62±0.13^{B}	3.78±0.18^{Ba}	3.98±1.18^{Ba}
OM	1.82±0.10^{A}	1.69±0.10^{A}	1.34±0.14^{A}	1.28±0.14^{A}	3.28±0.20^{A}	3.09±0.20^{A}
OF	1.65±0.12^{B}	1.51±0.12^{B}	1.19±0.17^{B}	1.04±0.17^{B}	2.98±0.23^{B}	2.60±0.23^{A}
Y	2.22±0.07^{*A}	2.46±0.07^{*B}	1.76±0.10^{A}	1.69±0.10^{B}	4.09±0.13^{A}	4.27±0.13^{B}
O	1.73±0.08^{A}	1.60±0.08^{B}	1.26±0.11^{A}	1.16±0.11^{B}	3.12±0.15^{A}	2.85±0.15^{B}
M	2.14±0.07^{a}	2.18±0.07^{b}	1.59±0.10	1.52±0.10	3.85±0.14^{a}	3.82±0.14^{b}
F	1.81±0.08^{a}	1.88±0.08^{b}	1.44±0.11	1.33±0.11	3.37±0.15^{a}	3.30±0.15^{b}

Data are mean±SE. *Posture effect in pairwise comparisons; Capital letters = age effect; Lower case letters = sex effect; Same letters or symbols denote differences within effect.

Table 3-6. Muscle Thickness at L3

Group	VL		VI		VL + VI	
	Stand	Supine	Stand	Supine	Stand	Supine
YM	1.43±0.10^{a}	1.35±0.10	1.66±0.13^{A}	1.85±0.13^{A}	3.18±0.18	3.31±0.18^{A}
YF	1.07±0.10^{a}	1.24±0.10	1.63±0.12	1.67±0.14^{B}	2.86±0.17	3.00±0.19^{B}
OM	1.48±0.12	1.46±0.11^{a}	1.16±0.15^{A}	1.00±0.14^{A}	2.76±0.21	2.55±0.20^{A}
OF	1.14±0.15	1.03±0.13^{a}	1.26±0.20	0.91±0.17^{B}	3.32±0.23	1.99±0.22^{B}
Y	1.25±0.07	1.30±0.07	1.64±0.09^{A}	1.76±0.09^{B}	3.02±0.13^{A}	3.16±0.13^{B}
O	1.30±0.10	1.26±0.09	1.21±0.12^{A}	0.95±0.11^{B}	2.53±0.15^{A}	2.27±0.15^{B}
M	1.46±0.08^{a}	1.40±0.08^{b}	1.41±0.10	1.43±0.10	2.97±0.14	2.93±0.13^{a}
F	1.09±0.09^{a}	1.15±0.08^{b}	1.44±0.12	1.29±0.11	2.58±0.14	2.49±0.14^{a}

Data are mean±SE. Capital letters = age effect; Lower case letters = sex effect; Same letters or symbols denote differences within effect.

Table 3-7. Pennation Angle

Group	L1 VL		L1 VI		L2 VL		L2 VI		L3 VL	
	Stand	Supine	Stand	Supine	Stand	Supine	Stand	Supine	Stand	Supine
YM	11.9±1.0	14.2±0.9^{A}	11.1±0.9^{A}	9.7±0.9^{A}	13.8±10.9^{*A}	16.6±0.9^{*Aa}	10.2±1.1	12.4±1.0^{Aa}	17.1±1.2^{a}	17.7±1.1^{Aa}
YF	11.7±0.9	12.5±0.9^{B}	9.0±0.9	10.0±0.9	11.0±0.9*	15.2±0.9^{*Ba}	11.8±1.0*	8.6±1.1^{*a}	12.5±1.3^{a}	13.1±1.1^{a}
OM	9.3±1.0	9.8±1.0^{A}	7.1±1.2^{A}	5.8±1.1^{A}	10.5±1.1^{A}	9.4±1.0^{A}	8.7±1.2	6.6±1.1^{A}	13.7±1.2	12.4±1.2^{A}
OF	9.0±1.2	9.3±1.2^{B}	7.0±1.5	6.5±1.9	9.6±1.2	8.3±1.2^{B}	8.0±1.8	8.0±1.3	12.3±1.3	13.0±1.2
Y	11.8±0.7^{A}	13.4±0.7^{B}	10.1±0.7^{A}	9.9±0.7^{B}	12.4±0.7^{*A}	15.9±0.7^{*B}	11.1±0.8^{A}	10.5±0.8^{B}	14.8±0.9	15.5±0.8^{A}
O	9.1±0.8^{A}	9.6±0.8^{B}	7.0±0.9^{A}	6.4±1.1^{B}	10.0±0.8^{A}	8.9±0.8^{B}	8.8±1.1^{A}	7.2±0.9^{B}	13.0±0.9	12.7±1.8^{A}
M	10.5±0.7	12.0±0.7	9.1±0.8	7.7±0.7	12.1±0.7	13.0±0.7	9.4±0.9	9.5±0.8	15.4±0.8^{a}	15.1±0.8
F	10.4±0.7	10.9±0.7	8.0±0.9	8.5±1.0	10.2±0.8	11.8±0.8	10.6±1.0	8.1±0.9	12.4±0.9^{a}	13.1±0.8

Data are mean±SE. *Posture effect in pairwise comparisons; Capital letters = age effect; Lower case letters = sex effect; Same letters or symbols denote differences within effect.

Table 3-8. Echogenicity at A1

Group	RF		VI	
	Stand	Supine	Stand	Supine
YM	27.8±4.4^{Aa}	31.9±4.2^{Aa}	31.3±3.4^{Aa}	35.7±3.3^{A}
YF	48.3±4.2^{a}	51.8±4.2^{a}	41.0±3.3^{a}	42.7±3.3
OM	42.0±5.1^{A}	50.7±4.9^{A}	46.7±4.0^{A}	54.2±3.8^{A}
OF	45.3±6.0	56.9±5.6	47.4±4.7*****	63.4±4.4*****
Y	38.1±3.0	41.8±3.0^{A}	36.2±2.4^{A}	39.2±2.3^{B}
O	43.8±3.9	53.6±3.7^{A}	47.3±3.1*****^{A}	58.5±2.9*****^{B}
M	34.9±3.4^{a}	41.3±3.2^{b}	38.7±2.6	45.2±2.5
F	47.0±3.6^{a}	54.0±3.5^{b}	44.7±2.8*****	52.6±2.7*****

Data are mean±SE. *Posture effect in pairwise comparisons; Capital letters = age effect; Lower case letters = sex effect; Same letters or symbols denote differences within effect.

Table 3-9. Echogenicity at A2

Group	RF		VI	
	Stand	Supine	Stand	Supine
YM	28.1±4.1^{a}	31.7±4.1^{Aa}	28.5±3.6	35.2±3.6^{A}
YF	44.3±4.1^{a}	49.9±4.1^{Aa}	38.3±3.6	41.9±3.6^{B}
OM	37.5±4.8	49.8±5.0	37.8±4.2	48.5±4.4^{A}
OF	43.1±5.2	49.1±5.2	44.1±4.6*****	58.0±4.6*****^{B}
Y	36.2±2.9	40.8±2.9	33.4±2.6	38.5±2.6^{A}
O	40.2±3.5	49.4±3.6	41.0±3.1*****	53.1±3.2*****^{A}
M	32.9±3.1^{a}	40.5±3.2	33.1±2.8*****^{a}	41.9±2.8*****^{b}
F	43.4±3.3^{a}	49.8±3.2	41.4±2.9*****^{a}	49.7±2.9*****^{b}

Data are mean±SE. *Posture effect in pairwise comparisons; Capital letters = age effect; Lower case letters = sex effect; Same letters or symbols denote differences within effect.

Table 3-10. Echogenicity at L1

Group	VL		VI	
	Stand	Supine	Stand	Supine
YM	32.4±4.4^{a}	30.7±4.4^{Aa}	38.2±4.5	35.2±4.5^{A}
YF	47.7±4.4^{a}	46.3±4.4^{Ba}	46.6±4.5	46.9±4.5^{B}
OM	42.3±5.3	50.4±5.1^{A}	38.2±5.4	52.1±5.1^{A}
OF	54.7±5.9	60.2±5.6^{B}	50.3±5.9	61.3±5.6^{B}
Y	40.1±3.1	38.5±3.1^{A}	42.4±3.2	41.0±3.2^{A}
O	48.4±4.0	55.4±3.8^{A}	44.2±4.0*	56.8±3.8^{*A}
M	37.4±3.4^{a}	40.5±3.4^{b}	38.3±3.5^{a}	43.5±3.4^{b}
F	51.1±3.6^{a}	53.4±3.5^{b}	48.3±3.7^{a}	54.3±3.6^{b}

Data are mean±SE. *Posture effect in pairwise comparisons; Capital letters = age effect; Lower case letters = sex effect; Same letters or symbols denote differences within effect.

Table 3-11. Echogenicity at L2

Group	VL		VI	
	Stand	Supine	Stand	Supine
YM	30.1±4.0^{Aa}	29.4±4.0^{Aa}	37.0±4.4	35.0±4.4^{Aa}
YF	51.1±4.0^{a}	52.1±4.0^{a}	45.9±4.4	47.6±4.4^{Ba}
OM	42.9±1.7^{A}	46.2±4.7^{A}	42.6±5.1	51.7±5.1^{A}
OF	43.1±5.1	53.1±5.1	48.1±5.6*	64.0±5.6^{*B}
Y	40.7±2.9	40.8±2.9^{A}	41.4±3.1	41.3±3.1
O	43.1±3.5	49.6±3.5^{A}	45.3±3.8*	57.8±3.8*
M	36.4±3.1^{a}	37.9±3.1^{b}	39.7±3.4	43.4±3.4^{a}
F	47.3±3.2^{a}	52.5±3.2^{b}	47.1±3.5	55.7±3.5^{a}

Data are mean±SE. *Posture effect in pairwise comparisons; Capital letters = age effect; Lower case letters = sex effect; Same letters or symbols denote differences within effect.

Table 3-12. Echogenicity at L3

Group	VL		VI	
	Stand	Supine	Stand	Supine
YM	34.7±6.0^{a}	30.9±5.6^{a}	24.8±4.1	20.5±4.0^{A}
YF	54.3±5.2^{a}	58.5±5.4^{a}	32.7±3.6	30.7±4.0^{B}
OM	43.6±6.9	45.7±6.9	34.8±4.7	41.5±4.7^{A}
OF	41.8±7.9	54.7±6.6	28.5±5.4*	53.3±4.5^{*B}
Y	44.6±4.0	44.7±3.9	29.0±2.8	25.5±2.9^{A}
O	42.7±5.3	50.2±4.8	32.0±3.7*	47.5±3.3^{*A}
M	39.2±4.3	38.4±4.5^{a}	29.5±3.2	31.3±3.1^{a}
F	48.2±4.7	56.6±4.3^{a}	31.5±3.2*	41.8±3.1^{*a}

Data are mean±SE. *Posture effect in pairwise comparisons; Capital letters = age effect; Lower case letters = sex effect; Same letters or symbols denote differences within effect.

Table 3-13**.** Test-Retest Intraclass Correlation Coefficients for Anterior Muscle Thickness

	A1			A2		
	RF	**VI**	**RF+VI**	**RF**	**VI**	**RF+VI**
			Supine			
M	0.940 *(0.871-0.972)*	0.784 *(0.573-0.897)*	0.910 *(0.817-0.957)*	0.853 *(0.703-0.930)*	0.945 *(0.883-0.974)*	0.936 *(0.867-0.970)*
UM	0.901 *(0.798-0.954)*	0.781 *(0.573-0.894)*	0.924 *(0.842-0.964)*	0.743 *(0.509-0.874)*	0.653 *(0.376-0.824)*	0.694 *(0.441-0.845)*
			Standing			
M	0.785 *(0.580-0.896)*	0.853 *(0.699-0.931)*	0.780 *(0.572-0.894)*	0.818 *(0.640-0.913)*	0.932 *(0.858-0.969)*	0.904 *(0.802-0.954)*
UM	0.865 *(0.710-0.940)*	0.809 *(0.606-0.913)*	0.887 *(0.766-0.947)*	0.722 *(0.475-0.863)*	0.876 *(0.745-0.943)*	0.836 *(0.682-0.922)*

Data are ICC (95% confidence interval). M, marked leg; UM, unmarked leg; A1, anterior quadriceps 56%; A2, anterior quadriceps 39%; RF, rectus femoris; VI, vastus intermedius.

Table 3-14. Test-Retest Intraclass Correlation Coefficients for Anterior Muscle Thickness in Young

	A1			A2		
	RF	**VI**	**RF+VI**	**RF**	**VI**	**RF+VI**
			Supine			
M	0.948 *(0.858-0.981)*	0.865 *(0.655-0.951)*	0.888 *(0.715-0.959)*	0.912 *(0.767-0.969)*	0.908 *(0.759-0.967)*	0.930 *(0.814-0.975)*
UM	0.942 *(0.843-0.979)*	0.749 *(0.413-0.905)*	0.900 *(0.745-0.964)*	0.849 *(0.628-0.944)*	0.833 *(0.594-0.938)*	0.830 *(0.578-0.937)*
			Standing			
M	0.942 *(0.846-0.979)*	0.872 *(0.672-0.953)*	0.897 *(0.730-0.963)*	0.851 *(0.628-0.945)*	0.948 *(0.859-0.981)*	0.931 *(0.817-0.975)*
UM	0.822 *(0.554-0.936)*	0.853 *(0.607-0.949)*	0.876 *(0.629-0.959)*	0.763 *(0.455-0.909)*	0.955 *(0.875-0.984)*	0.894 *(0.729-0.962)*

Data are ICC (95% confidence interval). M, marked leg; UM, unmarked leg; A1, anterior quadriceps 56%; A2, anterior quadriceps 39%; RF, rectus femoris; VI, vastus intermedius.

Table 3-15. Test-Retest Intraclass Correlation Coefficients for Anterior Muscle Thickness in Old

	A1			A2		
	RF	**VI**	**RF+VI**	**RF**	**VI**	**RF+VI**
			Supine			
M	0.934 *(0.766-0.983)*	0.684 *(0.112-0.912)*	0.905 *(0.706-0.972)*	0.767 *(0.327-0.932)*	0.942 *(0.798-0.984)*	0.910 *(0.717-0.973)*
UM	0.853 *(0.543-0.958)*	0.767 *(0.328-0.932)*	0.926 *(0.763-0.978)*	0.586 *(0.051-0.866)*	0.545 *(-0.002-0.850)*	0.598 *(0.087-0.863)*
			Standing			
M	0.602 *(0.006-0.877)*	0.784 *(0.327-0.942)*	0.552 *(-0.075-0.859)*	0.782 *(0.402-0.935)*	0.824 *(0.473-0.949)*	0.827 *(0.506-0.947)*
UM	0.939 *(0.730-0.987)*	0.709 *(0.163-0.925)*	0.898 *(0.674-0.971)*	0.650 *(0.120-0.892)*	0.682 *(0.137-0.910)*	0.733 *(0.287-0.916)*

Data are ICC (95% confidence interval). M, marked leg; UM, unmarked leg; A1, anterior quadriceps 56%; A2, anterior quadriceps 39%; RF, rectus femoris; VI, vastus intermedius.

Table 3-16. Test-Retest Intraclass Correlation Coefficients for Lateral Muscle Thickness

	L1			L2			L3		
	VL	**VI**	**VL+VI**	**VL**	**VI**	**VL+VI**	**VL**	**VI**	**VL+VI**
					Supine				
M	0.927 *(0.847-0.966)*	0.785 *(0.585-0.895)*	0.904 *(0.805-0.954)*	0.948 *(0.891-0.975)*	0.974 *(0.889-0.975)*	0.985 *(0.968-0.993)*	0.773 *(0.542-0.896)*	0.949 *(0.883-0.978)*	0.923 *(0.830-0.996)*
UM	0.903 *(0.799-0.955)*	0.875 *(0.746-0.941)*	0.900 *(0.795-0.952)*	0.907 *(0.811-0.956)*	0.837 *(0.677-0.921)*	0.920 *(0.835-0.962)*	0.568 *(0.237-0.780)*	0.740 *(0.484-0.879)*	0.677 *(0.389-0.844)*
					Standing				
M	0.756 *(0.541-0.879)*	0.592 *(0.285-0.788)*	0.705 *(0.453-0.852)*	0.683 *(.425-0.839)*	.859 *(0.718-0.932)*	0.883 *(0.763-0.944)*	0.541 *(0.188-.773)*	0.780 *(0.535-0.905)*	0.496 *(0.124-0.784)*
UM	0.840 *(0.674-0.926)*	0.768 *(0.547-0.889)*	0.852 *(0.702-0.930)*	0.816 *(0.641-0.910)*	0.720 *(0.483-0.859)*	0.915 *(0.826-0.960)*	0.715 *(0.424-0.871)*	0.871 *(0.719-0.944)*	0.687 *(0.395-0.852)*

Data are ICC (95% confidence interval). M, marked leg; UM, unmarked leg; L1, lateral quadriceps 56%; L2, lateral quadriceps 39%; L3, lateral quadriceps 22%; VL, vastus lateralis; VI, vastus intermedius.

Table 3-17. Test-Retest Intraclass Correlation Coefficients for Lateral Muscle Thickness in Young

	L1			L2			L3		
	VL	**VI**	**VL+VI**	**VL**	**VI**	**VL+VI**	**VL**	**VI**	**VL+VI**
					Supine				
M	0.937 *(0.833-0.977)*	0.557 *(0.121-0.817)*	0.837 *(0.601-0.940)*	0.940 *(0.839-0.979)*	0.937 *(0.833-0.978)*	0.972 *(0.924-0.990)*	0.822 *(0.547-0.937)*	0.944 *(0.838-0.981)*	0.940 *(0.822-0.980)*
UM	0.832 *(0.583-0.938)*	0.763 *(0.450-0.910)*	0.752 *(0.425-0.905)*	0.857 *(0.646-0.947)*	0.788 *(0.486-0.916)*	0.744 *(0.402-0.903)*	0.239 *(-0.311-0.654)*	0.494 *(-0.051-0.807)*	0.311 *(-0.278-0.717)*
					Standing				
M	0.838 *(0.593-0.940)*	0.699 *(0.339-0.882)*	0.842 *(0.615-0.941)*	0.832 *(0.589-0.938)*	0.867 *(0.665-0.951)*	0.931 *(0.814-0.975)*	0.492 *(0.008-0.793)*	0.697 *(0.284-0.892)*	0.376 *(-0.143-0.735)*
UM	0.746 *(0.420-0.903)*	0.298 *(-0.244-0.688)*	0.649 *(0.235-0.862)*	0.658 *(0.245-0.867)*	0.462 *(-0.013-0.771)*	0.816 *(0.560-0.931)*	0.664 *(0.236-0.874)*	0.901 *(0.507-0.973)*	0.753 *(0.421-0.909)*

Data are ICC (95% confidence interval). M, marked leg; UM, unmarked leg; L1, lateral quadriceps 56%; L2, lateral quadriceps 39%; L3, lateral quadriceps 22%; VL, vastus lateralis; VI, vastus intermedius.

Table 3-18. Test-Retest Intraclass Correlation Coefficients for Lateral Muscle Thickness in Old

	L1			L2			L3		
	VL	**VI**	**VL+VI**	**VL**	**VI**	**VL+VI**	**VL**	**VI**	**VL+VI**
					Supine				
M	0.826 *(0.468-0.950)*	0.902 *(0.674-0.973)*	0.869 *(0.604-0.961)*	0.812 *(0.489-0.941)*	0.915 *(0.735-0.975)*	0.971 *(0.905-0.992)*	0.733 *(0.170-0.933)*	0.855 *(0.503-0.965)*	0.845 *(0.499-0.959)*
UM	0.932 *(0.766-0.981)*	0.927 *(0.754-0.980)*	0.940 *(0.806-0.982)*	0.819 *(0.479-0.945)*	0.813 *(0.488-0.942)*	0.923 *(0.761-0.977)*	0.909 *(0.647-0.977)*	0.780 *(0.306-0.941)*	0.944 *(0.805-0.984)*
					Standing				
M	0.388 *(-0.199-0.773)*	0.483 *(-0.129-0.821)*	0.457 *(-0.148-0.808)*	-0.018 *(-0.625-0.557)*	0.710 *(0.263-0.907)*	0.698 *(0.218-0.904)*	0.795 *(0.311-0.954)*	0.894 *(0.504-0.981)*	0.840 *(0.433-0.965)*
UM	0.894 *(0.620-0.975)*	0.923 *(0.727-0.980)*	0.955 *(0.844-0.988)*	0.845 *(0.565-0.952)*	0.824 *(0.517-0.945)*	0.919 *(0.746-0.976)*	0.937 *(0.676-0.989)*	0.743 *(0.199-0.942)*	0.444 *(-0.282-0.842)*

Data are ICC (95% confidence interval). M, marked leg; UM, unmarked leg; L1, lateral quadriceps 56%; L2, lateral quadriceps 39%; L3, lateral quadriceps 22%; VL, vastus lateralis; VI, vastus intermedius.

Table 3-19. Test-Retest Intraclass Correlation Coefficients for Pennation Angle

	L1		L2		L3
	VL	VI	VL	VI	VL
			Supine		
M	0.822 *(0.646-.915)*	0.573 *(0.124-0.789)*	0.779 *(0.580-0.891)*	0.197 *(-0.257-0.605)*	0.751 *(0.510-0.882)*
U M	0.533 *(0.189-0.761)*	0.143 *(-0.513-0.658)*	0.771 *(0.555-0.890)*	0.439 *(-0.156-0.791)*	0.568 *(0.155-0.813)*
			Standing		
M	0.442 *(0.074-0.702)*	0.602 *(0.182-0.836)*	0.446 *(0.105-0.696)*	0.599 *(-0.018-0.884)*	0.373 *(-0.126-0.718)*
U M	0.674 *(0.404-0.835)*	0.310 *(-0.140-0.699)*	0.678 *(0.404-0.840)*	0.387 *(-0.218-0.767)*	0.721 *(0.418-0.880)*

Data are ICC (95% confidence interval). M, marked leg; UM, unmarked leg; L1, lateral quadriceps 56%; L2, lateral quadriceps 39%; L3, lateral quadriceps 22%; VL, vastus lateralis; VI, vastus intermedius.

Table 3-20. Test-Retest Intraclass Correlation Coefficients for Pennation Angle Young

	L1		L2		L3
	VL	VI	VL	VI	VL
			Supine		
M	0.841 *(0.605-0.941)*	0.436 *(-0.161-0.790)*	0.580 *(0.149-0.829)*	-0.077 *(-0.676-0.558)*	0.840 *(0.582-0.945)*
U M	0.439 *(-0.078-0.764)*	-0.414 *(-0.998-0.425)*	0.620 *(0.167-0.855)*	0.854 *(0.193-0.984)*	0.788 *(0.340-0.947)*
			Standing		
M	0.599 *(0.149-0.844)*	0.493 *(-0.119-0.825)*	0.285 *(-0.261-0.681)*	0.420 *(-0.502-0.873)*	0.341 *(-0.435-0.806)*
U M	0.703 *(0.325-0.886)*	0.326 *(-0.187-0.769)*	0.749 *(0.410-0.905)*	-0.806 *(-1.157-0.103)*	0.745 *(0.252-0.930)*

Data are ICC (95% confidence interval). M, marked leg; UM, unmarked leg; L1, lateral quadriceps 56%; L2, lateral quadriceps 39%; L3, lateral quadriceps 22%; VL, vastus lateralis; VI, vastus intermedius.

Table 3-21. Test-Retest Intraclass Correlation Coefficients for Pennation Angle Old

	L1		L2		L3
	VL	VI	VL	VI	VL
			Supine		
M	0.653 *(0.094-0.895)*	-0.048 *(-0.962-0.718)*	0.586 *(0.030-0.862)*	-0.298 *(-0.520-0.476)*	0.523 *(-0.106-0.847)*
U M	0.319 *(-0.356-0.773)*	0.541 *(-0.193-0.956)*	0.514 *(-0.069-0.840)*	-0.960 *(-1.247- -0.197)*	0.140 *(-0.640-0.723)*
			Standing		
M	0.191 *(-0.463-0.683)*	-0.560 *(-1.163-0.582)*	0.591 *(-0.017-0.870)*	0.929 *(0.202-0.998)*	0.225 *(-0.631-0.786)*
U M	0.474 *(-.147-0.818)*	0.099 *(-0.936-0.903)*	0.332 *(-0.367-0.770)*	0.727 *(-0.090-0.957)*	0.683 *(0.111-0.912)*

Data are ICC (95% confidence interval). M, marked leg; UM, unmarked leg; L1, lateral quadriceps 56%; L2, lateral quadriceps 39%; L3, lateral quadriceps 22%; VL, vastus lateralis; VI, vastus intermedius.

Table 3-22. Test-Retest Intraclass Correlation Coefficients for Echogenicity

	A1		A2		L1		L2		L3	
	RF	**VI**	**RF**	**VI**	**VL**	**VI**	**VL**	**VI**	**VL**	**VI**
					Supine					
M	0.742 *(0.507-0.874)*	0.631 *(0.340-0.813)*	0.661 *(0.377-0.830)*	0.752 *(0.517-0.880)*	0.735 *(0.504-0.869)*	0.836 *(0.670-0.922)*	0.540 *(0.204-0.761)*	0.807 *(0.622-0.907)*	0.533 *(0.166-0.768)*	0.653 *(0.338-0.836)*
UM	0.586 *(0.266-0.790)*	0.700 *(0.417-0.856)*	0.594 *(0.284-0.793)*	0.638 *(0.339-0.820)*	0.761 *(0.540-0.884)*	0.794 *(0.600-0.901)*	0.605 *(0.294-0.799)*	0.729 *(0.492-0.866)*	0.858 *(0.700-0.936)*	0.750 *(0.490-0.888)*
					Standing					
M	0.552 *(0.209-0.772)*	0.437 *(0.077-0.699)*	0.569 *(0.250-0.777)*	0.643 *(0.352-0.820)*	0.577 *(0.246-0.786)*	0.675 *(0.392-0.841)*	0.542 *(0.212-0.762)*	0.546 *(0.212-0.764)*	0.265 *(-0.222-0.639)*	0.416 *(-0.042-0.727)*
UM	0.587 *(0.253-0.797)*	0.467 *(0.076-0.730)*	0.380 *(-0.003-0.662)*	0.542 *(0.210-0.762)*	0.663 *(0.373-0.834)*	0.751 *(0.517-0.881)*	0.608 *(0.302-0.800)*	0.629 *(0.335-0.811)*	0.703 *(0.393-0.868)*	0.665 *(0.334-0.850)*

Data are ICC (95% confidence interval). M, marked leg; UM, unmarked leg; A1, anterior quadriceps 56%; A2, anterior quadriceps 39%; L1, lateral quadriceps 56%; L2, lateral quadriceps 39%; L3, lateral quadriceps 22%; RF, rectus femoris; VI, vastus intermedius; VL, vastus lateralis.

Table 3-23. Test-Retest Intraclass Correlation Coefficients for Echogenicity in Young

	A1		A2		L1		L2		L3	
	RF	**VI**	**RF**	**VI**	**VL**	**VI**	**VL**	**VI**	**VL**	**VI**
					Supine					
M	0.684 *(0.295-0.878)*	0.613 *(0.203-0.844)*	0.692 *(0.326-0.879)*	0.746 *(0.425-0.902)*	0.619 *(0.184-0.849)*	0.846 *(0.583-0.945)*	0.497 *(0.003-0.792)*	0.780 *(0.477-0.917)*	0.527 *(0.024-0.813)*	0.591 *(0.101-0.849)*
UM	0.555 *(0.100-0.818)*	0.587 *(0.158-0.832)*	0.604 *(0.185-0.840)*	0.634 *(0.236-0.853)*	0.742 *(0.402-0.902)*	0.803 *(0.579-0.937)*	0.595 *(0.153-0.838)*	0.817 *(0.562-0.932)*	0.871 *(0.657-0.956)*	0.519 *(-0.075-0.835)*
					Standing					
M	0.488 *(-0.01-0.788)*	0.571 *(0.111-0.827)*	0.560 *(0.093-0.822)*	0.630 *(0.232-0.851)*	0.644 *(0.234-0.859)*	0.722 *(0.383-0.892)*	0.599 *(0.152-0.840)*	0.663 *(0.261-0.868)*	0.226 *(-0.386-0.683)*	0.468 *(-0.067-0.799)*
UM	0.587 *(0.116-0.840)*	0.431 *(-0.101-0.767)*	0.434 *(-0.086-0.761)*	0.496 *(0.015-0.790)*	0.647 *(0.228-0.862)*	0.824 *(0.568-0.935)*	0.576 *(0.122-0.829)*	0.742 *(0.403-0.902)*	0.763 *(0.391-0.921)*	0.684 *(0.232-0.892)*

Data are ICC (95% confidence interval). M, marked leg; UM, unmarked leg; A1, anterior quadriceps 56%; A2, anterior quadriceps 39%; L1, lateral quadriceps 56%; L2, lateral quadriceps 39%; L3, lateral quadriceps 22%; RF, rectus femoris; VI, vastus intermedius; VL, vastus lateralis.

Table 3-24**.** Test-Retest Intraclass Correlation Coefficients for Echogenicity in Old

	A1		A2		L1		L2		L3	
	RF	**VI**	**RF**	**VI**	**VL**	**VI**	**VL**	**VI**	**VL**	**VI**
					Supine					
M	0.810 *(0.427-0.945)*	0.538 *(-0.051-0.850)*	0.488 *(-0.052-0.824)*	0.646 *(0.132-0.889)*	0.749 *(0.320-0.925)*	0.692 *(0.171-0.907)*	0.522 *(-0.021-0.839)*	0.770 *(0.333-0.933)*	0.577 *(-0.134-0.888)*	0.111 *(-0.647-0.708)*
UM	0.502 *(-0.182-0.850)*	0.720 *(0.234-0.921)*	0.382 *(-0.272-0.799)*	0.489 *(-0.193-0.845)*	0.706 *(0.251-0.910)*	0.643 *(0.150-0.887)*	0.510 *(-0.115-0.841)*	0.348 *(-0.331-0.775)*	0.830 *(0.460-0.955)*	0.665 *(0.110-0.905)*
					Standing					
M	0.799 *(0.404-0.945)*	0.336 *(-0.169-0.758)*	0.644 *(0.150-0.887)*	0.642 *(0.144-0.887)*	0.378 *(-0.233-0.792)*	0.589 *(0.043-0.875)*	0.228 *(-0.384-0.708)*	0.182 *(-0.365-0.672)*	0.636 *(-0.284-0.940)*	0.193 *(-0.812-0.837)*
UM	0.595 *(-0.01-0.889)*	0.485 *(-0.214-0.855)*	0.244 *(-0.458-0.729)*	0.602 *(0.008-0.877)*	0.666 *(0.081-0.906)*	0.327 *(-0.420-0.784)*	0.730 *(0.254-0.920)*	0.232 *(-0.421-0.717)*	0.300 *(-0.473-0.807)*	0.524 *(-0.309-0.886)*

Data are ICC (95% confidence interval). M, marked leg; UM, unmarked leg; A1, anterior quadriceps 56%; A2, anterior quadriceps 39%; L1, lateral quadriceps 56%; L2, lateral quadriceps 39%; L3, lateral quadriceps 22%; RF, rectus femoris; VI, vastus intermedius; VL, vastus lateralis.

Table 3-25. Muscle Thickness for A1 Rectus Femoris

Group	Stand				Supine			
	Marked		Unmarked		Marked		Unmarked	
	ABS (cm)	REL (%)	ABS (cm)	REL (%)	ABS (cm)	REL (%)	ABS (cm)	REL (%)
YM	0.10±0.06^{A}	5.94±3.21	0.14±0.06	6.20±3.43	0.11±0.06	5.36±3.21	0.10±0.06	4.55±3.21
YF	0.10±0.06	4.43±3.21$^{\#}$	0.25±0.06	15.2±3.21$^{\#}$	0.10±0.06	6.05±3.21	0.13±0.06	8.09±3.21
OM	0.38±0.06$^{*\#Aa}$	15.1±3.43	0.17±0.08$^{\#}$	6.58±4.54	0.16±0.07*	10.7±3.70	0.21±0.06	11.3±3.43
OF	0.15±0.08^{a}	7.10±4.54	0.12±0.08	5.85±4.54	0.12±0.08	6.36±5.54	0.26±0.08	16.5±4.54
Y	0.12±0.04^{A}	5.16±2.27	0.20±0.04	10.7±2.35	0.10±0.04	5.71±2.27	0.23±0.05	6.32±2.27^{B}
O	0.27±0.05^{A}	11.1±2.84	0.15±0.06	6.21±3.21	0.14±0.05	8.55±2.93	0.11±0.04	13.9±2.84^{B}
M	0.26±0.04^{*a}	10.5±2.35	0.16±0.05	6.39±2.84	0.13±0.05*	8.05±2.45	0.15±0.04	7.91±2.35
F	0.13±0.05^{a}	5.77±2.78$^{\#}$	0.19±0.05	10.5±2.78$^{\#}$	0.11±0.05	6.20±2.78	0.19±0.05	12.3±2.78

Data are mean±SE. Capital letters = age effect; Lower case letter = sex effect; *Denotes posture effects; $^{\#}$Denotes marking effects; same letters or symbols denote differences within effect; ABS, absolute day-to-day difference; REL; relative day-to-day difference; Y, young; O, old; M, male; F, female.

Table 3-26. Muscle Thickness for A1 Vastus Intermedius

Group	Stand				Supine			
	Marked		Unmarked		Marked		Unmarked	
	ABS	REL	ABS	REL	ABS	REL	ABS	REL
YM	0.22±0.07	10.5±3.60	0.16±0.08^{A}	6.33±3.85^{B}	0.12±0.07	6.58±3.60^{B}	0.11±0.07	5.86±3.60
YF	0.13±0.07	4.72±3.60	0.16±0.07	7.57±3.60	0.11±0.07	5.66±3.60	0.12±0.07	6.90±3.60
OM	0.31±0.08	14.2±3.85	0.43±0.09^{A}	22.8±4.60^{Bb}	0.34±0.09	21.1±4.15^{B}	0.24±0.08	12.8±3.85
OF	0.05±0.12	2.76±5.87	0.18±0.10	9.16±5.09^{b}	0.20±0.10	13.8±5.09	0.17±0.10	14.8±5.09
Y	0.17±0.05	7.63±2.54	0.16±0.05	6.95±2.63^{B}	0.12±0.05	6.12±2.54^{B}	0.13±0.05	6.38±2.54
O	0.18±0.07	8.47±3.51	0.31±0.07	16.0±3.41^{B}	0.27±0.07	17.5±3.28^{B}	0.21±0.07	13.8±3.19
M	0.27±0.05	12.4±2.63^{a}	0.30±0.06	14.6±2.98	0.23±0.06	13.8±2.75	0.18±0.05	9.33±2.63
F	0.09±0.07	3.74±3.44^{a}	0.17±0.06	8.36±3.12	0.16±0.06	9.75±3.12	0.140.06	10.8±3.12

Data are mean±SE. Capital letters = age effect; Lower case letter = sex effect; same letters or symbols denote differences within effect; ABS, absolute day-to-day difference; REL; relative day-to-day difference; Y, young; O, old; M, male; F, female.

Table 3-27. Muscle Thickness for A1 RF+VI

Group	Stand				Supine			
	Marked		Unmarked		Marked		Unmarked	
	ABS	REL	ABS	REL	ABS	REL	ABS	REL
YM	0.32±0.11	6.67±2.49	0.34±0.13	4.39±2.66	0.21±0.11	5.63±2.49	0.20±0.11	4.99±2.49
YF	0.13±0.11	2.61±2.49	0.31±0.11	8.51±2.49	0.20±0.11	5.60±2.49	0.20±0.11	5.75±2.49
OM	0.59±0.12	12.1±2.66	0.34±0.13	8.39±2.87	0.36±0.12	10.4±2.66	0.31±0.12	8.15±2.66
OF	0.22±0.15	5.17±3.52	0.08±0.14	2.07±3.15	0.20±0.14	5.93±3.15	0.17±0.14	5.81±3.15
Y	0.22±0.08	4.64±1.76	0.26±0.08	6.45±1.82	0.21±0.08	5.62±1.76	0.20±0.08	5.37±1.76
O	0.40±0.10	8.64±2.20	0.21±0.09	5.23±2.13	0.28±0.09	8.17±2.06	0.24±0.09	6.98±2.06
M	0.45±0.08[a]	9.39±1.82[b]	0.28±0.09	6.39±1.96	0.29±0.08	8.02±1.82	0.26±0.08	6.57±1.82
F	0.17±0.09[a]	3.89±2.15[b]	0.20±0.09	5.29±2.01	0.20±0.09	5.77±2.01	0.18±0.09	5.78±2.01

Data are mean±SE. Capital letters = age effect; Lower case letter = sex effect; *Denotes posture effects; #Denotes marking effects; same letters or symbols denote differences within effect; ABS, absolute day-to-day difference; REL; relative day-to-day difference; Y, young; O, old; M, male; F, female.

Table 3-28. Muscle Thickness for A2 Rectus Femoris

Group	Stand				Supine			
	Marked		Unmarked		Marked		Unmarked	
	ABS	REL	ABS	REL	ABS	REL	ABS	REL
YM	0.20±0.06	16.5±4.51	0.29±0.06	21.6±4.51	0.11±0.06	9.68±4.51	0.20±0.06	15.7±4.50
YF	0.16±0.06	8.71±4.51	0.18±0.06[A]	11.9±4.51	0.11±0.06	9.12±4.51	0.15±0.06	15.4±4.51
OM	0.26±0.07	14.4±4.82	0.17±0.07[a]	9.40±4.82	0.25±0.07	20.3±5.20	0.24±0.07	16.2±5.20
OF	0.21±0.09[#]	11.0±6.37	0.47±0.09[*#Aa]	24.2±6.37	0.09±0.08	9.12±5.70	0.14±0.08[*]	13.0±5.70
Y	0.18±0.05	12.6±3.19	0.24±0.05	16.7±3.19	0.11±0.05	9.40±3.19	0.18±0.05	15.5±3.19
O	0.23±0.06	12.7±3.99	0.32±0.06	16.8±3.99	0.17±0.06	14.7±3.86	0.19±0.06	14.6±3.86
M	0.23±0.05	15.5±3.30	0.23±0.05	15.5±3.30	0.18±0.05	15.0±3.44	0.22±0.05	15.9±3.44
F	0.18±0.06	9.88±3.90	0.33±0.06[*]	18.0±3.90	0.10±0.05	9.12±3.63	0.15±0.05[*]	14.2±3.63

Data are mean±SE. Capital letters = age effect; Lower case letter = sex effect; *Denotes posture effects; #Denotes marking effects; same letters or symbols denote differences within effect; ABS, absolute day-to-day difference; REL; relative day-to-day difference; Y, young; O, old; M, male; F, female.

Table 3-29. Muscle Thickness for A2 Vastus Intermedius

Group	Stand				Supine			
	Marked		Unmarked		Marked		Unmarked	
	ABS	REL	ABS	REL	ABS	REL	ABS	REL
YM	0.22±0.08	12.1±3.40	0.12±0.08	6.60±3.40	0.09±0.08	6.48±3.40	0.13±0.08^{A}	7.25±3.40
YF	0.07±0.08	3.39±3.40^{B}	0.16±0.08	7.54±3.40	0.10±0.08	5.81±3.40	0.09±0.08	6.02±3.40
OM	0.20±0.09	12.9±3.63	0.31±0.09	14.3±3.63	0.10±0.09$^{\#}$	7.82±3.92	0.37±0.09$^{\#A}$	16.6±3.90
OF	0.23±0.12	14.9±4.80^{B}	0.20±0.13	11.7±5.54	0.07±0.10	6.45±4.29	0.17±0.10	12.6±4.29
Y	0.14±0.06	7.76±2.40	0.14±0.06	7.07±2.40	0.10±0.06	6.15±2.40	0.11±0.06	6.64±2.40^{B}
O	0.22±0.08	13.9±3.01	0.25±0.08	13.0±3.31	0.09±0.07	7.13±2.91	0.27±0.07	14.6±2.91^{B}
M	0.21±0.06	12.5±2.49	0.21±0.06	10.5±2.49	0.10±0.06	7.15±2.59	0.25±0.06	11.9±2.59
F	0.15±0.07	9.13±2.94	0.18±0.08	9.61±3.25	0.08±0.07	6.13±2.74	0.13±0.07	9.29±2.74

Data are mean±SE. Capital letters = age effect; Lower case letter = sex effect; same letters denote differences within effect; ABS, absolute day-to-day difference; REL; relative day-to-day difference; Y, young; O, old; M, male; F, female.

Table 3-30. Muscle Thickness for A2 RF+VI

Group	Stand				Supine			
	Marked		Unmarked		Marked		Unmarked	
	ABS	REL	ABS	REL	ABS	REL	ABS	REL
YM	0.34±0.12	9.99±2.73	0.26±0.12	6.92±2.73	0.17±0.12	5.69±2.73	0.24±0.12	8.03±2.73
YF	0.21±0.12	4.99±2.73	0.36±0.12	10.4±2.73	0.13±0.12	4.22±2.73	0.27±0.12	9.81±2.73
OM	0.35±0.13	9.74±2.92	0.44±0.13	10.3±2.92	0.23±0.13	8.21±2.92	0.50±0.13	12.6±2.92
OF	0.26±0.15	7.05±3.45	0.34±0.15	10.4±3.45	0.13±0.15	5.12±3.45	0.20±0.15	7.84±3.45
Y	0.27±0.08	7.49±1.93	0.31±0.08	8.68±1.93	0.15±0.08	4.96±1.93	0.25±0.08	8.92±1.93
O	0.31±0.10	8.39±2.26	0.39±0.10	10.4±2.26	0.18±0.10	6.66±2.26	0.25±0.10	10.2±2.26
M	0.35±0.09	9.86±2.00	0.35±0.09	8.62±2.00	0.20±0.09	6.95±2.00	0.37±0.09	10.3±2.00
F	0.23±0.10	6.02±2.20	0.35±0.10	10.4±2.20	0.13±0.10	4.67±2.20	0.23±0.10	8.83±2.20

Data are mean±SE; ABS, absolute day-to-day difference; REL; relative day-to-day difference; Y, young; O, old; M, male; F, female.

Table 3-31. Muscle Thickness for L1 Vastus Lateralis

Group	Stand				Supine			
	Marked		Unmarked		Marked		Unmarked	
	ABS	REL	ABS	REL	ABS	REL	ABS	REL
YM	0.19±0.06$^{\#}$	7.25±4.30	0.38±0.06$^{\#Aa}$	18.2±4.30	0.14±0.06	5.07±4.30	0.28±0.06	10.7±4.30
YF	0.20±0.06^{A}	12.0±4.30^{B}	0.17±0.06^{a}	9.29±4.30	0.12±0.06	5.57±4.30	0.12±0.06	5.92±4.30
OM	0.28±0.07	15.6±4.59^{b}	0.16±0.08^{A}	7.22±4.96	0.16±0.07	8.10±4.59	0.13±0.07	7.32±4.59
OF	0.46±0.08$^{*\#A}$	35.1±5.44$^{*\#Bb}$	0.13±0.09$^{\#}$	10.1±6.08$^{\#}$	0.20±0.09*	14.1±6.08*	0.19±0.09	12.4±6.08
Y	0.20±0.04^{A}	9.62±3.04^{B}	0.27±0.04	13.8±3.04	0.13±0.04	5.32±3.04	0.20±0.04	8.32±3.04
O	0.37±0.05$^{*\#A}$	25.3±3.56$^{\#B}$	0.14±0.06$^{\#}$	8.65±3.92$^{\#}$	0.18±0.06*	11.1±3.81	0.16±0.06	9.85±3.81
M	0.23±0.05	11.4±3.15^{b}	0.27±0.05	12.7±3.28	0.15±0.05	6.58±3.15	0.21±0.05	9.01±3.15
F	0.33±0.05$^{*\#}$	23.5±3.46$^{*\#b}$	0.15±0.05$^{\#}$	9.68±3.72$^{\#}$	0.16±0.05*	9.84±3.72*	0.15±0.05	9.15±3.72

Data are mean±SE. Capital letters = age effect; Lower case letter = sex effect; *Denotes posture effects; #Denotes marking effects; same letters or symbols denote differences within effect; ABS, absolute day-to-day difference; REL; relative day-to-day difference; Y, young; O, old; M, male; F, female.

Table 3-32. Muscle Thickness for L1 Vastus Intermedius

Group	Stand				Supine			
	Marked		Unmarked		Marked		Unmarked	
	ABS	REL	ABS	REL	ABS	REL	ABS	REL
YM	0.24±0.09	11.7±5.67^{b}	0.25±0.09	15.7±5.67	0.37±0.09^{A}	20.8±5.67^{B}	0.30±0.09	14.1±5.67
YF	0.20±0.09	10.4±5.67	0.21±0.09	12.6±5.67	0.11±0.09	6.47±5.67^{B}	0.13±0.09	8.80±5.67
OM	0.48±0.10*	31.2±6.06^{*b}	0.23±0.11	14.7±6.55	0.06±0.10^{*A}	3.80±6.06^{*Bb}	0.19±0.10	15.1±6.06
OF	0.30±0.12	24.0±7.18	0.06±0.13	5.20±8.02	0.32±0.13	31.3±8.02^{Bb}	0.12±0.13	10.6±8.02
Y	0.22±0.07	11.1±4.01^{B}	0.23±0.07	14.2±4.01	0.24±0.07	13.6±4.01	0.21±0.07	11.4±4.01
O	0.39±0.08$^{\#}$	27.6±4.70$^{\#B}$	0.14±0.09$^{\#}$	9.96±5.18$^{\#}$	0.19±0.08	17.6±5.03	0.16±0.08	12.9±5.03
M	0.36±0.07	21.5±4.15	0.24±0.07	15.2±4.33	0.21±0.07	12.3±4.15	0.25±0.07	14.6±4.15
F	0.25±0.08	17.2±4.57	0.14±0.08	8.91±4.91	0.22±0.08	18.9±4.91	0.12±0.08	9.69±4.91

Data are mean±SE. Capital letters = age effect; Lower case letter = sex effect; *Denotes posture effects; #Denotes marking effects; same letters or symbols denote differences within effect; ABS, absolute day-to-day difference; REL; relative day-to-day difference; Y, young; O, old; M, male; F, female.

Table 3-33. Muscle Thickness for L1 VL+VI

Group	Stand				Supine			
	Marked		Unmarked		Marked		Unmarked	
	ABS	REL	ABS	REL	ABS	REL	ABS	REL
YM	0.39±0.13	7.97±3.89^{B}	0.59±0.13^{a}	15.9±3.89^{b}	0.37±0.13	7.81±3.89	0.48±0.13	10.0±3.89
YF	0.24±0.13^{A}	6.18±3.89^{B}	0.18±0.13^{a}	5.01±3.89^{b}	0.22±0.13	5.46±3.89	0.20±0.12	5.50±3.89
OM	0.70±0.14$^{*\#}$	20.2±4.16$^{*\#B}$	0.26±0.15$^{\#}$	7.44±4.49$^{\#}$	0.23±0.14*	6.43±4.16*	0.29±0.14	9.42±4.16
OF	0.73±0.16^{A}	27.0±4.92$^{\#B}$	0.24±0.16	7.95±4.92$^{\#}$	0.41±0.16	15.9±4.92	0.21±0.16	8.63±4.92
Y	0.31±0.09^{A}	7.08±2.75^{B}	0.39±0.09	10.5±2.75	0.29±0.09	6.63±2.75	0.34±0.09	7.75±2.75
O	0.72±0.11$^{*\#A}$	23.6±3.22$^{*\#B}$	0.25±0.11$^{\#}$	7.70±3.33$^{\#}$	0.32±0.11*	11.1±3.22*	0.25±0.11	9.02±3.22
M	0.54±0.10	14.1±2.85	0.42±0.10	11.7±2.97	0.30±0.10	7.12±2.85	0.39±0.10	9.71±2.85
F	0.49±0.10	16.6±3.14$^{\#}$	0.21±0.10	6.48±3.14$^{\#}$	0.31±0.10	10.7±3.14	0.21±0.10	7.07±3.14

Data are mean±SE. Capital letters = age effect; Lower case letter = sex effect; *Denotes posture effects; #Denotes marking effects; same letters or symbols denote differences within effect; ABS, absolute day-to-day difference; REL; relative day-to-day difference; Y, young; O, old; M, male; F, female.

Table 3-34. Muscle Thickness for L2 Vastus Lateralis

Group	Stand				Supine			
	Marked		Unmarked		Marked		Unmarked	
	ABS	REL	ABS	REL	ABS	REL	ABS	REL
YM	0.27±0.07	11.3±4.83	0.20±0.07	7.62±4.83	0.11±0.07	4.27±4.83	0.21±0.07	7.84±4.83
YF	0.14±0.07	7.11±4.83	0.24±0.07	13.3±4.83	0.15±0.07	6.88±4.83	0.16±0.07	7.60±4.83
OM	0.33±0.08$^{\#}$	21.5±5.16	0.11±0.08$^{\#}$	7.11±5.16	0.16±0.08	10.0±5.16	0.21±0.08	14.1±5.16
OF	0.25±0.09	15.0±6.11	0.11±0.09	7.46±6.11	0.15±0.09	10.5±6.11	0.20±0.09	15.1±6.11
Y	0.21±0.05	9.20±3.42	0.22±0.05	10.5±3.42	0.13±0.05	5.58±3.42	0.19±0.05	7.72±3.42
O	0.29±0.06$^{\#}$	18.3±4.00	0.11±0.06$^{\#}$	7.28±4.00	0.15±0.06	10.2±4.00	0.20±0.06	14.6±4.00
M	0.30±0.05$^{*\#}$	16.4±3.54	0.15±0.05$^{\#}$	7.36±3.54	0.13±0.05*	7.14±3.54	0.21±0.05	11.0±3.54
F	0.20±0.06	11.1±3.89	0.17±0.06	10.4±3.89	0.15±0.06	8.67±3.89	0.18±0.06	11.4±3.89

Data are mean±SE. *Denotes posture effects; #Denotes marking effects; same letters or symbols denote differences within effect; ABS, absolute day-to-day difference; REL; relative day-to-day difference; Y, young; O, old; M, male; F, female.

Table 3-35. Muscle Thickness for L2 Vastus Intermedius

Group	Stand				Supine			
	Marked		Unmarked		Marked		Unmarked	
	ABS	REL	ABS	REL	ABS	REL	ABS	REL
YM	0.22±0.08	10.5±5.26^{A}	0.31±0.08	18.8±5.62	0.10±0.08	5.36±5.26	0.23±0.08	13.6±5.26
YF	0.16±0.08	10.2±5.26	0.25±0.08	14.5±5.26	0.19±0.08	12.5±5.26	0.25±0.08	16.9±5.26
OM	0.29±0.08	30.0±5.62$^{\#A}$	0.14±0.08	6.65±5.62$^{\#a}$	0.21±0.08	18.5±5.62	0.23±0.08	20.3±5.62
OF	0.21±0.10	19.7±6.65	0.34±0.10	23.8±6.65^{a}	0.13±0.10	15.9±6.65	0.20±0.10	15.2±6.65
Y	0.19±0.05	10.4±3.72^{A}	0.28±0.05	16.7±3.72	0.14±0.05	8.95±3.72	0.24±0.05	15.2±3.72
O	0.25±0.06	24.9±4.36^{A}	0.24±0.06	15.2±4.36	0.17±0.06	17.2±4.36	0.22±0.06	17.8±4.36
M	0.26±0.06	20.3±3.85	0.23±0.06	12.7±3.85	0.16±0.06	11.9±3.85	0.23±0.06	16.9±3.85
F	0.19±0.06	15.0±4.24	0.30±0.06	19.2±4.24	0.16±0.06	14.2±4.24	0.23±0.06	16.1±4.24

Data are mean±SE. Capital letters = age effect; Lower case letter = sex effect; $^{\#}$Denotes marking effects; same letters or symbols denote differences within effect; ABS, absolute day-to-day difference; REL; relative day-to-day difference; Y, young; O, old; M, male; F, female.

Table 3-36. Muscle Thickness for L2 VL+VI

Group	Stand				Supine			
	Marked		Unmarked		Marked		Unmarked	
	ABS	REL	ABS	REL	ABS	REL	ABS	REL
YM	0.20±0.08	4.27±2.01	0.30±0.08	6.80±2.01	0.14±0.08$^{\#}$	2.99±2.01$^{\#}$	0.41±0.08$^{\#}$	9.23±2.01$^{\#}$
YF	0.27±0.08	7.30±2.01^{a}	0.16±0.08	4.00±2.01	0.19±0.08	5.16±2.01	0.31±0.08	8.45±2.01
OM	0.37±0.09*****	9.09±2.15	0.19±0.09	6.33±2.15	0.12±0.09*****	4.12±2.15	0.31±0.09	9.39±2.15
OF	0.43±0.10	14.7±2.54^{a}	0.33±0.10	10.2±2.54	0.23±0.10	9.59±2.54	0.12±0.10	5.19±2.54
Y	0.23±0.06	5.78±1.42^{A}	0.23±0.06	5.40±1.42	0.17±0.06$^{\#}$	4.08±1.42$^{\#}$	0.36±0.06$^{\#}$	8.84±1.42$^{\#}$
O	0.40±0.07*****	11.9±1.66*****^{A}	0.26±0.07	8.25±1.66	0.18±0.07*****	6.85±1.66*****	0.21±0.07	7.29±1.66
M	0.29±0.06	6.68±1.47^{a}	0.25±0.06	6.57±1.47	0.13±0.06$^{\#}$	3.56±1.47$^{\#}$	0.36±0.06$^{\#}$	9.31±1.47$^{\#}$
F	0.35±0.07	11.0±1.62^{a}	0.24±0.07	7.09±1.62	0.21±0.07	7.37±1.62	0.22±0.07	6.82±1.62

Data are mean±SE. Capital letters = age effect; Lower case letter = sex effect; *Denotes posture effects; $^{\#}$Denotes marking effects; same letters or symbols denote differences within effect; ABS, absolute day-to-day difference; REL; relative day-to-day difference; Y, young; O, old; M, male; F, female.

Table 3-37. Muscle Thickness for L3 Vastus Lateralis

Group	Stand				Supine			
	Marked		Unmarked		Marked		Unmarked	
	ABS	REL	ABS	REL	ABS	REL	ABS	REL
YM	0.42±0.09*	23.9±7.00	0.38±0.09^{A}	36.6±7.00^{B}	0.13±0.08*$^{\#}$	14.5±7.00$^{\#}$	0.38±0.08$^{\#}$	35.8±6.55$^{\#B}$
YF	0.21±0.08	18.5±6.55	0.20±0.08	19.4±6.55	0.20±0.09	10.1±6.55	0.28±0.08	23.9±6.66
OM	0.17±0.11	10.5±8.28	0.04±0.12^{A}	3.10±9.26^{B}	0.26±0.11	16.4±8.28	0.17±0.10	13.4±7.56^{B}
OF	0.12±0.14	10.2±10.7	0.11±0.14	10.9±10.7	0.11±0.12	10.8±9.26	0.10±0.12	10.9±9.26
Y	0.31±0.06	21.2±4.79	0.29±0.06^{A}	28.0±4.79^{B}	0.17±0.06	12.3±4.79$^{\#}$	0.33±0.06^{A}	29.9±4.63$^{\#B}$
O	0.15±0.09	10.3±6.76	0.08±0.09^{A}	6.98±7.07^{B}	0.19±0.08	13.6±6.21	0.13±0.08^{A}	12.1±5.98^{B}
M	0.30±0.07	17.2±5.42	0.21±0.08	19.9±5.80	0.20±0.07	13.3±5.28	0.27±0.06	24.6±5.00
F	0.16±0.08	14.3±6.27	0.16±0.08	15.1±6.27	0.16±0.08	12.6±5.80	0.19±0.07	17.4±5.70

Data are mean±SE. Capital letters = age effect; Lower case letter = sex effect; *Denotes posture effects; $^{\#}$Denotes marking effects; same letters or symbols denote differences within effect; ABS, absolute day-to-day difference; REL; relative day-to-day difference; Y, young; O, old; M, male; F, female.

Table 3-38. Muscle Thickness for L3 Vastus Intermedius

Group	Stand				Supine			
	Marked		Unmarked		Marked		Unmarked	
	ABS	REL	ABS	REL	ABS	REL	ABS	REL
YM	0.32±0.11	10.7±5.26	0.20±0.11	13.0±5.26	0.07±0.09$^{\#}$	4.25±4.56$^{\#B}$	0.41±0.10$^{\#A}$	17.6±4.87$^{\#}$
YF	0.24±0.09	18.2±4.56	0.14±0.09	9.60±4.56	0.16±0.11	12.1±5.26	0.21±0.10	14.7±4.87
OM	0.15±0.12	15.5±5.77	0.24±0.12	16.5±5.77	0.25±0.12	25.9±5.77$^{\#B}$	0.07±0.11^{A}	7.37±5.26$^{\#}$
OF	0.04±0.18	3.74±9.12	0.05±0.15	4.01±7.45	0.12±0.13	13.8±6.45	0.21±0.13	23.1±6.45
Y	0.28±0.07	14.5±3.48	0.17±0.07	11.3±3.48	0.12±0.07$^{\#}$	8.16±3.48^{B}	0.31±0.07$^{\#}$	16.2±3.45
O	0.10±0.11	9.62±5.39	0.15±0.09	10.3±4.71	0.18±0.09	19.9±4.33^{B}	0.14±0.08	15.2±4.16
M	0.23±0.08	13.1±3.91	0.22±0.08	14.7±3.90	0.16±0.07	15.1±3.68	0.24±0.07	12.5±3.59
F	0.14±0.10	11.0±5.10	0.10±0.09	6.81±4.37*	0.14±0.08	12.9±4.16	0.21±0.08	18.9±4.04*

Data are mean±SE. Capital letters = age effect; *Denotes posture effects; $^{\#}$Denotes marking effects; same letters or symbols denote differences within effect; ABS, absolute day-to-day difference; REL; relative day-to-day difference; Y, young; O, old; M, male; F, female.

Table 3-39. Muscle Thickness for L3 VL+VI

Group	Stand				Supine			
	Marked		Unmarked		Marked		Unmarked	
	ABS	REL	ABS	REL	ABS	REL	ABS	REL
YM	0.61±0.16[a]	12.5±4.05	0.42±0.16	15.5±4.05	0.20±0.15[#]	5.89±3.79[#]	0.69±0.16[#A]	19.4±4.05[#B]
YF	0.12±0.15[a]	4.16±3.79	0.20±0.15	7.90±3.79[*]	0.16±0.17	4.96±4.37[#]	0.52±0.16	20.2±4.05[*#]
OM	0.21±0.19	7.04±4.79	0.36±0.21	11.0±5.36	0.36±0.19	12.1±4.79	0.13±0.17[A]	5.26±4.37[B]
OF	0.22±0.25	10.5±6.18	0.32±0.19	14.0±4.79	0.21±0.19	10.7±4.79	0.19±0.19	8.89±4.79
Y	0.36±0.11	8.32±2.77	0.31±0.11	11.7±2.77[*]	0.18±0.12[#]	5.43±2.89[#]	0.60±0.11[#A]	19.8±2.86[*#B]
O	0.22±0.16	8.75±3.91	0.34±0.14	12.5±3.59	0.28±0.14	11.4±3.39	0.16±0.13[A]	7.07±3.24[B]
M	0.41±0.13	9.76±3.14	0.39±0.13	13.2±3.36	0.28±0.12	8.98±3.05	0.41±0.12	12.3±2.98
F	0.17±0.15	7.31±3.63	0.26±0.12	10.9±3.05	0.18±0.13	7.83±3.24	0.35±0.13	14.5±3.14

Data are mean±SE. Capital letters = age effect; Lower case letter = sex effect; *Denotes posture effects; #Denotes marking effects; same letters or symbols denote differences within effect; ABS, absolute day-to-day difference; REL; relative day-to-day difference; Y, young; O, old; M, male; F, female.

Table 3-40. Pennation Angle L1 Vastus Lateralis

Group	Stand				Supine			
	Marked		Unmarked		Marked		Unmarked	
	ABS	REL	ABS	REL	ABS	REL	ABS	REL
YM	2.85±0.80	33.3±8.61*	2.48±0.75*	23.5±8.05*	1.51±0.75#	9.26±8.05*#	5.45±0.75*#Aa	48.7±8.05*#a
YF	2.78±0.75	26.7±8.05	2.67±0.75	23.1±8.05	2.29±0.75	18.9±8.05	2.22±0.75a	18.3±8.05a
OM	4.34±0.80	51.9±8.61*	2.93±0.80	29.4±8.61	2.30±0.80	26.3±8.61*	1.90±0.87A	25.6±9.30
OF	3.69±0.95	39.2±10.2	2.85±0.95	31.8±10.2	2.27±1.06	27.6±11.4	2.86±1.06	26.1±11.4
Y	2.81±0.55	30.0±5.89	2.57±0.53	23.3±5.69	1.90±0.53#	14.1±5.69#	3.84±0.53#	33.5±5.69#
O	4.02±0.62	45.6±6.67	2.89±0.62	30.6±6.67	2.29±0.67	26.9±7.14	2.38±0.68	25.9±7.35
M	3.59±0.57*	42.6±6.09*	2.71±0.55	26.4±5.89	1.91±0.55*#	17.8±5.89*#	3.68±0.57#	37.2±6.15#
F	3.24±0.61	32.9±6.49	2.76±0.61	27.5±6.49	2.25±0.65	23.3±6.97	2.54±0.65	22.2±6.97

Data are mean±SE. Capital letters = age effect; Lower case letter = sex effect; *Denotes posture effects; #Denotes marking effects; same letters or symbols denote differences within effect; ABS, absolute day-to-day difference; REL; relative day-to-day difference; Y, young; O, old; M, male; F, female.

Table 3-41. Pennation Angle L1 Vastus Intermedius

Group	Stand				Supine			
	Marked		Unmarked		Marked		Unmarked	
	ABS	REL	ABS	REL	ABS	REL	ABS	REL
YM	3.87±0.92	47.6±15.8	4.16±1.12	36.6±19.3	2.83±1.00	34.6±17.3	4.33±1.00	51.6±17.3
YF	2.15±0.92	22.0±15.8A	2.27±1.00	25.7±17.3	2.71±0.79	32.8±13.6	4.14±1.30	27.6±22.3
OM	1.87±1.30	55.0±22.3	4.00±1.59	42.0±27.3	1.67±1.12	31.4±19.3	2.87±1.12	57.5±19.3
OF	3.88±1.59	86.7±27.3A	1.70±1.59	41.8±27.3	2.51±1.30	61.5±22.3	-	-
Y	3.01±0.65	34.8±11.1	3.22±0.75	31.2±12.9	2.77±0.64	33.7±11.0	4.23±0.82	39.6±14.1
O	2.87±1.02	70.8±17.6	2.85±1.12	41.9±19.3	2.09±0.86	46.5±14.7	2.87±1.12	57.5±19.3
M	2.87±0.79	51.3±13.6	4.08±0.97	39.3±16.7	2.25±0.75	33.0±12.9	3.60±0.75	54.6±12.9
F	3.01±0.92	54.3±15.8	1.98±0.94	33.8±16.2	2.61±0.76	47.1±13.1	4.14±1.30	27.6±22.3

Data are mean±SE. Capital letters = age effect; same letters or symbols denote differences within effect; ABS, absolute day-to-day difference; REL; relative day-to-day difference; Y, young; O, old; M, male; F, female.

Table 3-42. Pennation Angle L2 Vastus Lateralis

Group	Stand				Supine			
	Marked		Unmarked		Marked		Unmarked	
	ABS	REL	ABS	REL	ABS	REL	ABS	REL
YM	4.63±0.87	31.3±8.78	2.36±0.87	19.2±8.78	3.37±0.87	19.5±8.78	3.08±0.87	31.1±8.78
YF	3.04±0.87	28.3±8.78	2.99±0.87	33.6±8.78	1.88±0.87	12.9±8.78[A]	3.05±0.93	22.2±9.39
OM	2.21±0.93	28.8±11.1	2.98±1.01	32.8±10.1	2.10±0.93	25.8±9.39	1.92±1.01	17.3±10.1
OF	3.23±1.11	20.0±9.39	3.49±1.11	43.5±11.1	3.52±1.11	49.5±11.1[A]	1.33±1.11	19.6±11.1
Y	3.83±0.62	29.8±6.21	2.67±0.62	26.4±6.21	2.63±0.62	16.2±6.21[A]	3.07±0.64	26.6±6.43
O	2.72±0.72	24.4±7.27	3.23±0.75	38.1±7.52	2.81±0.72	37.7±7.27[A]	1.63±0.75	18.4±7.52
M	3.42±0.64	25.7±6.43	2.67±0.67	26.0±6.71	2.74±0.64	22.7±6.43	2.50±0.67	24.2±6.71
F	3.14±0.70	28.5±7.08	3.24±0.70	38.5±7.08	2.70±0.70	31.2±7.08	2.19±0.72	20.9±7.27

Data are mean±SE. Capital letters = age effect; same letters or symbols denote differences within effect; ABS, absolute day-to-day difference; REL; relative day-to-day difference; Y, young; O, old; M, male; F, female.

Table 3-43. Pennation Angle L2 Vastus Intermedius

Group	Stand				Supine			
	Marked		Unmarked		Marked		Unmarked	
	ABS	REL	ABS	REL	ABS	REL	ABS	REL
YM	4.47±1.41	50.4±24.1	1.88±2.00	21.4±34.0	3.60±1.26	21.9±21.5	1.53±2.00	18.7±34.0
YF	1.21±2.00	10.4±34.0	3.30±1.26	30.8±21.5	3.80±1.26	68.6±21.5	2.21±1.63	26.0±27.8
OM	0.66±1.63	11.7±27.8	2.07±1.41	23.2±24.1	2.16±1.41	24.1±24.1	3.35±1.41	76.8±24.1
OF	-	-	2.43±2.00	23.1±34.0	2.55±2.00	29.8±34.0	2.80±1.41	31.1±24.1
Y	2.84±1.22	30.4±20.8	2.59±1.18	26.1±20.1	3.70±0.89	45.2±15.2	1.87±1.29	22.3±22.0
O	0.66±1.63	11.7±27.8	2.25±1.22	23.1±20.8	2.36±1.22	26.9±20.8	3.07±1.00	54.0±17.0
M	2.57±1.08	31.0±18.4	1.98±1.22	22.3±20.8	2.88±0.95	23.0±16.1	2.44±1.22	47.8±20.8
F	1.21±2.00	10.4±34.0	2.87±1.18	26.9±20.1	3.17±1.18	49.2±20.1	2.50±1.08	28.5±18.4

Data are mean±SE; ABS, absolute day-to-day difference; REL; relative day-to-day difference; Y, young; O, old; M, male; F, female.

Table 3-44. Pennation Angle L3 Vastus Lateralis

Group	Stand				Supine			
	Marked		Unmarked		Marked		Unmarked	
	ABS	REL	ABS	REL	ABS	REL	ABS	REL
YM	4.75±1.19	51.0±13.2*****	2.95±1.19	19.4±13.2	2.02±1.01	12.9±11.1*****	2.73±1.34	16.0±14.7
YF	3.58±1.34	23.2±14.7	3.83±1.19	37.1±13.2	2.16±1.01	21.5±11.1	3.35±1.19	23.0±13.2
OM	2.59±1.34	23.8±14.7	2.13±1.09	14.9±12.0	3.06±1.09	25.3±12.0	5.03±1.34	47.9±14.7
OF	2.41±1.34	21.3±14.7	2.38±1.34	21.8±14.7	3.24±1.19	26.9±13.2	4.36±1.19	28.2±13.2
Y	4.17±0.90	37.1±9.88	3.39±0.84	28.3±9.32	2.09±0.71	17.2±7.87	3.04±0.90	19.5±9.88
O	2.50±0.94	22.5±10.4	2.26±0.86*****	18.4±9.51	3.15±0.81	26.0±8.92	4.69±0.90*****	38.1±9.88
M	3.67±0.90	37.4±9.88	2.54±0.81	17.2±8.92	2.54±0.74	19.0±8.20	3.88±0.94	32.0±10.4
F	3.00±0.94	22.2±10.4	3.11±0.90	29.5±9.88	2.70±0.78	24.2±8.63	3.86±0.84	25.6±9.32

Data are mean±SE. *Denotes posture effects; same letters or symbols denote differences within effect; ABS, absolute day-to-day difference; REL; relative day-to-day difference; Y, young; O, old; M, male; F, female.

Table 3-45. Echogenicity for A1 Rectus Femoris

Group	Stand				Supine			
	Marked		Unmarked		Marked		Unmarked	
	ABS	REL	ABS	REL	ABS	REL	ABS	REL
YM	6.02±3.15	20.8±5.40	4.70±3.41	15.3±5.84	3.06±3.15[A]	8.92±5.42	6.34±3.15	19.7±5.05
YF	8.26±2.95	16.9±5.05	9.26±2.95	14.8±5.05	10.6±2.95	17.4±5.05	9.50±2.95	20.8±5.05
OM	7.68±3.41	17.8±5.84	7.52±3.73	15.0±6.39	12.4±3.41[A]	24.1±5.84	9.29±3.41	16.7±5.84
OF	3.56±4.17	10.8±7.15	10.9±4.17	28.6±7.15	6.63±3.73	11.2±6.39	11.9±4.17	20.6±7.15
Y	7.14±2.16	18.9±3.70	6.98±2.25	15.1±3.86	6.82±2.16	13.2±3.70	7.92±2.16	20.2±3.70
O	5.62±2.69	14.3±4.61	9.23±2.80	21.8±4.79	9.53±2.53	17.7±4.33	10.6±2.69	18.7±4.61
M	6.85±2.32	19.3±3.98	6.11±2.56	15.2±4.33	7.75±2.32	16.5±3.98	7.82±2.32	18.2±3.98
F	5.91±2.56	13.9±4.38	10.1±2.56	21.7±4.38	8.61±2.38	14.3±4.07	10.7±2.56	20.7±4.38

Data are mean±SE. Capital letters = age effect; same letters or symbols denote differences within effect; ABS, absolute day-to-day difference; REL; relative day-to-day difference; Y, young; O, old; M, male; F, female.

Table 3-46. Echogenicity for A1 Vastus Intermedius

Group	Stand				Supine			
	Marked		Unmarked		Marked		Unmarked	
	ABS	REL	ABS	REL	ABS	REL	ABS	REL
YM	8.54±3.76	23.5±7.32	8.43±4.06	29.6±7.91	6.72±3.76	16.7±7.32	8.65±3.76	23.6±7.32
YF	7.01±3.52	17.1±6.85	9.30±3.52	18.9±6.85	11.4±3.52	23.2±6.85	11.3±3.52	31.7±6.85
OM	18.1±4.06	37.0±7.91	11.1±4.45	18.3±8.67	12.7±4.06	20.9±7.91	9.91±4.06	18.2±7.91
OF	8.45±4.97	15.2±9.69	5.48±4.97	14.0±9.69	8.30±4.45	15.1±8.67	11.3±4.97	21.0±9.69
Y	7.77±2.57	20.3±5.01	8.86±2.69	24.3±5.23	9.06±2.57	19.9±5.01	9.99±2.57	27.7±5.01
O	13.3±3.21	26.1±6.25	8.28±3.34	16.1±6.50	10.5±3.01	18.0±5.87	10.6±3.21	19.6±6.25
M	13.3±2.77	30.2±5.39	9.76±3.01	23.9±5.87	9.73±2.77	18.8±5.39	9.28±2.77	20.9±5.39
F	7.73±3.04	16.1±5.93	7.39±3.04	16.5±5.93	9.85±2.83	19.1±5.52	11.3±3.04	26.3±5.93

Data are mean±SE; ABS, absolute day-to-day difference; REL; relative day-to-day difference; Y, young; O, old; M, male; F, female.

Table 3-47. Echogenicity for A2 Rectus Femoris

Group	Stand				Supine			
	Marked		Unmarked		Marked		Unmarked	
	ABS	REL	ABS	REL	ABS	REL	ABS	REL
YM	4.46±3.14[a]	14.9±7.82	4.17±3.14[A]	13.3±7.82[A]	3.10±3.14[a]	9.03±7.82	7.79±3.14	25.8±7.82
YF	14.7±2.94[a]	34.6±7.31	10.9±2.94	26.7±7.31	13.3±2.94[a]	21.1±7.31	7.64±2.94	19.6±7.31
OM	6.66±3.39	16.2±8.45[#]	15.7±3.39[A]	45.5±8.45[*#A]	11.1±3.39	22.1±8.45	8.98±3.71	18.8±9.25[*]
OF	10.2±3.71	23.6±9.25	9.76±3.71	25.5±9.25	13.2±3.71	28.6±9.25	14.7±3.71	34.5±9.25
Y	9.61±2.15	24.8±5.35	7.52±2.15	19.9±5.35	8.18±2.15	15.1±5.35	7.72±2.15	22.7±5.35
O	8.42±2.51	19.9±6.26	12.7±2.51	35.5±6.26	12.2±2.51	25.4±6.26	11.8±2.63	26.6±6.54
M	5.56±2.31[a]	15.6±5.75	9.92±2.31	29.4±5.75	7.12±2.31	15.6±5.75	8.38±2.43	22.3±6.06
F	12.5±2.37[a]	29.1±5.90	10.3±2.37	26.1±5.90	13.2±2.37	24.9±5.90	11.2±2.37	27.0±5.90

Data are mean±SE. Capital letters = age effect; Lower case letter = sex effect; *Denotes posture effects; #Denotes marking effects; same letters or symbols denote differences within effect; ABS, absolute day-to-day difference; REL; relative day-to-day difference; Y, young; O, old; M, male; F, female.

Table 3-48. Echogenicity for A2 Vastus Intermedius

Group	Stand				Supine			
	Marked		Unmarked		Marked		Unmarked	
	ABS	REL	ABS	REL	ABS	REL	ABS	REL
YM	5.76±3.21	18.2±6.81	5.22±3.21	13.7±6.81	5.64±3.21	12.5±6.81	8.99±3.21	24.0±6.81
YF	11.1±3.00	26.7±6.37	8.77±3.00	20.2±6.37	4.46±3.00	14.5±6.37	9.05±3.00	19.9±6.37
OM	11.0±3.47	25.5±7.35	11.6±3.47	31.9±7.35	4.46±3.47	9.13±7.35	8.34±3.80	14.9±8.05
OF	5.93±3.80	13.6±8.05	6.55±3.80	18.9±8.05	12.5±3.80	22.3±8.05	11.2±3.80	23.4±8.05
Y	8.44±2.20	22.4±466	6.70±2.20	16.9±4.66	5.05±2.20	12.5±4.66	9.02±2.20	22.0±4.66
O	8.44±2.57	19.6±5.45	9.06±2.57	25.4±5.45	8.46±2.57	15.6±5.45	9.78±2.69	19.2±5.70
M	8.36±2.36	21.8±5.01	8.40±2.36	22.8±5.01	5.05±2.36	10.8±5.01	8.67±2.49	19.5±5.27
F	8.52±2.42	20.2±5.13	7.66±2.42	19.6±5.13	8.46±2.42	18.4±5.13	10.1±2.42	21.7±5.13

Data are mean±SE; ABS, absolute day-to-day difference; REL; relative day-to-day difference; Y, young; O, old; M, male; F, female.

Table 3-49. Echogenicity for L1 Vastus Lateralis

Group	Stand				Supine			
	Marked		Unmarked		Marked		Unmarked	
	ABS	REL	ABS	REL	ABS	REL	ABS	REL
YM	4.41±3.04	12.4±5.66	5.03±3.04	14.5±5.66^{A}	2.92±3.04	9.68±5.66$^{\#}$	8.25±3.04	30.1±5.66$^{\#a}$
YF	3.88±2.85	8.13±5.29	11.3±2.85	21.6±5.29	8.62±2.85	18.1±5.29	7.52±2.84	14.9±5.29^{a}
OM	10.9±3.60	24.9±6.70	12.4±3.29	31.0±6.11^{A}	9.54±3.29	22.7±6.11	9.32±3.29	15.4±6.11
OF	9.44±3.60	20.5±6.70	10.2±4.02	14.8±7.49	12.9±3.60	22.2±6.70	6.57±3.60	11.6±6.70
Y	4.14±2.08	10.3±3.88^{A}	8.16±2.08	18.0±3.88	5.77±2.08	13.9±3.88	7.88±2.08	22.4±3.88
O	10.2±2.55	22.7±4.74^{A}	11.8±2.60	22.9±4.83	11.3±2.44	22.5±4.53	7.94±2.44	13.5±4.53
M	7.65±2.36	18.6±4.38	9.21±2.24	22.7±4.17	6.23±2.24	16.2±4.17	8.78±2.24	22.7±4.17
F	6.60±2.29	14.3±4.27	10.8±2.46	18.2±4.59	10.8±2.29	20.2±4.27	7.04±2.29	13.3±4.27

Data are mean±SE. Capital letters = age effect; Lower case letter = sex effect; $^{\#}$Denotes marking effects; same letters or symbols denote differences within effect; ABS, absolute day-to-day difference; REL; relative day-to-day difference; Y, young; O, old; M, male; F, female.

Table 3-50. Echogenicity for L1 Vastus Intermedius

Group	Stand				Supine			
	Marked		Unmarked		Marked		Unmarked	
	ABS	REL	ABS	REL	ABS	REL	ABS	REL
YM	9.27±3.50	20.7±8.00	4.88±3.50	11.5±8.00^{A}	7.97±3.50	22.9±8.00	7.81±3.50	21.7±8.00
YF	9.28±3.27	23.7±7.49	9.58±3.27	22.7±7.49	7.92±3.27	17.6±7.29	10.7±3.27	18.3±7.49
OM	12.8±4.14	33.8±9.47	14.7±3.78	42.7±8.64^{*Aa}	9.60±3.78	18.6±8.64	9.13±3.78	14.6±8.64*
OF	8.82±4.14	18.5±9.47	6.52±4.63	11.5±10.6^{a}	8.73±4.14	14.8±9.47	7.33±4.14	11.7±9.47
Y	9.27±2.40	22.2±5.48	7.2±2.40	17.1±5.48	7.95±2.40	20.2±5.48	9.27±2.40	20.0±5.48
O	11.3±2.93	26.1±6.70	10.6±2.99	27.1±6.83	9.17±2.80	16.7±6.41	8.23±2.80	13.2±6.41
M	11.5±2.71	27.2±6.20	9.79±2.58	27.1±5.89	8.79±2.58	20.8±5.89	8.47±2.58	18.2±5.89
F	9.05±2.64	21.1±6.04	8.00±2.84	17.1±6.48	8.33±2.64	16.2±6.04	9.03±2.64	15.0±6.04

Data are mean±SE. Capital letters = age effect; Lower case letter = sex effect; *Denotes posture effects; same letters or symbols denote differences within effect; ABS, absolute day-to-day difference; REL; relative day-to-day difference; Y, young; O, old; M, male; F, female.

Table 3-51. Echogenicity for L2 Vastus Lateralis

Group	Stand				Supine			
	Marked		Unmarked		Marked		Unmarked	
	ABS	REL	ABS	REL	ABS	REL	ABS	REL
YM	2.55±4.12	7.38±6.71	5.68±4.12	15.2±6.71	1.94±4.12^{A}	7.76±6.71^{A}	7.00±4.12	21.7±6.71
YF	10.9±3.85	17.0±6.28	10.90±3.85	18.6±6.28	11.7±3.85	18.3±6.28	13.7±3.85	22.8±6.28
OM	10.8±4.45	25.0±7.25	10.4±4.45	23.2±7.25	15.6±4.45^{A}	34.3±7.25^{Aa}	6.51±4.45	20.6±7.25
OF	8.35±4.87	20.0±7.94	6.27±4.87	16.1±7.94	4.82±4.87	8.27±7.94^{a}	13.8±4.87	25.1±7.94
Y	6.73±2.82	12.2±4.59	8.29±2.82	16.9±4.59	6.84±2.82	13.0±4.59	10.4±2.82	22.2±4.59
O	9.58±3.30	22.5±5.37	8.34±3.30	19.6±5.37	10.2±3.30	21.3±5.37	10.1±3.30	22.8±5.37
M	6.68±3.03	16.2±4.94	8.05±3.03	19.2±4.94	8.77±3.03	21.0±4.94	6.76±3.03	21.1±4.94
F	9.63±3.11	18.5±5.06	8.58±3.11	17.3±5.06	8.28±3.11	13.3±5.06	12.7±3.11	23.9±5.06

Data are mean±SE. Capital letters = age effect; Lower case letter = sex effect;; same letters denote differences within effect; ABS, absolute day-to-day difference; REL; relative day-to-day difference; Y, young; O, old; M, male; F, female.

Table 3-52. Echogenicity for L2 Vastus Intermedius

Group	Stand				Supine			
	Marked		Unmarked		Marked		Unmarked	
	ABS	REL	ABS	REL	ABS	REL	ABS	REL
YM	5.35±2.97^{A}	15.5±7.10	4.26±2.97^{A}	11.4±7.10^{A}	7.66±2.97	18.4±7.10	7.80±2.97	22.5±7.10
YF	11.2±2.78	23.8±6.64	5.57±2.78	14.6±6.64	5.91±2.78	14.4±6.64	8.52±2.78	18.4±6.64
OM	17.6±3.21^{A}	35.4±7.67	14.1±3.21^{A}	40.9±7.67^{A}	10.7±3.21	20.8±7.67	15.3±3.21	29.7±7.67
OF	11.7±3.52	27.1±8.40	13.1±3.52	33.2±8.40	6.57±3.52	9.46±8.40	7.16±3.52	12.7±8.40
Y	8.27±2.03^{A}	19.6±4.9	4.91±2.03^{A}	13.0±4.86^{A}	6.79±2.03	16.4±4.86	8.16±2.03	20.5±4.86
O	14.7±2.38^{A}	31.2±5.69*****	13.6±2.38^{A}	37.1±5.69^{A}	8.64±2.38	15.1±5.69*****	11.2±2.38	21.2±5.69
M	11.5±2.19	25.4±5.23	9.17±2.19	26.2±5.23	9.18±2.19	19.6±5.23	11.6±2.19	26.1±5.23
F	11.532.24	25.4±5.36	9.35±2.24	23.9±5.36	6.24±2.24	11.9±5.36	7.84±2.24	15.5±5.36

Data are mean±SE. Capital letters = age effect; *Denotes posture effects; same letters or symbols denote differences within effect; ABS, absolute day-to-day difference; REL; relative day-to-day difference; Y, young; O, old; M, male; F, female.

Table 3-53. Echogenicity for L3 Vastus Lateralis

Group	Stand				Supine			
	Marked		Unmarked		Marked		Unmarked	
	ABS	REL	ABS	REL	ABS	REL	ABS	REL
YM	8.29±6.12	22.4±8.40	3.25±6.12	9.79±8.40^{A}	5.78±4.63	18.8±6.35	2.97±5.00	9.52±6.86
YF	15.1±4.33	21.4±5.94	8.89±4.33	16.0±5.94	17.8±4.63	22.7±6.35	11.9±4.33	18.1±5.94
OM	6.91±6.12	13.2±8.40$^{\#}$	14.8±5.48	38.4±7.52$^{\#A}$	6.56±6.12	13.7±8.40	9.04±5.48	20.7±7.52
OF	6.84±8.66	22.0±11.9	6.72±7.07	16.8±9.70	11.6±5.48	25.7±7.52	11.3±5.48	19.3±7.52
Y	11.7±3.75	21.9±5.15	6.07±3.75	12.9±5.15	11.8±3.27	20.7±4.49	7.45±3.31	13.8±4.54
O	6.87±5.30	17.6±7.28	10.7±4.47	27.6±6.14	9.06±4.11	19.7±5.64	10.2±3.87	20.0±5.31
M	7.60±4.33	17.8±5.94	9.00±4.11	24.1±5.64	6.17±3.84	16.2±5.27	6.00±3.71	15.1±5.09
F	11.0±4.84	21.7±6.64	7.81±4.15	16.4±5.69	14.7±3.59	24.2±4.92	11.6±3.49	18.7±4.79

Data are mean±SE. Capital letters = age effect; $^{\#}$Denotes marking effects; same letters or symbols denote differences within effect; ABS, absolute day-to-day difference; REL; relative day-to-day difference; Y, young; O, old; M, male; F, female.

Table 3-54. Echogenicity for L3 Vastus Intermedius

Group	Stand				Supine			
	Marked		Unmarked		Marked		Unmarked	
	ABS	REL	ABS	REL	ABS	REL	ABS	REL
YM	4.06±2.58	18.5±10.2	1.64±4.58	8.82±10.2^{A}	6.03±3.46	22.7±7.71	4.47±4.09	21.5±9.12
YF	8.34±3.24	25.6±7.21^{A}	9.13±3.24	20.7±7.21	9.74±3.74	24.0±8.32	9.22±3.46	25.3±7.71
OM	11.1±4.58	23.7±10.2^{a}	8.47±4.09	37.1±9.12^{A}	15.4±4.58	37.0±10.2	8.36±4.09	21.2±9.12
OF	11.5±6.47	59.9±14.4$^{\#Aa}$	2.14±5.29	11.1±11.8$^{\#}$	15.6±4.09	29.9±9.12	7.88±4.09	14.8±9.12
Y	6.20±2.80	22.0±6.24	5.38±2.80	14.8±6.24	7.89±2.55	23.3±5.67	6.84±2.68	23.4±5.97
O	11.3±3.96	41.8±8.83	5.31±3.34	24.1±7.44	15.5±3.07	33.4±6.84	8.12±2.90	18.0±6.45
M	7.59±3.24	21.1±7.21^{a}	5.06±3.07	22.9±6.84	10.7±2.87	29.8±6.39	6.41±2.90	21.4±6.45
F	9.93±3.62	42.8±8.06$^{\#a}$	5.63±3.10	15.9±6.90$^{\#}$	12.7±2.77	27.0±6.17	8.55±2.68	20.0±5.97

Data are mean±SE. Capital letters = age effect; Lower case letter = sex effect; $^{\#}$Denotes marking effects; same letters or symbols denote differences within effect; ABS, absolute day-to-day difference; REL; relative day-to-day difference; Y, young; O, old; M, male; F, female.

Table 3-55. Best Single Site Predictors of Peak Isometric Torque of the Quadriceps

Group	Variable	R	R^2	Sig.	Equation
			Supine		
Y	MT L2 VL+VI	0.825	0.620	0.001	PIT = -45.6 + 44.7 * MT L2 VL+VI
O	EG L1 VI	0.909	0.827	0.012	PIT = 191.0 – 1.60 * EG L1 VI
ALL	MT L2 VI	0.889	0.791	0.03	PIT = 41.1 + 56.5 * MT L2 VI
			Standing		
Y	MT L2 VI	0.936	0.876	0.019	PIT = 20.1 + 66.0 * MT L2 VI
O	EG L3 VI	0.998	0.996	0.041	PIT = 67.5 + 1.02 * EG L3 VI
ALL	MT L1 VL+VI	0.828	0.686	0.0001	PIT = -3.33 + 32.9 * MT L1 VL+VI

Y, young; O, old; MT, muscle thickness; EG, echogenicity; L1, lateral site 56%; L2, lateral site 39%; L3, lateral site 22%; VL, vastus lateralis; VI, vastus intermedius; PIT, peak isometric torque.

Table 3-56. Stepwise Linear Regression Predicting Peak Isometric Torque of the Quadriceps

Group	Model(s)	R^2	Sig.	Equation
		Supine		
Y	1. X_1: MT L2 VL+VI	0.620	0.001	1. PIT = -45.6 + 44.7*X_1
	2. X_1: MT L2 VL+VI, X_2: MT A2 VI	0.886	0.0001	2. PIT = 12.0 + 62.5*X_1 – 89.8*X_2
	3. X_1: MT L2 VL+VI, X_2: MT A2 VI, X_3: MT L3 VL+VI	0.938	0.0001	3. PIT = 6.30 + 43.2*X_1 – 109.4*X_2 + 37.2*X_3
	4. X_1: MT L2 VL+VI, X_2: MT A2 VI, X_3: MT L3 VL+VI, X_4: EG A1 RF	0.969	0.0001	4. PIT = -53.5 + 50.9*X_1 – 98.3*X_2 + 29.9*X_3 + 0.083*X_4
O	1. X_1: EG L1 VI	0.827	0.012	1. PIT = 191.0 – 1.60*X_1
	2. X_1: EG L1 VI, X_2: MT L2 VI	0.966	0.006	2. PIT = 166.8 – 1.40*X_1 + 14.1*X_2
ALL	1. X_1: MT L2 VI	0.791	0.03	1. PIT = 41.1 + 56.5*X_1
		Standing		
Y	1. X_1: MT L2 VI	0.876	0.019	1. PIT = 20.1 + 66.0*X_1
O	1. X_1: EG L3 VI	0.996	0.041	1. PIT = 67.5 + 1.02*X_1
	2. X_1: EG L3 VI, X_2: MT L3 VL	1.00	-	2. PIT = 65.2 + 0.68*X_1 + 10.3*X_2
ALL	1. X_1: MT L1 VL+VI	0.686	0.0001	1. PIT = -3.33 + 32.9*X_1
	2. X_1: MT L1 VL+VI, X_2: MT A2 VI	0.764	0.0001	2. PIT = 28.3 + 43.6*X_1 – 54.6*X_2
	3. X_1: MT L1 VL+VI, X_2: MT A2 VI, X_3: MT L3 VL+VI	0.854	0.0001	3. PIT = 23.3 + 28.6*X_1 – 83.1*X_2 + 37.0*X_3

Y, young; O, old; MT, muscle thickness; EG, echogenicity; A1, anterior site 56%; A2, anterior site 39%; L1, lateral site 56%; L2, lateral site 39%; L3, lateral site 22%; VL, vastus lateralis; VI, vastus intermedius; RF, rectus femoris; PIT, peak isometric torque.

Table 3-57. Mixed Model Results for Posture in Muscle Thickness- Anterior Sites

Group	A1			A2		
	RF	VI	RF+VI	RF	VI	RF+VI
Sex	**0.037**	0.373	**0.020**	0.534	0.551	0.330
Age	0.143	**0.000**	**0.000**	0.580	**0.000**	**0.006**
Posture	**0.000**	**0.000**	**0.000**	**0.000**	**0.000**	**0.000**
Marking	0.871	0.287	0.535	0.537	0.784	0.628
Age × Posture	0.390	0.442	0.819	**0.017**	0.291	0.619
Sex × Posture	0.601	0.758	0.648	0.105	0.611	0.416
Posture × Marking	0.817	0.736	0.969	0.801	0.643	0.681
Age × Sex	0.810	0.648	0.400	0.686	0.087	0.138

Data are *P*-values; Bonferroni adjusted when applicable. **Bold** indicates significant ($P < 0.05$). A1, anterior quadriceps 56%; A2, anterior quadriceps 39%; RF, rectus femoris; VI, vastus intermedius.

Table 3-58. Mixed Model Results for Posture in Muscle Thickness- Lateral Sites

Group	L1			L2			L3		
	VL	VI	VL+VI	VL	VI	VL+VI	VL	VI	VL+VI
Sex	**0.000**	**0.005**	**0.000**	**0.000**	0.098	**0.001**	**0.000**	0.617	**0.004**
Age	**0.000**	**0.000**	**0.000**	**0.000**	**0.000**	**0.000**	0.951	**0.000**	**0.000**
Posture	**0.008**	0.698	0.531	0.427	0.407	0.733	0.981	0.504	0.650
Marking	0.859	0.376	0.830	0.400	0.821	0.703	0.320	0.586	0.795
Age × Posture	0.822	0.220	0.173	**0.010**	0.890	0.115	0.577	0.080	0.150
Sex × Posture	0.991	0.760	0.715	0.830	0.839	0.867	0.456	0.405	0.858
Posture × Marking	0.966	0.453	0.972	0.602	0.848	0.914	0.932	0.434	0.883
Age × Sex	**0.007**	0.536	0.360	**0.046**	0.796	0.468	0.372	0.607	0.513

Data are *P*-values; Bonferroni adjusted when applicable. **Bold** indicates significant ($P < 0.05$). L1, lateral quadriceps 56%; L2, lateral quadriceps 39%; L3, lateral quadriceps 22%; VL, vastus lateralis; VI, vastus intermedius.

Table 3-59. Mixed Model Results for Posture in Pennation Angle- Lateral Sites

Group	L1		L2		L3
	VL	VI	VL	VI	VL
Sex	0.384	0.807	**0.045**	0.904	**0.004**
Age	**0.000**	**0.000**	**0.000**	**0.003**	**0.009**
Posture	0.171	0.605	0.113	0.205	0.818
Marking	0.563	0.894	0.134	0.950	0.800
Age × Posture	0.420	0.795	**0.003**	0.548	0.537
Sex × Posture	0.499	0.233	0.618	0.157	0.564
Posture × Marking	0.130	0.654	0.949	0.589	0.179
Age × Sex	0.745	0.443	0.448	0.324	**0.020**

Data are *P*-values; Bonferroni adjusted when applicable. **Bold** indicates significant ($P < 0.05$). L1, lateral quadriceps 56%; L2, lateral quadriceps 39%; L3, lateral quadriceps 22%; VL, vastus lateralis; VI, vastus intermedius.

Table 3-60. Mixed Model Results for Posture in Echogenicity- Anterior Sites

Group	A1		A2	
	RF	VI	RF	VI
Sex	**0.001**	**0.015**	**0.003**	**0.006**
Age	**0.013**	**0.000**	0.056	**0.000**
Posture	**0.051**	**0.009**	**0.035**	**0.003**
Marking	0.630	0.243	0.143	0.389
Age × Posture	0.378	0.133	0.474	0.227
Sex × Posture	0.919	0.799	0.848	0.933
Posture × Marking	0.457	0.929	0.858	0.831
Age × Sex	**0.027**	0.552	**0.027**	0.952

Data are *P*-values; Bonferroni adjusted when applicable. **Bold** indicates significant ($P < 0.05$). A1, anterior quadriceps 56%; A2, anterior quadriceps 39%; RF, rectus femoris; VI, vastus intermedius.

Table 3-61. Mixed Model Results for Posture in Echogenicity- Lateral Sites

Group	L1		L2		L3	
	VL	VI	VL	VI	VL	VI
Sex	**0.000**	**0.004**	**0.000**	**0.006**	**0.004**	0.055
Age	**0.000**	**0.015**	0.082	**0.004**	0.690	**0.000**
Posture	0.442	0.116	0.301	0.079	0.402	0.060
Marking	0.689	0.441	0.652	0.528	0.896	0.885
Age × Posture	0.224	**0.051**	0.319	0.072	0.420	**0.004**
Sex × Posture	0.892	0.914	0.552	0.476	0.301	0.176
Posture × Marking	0.825	0.938	0.989	0.700	0.799	0.820
Age × Sex	0.543	0.924	**0.005**	0.785	**0.031**	0.343

Data are *P*-values; Bonferroni adjusted when applicable. **Bold** indicates significant ($P < 0.05$). L1, lateral quadriceps 56%; L2, lateral quadriceps 39%; L3, lateral quadriceps 22%; VL, vastus lateralis; VI, vastus intermedius.

Table 3-62. Mixed Model Results for Absolute Reliability in Muscle Thickness- Anterior Sites

Group	A1			A2		
	RF	VI	RF+VI	RF	VI	RF+VI
Sex	0.703	0.067	0.057	0.388	0.223	0.271
Age	**0.035**	**0.009**	0.239	0.227	**0.054**	0.311
Posture	0.168	0.287	0.390	0.063	0.301	0.180
Marking	0.743	0.892	0.401	0.192	0.155	0.099
Sex × Marking	0.110	0.607	0.368	0.510	0.901	0.733
Age × Marking	0.384	0.803	0.267	0.699	0.171	0.591
Posture × Marking	0.473	0.454	0.722	0.946	0.464	0.516

Data are *P*-values; Bonferroni adjusted when applicable. **Bold** indicates significant ($P < 0.05$). A1, anterior quadriceps 56%; A2, anterior quadriceps 39%; RF, rectus femoris; VI, vastus intermedius.

Table 3-63. Mixed Model Results for Absolute Reliability in Muscle Thickness- Lateral Sites

Group	L1			L2			L3		
	VL	VI	VL+VI	VL	VI	VL+VI	VL	VI	VL+VI
Sex	0.373	0.082	0.063	0.534	0.984	0.926	0.079	0.335	0.104
Age	0.911	0.792	0.578	0.930	0.855	0.780	**0.009**	0.228	0.197
Posture	**0.022**	0.298	0.126	0.258	0.289	0.406	0.762	0.907	0.921
Marking	0.412	0.214	0.159	0.666	0.219	0.640	0.975	0.889	0.324
Sex × Marking	**0.028**	0.720	0.202	0.609	0.563	0.078	0.864	0.545	0.640
Age × Marking	**0.005**	0.253	**0.024**	0.201	0.276	0.087	0.159	0.493	0.258
Posture × Marking	0.320	0.408	0.243	0.085	0.661	**0.020**	0.193	0.171	0.319

Data are *P*-values; Bonferroni adjusted when applicable. **Bold** indicates significant ($P < 0.05$). L1, lateral quadriceps 56%; L2, lateral quadriceps 39%; L3, lateral quadriceps 22%; VL, vastus lateralis; VI, vastus intermedius.

Table 3-64. Mixed Model Results for Relative Reliability in Muscle Thickness- Anterior Sites

Group	A1			A2		
	RF	VI	RF+VI	RF	VI	RF+VI
Sex	0.603	0.113	0.146	0.214	0.261	0.377
Age	0.064	**0.000**	0.153	0.803	**0.007**	0.297
Posture	0.803	0.914	0.939	0.745	0.390	0.497
Marking	0.369	0.794	0.592	0.228	0.313	0.055
Sex × Marking	**0.049**	0.337	0.252	0.362	0.680	0.205
Age × Marking	0.456	0.739	0.251	0.406	0.288	0.880
Posture × Marking	0.802	0.344	0.936	0.968	0.302	0.397

Data are *P*-values; Bonferroni adjusted when applicable. **Bold** indicates significant ($P < 0.05$). A1, anterior quadriceps 56%; A2, anterior quadriceps 39%; RF, rectus femoris; VI, vastus intermedius.

Table 3-65. Mixed Model Results for Relatively Reliability in Muscle Thickness- Lateral Sites

Group	L1			L2			L3		
	VL	VI	Both	VL	VI	Both	VL	VI	Both
Sex	0.374	0.349	0.573	0.976	0.785	0.206	0.191	0.835	0.516
Age	0.106	0.250	**0.037**	0.085	**0.037**	**0.026**	**0.003**	0.418	0.509
Posture	**0.022**	0.414	0.114	0.406	0.557	0.544	0.889	0.705	0.628
Marking	0.235	0.173	0.133	0.756	0.866	0.769	0.266	0.693	0.075
Sex × Marking	**0.042**	0.486	0.109	0.483	0.596	**0.023**	0.304	0.642	0.677
Age × Marking	**0.009**	0.133	**0.012**	0.330	**0.044**	0.087	**0.048**	0.241	**0.043**
Posture × Marking	0.299	0.553	0.277	0.152	0.333	**0.022**	0.303	0.338	0.492

Data are *P*-values; Bonferroni adjusted when applicable. **Bold** indicates significant ($P < 0.05$). L1, lateral quadriceps 56%; L2, lateral quadriceps 39%; L3, lateral quadriceps 22%; VL, vastus lateralis; VI, vastus intermedius.

Table 3-66. Mixed Model Results for Absolute Reliability in Pennation Angle- Lateral Sites

Group	L1		L2		L3
	VL	VI	VL	VI	VL
Sex	0.419	0.250	0.814	0.957	0.930
Age	0.809	0.186	0.290	0.297	0.948
Posture	0.352	0.946	0.258	0.561	0.897
Marking	0.802	0.439	0.556	0.867	0.546
Sex × Marking	0.326	0.392	0.581	0.501	0.606
Age × Marking	0.086	0.693	0.853	0.154	0.839
Posture × Marking	**0.036**	0.496	0.790	0.574	0.120

Data are *P*-values; Bonferroni adjusted when applicable. **Bold** indicates significant ($P < 0.05$). L1, lateral quadriceps 56%; L2, lateral quadriceps 39%; L3, lateral quadriceps 22%; VL, vastus lateralis; VI, vastus intermedius.

Table 3-67. Mixed Model Results for Relative Reliability in Pennation Angle- Lateral Sites

Group	L1		L2		L3
	VL	VI	VL	VI	VL
Sex	0.259	0.553	0.387	0.857	0.969
Age	0.123	0.151	0.381	0.780	0.921
Posture	0.132	0.962	0.291	0.433	0.711
Marking	0.785	0.758	0.857	0.952	0.976
Sex × Marking	0.425	0.478	0.977	0.425	0.556
Age × Marking	0.092	0.625	0.582	0.313	0.756
Posture × Marking	**0.016**	0.378	0.605	0.788	0.265

Data are *P*-values; Bonferroni adjusted when applicable. **Bold** indicates significant ($P < 0.05$). L1, lateral quadriceps 56%; L2, lateral quadriceps 39%; L3, lateral quadriceps 22%; VL, vastus lateralis; VI, vastus intermedius.

Table 3-68. Mixed Model Results for Absolute Reliability in Echogenicity- Anterior Sites

Group	A1		A2	
	RF	VI	RF	VI
Sex	0.191	0.688	**0.008**	0.480
Age	0.318	0.344	0.062	0.341
Posture	0.447	0.814	0.935	0.762
Marking	0.497	0.664	0.845	0.479
Sex × Marking	0.438	0.568	0.109	0.697
Age × Marking	0.644	0.369	0.323	0.953
Posture × Marking	0.917	0.614	0.691	0.276

Data are *P*-values; Bonferroni adjusted when applicable. **Bold** indicates significant (*P* < 0.05). A1, anterior quadriceps 56%; A2, anterior quadriceps 39%; RF, rectus femoris; VI, vastus intermedius.

Table 3-69. Mixed Model Results for Absolute Reliability in Echogenicity- Lateral Sites

Group	L1		L2		L3	
	VL	VI	VL	VI	VL	VI
Sex	0.453	0.794	0.132	0.468	**0.045**	0.218
Age	**0.019**	0.418	0.455	**0.002**	0.893	0.082
Posture	0.877	0.625	0.597	0.405	0.935	0.388
Marking	0.427	0.849	0.743	0.925	0.713	0.092
Sex × Marking	0.618	0.702	0.703	0.899	0.437	0.867
Age × Marking	0.250	0.968	0.448	0.586	0.198	0.146
Posture × Marking	0.271	0.665	0.772	0.143	0.942	0.795

Data are *P*-values; Bonferroni adjusted when applicable. **Bold** indicates significant (*P* < 0.05). L1, lateral quadriceps 56%; L2, lateral quadriceps 39%; L3, lateral quadriceps 22%; VL, vastus lateralis; VI, vastus intermedius.

Table 3-70. Mixed Model Results for Relative Reliability in Echogenicity- Anterior Sites

Group	A1		A2	
	RF	VI	RF	VI
Sex	0.879	0.419	0.120	0.694
Age	0.648	0.483	0.120	0.678
Posture	0.934	0.987	0.453	0.295
Marking	0.435	0.946	0.223	0.371
Sex × Marking	0.288	0.547	0.171	0.589
Age × Marking	0.745	0.190	0.373	0.624
Posture × Marking	0.496	0.316	0.940	0.302

Data are *P*-values; Bonferroni adjusted when applicable. **Bold** indicates significant (*P* < 0.05). A1, anterior quadriceps 56%; A2, anterior quadriceps 39%; RF, rectus femoris; VI, vastus intermedius.

Table 3-71. Mixed Model Results for Relative Reliability in Echogenicity- Lateral Sites

Group	L1		L2		L3	
	VL	VI	VL	VI	VL	VI
Sex	0.308	0.296	0.996	0.263	0.499	0.799
Age	0.168	0.794	0.115	**0.020**	0.266	0.178
Posture	0.974	0.213	0.514	0.134	0.693	0.945
Marking	0.504	0.760	0.449	0.536	0.969	0.120
Sex × Marking	0.264	0.994	0.837	0.728	0.431	0.363
Age × Marking	**0.048**	0.785	0.272	0.343	0.103	0.289
Posture × Marking	0.459	0.980	0.593	0.385	0.500	0.935

Data are *P*-values; Bonferroni adjusted when applicable. **Bold** indicates significant (*P* < 0.05). L1, lateral quadriceps 56%; L2, lateral quadriceps 39%; L3, lateral quadriceps 22%; VL, vastus lateralis; VI, vastus intermedius.

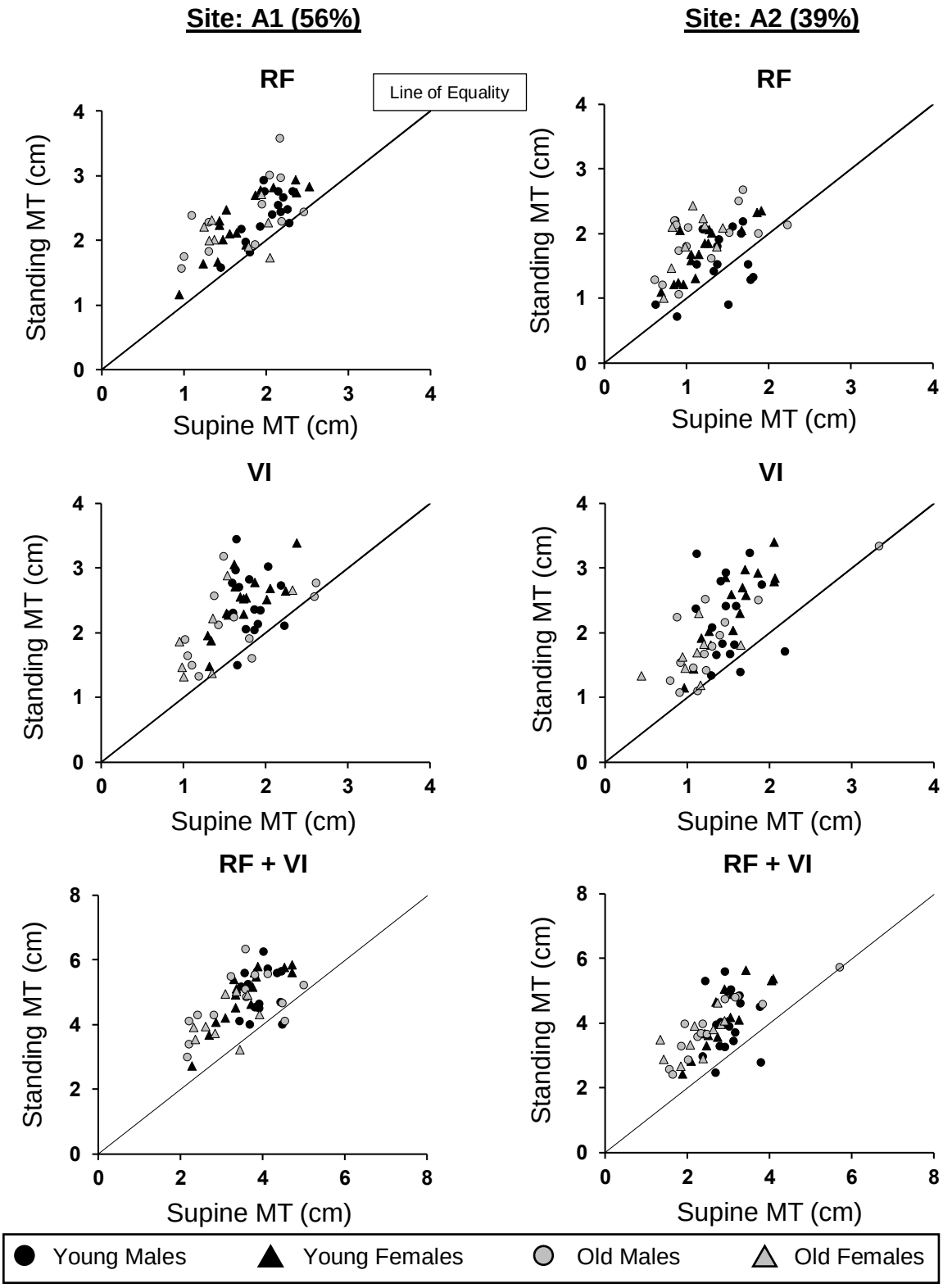


Figure 3-2. Skeletal muscle thickness of the anterior quadriceps measured while standing and supine. A1, anterior quadriceps 56% proximal from knee; A2, anterior quadriceps 39% proximal from knee; RF, rectus femoris; VI, vastus intermedius; MT, muscle thickness.

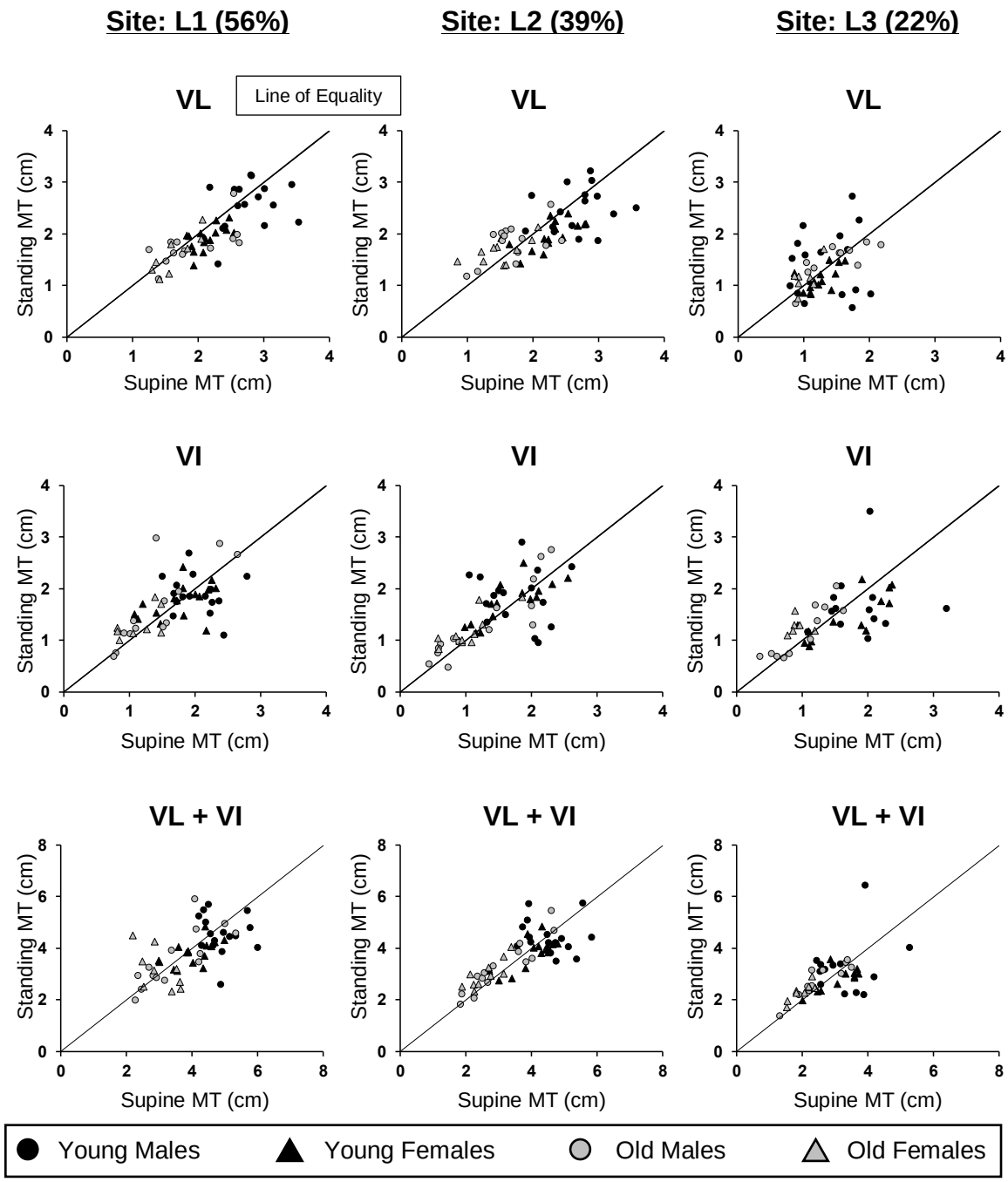


Figure 3-3. Skeletal muscle thickness of the lateral quadriceps measured while standing and supine. L1, lateral quadriceps 56% proximal from knee; L2, anterior quadriceps 39% proximal from knee; L3, lateral quadriceps 22% proximal from knee; VL, vastus lateralis; VI, vastus intermedius; MT, muscle thickness.

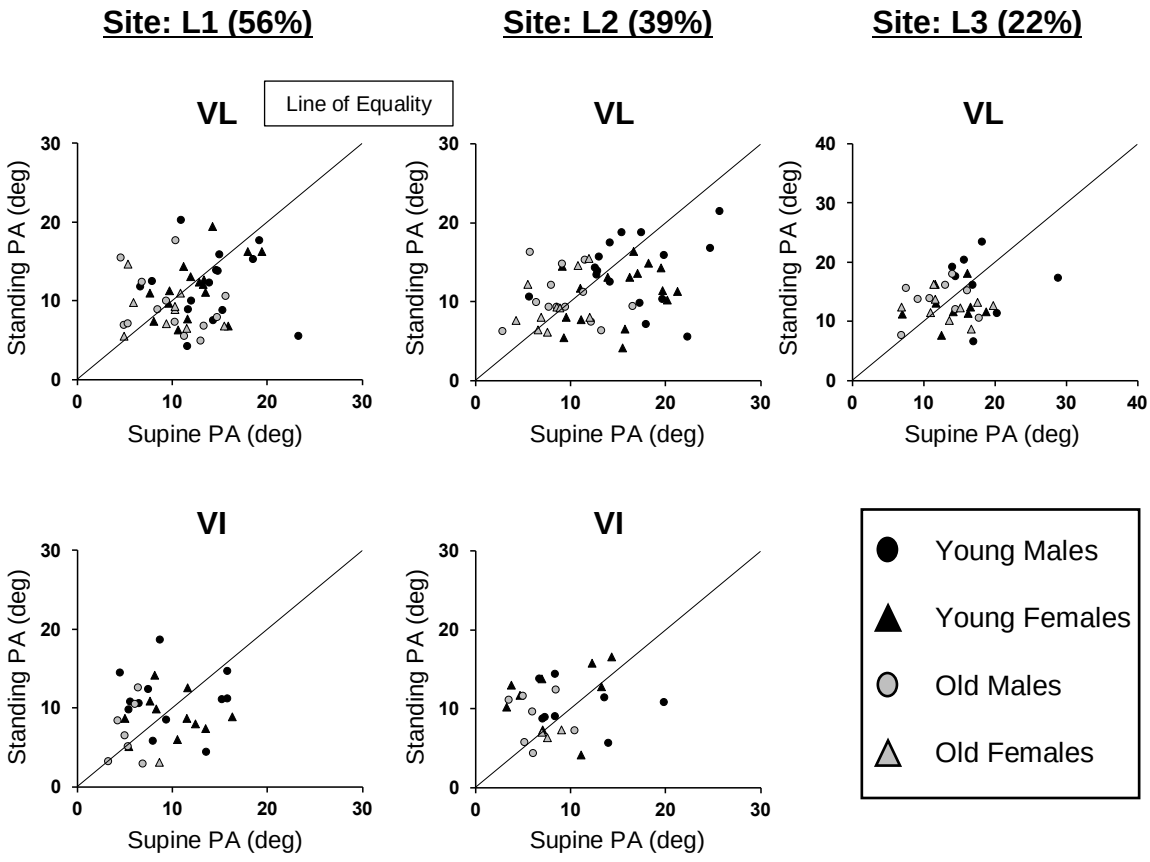


Figure 3-4. Skeletal muscle pennation angle of the lateral quadriceps measured while standing and supine. L1, lateral quadriceps 56% proximal from knee; L2, anterior quadriceps 39% proximal from knee; L3, lateral quadriceps 22% proximal from knee; VL, vastus lateralis; VI, vastus intermedius; PA, pennation angle.

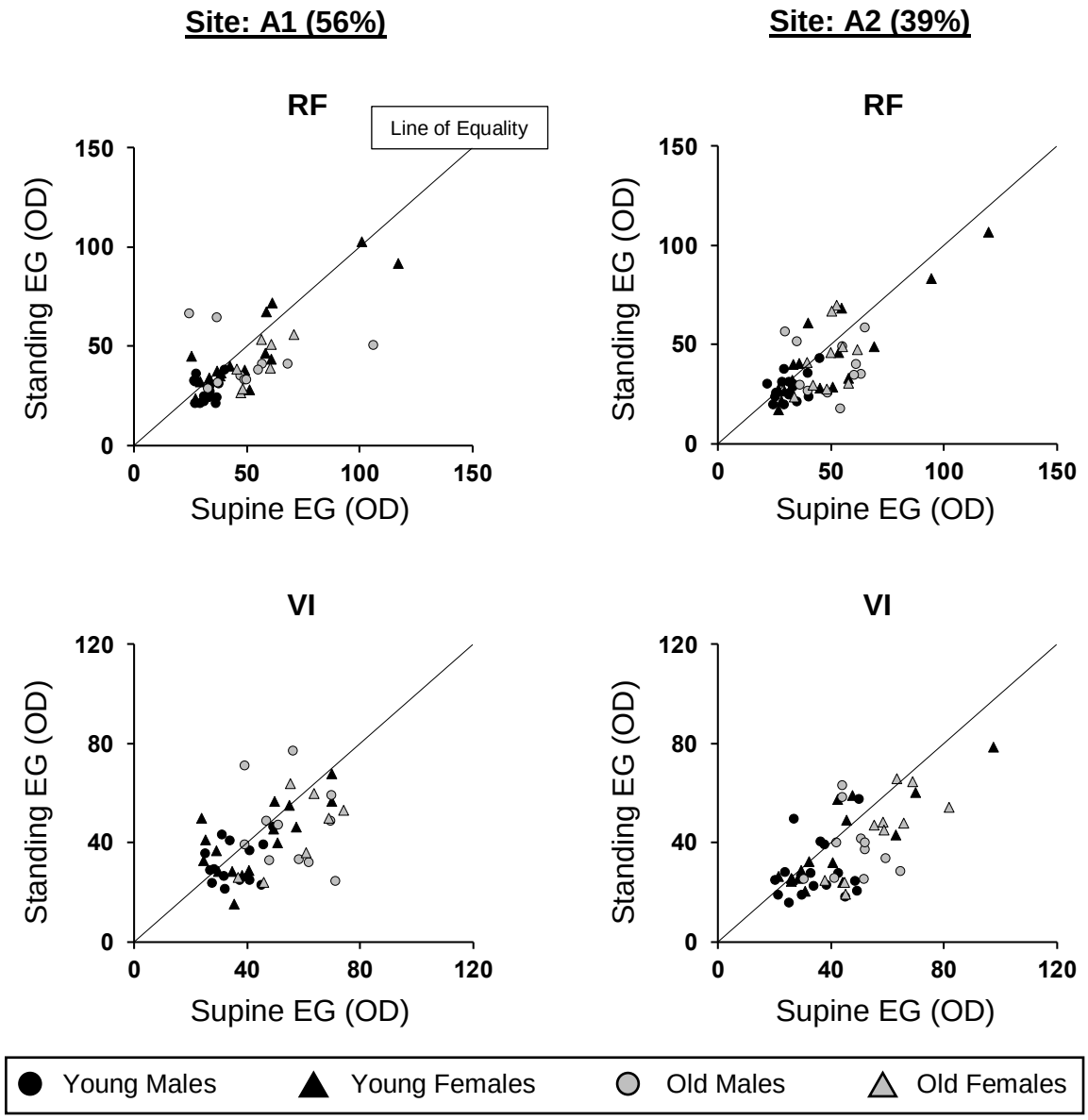


Figure 3-5. Skeletal muscle echogenicity of the anterior quadriceps measured while standing and supine. A1, anterior quadriceps 56% proximal from knee; A2, anterior quadriceps 39% proximal from knee; RF, rectus femoris; VI, vastus intermedius; EG, echogenicity; OD, optical density.

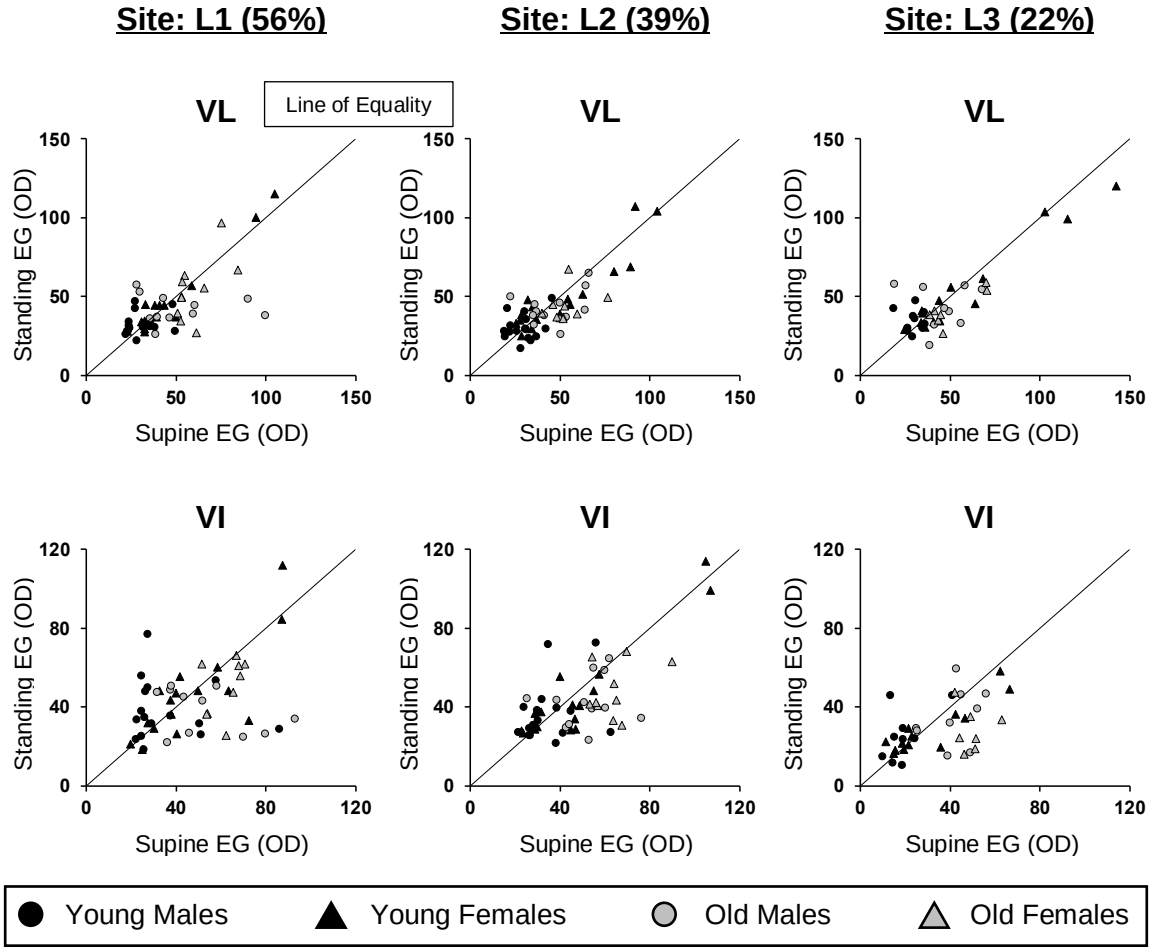


Figure 3-6. Skeletal muscle echogenicity of the lateral quadriceps measured while standing and supine. L1, lateral quadriceps 56% proximal from knee; L2, anterior quadriceps 39% proximal from knee; L3, lateral quadriceps 22% proximal from knee; VL, vastus lateralis; VI, vastus intermedius; EG, echogenicity.

CHAPTER 4

REDUCED SATELLITE CELL AND CAPILLARY ABUNDANCE IN RAT SKELETAL MUSCLE FOLLOWING CHRONIC DOXORUBICIN ADMINISTRATION

Andrew C. D'Lugos[1], Christopher S. Fry[2], Jordan C. Ormsby[1], Kaylin R. Sweeney[1]; Taben M. Hale[3], Rayna J. Gonzales[3], Siddhartha S. Angadi[1], Chad C. Caroll[4,5], and Jared M. Dickinson[1]

[1]School of Nutrition and Health Promotion, Healthy Lifestyles Research Center, Exercise Science and Health Promotion, Arizona State University, Phoenix, AZ, USA, [2]Department of Nutrition and Metabolism, University of Texas Medical Branch, Galveston, TX, USA, [3]Department of Basic Medical Sciences, College of Medicine-Phoenix, University of Arizona, Phoenix, AZ, USA, [4]Department of Physiology, Midwestern University, Glendale, AZ, USA, [5]Department of Health and Kinesiology, Purdue University, West Lafayette, IN, USA

INTRODUCTION

Doxorubicin (DOX) is an anthracycline-class chemotherapeutic agent that is very effective for treating various cancers (162). However, the clinical utility of DOX is limited due to well-known off-target effects (90, 130, 226-228), including the induction of skeletal muscle atrophy (27, 32) and dysfunction (33, 91, 111, 122). While the cellular mechanisms through which DOX may exert these deleterious effects on skeletal muscle remain to be fully understood, previous studies have demonstrated increased formation of reactive oxygen species (91), as well as increased inflammatory (90, 92) and proteolytic markers (130, 227) in skeletal muscle within days following the administration of a large, single bolus of DOX. When administering smaller doses of DOX over biweekly intervals, to mimic the clinical utility of DOX, we have recently shown reduced muscle fiber size to coincide with impaired skeletal muscle mammalian target of rapamycin (mTOR) signaling (58). Indeed, the mTOR pathway is implicated in a variety of cellular processes related to muscle size including protein translation, cell proliferation, and autophagy (212). Thus, a more precise characterization of the cellular response of skeletal muscle to chronic DOX administration may provide valuable therapeutic targets to reduce side effects and improve clinical utility.

Since their discovery (129, 154), satellite cells have been purported to serve an essential role in skeletal muscle growth and regeneration (135). Indeed, *in vitro* exposure to DOX has been shown to interfere with myogenic processes associated with satellite cells, including repressed activity of a key myogenic regulatory factor, myogenic differentiation factor 1 (MyoD) (137, 138), and impaired progression of myoblasts through the myogenic lineage (137, 179, 197). Furthermore, the administration of a single bolus of DOX appears to exacerbate muscle fiber loss when injected during the peak satellite cell activation window following an injury (185). Moreover, satellite cells have also been reported to actively engage in unique crosstalk with neighboring capillaries to facilitate myogenic and angiogenic processes (6, 45). Interestingly, chronic administration of DOX also appears to reduce cardiac muscle capillaries by ~50% (12). While there appears to be a potential role for satellite cells and capillaries as therapeutic targets for attenuating DOX-induced toxicities in skeletal muscle, the impact of DOX on satellite cell and capillary content, and their relation to muscle fiber size has not been thoroughly investigated.

Recently, the dependence on satellite cells for the non-injurious maintenance of muscle fiber size in adulthood has garnered review (170). Specifically, the role of satellite cells in the maintenance of fiber size may differ between skeletal muscles of various fiber types (88, 132), functions (127) and capillarization (182). Thus, there not only remains a need to explore the impact of *in vivo* DOX administration on satellite cells and capillary contents in skeletal muscle, but in particular, there is a need to assess this relationship in skeletal muscles of varying fiber type and function. Therefore, the purpose of this study was to determine the impact of chronic biweekly DOX administration on satellite cell and capillary content in the soleus (SOL) and extensor digitorum longus (EDL) muscles. These muscles were selected as they differ substantially in fiber size (231), fiber type (231), and capillarization (171), and the function of these muscles appears to be differentially impacted by DOX (111, 122). We hypothesized that chronic DOX administration would be associated with reduced satellite cell and capillary content as well as reduced fiber size, in both muscles.

METHODS

Study Design

Eight-week-old ovariectomized female Sprague-Dawley rats were purchased (Charles River Labs, Wilmington, MA) and acclimated to the laboratory for 1 week as previously described (58). Rats included in the current study were randomized to receive either Doxorubicin (DOX, n = 8) or a saline vehicle (VEH, n = 8). Rats were pair-housed with an animal in the same group, allowed access to food and water *ad libitum*, and maintained on a 12-h light-12-h dark cycle. All methods used in this investigation were approved by the Midwestern University Institutional Animal Care and Use Committee.

Rats were injected (I.P.) on three occasions with DOX (doxorubicin hydrochloride >99%; LC Laboratories, Woburn, MA) dissolved in 0.9% normal saline or vehicle (0.9% normal saline). Injections were separated by 2 week intervals. The dosing strategy was designed to closely mimic strategies used in the clinical treatment of human cancer patients (250) and has been previously detailed (58). Briefly, during each injection, DOX was administered in doses of $4mg \cdot kg^{-1}$; totaling 12mg/kg received by each animal by the end the experimental protocol. Five days following the final injection, rats were anesthetized with isoflurane then decapitated. Upon euthanasia, the SOL and EDL muscles were removed from each leg. The muscles from one leg were immediately frozen in liquid nitrogen for RT-qPCR analysis while the muscles from the opposite leg were carefully embedded on a foil-wrapped cork in Tissue Tek optimal cutting temperature medium (OCT; Thermo Fisher Scientific, Rockford, IL) and frozen in liquid nitrogen-cooled isopentane for immunohistochemical analysis. All samples were stored at -80°C for subsequent analyses.

Immunohistochemistry

Seven-micron-thick sections were cut in a cryostat (HM525X; ThermoFisher, Waltham, MA), and sections were allowed to air dry for 1 h. Determination of cross-sectional area (CSA) was performed as previously described for these animals in which fiber type-specific CSA in the SOL has been previously reported (58). Briefly, unfixed slides were incubated for 90 min at room temperature with an antibody directed against laminin [2E8, IgG2a, supernatant; Developmental

Studies Hybridoma Bank (DSHB, Iowa City, IA)]. Following a series of washes in phosphate-buffered saline (PBS), slides were incubated for 60 min at room temperature in goat anti-mouse IgG2a Alexa Fluor (AF) 633 (#A21136; Invitrogen, Grand Island, NY), washed in PBS, and mounted with fluorescent mounting media (Fluormount G, #0100-01; Southern Biotech, Birmingham, AL).

For Pax7/laminin/DAPI staining (visualization of myonuclei and satellite cells), immunohistochemical procedures were adapted from Finnerty et al. (71). Briefly, slides were fixed in 4% paraformaldehyde followed by epitope retrieval using sodium citrate (10 mM, pH 6.5) at 92°C for 20 min. Endogenous peroxidases were blocked with 3% hydrogen peroxide in PBS, and then slides were incubated overnight at 4°C in anti-laminin (no. L9393; Sigma Aldrich, St. Louis, MO) and anti-Pax7 antibody (DSHB). The next day, slides were incubated for 70 min at room temperature in goat anti-rabbit AF488 (#A11034; Invitrogen, laminin) and goat anti-mouse biotinylated secondary antibody (no. 115-065-205; Jackson ImmunoResearch, West Grove, PA), and then reacted with streptavidin-horseradish peroxidase (HRP) and AF555 tyramide included with the tyramide signal amplification (TSA) kit (#T20932; Invitrogen). TSA-AF555 was used to visualize Pax7 antibody-binding. Slides were co-stained with 4',6-diamidino-2-phenylindole (DAPI, no. D35471; Invitrogen) before being mounted with Vectashield fluorescent mounting media (Vector Laboratories, Burlingame, CA).

For visualization of capillaries, slides were fixed for 10 min in ice-cold acetone (-20°C) and then blocked for 1 h in 2.5% normal horse serum (Vector Laboratories). Slides were incubated overnight at 4°C in antibody against CD31/PECAM (#550300, BD Biosciences, San Jose, CA). The next day, slides were incubated for 1 h at room temperature in goat anti-mouse AF555 (#A21127, Invitrogen) and AF488 conjugated-wheat germ agglutinin (WGA, #W11261, Invitrogen).

Image acquisition and analysis

Images were captured at 100x total magnification at room temperature with a Zeiss upright microscope equipped with an automated stage (AxioImager M1; Zeiss, Oberkochen, Germany). Muscle fiber CSA was analyzed from images of laminin staining using a semiautomated threshold analysis (ImageJ, NIH, Bethesda, MD) as previously detailed (58). Image analysis for satellite cells, myonuclei, and capillaries was performed using the AxioVision Rel software (v. 4.9) by a single

assessor blinded to group. Satellite cell abundance was assessed as previously described (71). Briefly, $Pax7^+/DAPI^+$ loci residing within the laminin border were counted as satellite cells. $DAPI^+$ nuclei residing within the laminin border were counted as myonuclei. A nucleus was identified as a myonucleus if it met one of the following criteria: *1*) it was clearly located within the laminin boundary; *2*) it was on the laminin boundary facing inside the fiber; or *3*) 50% of the area fell inside the laminin boundary. Cellular structures positive for $CD31^+$ were counted as capillaries. All satellite cells, myonuclei, and capillary counts were normalized to muscle area (mm^2).

RNA Extraction and Semiquantitative real-time PCR

RNA isolation, cDNA synthesis, and real-time quantitative PCR were performed as our laboratory has previously described (58). Briefly, frozen muscle tissue was weighed (mean ± SD, 25.84 ± 6.5mg) at 4ºC and homogenized with a hand-held homogenizing dispenser (Bio-Gen PRO200, Pro Scientific, Oxford, CT) in 1 ml of Tri reagent (Molecular Research Center, Cincinnati, OH). RNA concentration was determined using a Take3 plate (Biotek, Winooski, VT) and Biotek H1 Synergy. RNA (5 µg) was DNase-treated using a commercially available kit (DNA-free, Ambion, Austin, TX). A total of 1 µg of RNA was reverse transcribed into cDNA according to the directions provided by the manufacturer (SensiFAST, Bioline, Taunton, MA). Real-time qPCR was carried out with a CFX Connect Real-Time PCR Detection System (BioRad). cDNA was analyzed with SYBR green fluorescence (iTaq Universal SYBR green supermix; BioRad). Primer sequences were designed using the National Center for Biotechnology Information database (265) to be mRNA specific and compatible with SYBR green chemistry. Primer pairs (Table 1) were purchased from Invitrogen (Carlsbad, CA) and carefully optimized as previously described (52). β_2-Microglobulin was utilized as a normalization/housekeeping gene. Relative fold changes from VEH were determined from the Cq values using the $2^{-\Delta\Delta Ct}$ method (147).

Statistical Analyses

All data were tested for normality through skewness and kurtosis analyses and visual inspection of the normality plots using SPSS v.24 (IBM). Satellite cell, myonuclei, capillary, and

mRNA expression data were analyzed using an independent samples *t*-test. To account for multiple measures obtained from the same animal, all individual fiber CSA data from an individual animal were nested and data were analyzed using a multi-level mixed model (nested ANOVA) (58). This statistical model allows for the inclusion of the multiple measures (i.e., all fibers analyzed), but avoids treating each fiber as an independent observation and takes into account variability for measures obtained both within and between animals. Statistical analyses were conducted using SPSS v.24 (IBM). Significance was set *a priori* at $P \leq 0.05$. Data are presented as mean ± standard error (SE) where individual data are not shown.

RESULTS

Muscle fiber CSA

To assess the impact of DOX administration on muscle fiber size, we examined SOL and EDL fiber CSA. Similar to the fiber type specific data previously reported (58), DOX administration was associated with ~26% smaller pooled-fiber CSA in the SOL (Fig. 1A; $P = 0.022$). Similarly, fiber CSA in the EDL was ~33% smaller in DOX animals (Fig. 1C; $P = 0.009$). The distribution of fiber CSA in each muscle displayed a clear leftward shift toward smaller fibers in both the SOL and EDL in DOX animals (Fig. 1B,D). The average number of SOL fibers analyzed per animal were 162 ± 5 for VEH and 209 ± 15 for DOX, while the average EDL fibers analyzed per animal were 228 ± 74 for VEH and 403 ± 100 for DOX.

Satellite cell and myonuclei content

Representative immunohistochemical images of satellite cell and myonuclei analyses are shown in Figure 2. Pax7-positive satellite cell content in the SOL was ~39% lower in DOX animals (Fig. 3A; $P = 0.002$). Notably, the SC content in the SOL of all animals that were administered DOX was lower than every animal in VEH (Fig. 3A). On the other hand, SC content was not statistically impacted by DOX administration in the EDL (Fig. 3C; $P = 0.18$). Myonuclei content in the SOL (Fig. 3B) and EDL (Fig. 3D) were not affected by DOX administration ($P = 0.292$ and $P = 0.66$, respectively). The muscle area (mm^2) analyzed for SC and myonuclei content was similar for each muscle between groups ($P > 0.05$; SOL: VEH = 3.43 ± 0.35, DOX = 5.03 ± 0.98; EDL: VEH = 5.81 ± 0.74, DOX = 5.21 ± 0.53 mm^2).

Capillary content

Capillary content in the SOL was ~35% lower in DOX animals (Fig. 4A-D; $P = 0.021$). Notably, the SOL capillary content of all animals that were administered DOX was lower than every VEH animal (Fig 4D). Capillary content of the EDL was not impacted by DOX administration (Fig. 4E-H; $P = 0.959$). The muscle area (mm^2) analyzed for capillary content was similar for each muscle across treatments ($P > 0.05$; SOL: VEH= 1.23 ± 0.47, DOX = 5.50 ± 1.92; EDL: VEH = 3.64 ± 1.05, DOX = 2.89 ± 0.54 mm^2).

Myogenic gene expression

The mRNA expression of MYF5 was higher in animals administered DOX only in the SOL (P = 0.026). MGF mRNA expression was lower in animals administered DOX only in the EDL (P = 0.048). The mRNA expression of several other genes associated with myogenesis in the SOL and EDL were unaffected by DOX administration (Table 2).

DISCUSSION

The purpose of the current study was to determine the impact of chronic DOX administration on satellite cell and capillary densities in different skeletal muscles. Several novel findings resulted from this study. First, chronic DOX administration was associated with lower skeletal muscle satellite cell density in the SOL muscle. The lower satellite cell density in the SOL of DOX animals coincided with lower capillary density and reduced muscle fiber CSA. Conversely, while chronic DOX administration was also associated with reduced CSA in the EDL, satellite cell and capillary densities were not impacted. These findings suggest that 1) DOX administration impacts satellite cell and capillary densities in a muscle-specific manner, 2) DOX impairs the regulation of muscle fiber CSA across multiple muscles of varying fiber type, 3) the role of satellite cells in the regulation of muscle fiber size may differ across muscles.

We have previously reported reduced MHC I and MHC II fiber CSA in the SOL of animals that underwent chronic DOX administration (58). DOX has been shown to impact the function of both the SOL and EDL (111, 122), however, to what extent chronic DOX administration impacts fiber size in the EDL has not been investigated. In the current study, chronic DOX administration was associated with a similar relative reduction in fiber CSA in both the SOL and EDL muscles despite the fact that these muscles differ considerably in fiber type profile and fiber size (231), and may also differ in their accumulation of DOX (111). Nonetheless, these results indicate that DOX exerts an impact on muscle fiber size across different skeletal muscles.

Satellite cells are understood to contribute to the regulation of muscle fiber size (131), however, the role of satellite cells in maintaining fiber size may differ depending on the muscular environment in which they reside. Therefore, to more precisely identify the impact of DOX on the regulation of muscle fiber size, we examined satellite cell density in the SOL and EDL following chronic DOX administration as these muscles are comprised of different fiber type profiles (88, 132), functions (127) and capillarization (36). While chronic DOX administration reduced muscle fiber size in both the SOL and EDL, the reduced fiber size was accompanied by reduced satellite cell density only in the SOL, whereas satellite cell density was unaffected by DOX in the EDL. Indeed, the work of Kelly et al. (132) propose that fiber size in the SOL is more associated with

satellite cell fusion whereas fiber size in the EDL is more a product of cytoplasmic expansion. While satellite cells in the EDL were not affected by DOX administration, the EDL muscle of the DOX group exhibited reduced MGF mRNA expression which has been shown to be regulated by circulating growth hormone (124) and positively correlated to lean mass (193). Thus, it is likely that the role of satellite cells as a contributing factor to the maintenance of fiber size may differ between the SOL and EDL. Collectively, these data highlight that the mechanisms through which DOX administration impacts fiber size may vary between muscles of different phenotype.

An interesting finding in the current study was that chronic DOX administration was associated with a muscle-specific reduction of satellite cell density in the SOL. However, despite reductions in satellite cell density, the myonuclear density was maintained in the SOL following DOX administration. Previous research has shown that a large, single bolus injection of DOX increases the occurrence of apoptotic myonuclei in the SOL (227). Importantly, maintenance of the myonuclear population is reliant on satellite cell fusion as the primary source of new myonuclei (168). In addition, DOX is a known inhibitor of cell proliferation (106), thus it is possible that satellite cell proliferation may also be blunted by DOX administration. Collectively, the reduced satellite cell density observed specifically in the SOL of the DOX group may be the result of a greater reliance on satellite cells to replenish apoptotic nuclei coupled with an impaired ability to maintain the satellite cell pool through blunted proliferation/self-renewal. Further, this interpretation is supported by increased mRNA expression of Myf5 in the SOL of DOX, which may be upregulated in an attempt to recuperate proliferation (266) and self-renewal (210) that may be compromised by DOX. Further research is needed to identify the precise mechanisms regulating satellite cell dynamics in otherwise sedentary skeletal muscle and how they are affected by myotoxic drugs such as DOX.

Similar to previous studies (88, 132), we also detected reduced satellite cell density in the EDL compared to the SOL, supporting the notion that satellite cells may have unique roles within various skeletal muscles. Further, similar to satellite cell density, myonuclear density was also not impacted by chronic DOX administration in the EDL. Previous reports indicate satellite cells and myonuclei within the EDL are less mitotically and transcriptionally active, respectively, compared to those within SOL (97, 132). Previous research has also demonstrated that under non-injurious

conditions, the number of myonuclei in the EDL of satellite cell-ablated mice do not appear to differ from that of control mice (131). This latter observation would seem to indicate that satellite cells in the EDL may not measurably contribute to myonuclear number in the maintenance of muscle homeostasis. Thus, in the uninjured state (i.e., sedentary) the satellite cell pool in the EDL may be less susceptible to the deleterious effects of DOX. On the other hand, future research is necessary to determine the extent to which DOX administration impacts satellite cell in the EDL in the presence of a (damaging) stimulus that may accompany clinical treatment (i.e., exercise/rehabilitation).

It is well known that muscle capillaries serve a vital role in maintaining skeletal muscle by delivering oxygen, substrates, and circulating factors. More recently, mounting evidence indicates that capillaries and satellite cells communicate through paracrine interactions to facilitate myogenic and angiogenic processes (6, 45). Indeed, satellite cells and capillaries appear to share a general proximity within skeletal muscle (45, 181). Given the vital role of skeletal muscle capillaries and their proposed relationship with satellite cells, we examined the impact of chronic DOX administration on capillary density in the SOL and EDL. Similar to our findings regarding satellite cell density, we also show that DOX administration was associated with lower capillary density in the SOL, but not the EDL. Our findings are consistent with a previous study (12) demonstrating reduced capillaries in the myocardium of diabetic rats following chronic DOX administration. Interestingly, myocardial capillary content was increased when stem cells were administered along with DOX administration (12). These findings indicate that stem cells may aid in the maintenance of capillary networks. Indeed, cell culture models demonstrate capillary density (200) and capillary growth (206) are greater in the presence of satellite cells. Therefore, it is interesting to speculate that in the current study the lower capillary density observed in the SOL of the DOX group may, in part, result from the reduction in satellite cell density in the same muscle.

Consistent with the satellite cell data, capillary density in the EDL was unaffected by chronic DOX administration. Recently, Nissinen *et al.* (186) showed that chronic DOX administration did not impact capillary density of the tibialis anterior (TA) muscle in mice. Given the strikingly similar fiber type profiles between the TA and EDL (231), the findings from Nissinen et al.

(186) indirectly support our findings in the predominantly MHC II EDL. Similar to observations made in the SOL, it is interesting to speculate that the preservation of capillary density in the EDL following chronic DOX administration may be, in part, related to the lack of effect on satellite cell density. However, it is important to note that much of the work investigating the relationship between satellite cells and capillaries has occurred during times of active muscle repair (181, 182, 187), therefore more research is needed to clarify the relationship between satellite cells and capillaries in relation to uninjured, skeletal muscle maintenance as was employed in the current investigation (i.e., sedentary animals). Nonetheless, our findings further promote an intricately regulated connection between satellite cell and capillary populations across skeletal muscles.

In conclusion, we show for the first time that chronic DOX administration is associated with reduced satellite cell and capillary densities in the SOL. On the other hand, while DOX administration was associated with reduced muscle fiber size in both the SOL and EDL, satellite cell and capillary density were unaffected by chronic DOX administration in the EDL. These findings indicate that varying skeletal muscles may rely on different mechanisms to maintain fiber size and that chronic DOX administration may impact fiber size of various skeletal muscles through different cellular mechanisms. While the current study did not examine functional parameters of these muscles, DOX appears to cause dysfunction in both the SOL and EDL (111, 122). Coupled with previous findings in which chronic DOX administration attenuated mTORC1 signaling (58) and mitochondrial dysfunction (102), these findings contribute to a growing body of literature highlighting the myotoxicity associated with DOX. Future studies are encouraged to examine skeletal muscle satellite cells and capillaries as therapeutic targets in mitigating the deleterious impact of DOX in skeletal muscle.

Table 4-1. Primer sequences used for real-time PCR

mRNA	Accession No.		Primer Sequence (5'-3')	Product Size (bp)
Id2	NM_013060.3	Sense	GGACAGAACCAAACGTCCAG	94
		Antisense	TAAGCTCAGAAGGGAATTCAGAC	
MGF	NM_001082478.1	Sense	TGACATGCCCAAGACTCAGAAGT	70
		Antisense	CCTTCTCCTTTGCAGCTTCCT	
MYF5	NM_001106783.1	Sense	TGTCTGGTCCCGAAAGAACA	103
		Antisense	CAAGCAATCCAAGCTGGACA	
MYF6	NM_013172.2	Sense	CCCTTACAGCTACAAACCCAAG	130
		Antisense	TGCTCCTCCTTCCTTAGCAG	
MyoD	NM_176079.1	Sense	GGAGACATCCTCAAGCGATGC	104
		Antisense	GCACCTGGTAAATCGGATTG	
Myogenin	NM_017115.2	Sense	CAGTGAATGCAACTCCCACA	85
		Antisense	CAAATGATCTCCTGGGTTGG	
Myostatin	NM_019151.1	Sense	GGCAGAGTATTGATGTGAAGAC	119
		Antisense	TGGGAAGGTTACAGCAAGATC	
Mdm2	NM_001108099.1	Sense	CCGAGCGAAATGGTCTCTCA	93
		Antisense	CTGCAGACCGCTGCTACTC	
Npm1	NM_012992.4	Sense	TCAAGTGCGCGCCTCC	97
		Antisense	CAGCCTTTAGTTCACAACCGAA	
Rb1	NM_017045.1	Sense	TGTATGGCATCTGCAAGGTGA	100
		Antisense	CGTTTAAAGGTCTCCTGGGC	

Id2, Inhibitor of DNA Binding 2; MGF, Mechano growth factor; MYF5, Myogenic factor 5; MYF6, Myogenic factor 6; MyoD, Myogenic differentiation factor 1; Mdm2, mouse double minute 2 homolog; Npm1, Nucleophosmin 1; Rb1, Retinablastoma 1.

Table 4-2. Soleus and extensor digitorum longus muscle mRNA analyses for markers of myogenic activity.

	Soleus		Extensor Digitorum Longus	
mRNA	VEH	DOX	VEH	DOX
Id2	1.24 ± 0.33	1.30 ± 0.24	1.03 ± 0.14	0.92 ± 0.16
Mdm2	1.05 ± 0.42	0.76 ± 0.21	1.08 ± 0.25	0.79 ± 0.24
MGF	1.25 ± 0.30	1.18 ± 0.13	1.01 ± 0.07	0.80 ± 0.01*
MYF5	1.07 ± 0.16	1.59 ± 0.13*	1.02 ± 0.11	0.80 ± 0.01
MYF6	1.08 ± 0.16	0.89 ± 0.09	1.14 ± 0.34	0.54 ± 0.04
MYOD	1.25 ± 0.35	1.90 ± 0.23	1.18 ± 0.40	0.57 ± 0.08
Myogenin	1.43 ± 0.54	1.25 ± 0.15	1.16 ± 0.39	0.96 ± 0.17
Myostatin	1.38 ± 0.38	1.31 ± 0.25	1.18 ± 0.43	0.90 ± 0.24
Npm1	1.31 ± 0.49	0.94 ± 0.11	1.02 ± 0.12	1.16 ± 0.19
Rb1	1.23 ± 0.38	0.78 ± 0.11	1.03 ± 0.15	0.93 ± 0.15

Data are mean ± SE. Values represent relative fold change from vehicle (VEH) as determined from the Cq values using the $2^{-\Delta\Delta Ct}$ method (28). *P < 0.05 VEH vs DOX. Inhibitor of DNA Binding 2; MGF, Mechano growth factor; MYF5, Myogenic factor 5; MYF6, Myogenic factor 6; MyoD, Myogenic differentiation factor 1; Mdm2, mouse double minute 2 homolog; Npm1, Nucleophosmin 1; Rb1, Retinablastoma 1. Soleus: VEH, n=8; DOX, n=8; EDL: VEH, n=4; DOX, n=6.

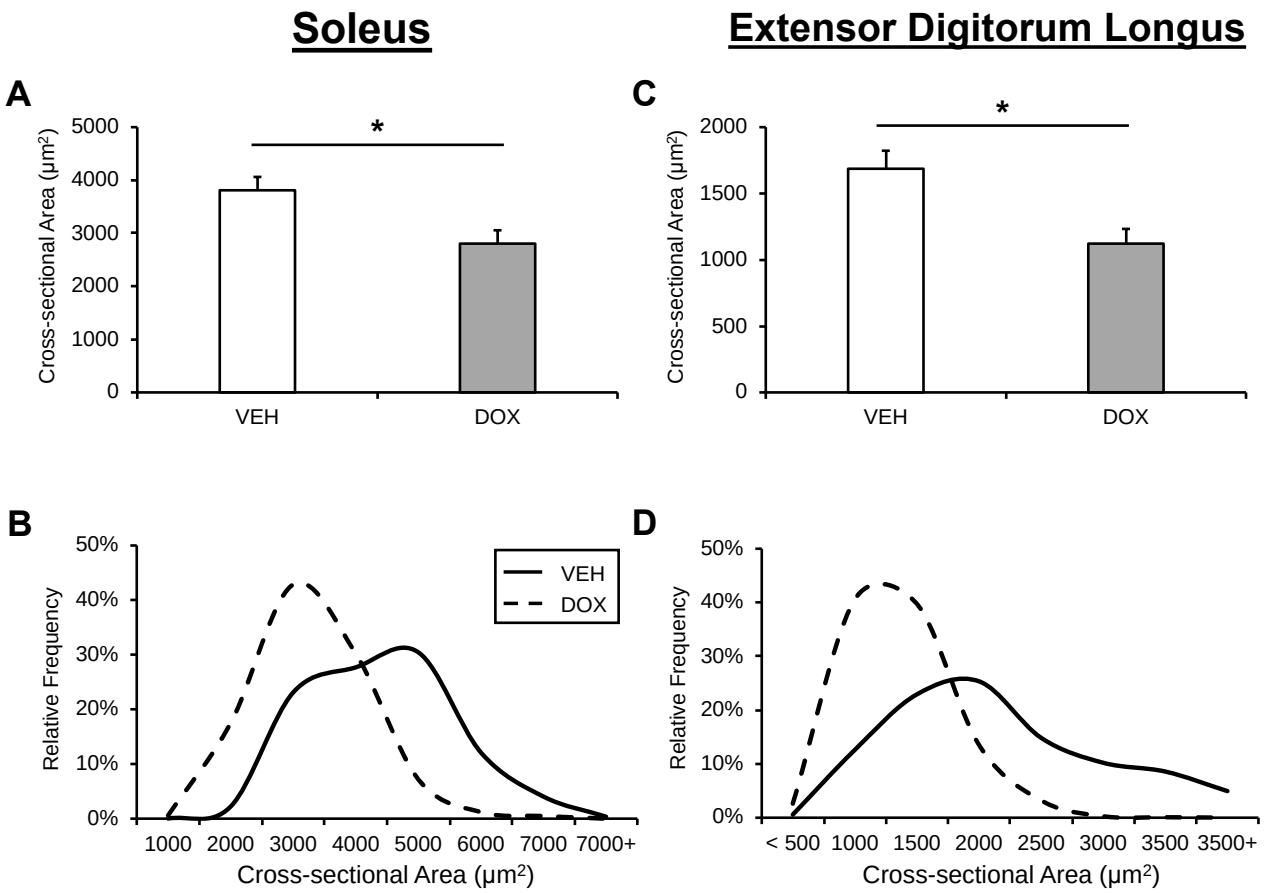


Figure 4-1. The effect of chronic doxorubicin administration on muscle fiber cross-sectional area (CSA). Mean fiber CSA of soleus (A) and extensor digitorum longus (C) presented as mean ± SE. Histogram distribution of fiber CSA in soleus (B) and extensor digitorum longus (D). VEH, vehicle group; DOX, doxorubicin group. Soleus (VEH, n = 4; DOX, n = 4); extensor digitorum longus (VEH, n = 4; DOX, n = 6). *P < 0.05 VEH vs DOX.

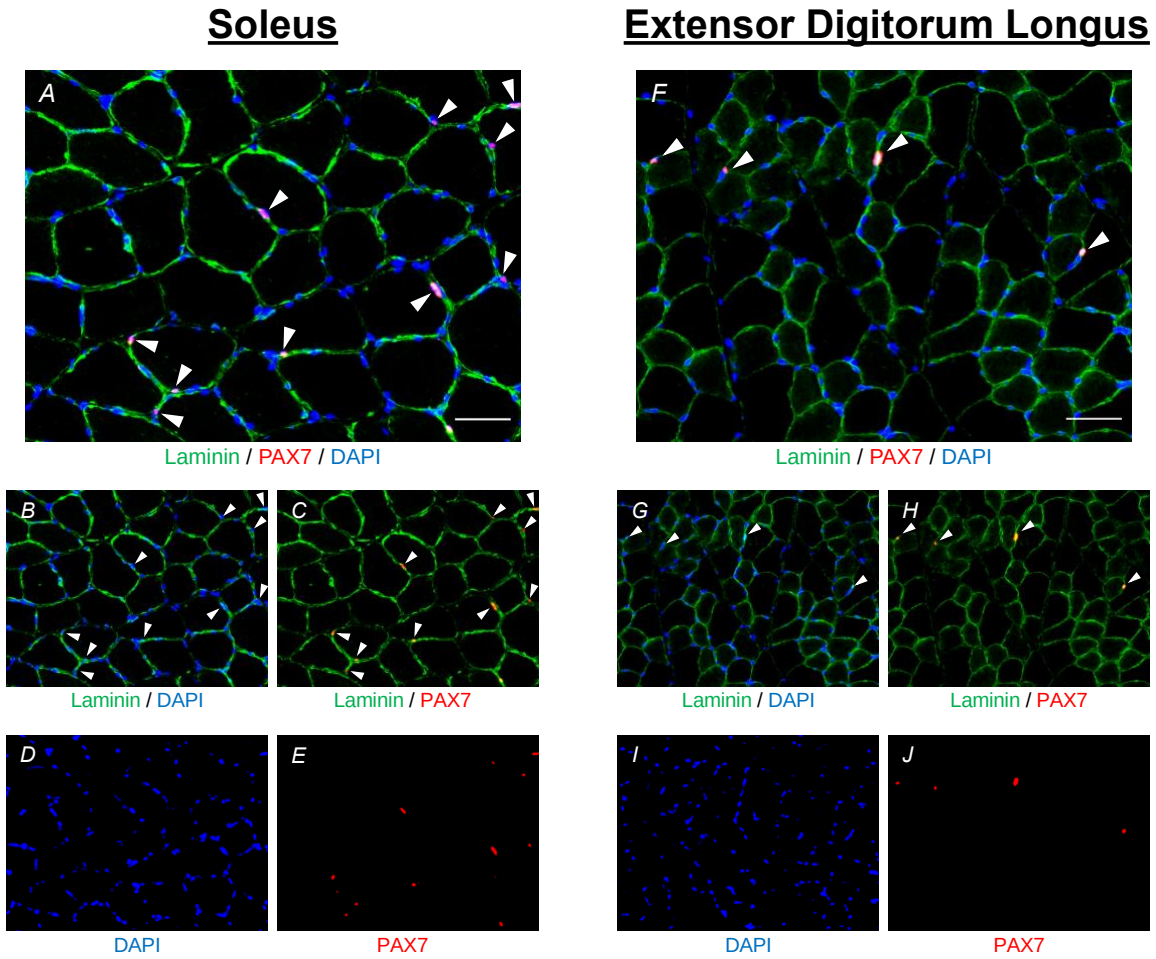


Figure 4-2. Representative immunohistochemical image of satellite cell detection in the soleus and extensor digitorum longus. Merged images (A,F) demonstrating laminin (green), Pax7 (red), and 4′ ,6-diamidino-2-phenylindole (DAPI, blue) with satellite cells denoted by white arrowheads. Scale bar represents 50 µm. Merged images (B, G) demonstrating satellite cell (red) location within laminin (green), costained with DAPI (blue; C, H) and denoted by white arrowheads. Single-channel image (D, I) demonstrating DAPI (blue). Single-channel image (E, J) demonstrating Pax7 (red).

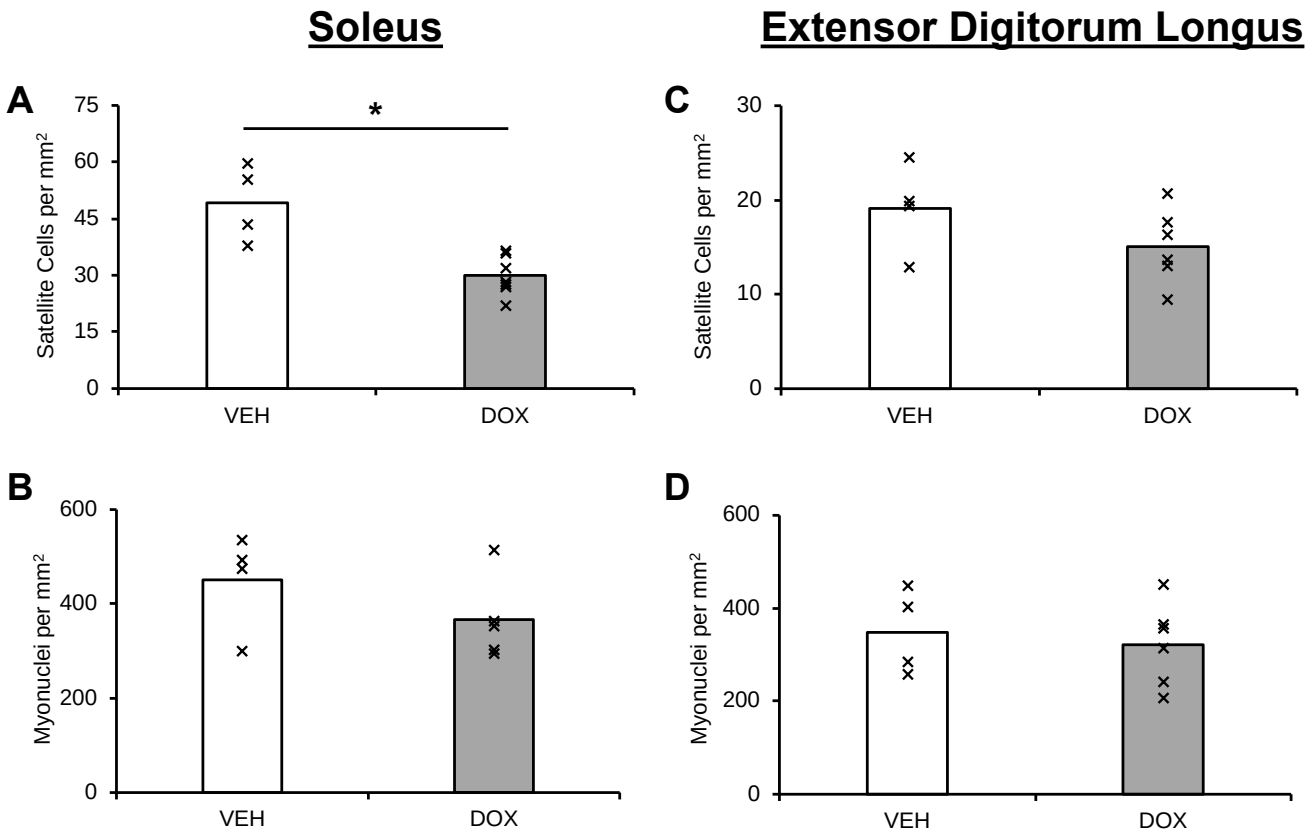


Figure 4-3. The effect of chronic doxorubicin administration on satellite cell and myonuclei densities. Mean satellite cell density of soleus (A) and extensor digitorum longus (C) presented as mean (bar) with individual animals represented by an "X". Mean myonuclei density of soleus (C) and extensor digitorum longus (D). VEH, vehicle group; DOX, doxorubicin group. Soleus (satellite cell: VEH, n = 4; DOX, n = 6; myonuclei: VEH, n = 4; DOX, n = 5); extensor digitorum longus (satellite cell: VEH, n = 4; DOX, n = 6; myonuclei: VEH, n = 4; DOX, n = 6). *P < 0.05 VEH vs DOX.

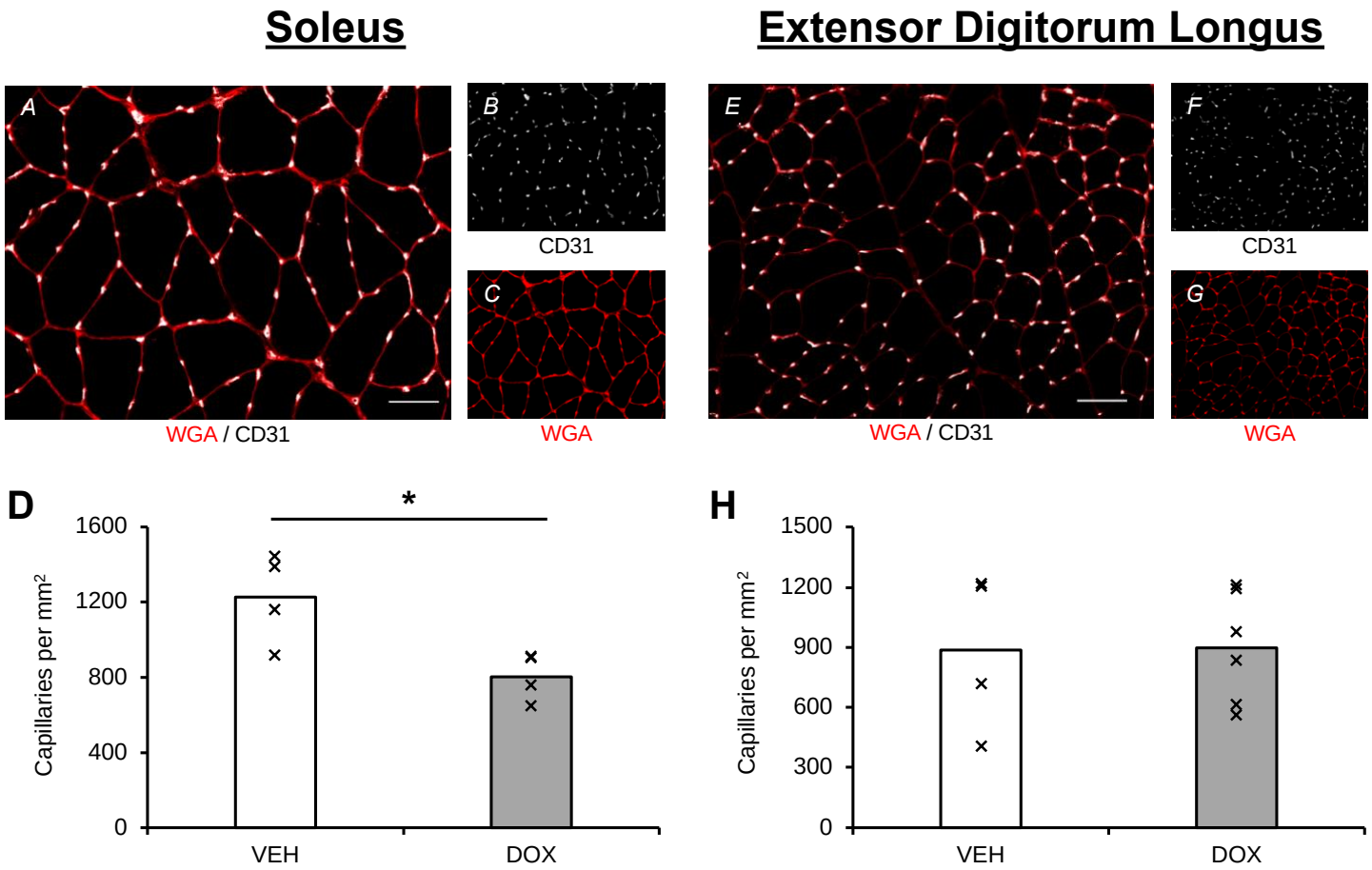


Figure 4-4. The effect of chronic doxorubicin administration on capillary density. Merged images (A, E) demonstrating CD31 (white) and wheat germ agglutinin (WGA, red). Scale bar represents 50 µm. Single-channel images (B, F) demonstrating CD31 (white). Single-channel images demonstrating WGA (red). Mean capillary density of soleus (D) and extensor digitorum longus (H) presented as mean (bar) with individual animals represented by an "X". VEH, vehicle group; DOX, doxorubicin group. Soleus (VEH, n = 4; DOX, n = 4); extensor digitorum longus (VEH, n = 4; DOX, n = 6). *P < 0.05 VEH vs DOX.

CHAPTER FIVE

CONCLUSION

The aim of this dissertation was to advance our ability to develop these strategies by addressing challenges to skeletal muscle faced throughout advancing age. Specifically, this dissertation is comprised of two distinct studies which aimed to 1) develop noninvasive strategies to assess skeletal muscle size, architecture, and composition in young and old adults and 2) evaluate the impact of chemotherapeutic treatment on skeletal muscle satellite cells and capillaries. The major findings from this dissertation aid in our ability to preserve skeletal muscle health and function throughout aging.

The goal of the first project was to assess the reliability of two predominate methodologies for ultrasound-based examination of quadriceps muscle size, architecture, and composition in young and old individuals. Ultrasound has been a valuable tool for examining the age-related decline in muscle size, pennation angle, and composition, which together, largely dictate the functional capacity of a muscle (140, 173). However, there lacks consensus on a standardized method to assess skeletal muscle characteristics, with the two predominant methodologies being practiced largely differing in the posture of the subject during imaging (4, 25). The findings from the first study highlight sources of variability associated the use of ultrasound to examine skeletal muscle characteristics. Overall, our findings suggest that US measurements of the lateral quadriceps are ideal for assessing functional changes in skeletal muscle, particularly given their collective relationship with muscle function and resistance to posture in both young and old. However, older age was associated with generally lower reliability which may impede the ability to accurately detect changes in the skeletal muscle of older adults. The findings from this study can be used to improve reproducibility and generalizability across

and within scientific investigations. This is particularly relevant given the emerging use of ultrasound to assess skeletal muscle characteristics in healthy and clinical populations. Future directions for these works include the assessment of the reliability of skeletal muscle ultrasound measures in clinical populations in order to more accurately detect functionally-relevant changes in skeletal muscle characteristics.

In addition to aging, disease and associated treatments can accelerate reductions in muscle quality. The common chemotherapeutic drug DOX is associated with many negative side effects in skeletal muscle including muscle atrophy (27, 32) and dysfunction (33, 91, 111, 122), however the cellular mechanisms responsible are still unclear. In this regard, satellite cells are a population of resident stem cells that govern the regenerative program in skeletal muscle (229). In addition, these cells engage in unique crosstalk with neighboring capillaries to facilitate myogenic and angiogenic processes, both of which are critical to skeletal muscle health (6, 45). The purpose of the second study was, therefore, to determine the impact of the common chemotherapeutic drug, DOX, on the satellite cell and capillary content in the soleus and extensor digitorum longus muscles. Specifically, these two muscles were studied as they differ substantially in fiber size (231), fiber type (88, 132), and capillarization (36), and the function of these muscles appears to be differentially impacted by DOX (111, 122). The results from our preclinical animal model indicate the chronic DOX administration is associated with reduced fiber size in multiple skeletal muscles, however the satellite cell and capillary densities were more impacted in the soleus compared to the extensor digitorum longus, indicating that DOX appears to impact molecular processes in a muscle-specific manner. These findings indicate that varying skeletal muscles may rely on different mechanisms to maintain fiber size and that chronic DOX administration may impact fiber size of various skeletal muscles through different cellular mechanisms. These findings contribute to a growing body of literature

highlighting the myotoxicity associated with DOX and highlight novel therapeutic targets for the development of strategies aimed at preserving skeletal muscle throughout DOX treatment (33, 58, 90, 122, 186). Future studies are encouraged to examine satellite cells and capillaries as therapeutic targets in human cancer patients receiving DOX.

In summary, advancing age is accompanied by an inevitable physiological decline over time. Skeletal muscle mass and function steadily decline with old age, leading to reduced independence and diminished quality of life in older adults. Unfortunately, this decline is often exacerbated by occurrences including injury, illness, or the direct and indirect effect of drug treatments. These occurrences present particularly difficult challenges to skeletal muscle by accelerating the normal age-related decline in muscle quality, increasing the risk for disability or frailty. Thus, in order to sustain quality of life and independence into old age, focus must be placed on the development of therapeutic strategies aimed at preserving skeletal muscle health and function through advancing age. Collectively, the findings from this dissertation 1) improve the ability to non-invasively examine changes in muscle size, composition, and function that can be used to monitor changes with age-related impairments or improvements following rehabilitation, and 2) identify promising therapeutic targets to protect skeletal muscle from the harmful effects of chemotherapy treatment. The works from this dissertation aid in the development of strategies aimed at returning muscle back to a normal, healthy state of aging following these challenges.

REFERENCES

1. **Aagaard P, Andersen JL, Dyhre-Poulsen P, Leffers AM, Wagner A, Magnusson SP, Halkjaer-Kristensen J, and Simonsen EB**. A mechanism for increased contractile strength of human pennate muscle in response to strength training: changes in muscle architecture. *J Physiol* 534: 613-623, 2001.

2. **Abe T, Kawakami Y, Suzuki Y, Gunji A, and Fukunaga T**. Effects of 20 days bed rest on muscle morphology. *Journal of gravitational physiology : a journal of the International Society for Gravitational Physiology* 4: S10-14, 1997.

3. **Abe T, Kojima K, and Stager JM**. Skeletal muscle mass and muscular function in master swimmers is related to training distance. *Rejuvenation Res* 17: 415-421, 2014.

4. **Abe T, Kondo M, Kawakami Y, and Fukunaga T**. Prediction equations for body composition of Japanese adults by B-mode ultrasound. *Am J Hum Biol* 6: 161-170, 1994.

5. **Abe T, Loenneke JP, and Thiebaud RS**. Morphological and functional relationships with ultrasound measured muscle thickness of the lower extremity: a brief review. *Ultrasound* 23: 166-173, 2015.

6. **Abou-Khalil R, Mounier R, and Chazaud B**. Regulation of myogenic stem cell behavior by vessel cells: the "menage a trois" of satellite cells, periendothelial cells and endothelial cells. *Cell Cycle* 9: 892-896, 2010.

7. **Agyapong-Badu S, Warner M, Samuel D, Narici M, Cooper C, and Stokes M**. Anterior thigh composition measured using ultrasound imaging to quantify relative thickness of muscle and non-contractile tissue: a potential biomarker for musculoskeletal health. *Physiol Meas* 35: 2165-2176, 2014.

8. **Akima H, Hioki M, Yoshiko A, Koike T, Sakakibara H, Takahashi H, and Oshida Y**. Intramuscular adipose tissue determined by T1-weighted MRI at 3T primarily reflects extramyocellular lipids. *Magn Reson Imaging* 34: 397-403, 2016.

9. **Akima H, Yoshiko A, Tomita A, Ando R, Saito A, Ogawa M, Kondo S, and Tanaka NI**. Relationship between quadriceps echo intensity and functional and morphological characteristics in older men and women. *Arch Gerontol Geriatr* 70: 105-111, 2017.

10. **Alegre LM, Ferri-Morales A, Rodriguez-Casares R, and Aguado X**. Effects of isometric training on the knee extensor moment-angle relationship and vastus lateralis muscle architecture. *Eur J Appl Physiol* 114: 2437-2446, 2014.

11. **Alegre LM, Jimenez F, Gonzalo-Orden JM, Martin-Acero R, and Aguado X**. Effects of dynamic resistance training on fascicle length and isometric strength. *J Sports Sci* 24: 501-508, 2006.

12. **Ammar HI, Sequiera GL, Nashed MB, Ammar RI, Gabr HM, Elsayed HE, Sareen N, Rub EA, Zickri MB, and Dhingra S**. Comparison of adipose tissue- and bone marrow- derived mesenchymal stem cells for alleviating doxorubicin-induced cardiac dysfunction in diabetic rats. *Stem Cell Res Ther* 6: 148, 2015.

13. **Ando R, Saito A, Umemura Y, and Akima H**. Local architecture of the vastus intermedius is a better predictor of knee extension force than that of the other quadriceps femoris muscle heads. *Clin Physiol Funct Imaging* 35: 376-382, 2015.

14. **Angadi SS, Mookadam F, Lee CD, Tucker WJ, Haykowsky MJ, and Gaesser GA**. High-intensity interval training vs. moderate-intensity continuous exercise training in heart failure with preserved ejection fraction: a pilot study. *J Appl Physiol (1985)* 119: 753-758, 2015.

15. **Antoun S, Borget I, and Lanoy E**. Impact of sarcopenia on the prognosis and treatment toxicities in patients diagnosed with cancer. *Current opinion in supportive and palliative care* 7: 383-389, 2013.

16. **Arcamone F, Franceschi G, Penco S, and Selva A**. Adriamycin (14-hydroxydaunomycin), a novel antitumor antibiotic. *Tetrahedron Letters* 10: 1007-1010, 1969.

17. **Arts IM, Pillen S, Schelhaas HJ, Overeem S, and Zwarts MJ**. Normal values for quantitative muscle ultrasonography in adults. *Muscle Nerve* 41: 32-41, 2010.

18. **Baekkerud FH, Solberg F, Leinan IM, Wisloff U, Karlsen T, and Rognmo O**. Comparison of Three Popular Exercise Modalities on V O2max in Overweight and Obese. *Med Sci Sports Exerc* 48: 491-498, 2016.

19. **Balagopal P, Rooyackers OE, Adey DB, Ades PA, and Nair KS**. Effects of aging on in vivo synthesis of skeletal muscle myosin heavy-chain and sarcoplasmic protein in humans. *Am J Physiol* 273: E790-800, 1997.

20. **Baroni BM, Geremia JM, Rodrigues R, De Azevedo Franke R, Karamanidis K, and Vaz MA**. Muscle architecture adaptations to knee extensor eccentric training: rectus femoris vs. vastus lateralis. *Muscle Nerve* 48: 498-506, 2013.

21. **Bartlett JD, Hwa Joo C, Jeong TS, Louhelainen J, Cochran AJ, Gibala MJ, Gregson W, Close GL, Drust B, and Morton JP**. Matched work high-intensity interval and continuous running induce similar increases in PGC-1alpha mRNA, AMPK, p38, and p53 phosphorylation in human skeletal muscle. *J Appl Physiol (1985)* 112: 1135-1143, 2012.

22. **Berg HE, Tedner B, and Tesch PA**. Changes in lower limb muscle cross-sectional area and tissue fluid volume after transition from standing to supine. *Acta Physiol Scand* 148: 379-385, 1993.

23. **Bickel CS, Slade J, Mahoney E, Haddad F, Dudley GA, and Adams GR**. Time course of molecular responses of human skeletal muscle to acute bouts of resistance exercise. *J Appl Physiol (1985)* 98: 482-488, 2005.

24. **Blazevich AJ, Gill ND, Bronks R, and Newton RU**. Training-specific muscle architecture adaptation after 5-wk training in athletes. *Med Sci Sports Exerc* 35: 2013-2022, 2003.

25. **Blazevich AJ, Gill ND, and Zhou S**. Intra- and intermuscular variation in human quadriceps femoris architecture assessed in vivo. *J Anat* 209: 289-310, 2006.

26. **Bloemberg D, and Quadrilatero J**. Rapid determination of myosin heavy chain expression in rat, mouse, and human skeletal muscle using multicolor immunofluorescence analysis. *PLoS One* 7: e35273, 2012.

27. **Bonifati DM, Ori C, Rossi CR, Caira S, Fanin M, and Angelini C**. Neuromuscular damage after hyperthermic isolated limb perfusion in patients with melanoma or sarcoma treated with chemotherapeutic agents. *Cancer Chemother Pharmacol* 46: 517-522, 2000.

28. **Booth FW, and Baldwin KM**. Muscle plasticity: energy demand and supply processes. *Comprehensive Physiology* 1996.

29. **Bottinelli R, Canepari M, Pellegrino MA, and Reggiani C**. Force-velocity properties of human skeletal muscle fibres: myosin heavy chain isoform and temperature dependence. *J Physiol* 495 (Pt 2): 573-586, 1996.

30. **Bottinelli RP, M.A., Canepari M, Rossi R, and Reggiani C**. Specific contributions of various muscle fibre types to human muscle performance: an in vitro study. *J Electromyogr Kinesiol* 9: 87-95, 1999.

31. **Bouchard C, Malina RM, and P'Russe L**. *Genetics of fitness and physical performance*. Human Kinetics, 1997.

32. **Braun TP, Szumowski M, Levasseur PR, Grossberg AJ, Zhu X, Agarwal A, and Marks DL**. Muscle atrophy in response to cytotoxic chemotherapy is dependent on intact glucocorticoid signaling in skeletal muscle. *PLoS One* 9: e106489, 2014.

33. **Bredahl EC, Pfannenstiel KB, Quinn CJ, Hayward R, and Hydock DS**. Effects of Exercise on Doxorubicin-Induced Skeletal Muscle Dysfunction. *Med Sci Sports Exerc* 48: 1468-1473, 2016.

34. **Brockmann H**. Anthracyclinones and anthracyclines.(Rhodomycinone, pyrromycinone and their glycosides). *Fortschritte der Chemie organischer Naturstoffe= Progress in the chemistry of organic natural products Progres dans la chimie des substances organiques naturelles* 21: 121, 1963.

35. **Brooks G, Fahey T, Baldwin K, and White T**. Exercise physiology: Human bioenergetics and its applications. McGraw-Hill, 2005.

36. **Brown MD, Cotter MA, Hudlicka O, and Vrbova G**. The effects of different patterns of muscle activity on capillary density, mechanical properties and structure of slow and fast rabbit muscles. *Pflugers Arch* 361: 241-250, 1976.

37. **Burgomaster KA, Howarth KR, Phillips SM, Rakobowchuk M, Macdonald MJ, McGee SL, and Gibala MJ**. Similar metabolic adaptations during exercise after low volume sprint interval and traditional endurance training in humans. *J Physiol* 586: 151-160, 2008.

38. **Burgomaster KA, Hughes SC, Heigenhauser GJ, Bradwell SN, and Gibala MJ**. Six sessions of sprint interval training increases muscle oxidative potential and cycle endurance capacity in humans. *J Appl Physiol (1985)* 98: 1985-1990, 2005.

39. **Burkholder TJ, Fingado B, Baron S, and Lieber RL**. Relationship between muscle fiber types and sizes and muscle architectural properties in the mouse hindlimb. *Journal of morphology* 221: 177-190, 1994.

40. **Cadore EL, Izquierdo M, Conceicao M, Radaelli R, Pinto RS, Baroni BM, Vaz MA, Alberton CL, Pinto SS, Cunha G, Bottaro M, and Kruel LF**. Echo intensity is associated with skeletal muscle power and cardiovascular performance in elderly men. *Exp Gerontol* 47: 473-478, 2012.

41. **Camera DM, Smiles WJ, and Hawley JA**. Exercise-induced skeletal muscle signaling pathways and human athletic performance. *Free Radical Biology and Medicine* 98: 131-143, 2016.

42. **Carroll CC, Dickinson JM, Haus JM, Lee GA, Hollon CJ, Aagaard P, Magnusson SP, and Trappe TA**. Influence of aging on the in vivo properties of human patellar tendon. *J Appl Physiol (1985)* 105: 1907-1915, 2008.

43. **Cartee GD, Hepple RT, Bamman MM, and Zierath JR**. Exercise Promotes Healthy Aging of Skeletal Muscle. *Cell Metab* 23: 1034-1047, 2016.

44. **Carvalho C, Santos RX, Cardoso S, Correia S, Oliveira PJ, Santos MS, and Moreira PI**. Doxorubicin: the good, the bad and the ugly effect. *Current medicinal chemistry* 16: 3267-3285, 2009.

45. **Christov C, Chretien F, Abou-Khalil R, Bassez G, Vallet G, Authier FJ, Bassaglia Y, Shinin V, Tajbakhsh S, Chazaud B, and Gherardi RK**. Muscle satellite cells and endothelial cells: close neighbors and privileged partners. *Mol Biol Cell* 18: 1397-1409, 2007.

46. **Coffey VG, and Hawley JA**. The molecular bases of training adaptation. *Sports Med* 37: 737-763, 2007.

47. **Coffey VG, Zhong Z, Shield A, Canny BJ, Chibalin AV, Zierath JR, and Hawley JA**. Early signaling responses to divergent exercise stimuli in skeletal muscle from well-trained humans. *The FASEB Journal* 20: 190-192, 2005.

48. **Courneya KS, Mackey JR, Bell GJ, Jones LW, Field CJ, and Fairey AS**. Randomized controlled trial of exercise training in postmenopausal breast cancer survivors: cardiopulmonary and quality of life outcomes. *Journal of clinical oncology* 21: 1660-1668, 2003.

49. **Curie J, and Curie P**. Contractions et dilatations produites par des tensions dans les cristaux hémièdres à faces inclinées. *C R Acad Sci Gen* 93: 1137-1140, 1880.

50. **Curie J, and Curie P**. Développement, par pression, de l'électricité polaire dans les cristaux hémièdres à faces inclinées. *Comptes Rendus de l'Académie des Sciences* 91: 294-295, 1880.

51. **Curie J, and Curie P**. Sur l'électricité polaire dans les cristaux hémièdres à faces inclinées. *C R Acad Sci Gen* 91: 383-386, 1880.

52. **D'Lugos AC, Patel SH, Ormsby JC, Curtis DP, Fry CS, Carroll CC, and Dickinson JM**. Prior acetaminophen consumption impacts the early adaptive cellular response of human skeletal muscle to resistance exercise. *J Appl Physiol (1985)* 2018.

53. **Daussin FN, Zoll J, Dufour SP, Ponsot E, Lonsdorfer-Wolf E, Doutreleau S, Mettauer B, Piquard F, Geny B, and Richard R**. Effect of interval versus continuous training on cardiorespiratory and mitochondrial functions: relationship to aerobic performance improvements in sedentary subjects. *Am J Physiol Regul Integr Comp Physiol* 295: R264-272, 2008.

54. **De Lorenzo A, Andreoli A, and Deurenberg P**. Impedance ratio as a measure of water shifts. *Annals of nutrition & metabolism* 41: 22-28, 1997.

55. **de Moor JS, Mariotto AB, Parry C, Alfano CM, Padgett L, Kent EE, Forsythe L, Scoppa S, Hachey M, and Rowland JH**. Cancer survivors in the United States: prevalence across the survivorship trajectory and implications for care. *Cancer Epidemiol Biomarkers Prev* 22: 561-570, 2013.

56. **Delmonico MJ, Harris TB, Visser M, Park SW, Conroy MB, Velasquez-Mieyer P, Boudreau R, Manini TM, Nevitt M, Newman AB, Goodpaster BH, Health A, and Body**. Longitudinal study of muscle strength, quality, and adipose tissue infiltration. *Am J Clin Nutr* 90: 1579-1585, 2009.

57. **Der-Torossian H, Couch ME, Dittus K, and Toth MJ**. Skeletal muscle adaptations to cancer and its treatment: their fundamental basis and contribution to functional disability. *Critical Reviews™ in Eukaryotic Gene Expression* 23: 2013.

58. **Dickinson JM, D'Lugos AC, Mahmood TN, Ormsby JC, Salvo L, Dedmon WL, Patel SH, Katsma MS, Mookadam F, Gonzales RJ, Hale TM, Carroll CC, and Angadi SS**. Exercise Protects Skeletal Muscle during Chronic Doxorubicin Administration. *Med Sci Sports Exerc* 49: 2394-2403, 2017.

59. **Dickinson JM, D'Lugos AC, Naymik MA, Siniard AL, Wolfe AJ, Curtis DP, Huentelman MJ, and Carroll CC**. Transcriptome response of human skeletal muscle to divergent exercise stimuli. *J Appl Physiol (1985)* 2018.

60. **Doherty TJ**. Invited review: Aging and sarcopenia. *J Appl Physiol (1985)* 95: 1717-1727, 2003.

61. **Donald I, Macvicar J, and Brown T**. Investigation of abdominal masses by pulsed ultrasound. *The Lancet* 271: 1188-1195, 1958.

62. **Dussik K**. On the possibility of using ultrasound waves as a diagnostic aid. *Neurol Psychiat* 174: 153-168, 1942.

63. **Egan B, Carson BP, Garcia-Roves PM, Chibalin AV, Sarsfield FM, Barron N, McCaffrey N, Moyna NM, Zierath JR, and O'Gorman DJ**. Exercise intensity-dependent regulation of peroxisome proliferator-activated receptor coactivator-1 mRNA abundance is associated with differential activation of upstream signalling kinases in human skeletal muscle. *J Physiol* 588: 1779-1790, 2010.

64. **Egan B, and Zierath JR**. Exercise metabolism and the molecular regulation of skeletal muscle adaptation. *Cell Metab* 17: 162-184, 2013.

65. **Elbl L, Vasova I, Tomaskova I, Jedlicka F, Kral Z, Navratil M, Smardova L, Wagnerova B, and Vorlicek J**. Cardiopulmonary exercise testing in the evaluation of functional capacity after treatment of lymphomas in adults. *Leukemia & lymphoma* 47: 843-851, 2006.

66. **Ema R, Wakahara T, Miyamoto N, Kanehisa H, and Kawakami Y**. Inhomogeneous architectural changes of the quadriceps femoris induced by resistance training. *Eur J Appl Physiol* 113: 2691-2703, 2013.

67. **English C, Fisher L, and Thoirs K**. Reliability of real-time ultrasound for measuring skeletal muscle size in human limbs in vivo: a systematic review. *Clin Rehabil* 26: 934-944, 2012.

68. **Farup J, Kjolhede T, Sorensen H, Dalgas U, Moller AB, Vestergaard PF, Ringgaard S, Bojsen-Moller J, and Vissing K**. Muscle morphological and strength adaptations to endurance vs. resistance training. *Journal of strength and conditioning research* 26: 398-407, 2012.

69. **Feinstein B, Lindegard B, Nyman E, and Wohlfart G**. Morphologic studies of motor units in normal human muscles. *Acta anatomica* 23: 127-142, 1955.

70. **Fink WJ, Costill DL, and Pollock ML**. Submaximal and maximal working capacity of elite distance runners. Part II. Muscle fiber composition and enzyme activities. *Ann N Y Acad Sci* 301: 323-327, 1977.

71. **Finnerty CC, McKenna CF, Cambias LA, Brightwell CR, Prasai A, Wang Y, El Ayadi A, Herndon DN, Suman OE, and Fry CS**. Inducible satellite cell depletion attenuates skeletal muscle regrowth following a scald-burn injury. *J Physiol* 595: 6687-6701, 2017.

72. **Fluck M**. Functional, structural and molecular plasticity of mammalian skeletal muscle in response to exercise stimuli. *J Exp Biol* 209: 2239-2248, 2006.

73. **Forsberg AM, Nilsson E, Werneman J, Bergstrom J, and Hultman E**. Muscle composition in relation to age and sex. *Clin Sci (Lond)* 81: 249-256, 1991.

74. **Franchi MV, Atherton PJ, Reeves ND, Fluck M, Williams J, Mitchell WK, Selby A, Beltran Valls RM, and Narici MV**. Architectural, functional and molecular responses to concentric and eccentric loading in human skeletal muscle. *Acta Physiol (Oxf)* 210: 642-654, 2014.

75. **Freilich RJ, Kirsner RL, and Byrne E**. Isometric strength and thickness relationships in human quadriceps muscle. *Neuromuscul Disord* 5: 415-422, 1995.

76. **Frontera WR, and Ochala J**. Skeletal muscle: a brief review of structure and function. *Calcif Tissue Int* 96: 183-195, 2015.

77. **Fuentes T, Ponce-Gonzalez JG, Morales-Alamo D, de Torres-Peralta R, Santana A, De Pablos-Velasco P, Olmedillas H, Guadalupe-Grau A, Rodriguez-Garcia L, Serrano-Sanchez JA, Guerra B, and Calbet JA**. Isoinertial and isokinetic sprints: muscle signalling. *Int J Sports Med* 34: 285-292, 2013.

78. **Fukumoto Y, Ikezoe T, Yamada Y, Tsukagoshi R, Nakamura M, Mori N, Kimura M, and Ichihashi N**. Skeletal muscle quality assessed from echo intensity is associated with muscle strength of middle-aged and elderly persons. *Eur J Appl Physiol* 112: 1519-1525, 2012.

79. **Fukunaga T, Ichinose Y, Ito M, Kawakami Y, and Fukashiro S**. Determination of fascicle length and pennation in a contracting human muscle in vivo. *J Appl Physiol (1985)* 82: 354-358, 1997.

80. **Fukunaga T, Matsuo A, Ishida Y, Tsunoda N, Uchino S, and Ohkubo M**. Study for measurement of muscle and subcutaneous fat thickness by means of ultrasonic B-mode method. *Jpn J Med Ultrasonics* 16: 170-177, 1989.

81. **Furmaniak AC, Menig M, and Markes MH**. Exercise for women receiving adjuvant therapy for breast cancer. *The Cochrane Library* 2016.

82. **Gan Z, Rumsey J, Hazen BC, Lai L, Leone TC, Vega RB, Xie H, Conley KE, Auwerx J, Smith SR, Olson EN, Kralli A, and Kelly DP**. Nuclear receptor/microRNA circuitry links muscle fiber type to energy metabolism. *J Clin Invest* 123: 2564-2575, 2013.

83. **Gans C, and Bock WJ**. The functional significance of muscle architecture--a theoretical analysis. *Ergebnisse der Anatomie und Entwicklungsgeschichte* 38: 115-142, 1965.

84. **Gans C, and de Vree F**. Functional bases of fiber length and angulation in muscle. *Journal of morphology* 192: 63-85, 1987.

85. **Gewirtz D**. A critical evaluation of the mechanisms of action proposed for the antitumor effects of the anthracycline antibiotics adriamycin and daunorubicin. *Biochemical pharmacology* 57: 727-741, 1999.

86. **Gibala MJ, Little JP, van Essen M, Wilkin GP, Burgomaster KA, Safdar A, Raha S, and Tarnopolsky MA**. Short-term sprint interval versus traditional endurance training: similar initial adaptations in human skeletal muscle and exercise performance. *J Physiol* 575: 901-911, 2006.

87. **Gibala MJ, McGee SL, Garnham AP, Howlett KF, Snow RJ, and Hargreaves M**. Brief intense interval exercise activates AMPK and p38 MAPK signaling and increases the expression of PGC-1alpha in human skeletal muscle. *J Appl Physiol (1985)* 106: 929-934, 2009.

88. **Gibson MC, and Schultz E**. Age-related differences in absolute numbers of skeletal muscle satellite cells. *Muscle Nerve* 6: 574-580, 1983.

89. **Gillen JB, Martin BJ, MacInnis MJ, Skelly LE, Tarnopolsky MA, and Gibala MJ**. Twelve Weeks of Sprint Interval Training Improves Indices of Cardiometabolic Health Similar to Traditional Endurance Training despite a Five-Fold Lower Exercise Volume and Time Commitment. *PLoS One* 11: e0154075, 2016.

90. **Gilliam LA, Ferreira LF, Bruton JD, Moylan JS, Westerblad H, St Clair DK, and Reid MB**. Doxorubicin acts through tumor necrosis factor receptor subtype 1 to cause dysfunction of murine skeletal muscle. *J Appl Physiol (1985)* 107: 1935-1942, 2009.

91. **Gilliam LA, Lark DS, Reese LR, Torres MJ, Ryan TE, Lin CT, Cathey BL, and Neufer PD**. Targeted overexpression of mitochondrial catalase protects against cancer chemotherapy-induced skeletal muscle dysfunction. *Am J Physiol Endocrinol Metab* 311: E293-301, 2016.

92. **Gilliam LA, Moylan JS, Ferreira LF, and Reid MB**. TNF/TNFR1 signaling mediates doxorubicin-induced diaphragm weakness. *Am J Physiol Lung Cell Mol Physiol* 300: L225-231, 2011.

93. **Gilliam LA, Moylan JS, Patterson EW, Smith JD, Wilson AS, Rabbani Z, and Reid MB**. Doxorubicin acts via mitochondrial ROS to stimulate catabolism in C2C12 myotubes. *Am J Physiol Cell Physiol* 302: C195-202, 2012.

94. **Gilliam LA, and St Clair DK**. Chemotherapy-induced weakness and fatigue in skeletal muscle: the role of oxidative stress. *Antioxid Redox Signal* 15: 2543-2563, 2011.

95. **Gliemann L, Gunnarsson TP, Hellsten Y, and Bangsbo J**. 10-20-30 training increases performance and lowers blood pressure and VEGF in runners. *Scand J Med Sci Sports* 25: e479-489, 2015.

96. **Godin G, Valois P, and Lepage L**. The pattern of influence of perceived behavioral control upon exercising behavior: An application of Ajzen's theory of planned behavior. *Journal of behavioral medicine* 16: 81-102, 1993.

97. **Goldberg AL**. Protein synthesis in tonic and phasic skeletal muscles. *Nature* 216: 1219-1220, 1967.

98. **Gollnick PD, Armstrong RB, Saltin B, Saubert CWt, Sembrowich WL, and Shepherd RE**. Effect of training on enzyme activity and fiber composition of human skeletal muscle. *J Appl Physiol* 34: 107-111, 1973.

99. **Goodpaster BH, Chomentowski P, Ward BK, Rossi A, Glynn NW, Delmonico MJ, Kritchevsky SB, Pahor M, and Newman AB**. Effects of physical activity on strength and skeletal muscle fat infiltration in older adults: a randomized controlled trial. *J Appl Physiol (1985)* 105: 1498-1503, 2008.

100. **Goodpaster BH, He J, Watkins S, and Kelley DE**. Skeletal muscle lipid content and insulin resistance: evidence for a paradox in endurance-trained athletes. *The Journal of Clinical Endocrinology & Metabolism* 86: 5755-5761, 2001.

101. **Goodpaster BH, Park SW, Harris TB, Kritchevsky SB, Nevitt M, Schwartz AV, Simonsick EM, Tylavsky FA, Visser M, and Newman AB**. The loss of skeletal muscle strength, mass, and quality in older adults: the health, aging and body composition study. *J Gerontol A Biol Sci Med Sci* 61: 1059-1064, 2006.

102. **Gouspillou G, Scheede-Bergdahl C, Spendiff S, Vuda M, Meehan B, Mlynarski H, Archer-Lahlou E, Sgarioto N, Purves-Smith FM, Konokhova Y, Rak J, Chevalier S, Taivassalo T, Hepple RT, and Jagoe RT**. Anthracycline-containing chemotherapy causes long-term impairment of mitochondrial respiration and increased reactive oxygen species release in skeletal muscle. *Sci Rep* 5: 8717, 2015.

103. **Granata C, Oliveira RS, Little JP, Renner K, and Bishop DJ**. Sprint-interval but not continuous exercise increases PGC-1alpha protein content and p53 phosphorylation in nuclear fractions of human skeletal muscle. *Sci Rep* 7: 44227, 2017.

104. **Granata C, Oliveira RS, Little JP, Renner K, and Bishop DJ**. Training intensity modulates changes in PGC-1alpha and p53 protein content and mitochondrial respiration, but not markers of mitochondrial content in human skeletal muscle. *FASEB J* 30: 959-970, 2016.

105. **Guilhem G, Cornu C, Maffiuletti NA, and Guevel A**. Neuromuscular adaptations to isoload versus isokinetic eccentric resistance training. *Med Sci Sports Exerc* 45: 326-335, 2013.

106. **Hanusova V, Bousova I, and Skalova L**. Possibilities to increase the effectiveness of doxorubicin in cancer cells killing. *Drug metabolism reviews* 43: 540-557, 2011.

107. **Harber MP, Konopka AR, Undem MK, Hinkley JM, Minchev K, Kaminsky LA, Trappe TA, and Trappe S**. Aerobic exercise training induces skeletal muscle hypertrophy and age-dependent adaptations in myofiber function in young and older men. *J Appl Physiol (1985)* 113: 1495-1504, 2012.

108. **Hasten DL, Pak-Loduca J, Obert KA, and Yarasheski KE**. Resistance exercise acutely increases MHC and mixed muscle protein synthesis rates in 78-84 and 23-32 yr olds. *Am J Physiol Endocrinol Metab* 278: E620-626, 2000.

109. **Hawley JA**. Adaptations of skeletal muscle to prolonged, intense endurance training. *Clinical and experimental pharmacology and physiology* 29: 218-222, 2002.

110. **Hawley JA**. Molecular responses to strength and endurance training: are they incompatible? *Appl Physiol Nutr Metab* 34: 355-361, 2009.

111. **Hayward R, Hydock D, Gibson N, Greufe S, Bredahl E, and Parry T**. Tissue retention of doxorubicin and its effects on cardiac, smooth, and skeletal muscle function. *J Physiol Biochem* 69: 177-187, 2013.

112. **Heckmatt JZ, Dubowitz V, and Leeman S**. Detection of pathological change in dystrophic muscle with B-scan ultrasound imaging. *Lancet* 1: 1389-1390, 1980.

113. **Henneman E**. The size-principle: a deterministic output emerges from a set of probabilistic connections. *J Exp Biol* 115: 105-112, 1985.

114. **Hilton TN, Tuttle LJ, Bohnert KL, Mueller MJ, and Sinacore DR**. Excessive adipose tissue infiltration in skeletal muscle in individuals with obesity, diabetes mellitus, and peripheral neuropathy: association with performance and function. *Phys Ther* 88: 1336-1344, 2008.

115. **Hoier B, Passos M, Bangsbo J, and Hellsten Y**. Intense intermittent exercise provides weak stimulus for vascular endothelial growth factor secretion and capillary growth in skeletal muscle. *Exp Physiol* 98: 585-597, 2013.

116. **Holloszy JO**. Adaptations of skeletal muscle mitochondria to endurance exercise: a personal perspective. *Exerc Sport Sci Rev* 32: 41-43, 2004.

117. **Holloszy JO**. Biochemical adaptations in muscle. Effects of exercise on mitochondrial oxygen uptake and respiratory enzyme activity in skeletal muscle. *J Biol Chem* 242: 2278-2282, 1967.

118. **Holloszy JO**. The biology of aging. *Mayo Clinic proceedings* 75 Suppl: S3-8; discussion S8-9, 2000.

119. **Hood MS, Little JP, Tarnopolsky MA, Myslik F, and Gibala MJ**. Low-volume interval training improves muscle oxidative capacity in sedentary adults. *Med Sci Sports Exerc* 43: 1849-1856, 2011.

120. **Huxley AF, and Niedergerke R**. Structural changes in muscle during contraction; interference microscopy of living muscle fibres. *Nature* 173: 971-973, 1954.

121. **Huxley H, and Hanson J**. Changes in the cross-striations of muscle during contraction and stretch and their structural interpretation. *Nature* 173: 973-976, 1954.

122. **Hydock DS, Lien CY, Jensen BT, Schneider CM, and Hayward R**. Characterization of the effect of in vivo doxorubicin treatment on skeletal muscle function in the rat. *Anticancer Res* 31: 2023-2028, 2011.

123. **Ihnatsenka B, and Boezaart AP**. Ultrasound: Basic understanding and learning the language. *International Journal of Shoulder Surgery* 4: 55-62, 2010.

124. **Iida K, Itoh E, Kim DS, del Rincon JP, Coschigano KT, Kopchick JJ, and Thorner MO**. Muscle mechano growth factor is preferentially induced by growth hormone in growth hormone-deficient lit/lit mice. *J Physiol* 560: 341-349, 2004.

125. **Jacobs RA, Fluck D, Bonne TC, Burgi S, Christensen PM, Toigo M, and Lundby C**. Improvements in exercise performance with high-intensity interval training coincide with an increase in skeletal muscle mitochondrial content and function. *J Appl Physiol (1985)* 115: 785-793, 2013.

126. **Joanisse S, McKay BR, Nederveen JP, Scribbans TD, Gurd BJ, Gillen JB, Gibala MJ, Tarnopolsky M, and Parise G**. Satellite cell activity, without expansion, after nonhypertrophic stimuli. *Am J Physiol Regul Integr Comp Physiol* 309: R1101-1111, 2015.

127. **Kalhovde JM, Jerkovic R, Sefland I, Cordonnier C, Calabria E, Schiaffino S, and Lomo T**. "Fast" and "slow" muscle fibres in hindlimb muscles of adult rats regenerate from intrinsically different satellite cells. *J Physiol* 562: 847-857, 2005.

128. **Karlsen T, Aamot IL, Haykowsky M, and Rognmo O**. High Intensity Interval Training for Maximizing Health Outcomes. *Prog Cardiovasc Dis* 60: 67-77, 2017.

129. **Katz B**. The terminations of the afferent nerve fibre in the muscle spindle of the frog. *Philosophical Transactions of the Royal Society of London Series B, Biological Sciences* 221-240, 1961.

130. **Kavazis AN, Smuder AJ, and Powers SK**. Effects of short-term endurance exercise training on acute doxorubicin-induced FoxO transcription in cardiac and skeletal muscle. *J Appl Physiol (1985)* 117: 223-230, 2014.

131. **Keefe AC, Lawson JA, Flygare SD, Fox ZD, Colasanto MP, Mathew SJ, Yandell M, and Kardon G**. Muscle stem cells contribute to myofibres in sedentary adult mice. *Nat Commun* 6: 7087, 2015.

132. **Kelly AM**. Satellite cells and myofiber growth in the rat soleus and extensor digitorum longus muscles. *Developmental biology* 65: 1-10, 1978.

133. **Kjaer M**. Role of extracellular matrix in adaptation of tendon and skeletal muscle to mechanical loading. *Physiol Rev* 84: 649-698, 2004.

134. **Kristensen DE, Albers PH, Prats C, Baba O, Birk JB, and Wojtaszewski JF**. Human muscle fibre type-specific regulation of AMPK and downstream targets by exercise. *J Physiol* 593: 2053-2069, 2015.

135. **Kuang S, and Rudnicki MA**. The emerging biology of satellite cells and their therapeutic potential. *Trends Mol Med* 14: 82-91, 2008.

136. **Kumagai K, Abe T, Brechue WF, Ryushi T, Takano S, and Mizuno M**. Sprint performance is related to muscle fascicle length in male 100-m sprinters. *J Appl Physiol (1985)* 88: 811-816, 2000.

137. **Kurabayashi M, Jeyaseelan R, and Kedes L**. Antineoplastic agent doxorubicin inhibits myogenic differentiation of C2 myoblasts. *J Biol Chem* 268: 5524-5529, 1993.

138. **Kurabayashi M, Jeyaseelan R, and Kedes L**. Doxorubicin represses the function of the myogenic helix-loop-helix transcription factor MyoD. Involvement of Id gene induction. *J Biol Chem* 269: 6031-6039, 1994.

139. **Kwah LK, Pinto RZ, Diong J, and Herbert RD**. Reliability and validity of ultrasound measurements of muscle fascicle length and pennation in humans: a systematic review. *J Appl Physiol (1985)* 114: 761-769, 2013.

140. **Leiber R, and Friden J**. Functional and clinical significance of skeletal muscle architecture. *Muscle & Nerve* 23: 1647-1666, 2000.

141. **Lexell J, and Taylor CC**. Variability in muscle fibre areas in whole human quadriceps muscle: effects of increasing age. *J Anat* 174: 239-249, 1991.

142. **Lieber RL**. *Skeletal Muscle Structure, Function, and plasticity*. Baltimore: Lippincott Williams & Wilkins, 2002.

143. **Lieber RL, and Ward SR**. Skeletal muscle design to meet functional demands. *Philos Trans R Soc Lond B Biol Sci* 366: 1466-1476, 2011.

144. **Little JP, Safdar A, Bishop D, Tarnopolsky MA, and Gibala MJ**. An acute bout of high-intensity interval training increases the nuclear abundance of PGC-1alpha and activates mitochondrial biogenesis in human skeletal muscle. *Am J Physiol Regul Integr Comp Physiol* 300: R1303-1310, 2011.

145. **Little JP, Safdar A, Wilkin GP, Tarnopolsky MA, and Gibala MJ**. A practical model of low-volume high-intensity interval training induces mitochondrial biogenesis in human skeletal muscle: potential mechanisms. *J Physiol* 588: 1011-1022, 2010.

146. **Liu J, Liang X, Zhou D, Lai L, Xiao L, Liu L, Fu T, Kong Y, Zhou Q, Vega RB, Zhu MS, Kelly DP, Gao X, and Gan Z**. Coupling of mitochondrial function and skeletal muscle fiber type by a miR-499/Fnip1/AMPK circuit. *EMBO Mol Med* 8: 1212-1228, 2016.

147. **Livak KJ, and Schmittgen TD**. Analysis of relative gene expression data using real-time quantitative PCR and the 2(-Delta Delta C(T)) Method. *Methods* 25: 402-408, 2001.

148. **Lopez P, Wilhelm EN, Rech A, Minozzo F, Radaelli R, and Pinto RS**. Echo intensity independently predicts functionality in sedentary older men. *Muscle Nerve* 55: 9-15, 2017.

149. **MacInnis MJ, Zacharewicz E, Martin BJ, Haikalis ME, Skelly LE, Tarnopolsky MA, Murphy RM, and Gibala MJ**. Superior mitochondrial adaptations in human skeletal muscle after interval compared to continuous single-leg cycling matched for total work. *J Physiol* 595: 2955-2968, 2017.

150. **MacIntosh BR, Gardiner PF, and McComas AJ**. *Skeletal Muscle: Form and Function*. Human Kinetics, 2006.

151. **Marcus RL, Addison O, Kidde JP, Dibble LE, and Lastayo PC**. Skeletal muscle fat infiltration: impact of age, inactivity, and exercise. *J Nutr Health Aging* 14: 362-366, 2010.

152. **Matta TT, Nascimento FX, Fernandes IA, and Oliveira LF**. Heterogeneity of rectus femoris muscle architectural adaptations after two different 14-week resistance training programmes. *Clin Physiol Funct Imaging* 35: 210-215, 2015.

153. **Matthews DE, and Battezzati A**. Regulation of protein metabolism during stress. *Current opinion in general surgery* 72-77, 1993.

154. **Mauro A**. Satellite cell of skeletal muscle fibers. *J Biophys Biochem Cytol* 9: 493-495, 1961.

155. **Maw GJ, Mackenzie IL, and Taylor NA**. Redistribution of body fluids during postural manipulations. *Acta Physiol Scand* 155: 157-163, 1995.

156. **McMahon G, Morse CI, Burden A, Winwood K, and Onambele GL**. Muscular adaptations and insulin-like growth factor-1 responses to resistance training are stretch-mediated. *Muscle Nerve* 49: 108-119, 2014.

157. **McMahon GE, Morse CI, Burden A, Winwood K, and Onambele GL**. Impact of range of motion during ecologically valid resistance training protocols on muscle size, subcutaneous fat, and strength. *Journal of strength and conditioning research* 28: 245-255, 2014.

158. **Metcalfe RS, Koumanov F, Ruffino JS, Stokes KA, Holman GD, Thompson D, and Vollaard NB**. Physiological and molecular responses to an acute bout of reduced-exertion high-intensity interval training (REHIT). *Eur J Appl Physiol* 115: 2321-2334, 2015.

159. **Mijwel S, Cardinale DA, Norrbom J, Chapman M, Ivarsson N, Wengstrom Y, Sundberg CJ, and Rundqvist H**. Exercise training during chemotherapy preserves skeletal muscle fiber area, capillarization, and mitochondrial content in patients with breast cancer. *FASEB J* fj201700968R, 2018.

160. **Miller BF, Olesen JL, Hansen M, Døssing S, Crameri RM, Welling RJ, Langberg H, Flyvbjerg A, Kjaer M, Babraj JA, Smith K, and Rennie MJ**. Coordinated collagen and muscle protein synthesis in human patella tendon and quadriceps muscle after exercise. *The Journal of Physiology* 567: 1021-1033, 2005.

161. **Min K, Kwon OS, Smuder AJ, Wiggs MP, Sollanek KJ, Christou DD, Yoo JK, Hwang MH, Szeto HH, Kavazis AN, and Powers SK**. Increased mitochondrial emission of reactive oxygen species and calpain activation are required for doxorubicin-induced cardiac and skeletal muscle myopathy. *J Physiol* 593: 2017-2036, 2015.

162. **Minotti G, Menna P, Salvatorelli E, Cairo G, and Gianni L**. Anthracyclines: molecular advances and pharmacologic developments in antitumor activity and cardiotoxicity. *Pharmacol Rev* 56: 185-229, 2004.

163. **Molino S, Dossena M, Buonocore D, and Verri M**. Sarcopenic Obesity: An Appraisal of the Current Status of Knowledge and Management in Elderly People. *J Nutr Health Aging* 20: 780-788, 2016.

164. **Moreau NG, Teefey SA, and Damiano DL**. In vivo muscle architecture and size of the rectus femoris and vastus lateralis in children and adolescents with cerebral palsy. *Dev Med Child Neurol* 51: 800-806, 2009.

165. **Morgan TE, Cobb LA, Short FA, Ross R, and Gunn DR**. Effects of long-term exercise on human muscle mitochondria. In: *Muscle Metabolism During Exericse*, edited by Pernow B, and Saltin B. Plenum, New York: 1971, p. 87-95.

166. **Morgan WP, and Costill DL**. Psychological characteristics of the marathon runner. *J Sports Med Phys Fitness* 12: 42-46, 1972.

167. **Morse CI, Thom JM, Reeves ND, Birch KM, and Narici MV**. In vivo physiological cross-sectional area and specific force are reduced in the gastrocnemius of elderly men. *J Appl Physiol (1985)* 99: 1050-1055, 2005.

168. **Moss FP, and Leblond CP**. Satellite cells as the source of nuclei in muscles of growing rats. *The Anatomical record* 170: 421-435, 1971.

169. **Murach K, Greever C, and Luden ND**. Skeletal muscle architectural adaptations to marathon run training. *Appl Physiol Nutr Metab* 40: 99-102, 2015.

170. **Murach KA, Fry CS, Kirby TJ, Jackson JR, Lee JD, White SH, Dupont-Versteegden EE, McCarthy JJ, and Peterson CA**. Starring or Supporting Role? Satellite Cells and Skeletal Muscle Fiber Size Regulation. *Physiology (Bethesda, Md)* 33: 26-38, 2018.

171. **Murakami S, Fujino H, Takeda I, Momota R, Kumagishi K, and Ohtsuka A**. Comparison of capillary architecture between slow and fast muscles in rats using a confocal laser scanning microscope. *Acta Med Okayama* 64: 11-18, 2010.

172. **Narici M, Franchi M, and Maganaris C**. Muscle structural assembly and functional consequences. *J Exp Biol* 219: 276-284, 2016.

173. **Narici MV, and Maffulli N**. Sarcopenia: characteristics, mechanisms and functional significance. *Br Med Bull* 95: 139-159, 2010.

174. **Narici MV, Maganaris C, and Reeves N**. Myotendinous alterations and effects of resistive loading in old age. *Scand J Med Sci Sports* 15: 392-401, 2005.

175. **Narici MV, Maganaris CN, Reeves ND, and Capodaglio P**. Effect of aging on human muscle architecture. *J Appl Physiol (1985)* 95: 2229-2234, 2003.

176. **Narici MV, Roi G, Landoni L, Minetti A, and Cerretelli P**. Changes in force, cross-sectional area and neural activation during strength training and detraining of the human quadriceps. *European journal of applied physiology and occupational physiology* 59: 310-319, 1989.

177. **Narkar VA, Fan W, Downes M, Yu RT, Jonker JW, Alaynick WA, Banayo E, Karunasiri MS, Lorca S, and Evans RM**. Exercise and PGC-1alpha-independent synchronization of type I muscle metabolism and vasculature by ERRgamma. *Cell Metab* 13: 283-293, 2011.

178. **Nava S, Teresa Larovere M, Fanfulla F, Navalesi P, Delmastro M, and Mortara A**. Orthopnea and inspiratory effort in chronic heart failure patients. *Respiratory Medicine* 97: 647-653, 2003.

179. **Necco A, and Ferraguti M**. Influence of doxorubicin on myogenic cell fusion. *Exp Mol Pathol* 31: 353-360, 1979.

180. **Nederveen JP, Joanisse S, Seguin CM, Bell KE, Baker SK, Phillips SM, and Parise G**. The effect of exercise mode on the acute response of satellite cells in old men. *Acta Physiol (Oxf)* 215: 177-190, 2015.

181. **Nederveen JP, Joanisse S, Snijders T, Ivankovic V, Baker SK, Phillips SM, and Parise G**. Skeletal muscle satellite cells are located at a closer proximity to capillaries in healthy young compared with older men. *J Cachexia Sarcopenia Muscle* 7: 547-554, 2016.

182. **Nederveen JP, Joanisse S, Snijders T, Thomas ACQ, Kumbhare D, and Parise G**. The influence of capillarization on satellite cell pool expansion and activation following exercise-induced muscle damage in healthy young men. *J Physiol* 596: 1063-1078, 2018.

183. **Neidhart JA, Gochnour D, Roach R, Hoth D, and Young D**. A comparison of mitoxantrone and doxorubicin in breast cancer. *Journal of Clinical Oncology* 4: 672-677, 1986.

184. **Nguyen LT, McLoon LK, and Wirtschafter JD**. Doxorubicin chemomyectomy is enhanced when performed two days following bupivacaine injections the effect coincides witht he peak of muscle satellite cell division. *Invest Opthalmol Vis Sci* 39: 203-206, 1998.

185. **Nguyen LT, McLoon LK, and Wirtschafter JD**. Doxorubicin chemomyectomy is enhanced when performed two days following bupivacaine injections: the effect coincides with the peak of muscle satellite cell division. *Invest Ophthalmol Vis Sci* 39: 203-206, 1998.

186. **Nissinen TA, Degerman J, Rasanen M, Poikonen AR, Koskinen S, Mervaala E, Pasternack A, Ritvos O, Kivela R, and Hulmi JJ**. Systemic blockade of ACVR2B ligands prevents chemotherapy-induced muscle wasting by restoring muscle protein synthesis without affecting oxidative capacity or atrogenes. *Sci Rep* 6: 32695, 2016.

187. **Ochoa O, Sun D, Reyes-Reyna SM, Waite LL, Michalek JE, McManus LM, and Shireman PK**. Delayed angiogenesis and VEGF production in CCR2-/- mice during impaired skeletal muscle regeneration. *Am J Physiol Regul Integr Comp Physiol* 293: R651-661, 2007.

188. **Parker L, Trewin A, Levinger I, Shaw CS, and Stepto NK**. The effect of exercise-intensity on skeletal muscle stress kinase and insulin protein signaling. *PLoS One* 12: e0171613, 2017.

189. **Perry CG, Lally J, Holloway GP, Heigenhauser GJ, Bonen A, and Spriet LL**. Repeated transient mRNA bursts precede increases in transcriptional and mitochondrial proteins during training in human skeletal muscle. *J Physiol* 588: 4795-4810, 2010.

190. **Phillips SM, Tipton KD, Aarsland A, Wolf SE, and Wolfe RR**. Mixed muscle protein synthesis and breakdown after resistance exercise in humans. *Am J Physiol* 273: E99-107, 1997.

191. **Pillen S**. Skeletal Muscle Ultrasound. *Eur J Trans Myolog* 1: 145-155, 2010.

192. **Pillen S, Tak RO, Zwarts MJ, Lammens MM, Verrijp KN, Arts IM, van der Laak JA, Hoogerbrugge PM, van Engelen BG, and Verrips A**. Skeletal muscle ultrasound: correlation between fibrous tissue and echo intensity. *Ultrasound Med Biol* 35: 443-446, 2009.

193. **Pollanen E, Ronkainen PH, Horttanainen M, Takala T, Puolakka J, Suominen H, Sipila S, and Kovanen V**. Effects of combined hormone replacement therapy or its effective agents on the IGF-1 pathway in skeletal muscle. *Growth Horm IGF Res* 20: 372-379, 2010.

194. **Powell PL, Roy RR, Kanim P, Bello MA, and Edgerton VR**. Predictability of skeletal muscle tension from architectural determinations in guinea pig hindlimbs. *Journal of applied physiology: respiratory, environmental and exercise physiology* 57: 1715-1721, 1984.

195. **Pretorius A, and Keating J**. Validity of real time ultrasound for measuring skeletal muscle size. *Physical Therapy Reviews* 13: 415-426, 2008.

196. **Primack SJ**. Past, Present, and Future Considerations for Musculoskeletal Ultrasound. *Phys Med Rehabil Clin N Am* 27: 749-752, 2016.

197. **Puri PL, Medaglia S, Cimino L, Maselli C, Germani A, De Marzio E, Levrero M, and Balsano C**. Uncoupling of p21 induction and MyoD activation results in the failure of irreversible cell cycle arrest in doxorubicin-treated myocytes. *J Cell Biochem* 66: 27-36, 1997.

198. **Rabbani A, and Davoodi J**. Effects of anthracycline antibiotic, daunomycin on thymus chromatin: the role of chromosomal proteins. *General Pharmacology: The Vascular System* 25: 787-793, 1994.

199. **Radaelli R, Botton CE, Wilhelm EN, Bottaro M, Lacerda F, Gaya A, Moraes K, Peruzzolo A, Brown LE, and Pinto RS**. Low- and high-volume strength training induces similar neuromuscular improvements in muscle quality in elderly women. *Exp Gerontol* 48: 710-716, 2013.

200. **Rahbarghazi R, Nassiri SM, Khazraiinia P, Kajbafzadeh AM, Ahmadi SH, Mohammadi E, Molazem M, and Zamani-Ahmadmahmudi M**. Juxtacrine and paracrine interactions of rat marrow-derived mesenchymal stem cells, muscle-derived satellite cells, and neonatal cardiomyocytes with endothelial cells in angiogenesis dynamics. *Stem Cells Dev* 22: 855-865, 2013.

201. **Rangwala SM, Wang X, Calvo JA, Lindsley L, Zhang Y, Deyneko G, Beaulieu V, Gao J, Turner G, and Markovits J**. Estrogen-related receptor gamma is a key regulator of muscle mitochondrial activity and oxidative capacity. *J Biol Chem* 285: 22619-22629, 2010.

202. **Rayment I, Rypniewski WR, Schmidt-Base K, Smith R, Tomchick DR, Benning MM, Winkelmann DA, Wesenberg G, and Holden HM**. Three-dimensional structure of myosin subfragment-1: a molecular motor. *Science* 261: 50-58, 1993.

203. **Reeves ND, Maganaris CN, Longo S, and Narici MV**. Differential adaptations to eccentric versus conventional resistance training in older humans. *Exp Physiol* 94: 825-833, 2009.

204. **Reeves ND, Narici MV, and Maganaris CN**. In vivo human muscle structure and function: adaptations to resistance training in old age. *Exp Physiol* 89: 675-689, 2004.

205. **Rekabizaheh M, Rezasoltani A, Lahouti B, and Namavarian N**. Pennation Angle and Fascicle Length of Human Skeletal Muscles to Predict the Strength of an Individual Muscle Using Real-Time Ultrasonography: A Review of Literature. *J Clin Physiother Res* 1: 42-48, 2016.

206. **Rhoads RP, Johnson RM, Rathbone CR, Liu X, Temm-Grove C, Sheehan SM, Hoying JB, and Allen RE**. Satellite cell-mediated angiogenesis in vitro coincides with a functional hypoxia-inducible factor pathway. *Am J Physiol Cell Physiol* 296: C1321-1328, 2009.

207. **Rockl KS, Witczak CA, and Goodyear LJ**. Signaling mechanisms in skeletal muscle: acute responses and chronic adaptations to exercise. *IUBMB life* 60: 145-153, 2008.

208. **Roth SM**. *Genetics primer for exercise science and health*. Human Kinetics, 2007.

209. **Rutherford OM, and Jones DA**. Measurement of fibre pennation using ultrasound in the human quadriceps in vivo. *Eur J Appl Physiol Occup Physiol* 65: 433-437, 1992.

210. **Sabourin LA, Girgis-Gabardo A, Seale P, Asakura A, and Rudnicki MA**. Reduced Differentiation Potential of PrimaryMyoD−/− Myogenic Cells Derived from Adult Skeletal Muscle. *The Journal of Cell Biology* 144: 631-643, 1999.

211. **Sawyer DB, Peng X, Chen B, Pentassuglia L, and Lim CC**. Mechanisms of anthracycline cardiac injury: can we identify strategies for cardioprotection? *Prog Cardiovasc Dis* 53: 105-113, 2010.

212. **Saxton RA, and Sabatini DM**. mTOR Signaling in Growth, Metabolism, and Disease. *Cell* 168: 960-976, 2017.

213. **Scalzo RL, Peltonen GL, Binns SE, Shankaran M, Giordano GR, Hartley DA, Klochak AL, Lonac MC, Paris HL, Szallar SE, Wood LM, Peelor FF, 3rd, Holmes WE, Hellerstein MK, Bell C, Hamilton KL, and Miller BF**. Greater muscle protein synthesis and mitochondrial biogenesis in males compared with females during sprint interval training. *FASEB J* 28: 2705-2714, 2014.

214. **Scanlon TC, Fragala MS, Stout JR, Emerson NS, Beyer KS, Oliveira LP, and Hoffman JR**. Muscle architecture and strength: adaptations to short-term resistance training in older adults. *Muscle Nerve* 49: 584-592, 2014.

215. **Schrauwen P, van Aggel-Leijssen DP, Hul G, Wagenmakers AJ, Vidal H, Saris WH, and van Baak MA**. The effect of a 3-month low-intensity endurance training program on fat oxidation and acetyl-CoA carboxylase-2 expression. *Diabetes* 51: 2220-2226, 2002.

216. **Schwartz AL, Winters-Stone K, and Gallucci B**. Exercise effects on bone mineral density in women with breast cancer receiving adjuvant chemotherapy. In: *Oncology nursing forum*2007.

217. **Scott JM, Khakoo A, Mackey JR, Haykowsky MJ, Douglas PS, and Jones LW**. Modulation of anthracycline-induced cardiotoxicity by aerobic exercise in breast cancer: current evidence and underlying mechanisms. *Circulation* 124: 642-650, 2011.

218. **Scribbans TD, Edgett BA, Vorobej K, Mitchell AS, Joanisse SD, Matusiak JB, Parise G, Quadrilatero J, and Gurd BJ**. Fibre-specific responses to endurance and low volume high intensity interval training: striking similarities in acute and chronic adaptation. *PLoS One* 9: e98119, 2014.

219. **Selva Raj I, Bird SR, and Shield AJ**. Ultrasound Measurements of Skeletal Muscle Architecture Are Associated with Strength and Functional Capacity in Older Adults. *Ultrasound Med Biol* 43: 586-594, 2017.

220. **Seynnes OR, de Boer M, and Narici MV**. Early skeletal muscle hypertrophy and architectural changes in response to high-intensity resistance training. *J Appl Physiol (1985)* 102: 368-373, 2007.

221. **Shepherd SO, Cocks M, Tipton KD, Ranasinghe AM, Barker TA, Burniston JG, Wagenmakers AJ, and Shaw CS**. Sprint interval and traditional endurance training increase net intramuscular triglyceride breakdown and expression of perilipin 2 and 5. *J Physiol* 591: 657-675, 2013.

222. **Shrout PE, and Fleiss JL**. Intraclass correlations: uses in assessing rater reliability. *Psychological bulletin* 86: 420-428, 1979.

223. **Sin TK, Tam BT, Yu AP, Yip SP, Yung BY, Chan LW, Wong CS, Rudd JA, and Siu PM**. Acute Treatment of Resveratrol Alleviates Doxorubicin-Induced Myotoxicity in Aged Skeletal Muscle Through SIRT1-Dependent Mechanisms. *J Gerontol A Biol Sci Med Sci* 71: 730-739, 2016.

224. **Skovsgaard T, and Nissen NI**. Membrane transport of anthracyclines. *Pharmacology & therapeutics* 18: 293-311, 1982.

225. **Smerdu V, Karsch-Mizrachi I, Campione M, Leinwand L, and Schiaffino S**. Type IIx myosin heavy chain transcripts are expressed in type IIb fibers of human skeletal muscle. *Am J Physiol* 267: C1723-1728, 1994.

226. **Smuder AJ, Kavazis AN, Min K, and Powers SK**. Doxorubicin-induced markers of myocardial autophagic signaling in sedentary and exercise trained animals. *J Appl Physiol (1985)* 115: 176-185, 2013.

227. **Smuder AJ, Kavazis AN, Min K, and Powers SK**. Exercise protects against doxorubicin-induced markers of autophagy signaling in skeletal muscle. *J Appl Physiol (1985)* 111: 1190-1198, 2011.

228. **Smuder AJ, Kavazis AN, Min K, and Powers SK**. Exercise protects against doxorubicin-induced oxidative stress and proteolysis in skeletal muscle. *J Appl Physiol (1985)* 110: 935-942, 2011.

229. **Snijders T, Nederveen JP, McKay BR, Joanisse S, Verdijk LB, van Loon LJ, and Parise G**. Satellite cells in human skeletal muscle plasticity. *Front Physiol* 6: 283, 2015.

230. **Snijders T, Verdijk LB, and van Loon LJ**. The impact of sarcopenia and exercise training on skeletal muscle satellite cells. *Ageing Res Rev* 8: 328-338, 2009.

231. **Staron RS, Kraemer WJ, Hikida RS, Fry AC, Murray JD, and Campos GE**. Fiber type composition of four hindlimb muscles of adult Fisher 344 rats. *Histochem Cell Biol* 111: 117-123, 1999.

232. **Stasinaki AN, Gloumis G, Spengos K, Blazevich AJ, Zaras N, Georgiadis G, Karampatsos G, and Terzis G**. Muscle Strength, Power, and Morphologic Adaptations After 6 Weeks of Compound vs. Complex Training in Healthy Men. *Journal of strength and conditioning research* 29: 2559-2569, 2015.

233. **Štěrba M, Popelová O, Vávrová A, Jirkovský E, Kovaříková P, Geršl V, and Šimůnek T**. Oxidative stress, redox signaling, and metal chelation in anthracycline cardiotoxicity and pharmacological cardioprotection. *Antioxidants & redox signaling* 18: 899-929, 2013.

234. **Stock MS, Mota JA, Hernandez JM, and Thompson BJ**. Echo intensity and muscle thickness as predictors Of athleticism and isometric strength in middle-school boys. *Muscle Nerve* 55: 685-692, 2017.

235. **Stone P, Hardy J, Broadley K, Tookman A, Kurowska A, and A'Hern R**. Fatigue in advanced cancer: a prospective controlled cross-sectional study. *British journal of cancer* 79: 1479, 1999.

236. **Strasser EM, Draskovits T, Praschak M, Quittan M, and Graf A**. Association between ultrasound measurements of muscle thickness, pennation angle, echogenicity and skeletal muscle strength in the elderly. *Age (Dordr)* 35: 2377-2388, 2013.

237. **Suetta C, Andersen JL, Dalgas U, Berget J, Koskinen S, Aagaard P, Magnusson SP, and Kjaer M**. Resistance training induces qualitative changes in muscle morphology, muscle architecture, and muscle function in elderly postoperative patients. *J Appl Physiol (1985)* 105: 180-186, 2008.

238. **Takemura G, and Fujiwara H**. Doxorubicin-induced cardiomyopathy: from the cardiotoxic mechanisms to management. *Progress in cardiovascular diseases* 49: 330-352, 2007.

239. **Taylor CW, Ingham SA, Hunt JE, Martin NR, Pringle JS, and Ferguson RA**. Exercise duration-matched interval and continuous sprint cycling induce similar increases in AMPK phosphorylation, PGC-1alpha and VEGF mRNA expression in trained individuals. *Eur J Appl Physiol* 116: 1445-1454, 2016.

240. **Therkelsen KE, Pedley A, Speliotes EK, Massaro JM, Murabito J, Hoffmann U, and Fox CS**. Intramuscular Fat and Associations with Metabolic Risk Factors in the Framingham Heart Study. *Arteriosclerosis, thrombosis, and vascular biology* 33: 863-870, 2013.

241. **Thoirs K, and English C**. Ultrasound measures of muscle thickness: intra-examiner reliability and influence of body position. *Clin Physiol Funct Imaging* 29: 440-446, 2009.

242. **Tillquist M, Kutsogiannis DJ, Wischmeyer PE, Kummerlen C, Leung R, Stollery D, Karvellas CJ, Preiser JC, Bird N, Kozar R, and Heyland DK**. Bedside ultrasound is a practical and reliable measurement tool for assessing quadriceps muscle layer thickness. *JPEN J Parenter Enteral Nutr* 38: 886-890, 2014.

243. **Tisdale MJ**. Mechanisms of cancer cachexia. *Physiological reviews* 89: 381-410, 2009.

244. **Toth MJ, Miller MS, Callahan DM, Sweeny AP, Nunez I, Grunberg SM, Der-Torossian H, Couch ME, and Dittus K**. Molecular mechanisms underlying skeletal muscle weakness in human cancer: reduced myosin-actin cross-bridge formation and kinetics. *Journal of applied physiology* 114: 858-868, 2013.

245. **Trappe S, Gallagher P, Harber M, Carrithers J, Fluckey J, and Trappe T**. Single muscle fibre contractile properties in young and old men and women. *J Physiol* 552: 47-58, 2003.

246. **Trappe TA, White F, Lambert CP, Cesar D, Hellerstein M, and Evans WJ**. Effect of ibuprofen and acetaminophen on postexercise muscle protein synthesis. *Am J Physiol Endocrinol Metab* 282: E551-556, 2002.

247. **Tsubahara A, Chino N, Akaboshi K, Okajima Y, and Takahashi H**. Age-related changes of water and fat content in muscles estimated by magnetic resonance (MR) imaging. *Disability and rehabilitation* 17: 298-304, 1995.

248. **Turner-Gomes SO, Lands LC, Halton J, Hanning RM, Heigenhauser GJ, Pai M, and Barr R**. Cardiorespiratory status after treatment for acute lymphoblastic leukemia. *Medical and Pediatric Oncology: The Official Journal of SIOP—International Society of Pediatric Oncology (Societé Internationale d'Oncologie Pédiatrique* 26: 160-165, 1996.

249. **Tzanis G, Philippou A, Karatzanos E, Dimopoulos S, Kaldara E, Nana E, Pitsolis T, Rontogianni D, Koutsilieris M, and Nanas S**. Effects of High-Intensity Interval Exercise Training on Skeletal Myopathy of Chronic Heart Failure. *J Card Fail* 23: 36-46, 2017.

250. **van Dalen EC, van der Pal HJ, and Kremer LC**. Different dosage schedules for reducing cardiotoxicity in people with cancer receiving anthracycline chemotherapy. *Cochrane Database Syst Rev* 3: CD005008, 2016.

251. **van Norren K, van Helvoort A, Argiles JM, van Tuijl S, Arts K, Gorselink M, Laviano A, Kegler D, Haagsman HP, and van der Beek EM**. Direct effects of doxorubicin on skeletal muscle contribute to fatigue. *Br J Cancer* 100: 311-314, 2009.

252. **Varanoske AN, Fukuda DH, Boone CH, Beyer KS, Stout JR, and Hoffman JR**. Homogeneity of echo intensity values in transverse ultrasound images. *Muscle Nerve* 56: 93-98, 2017.

253. **Villani F, Busia A, Villani M, Laffranchi A, Viviani S, and Bonfante V**. Cardiopulmonary response to exercise in patients with different degrees of lung toxicity after radio-chemotherapy for Hodgkin's disease. *Anticancer research* 29: 777-783, 2009.

254. **Vogiatzis I, Terzis G, Nanas S, Stratakos G, Simoes DC, Georgiadou O, Zakynthinos S, and Roussos C**. Skeletal muscle adaptations to interval training in patients with advanced COPD. *Chest* 128: 3838-3845, 2005.

255. **Walker DK, Dickinson JM, Timmerman KL, Drummond MJ, Reidy PT, Fry CS, Gundermann DM, and Rasmussen BB**. Exercise, amino acids, and aging in the control of human muscle protein synthesis. *Med Sci Sports Exerc* 43: 2249-2258, 2011.

256. **Watanabe Y, Yamada Y, Fukumoto Y, Ishihara T, Yokoyama K, Yoshida T, Miyake M, Yamagata E, and Kimura M**. Echo intensity obtained from ultrasonography images reflecting muscle strength in elderly men. *Clin Interv Aging* 8: 993-998, 2013.

257. **Weiss RB**. The Anthracyclines: Will we ever find a better doxorubicin? *Seminars in Oncology* 19: 670-686, 1992.

258. **Wells AJ, Fukuda DH, Hoffman JR, Gonzalez AM, Jajtner AR, Townsend JR, Mangine GT, Fragala MS, and Stout JR**. Vastus lateralis exhibits non-homogenous adaptation to resistance training. *Muscle Nerve* 50: 785-793, 2014.

259. **Widrick JJ, Trappe SW, Blaser CA, Costill DL, and Fitts RH**. Isometric force and maximal shortening velocity of single muscle fibers from elite master runners. *Am J Physiol* 271: C666-675, 1996.

260. **Widrick JJ, Trappe SW, Costill DL, and Fitts RH**. Force-velocity and force-power properties of single muscle fibers from elite master runners and sedentary men. *Am J Physiol* 271: C676-683, 1996.

261. **Wilhelm EN, Rech A, Minozzo F, Radaelli R, Botton CE, and Pinto RS**. Relationship between quadriceps femoris echo intensity, muscle power, and functional capacity of older men. *Age (Dordr)* 36: 9625, 2014.

262. **Williamson DL, Gallagher PM, Carroll CC, Raue U, and Trappe SW**. Reduction in hybrid single muscle fiber proportions with resistance training in humans. *J Appl Physiol (1985)* 91: 1955-1961, 2001.

263. **Williamson DL, Godard MP, Porter DA, Costill DL, and Trappe SW**. Progressive resistance training reduces myosin heavy chain coexpression in single muscle fibers from older men. *J Appl Physiol (1985)* 88: 627-633, 2000.

264. **Yang Y, Creer A, Jemiolo B, and Trappe S**. Time course of myogenic and metabolic gene expression in response to acute exercise in human skeletal muscle. *J Appl Physiol (1985)* 98: 1745-1752, 2005.

265. **Ye J, Coulouris G, Zaretskaya I, Cutcutache I, Rozen S, and Madden TL**. Primer-BLAST: a tool to design target-specific primers for polymerase chain reaction. *BMC bioinformatics* 13: 134, 2012.

266. **Yin H, Price F, and Rudnicki MA**. Satellite cells and the muscle stem cell niche. *Physiol Rev* 93: 23-67, 2013.

267. **Yoshiko A, Kaji T, Sugiyama H, Koike T, Oshida Y, and Akima H**. Effect of 12-month resistance and endurance training on quality, quantity, and function of skeletal muscle in older adults requiring long-term care. *Exp Gerontol* 98: 230-237, 2017.

268. **Young A, Stokes M, and Crowe M**. The size and strength of the quadriceps muscles of old and young men. *Clinical physiology (Oxford, England)* 5: 145-154, 1985.

269. **Young HJ, Jenkins NT, Zhao Q, and McCully KK**. Measurement of intramuscular fat by muscle echo intensity. *Muscle Nerve* 52: 963-971, 2015.

270. **Young HJ, Southern WM, and McCully KK**. Comparisons of ultrasound-estimated intramuscular fat with fitness and health indicators. *Muscle Nerve* 54: 743-749, 2016.

271. **Zamboni M, Mazzali G, Fantin F, Rossi A, and Di Francesco V**. Sarcopenic obesity: a new category of obesity in the elderly. *Nutr Metab Cardiovasc Dis* 18: 388-395, 2008.

272. **Zierath JR, and Hawley JA**. Skeletal muscle fiber type: influence on contractile and metabolic properties. *PLoS Biol* 2: e348, 2004.

APPENDIX A

ULTRASOUND STUDY CONSENT FORM

Title of research study: A comparison of two ultrasound techniques for measuring muscle thickness, muscle fiber angle, and their association with muscle function among young and older adults.

Investigator: Jared Dickinson, PhD
School of Nutrition and Health Promotion
Arizona State University

Siddhartha Angadi, PhD
College of Nursing and Health Innovation
Arizona State University

Andrew D'Lugos, MS
College of Nursing and Health Innovation
Arizona State University

Why am I being invited to take part in a research study?

We invite you to take part in a research study because:

- You are either between 18 and 35 years of age or 60 and 85 years of age
- You are healthy, and do not have any major health problems such as heart trouble, lung, kidney or liver problems, active cancer, infections, or existing muscle/ bone injuries
- You do not participate in regularly scheduled heavy weight lifting exercise.

Why is this research being done?

Changes in muscle size are often related to changes in muscle function or strength. For instance, a bigger muscle is usually a stronger muscle. Ultrasound imaging is a safe and painless way of taking pictures of your muscles to deterimine their size.

Two common methods are used by researchers to measure muscle size using ultrasound. The main difference between protocols is the position of the patient while the images are captured, either standing or laying down. Nobody has compared the standing protocol versus the laying down protocol on the same set of individuals.

The purpose of this study is to determine which ultrasound imaging protocol of the thigh muscles is more accurate and reliable. We will also want to examine which protocol is more closely related to the strength of your thigh muscles and which protocol is more closley related to the total amount of muscle you have in your legs. Lastly, we also want to see whether these relationships are similar or different in younger and older men and women.

All subjects will perform and participate in the same number of tests and visits to the lab. These tests and visits are described below.

How long will the research last?

We expect that individuals participating in the proposed activities will spend about 4 hours at our lab, which is located in the Arizona Biomedical Collaborative Building on the Downtown Phoenix Campus of Arizona State University. You will be asked to visit the lab on two (2) separate occasions. The visits should require you to be in our lab for ~ 120 minutes (or 2 hours) for each of the visits. We expect that you will be able to complete all these visits over a 1-2 week period depending on scheduling.

How many people will be studied?

We expect about 80 people from the Phoenix area will participate in this research study.

What happens if I say yes, I want to be in this research?

It is up to you to decide whether or not to participate.

If you decide to participate, then as a study participant you will join a study involving research to determine which ultrasound imaging protocol is more reliable in measuring muscle characteristics (muscle size, muscle fiber angle) and is more closely related to muscular strength. All visits will take place at the Arizona Biomedical Collaborative building on the Downtown Phoenix campus of Arizona State University. You will only interact with members of the research team. As part of your participation you will be asked to perform the following tests:

Visit #1 (Consent, Familiarization, Trial 1)
Time Commitment: 120 minutes

1) You will be asked to arrive to the lab after a three (3) hour fast. We will ask you not to consume anything except water for three (3) hours before your scheduled arrival time. We will ask you to wear or bring with you a pair of shorts that can be worn during the visit.
2) You have been invited to Arizona State University for an initial visit, review of the information provided on the online questionnaire, distribution of the consent form, and an explanation of the study procedures.
3) If you agree to participate and sign this consent form, you will complete the first of two visits. Before the initiation of any measurement, you will have your height, weight, and blood pressure measured.
4) We will ask you to perform a Physical Activity Readiness Questionnaire to determine how safe it is for you to exercise.
5) We will measure the size of your muscles in your upper leg and the angle of muscle fibers within these muscles, using ultrasound imaging. You will be asked to either stand on a cushioned mat or lie down on a padded examination table and relax for twenty (20) minutes. During this time the researcher will measure and mark imaging sites along the upper leg, using a tape measure and medical marker. Next, the researcher will place the ultrasound device on the skin and proceed to capture pictures of the upper leg muscles. We will take these measures on both your right and left leg. You will be asked to stand up for some measures and lay down for some measures.
6) We will ask you to perform exercises that will familiarize you (like practice) with exercises we will ask you to perform at the second visit.
    a. <u>Muscle Performance</u>: This exercise will be performed for each leg on a specialized piece of exercise equipment. For this test, you will be seated on the exercise equipment and strapped in around your shoulders and hips to keep you in position. One of your legs will be attached to the leg attachment with a padded ankle strap. For this test, you will be asked to move your knee from a bent position to a straighten position and then from a straightened position to a bent position using your leg muscles to push and pull the bar as hard as you can in both directions. For a separate test, you will be asked to push against a stationary bar as hard as you can.
7) We will establish a schedule for Visit #2, ranging from five (5) to fifteen (15) days from Visit #1.

Visit #2 (Trial 2)
Time Commitment: 120 minutes

1) You will be asked to arrive to the lab after a three (3) hour fast. We will ask you not to consume anything except water for three (3) hours before your scheduled arrival time. We will ask you to wear or bring with you a pair of shorts that can be worn during the visit.
2) Before the initiation of any measurement, you will have your height, weight, and blood pressure measured.
3) We will repeat the same ultrasound measures as described for Visit #1
4) We will ask you to perform the same muscular performance test as Visit #1.
5) You will be asked to receive a DXA scan (similar to a low-dose x-ray). You will be escorted to the second floor of the ABC building and positioned on a padded, examination table lying face up. The DXA scan will last no more than five (5) minutes and will consist of a scanning head that will travel over top of the body. A licensed radiology technician will perform the DXA scan. If you are of child-bearing age, before you receive the DXA scan we will ask you to perform a pregnancy test that we provide and use this test to determine that you are not pregnant prior to performing the DXA scan.

Dietary and Activity Control: Three days prior visits #1 and #2 you will be asked to maintain your normal dietary habits. You will be asked to abstain from consuming any food (except water) 3 hours prior to visits #1 and #2. *You will also be asked to refrain from alcohol consumption 24 hours prior to visits #1 and #2 and any unordinary physical activity beginning three days prior to visits #1 and #2.*

What happens if I say yes, but I change my mind later?

You can leave the research at any time it will not be held against you.

If you stop being in the research project, data collected up to the point of your withdrawal from the study will remain with the research team to ensure the integrity of the research project. These data will be handled the same as research data.

If you decide to stop the research project, no explanation is required.

Is there any way being in this study could be bad for me?

If you decide to participate in this study, then you may face a risk. These risks include:

1) **Muscle Performance Testing.** Muscle soreness or cramps may occur. These are the most likely side effects of exercise, and can be reduced with an adequate warm-up. Exercise may also expose you to a low risk of cardiovascular events, such as a heart attack, especially if you have a predisposing condition. However, a cardiovascular event such as a heart attack is a very rare potential risk in individuals without a predisposing condition. The exercise portion of this study is considered minimal, and our screening procedures are specifically designed to minimize your risk.

2) **Dietary and Activity control**. No known risks

3) **Ultrasonography.** Ultrasound imaging has been used for over 20 years and has an excellent safety record. It does not have the same risks as x-rays or other types of imaging. Even though there are no known risks of ultrasound imaging, it can heat the tissues slightly. However, we do not anticipate that the time it takes for us to image your muscles will produce any noticeable heating effects on your body.

4) **DXA Scan**. This procedure will expose you to a very small amount of radiation, much less than most routine X-ray procedures, and less than the amount of radiation you would be exposed to in a 2-hour airplane flight. Exposure to radiation can increase the risk of getting cancer and birth defects. The amount of radiation to which you will be exposed during the DXA scan is so small that the exact risk is unknown. The exposure of radiation via X-ray during DXA scans is especially risky for women who are pregnant or have a risk of being pregnant.

5) **Confidentiality**. There is a general risk of disclosure of personal sensitive data in a clinical investigation. To minimize this risk only the investigators and the laboratory personnel will have access to your personal information. All research data containing your name will be locked in the Principal Investigator's office. To preserve confidentiality, immediately after enrollment you will be assigned a code by which each research sample will be identified for further analysis, thus avoiding identification by technicians or non-qualified individuals.

Other unforeseen or unknown risks may occur. And as with any research, there is some possibility that you may be subject to risks that have not yet been identified. You will be closely monitored for any unforeseen risks.

You should not be or become pregnant while in this research study.

Alternative Treatment. There are no feasible alternative procedures available for the procedures utilized in this study. An alternative would be not to participate in this study.

Will being in this study help me any way?

We cannot promise any benefits to you or others from your taking part in this research.

However, the knowledge gained from this study could have a benefit to society by providing new data regarding whether standing or lying down during ultrasound imaging results in more reliable measurements and which protocol relates more to muscular strength.

What happens to the information collected for the research?

Efforts will be made to limit the use and disclosure of your personal information to people who have a need to review this information. We cannot promise complete secrecy. Organizations that may inspect and copy your information include the IRB and other representatives of this organization.

Federal law provides additional protections of your medical records and related health information. These are described in an attached document.

What else do I need to know?

If you agree to take part in this research study, we will pay you for your time and effort. You will be paid $20 for completion of the protocol. If you drop out or are excluded, you will not receive any payment. You will receive the full $20 only for the completion of all research visits. Also, please note that in the unlikely event that a visit or test needs to be repeated, you will not receive additional compensation or payment.

All study-related costs associated with your participation will be paid by funds allocated to the research team. There will be no cost to you, the subject, during your participation in this study other than the cost of travel to and from the Arizona Biomedical Collaborative Building.

If you agree to participate in this study, then your consent does not waive your legal rights. However, no funds have been set aside to compensate you in the event of injury. However, if any injury occurs due to the experimental procedures, first aid will be provided. If there is a situation that the research team believes needs attention by a primary care practitioner, you will be referred to the Nurse Practitioner Clinic on the Downtown Arizona State University campus (approximately two (2) blocks from the lab). If any injury occurs after the Nurse Practitioner Clinic is closed you should seek attention at an urgent care facility. If a medical emergency were to occur during this study, we will call "911" to bring emergency medical personnel to the lab. You will be responsible for any costs incurred.

Your participation may be stopped by the research team without consent if

1) You do not meet the inclusion/exclusion criteria of this study.
2) You experience adverse events such as extreme muscle soreness or inability to complete the measurements during Visits #1 and #2.
3) You are not compliant with the pre-study instructions.

Who can I talk to?

If you have questions, concerns, or complaints, or think the research has hurt you, please contact the research team at ###-###-#### (business hours)**,** jared.dickinson@asu.edu (any time) or ###-###-#### (business hours), andrew.dlugos@asu.edu (any time).

This research has been reviewed and approved by the Bioscience IRB ("IRB"). You may talk to them at (480) 965-6788 or research.integrity@asu.edu if:

- Your questions, concerns, or complaints are not being answered by the research team.
- You cannot reach the research team.
- You want to talk to someone besides the research team.
- You have questions about your rights as a research participant.
- You want to get information or provide input about this research.

Written Informed Consent

- Your participation in this study is completely voluntary and you have been told that you may refuse to participate or stop your participation in this project at any time without penalty or loss of benefits and without jeopardizing any relationships with Arizona State University. If you decide to stop your participation in this project and revoke your authorization for the use and disclosure of your health information, Arizona State University may continue to use and disclose your health information in some instances. This would include any health information that was used or disclosed prior to your decision to stop participation and needed in order to maintain the integrity of the research study. If we get any information that might change your mind about participating, we will give you the information and allow you to reconsider whether or not to continue.

- The purpose of this research study, procedures to be followed, risks and benefits have been explained to you. You have been allowed to ask questions and your questions have been answered to your satisfaction. You have been told who to contact if you have additional questions. You have read this consent form and voluntarily agree to participate as a subject in this study. You are free to withdraw your consent, including your authorization for the use and disclosure of your health information, at any time. You may withdraw your consent by notifying Andrew D'Lugos, MS at 602-827-6328. You will be given a copy of the consent form you have signed.

Informed consent is required of all persons in this project. Whether or not you provide a signed informed consent for this research study will have no effect on your current or future relationship with Arizona State University.

Your signature below documents your permission to take part in this research.

Signature of participant	Date
Printed name of participant	
Signature of person obtaining consent	Date
Printed name of person obtaining consent	

APPENDIX B

ULTRASOUND IMAGE COLLECTION PROTOCOL

ULTRASOUND IMAGE COLLECTION PROTOCOL

Supplies Needed / Used	Item Number
Terason Ultrasound	Terason: uSmart 3300
Ultrasound Probe	Terason: Linear Phased Array 15-4 mHz
Bed	Medical Positioning, Inc. Ultra Scan Plus
Ultrasound Gel	Parker Aquasonics 100
Surgical Skin Markers	AliMed: 933294
General Lab Equipment	
Tape Measure	

1. Positioning Subject
    a. Position subject supine on bed or standing on mat with selected leg closest to researcher
    b. If supine, place foot of selected leg in foot holder
    c. If supine, place rolled towel under knee to achieve ~10^{o} knee bend
    d. Allow subject to rest for 15 min

2. Mark Imaging Sites
    a. **Tip: Mark measurement points with "•" and imaging sites with "X"*
    b. Create lateral plane on quadriceps by measuring from the head of the greater trochanter of femur to lateral epicondyle of knee
    c. Record distance (cm) as "leg length".
    d. Calculate 22%, 39%, 55% of this length.
    e. Mark points on leg corresponding to desired imaging sites
    i. 22%, 39%, 56% up from the knee
    f. With tape measure, create anterior plane from anterior superior iliac spine to proximal border of patella (no need to measure length, this is just to create an anterior line on quadriceps)
    g. Mark *anterior* imaging sites by tracing 22%, 39% and 56% points from the lateral plane to the anterior plane
    h. Mark *lateral* imaging sites as the midpoint between lateral and anterior points
    i. *Note distance from anterior point

3. Imaging
    a. Open U smart software

b. Enter Patient ID, Select Exam Type: Musculoskeletal
c. Press ‘Preset’, and select D’Lugos Protocol- Muscle Thickness
    i. Gain= 50, Dynamic Range= 55, Focal Zones= 4
d. Coat probe with generous amount of gel
e. Orient probe so horizontal bevel is proximal, angled toward the midline of the body
f. Without applying any pressure on the leg, manipulate probe until desirable image is visible
g. Adjust depth so that the superior border of femur is visible
h. Adjust dynamic range and/or frequency so that aponeuroses of muscles and fascicles (for pennation angle) are clearly visible
i. Once a sufficient image is obtained, select ‘Freeze’
j. Scroll backward to select best image then select ‘Store’

APPENDIX C

ULTRASOUND IMAGE ANALYSES PROTOCOL – THICKNESS

ULTRASOUND IMAGE ANALYSES PROTOCOL
Muscle Thickness of the Quadriceps

Supplies Needed / Used	Item Number
iMac	Apple
NIH Image J	https://imagej.nih.gov/ij/index.html

1. Open ImageJ with photo.
    a. Drag image file onto ImageJ icon on Dashboard
2. Process -> Sharpen
3. Image Navigation
    a. Zoom In = “Command” plus “+”
    b. Zoom Out= “Command” plus “-“
    c. Draw Straight, 90^{o} line = Hold “Shift” while drawing line
4. Calibrate Image J
    a. Using the Straight Line Tool, draw line (while holding ‘Shift’) from 0cm to 2cm marks along teal ruler on right of screen.
    b. Click ‘Enter’
    c. Analyze -> Set Scale -> Enter ‘Known distance’ to 2.0 and ‘Unit of Length’ to cm; click OK
    d. From this point on, the measurements for the opened image will be presented in centimeters (cm).
5. Define 10%, 50%, 90% of Field of View (FOV)
    a. Using the Straight Line Tool, draw line (while holding Shift) from the left border of the image to the right. Zoom in to ensure accurate line placement.
    b. After positioning your horizontal line, hover over the left end-point with cursor and enter the “x=” value into “X-Coord. LEFT” cell on line locator spreadsheet. Do the same with the right end-point of the line.
    c. Based on the three “x=” values generated from the spreadsheet, begin to place your vertical lines (while holding Shift) at each corresponding “x-coordinate”.
6. Drawing your Vertical Thickness Lines
    a. At each determined “x-coordinate” draw your line from the superficial fascia to the deep fascia (while holding Shift).
    b. Place the end points of your lines on the interior borders of the fascia. Zoom in to refine the positioning of each end point of your line.
    c. After drawing your line, click “T”. A new window titled “ROI Manager” will appear.

i. Repeat for each new line drawn

ii. Each new line will be assigned a number (i.e. 1-12)

d. In the “ROI Manager” window, check “Show All” and “Labels”.

e. Begin drawing your lines from left to right (10% to 90%), beginning with the most superficial muscle, then the deep muscle, then both muscle combined, finishing with the subcutaneous fat.

7. Obtaining your Thickness Measurements

   a. After drawing your thickness lines, click “Measure” in the “ROI Manager” window.

   b. All angles should be either 90 or -90. Enter the “Length” number into the US Data Spreadsheet.

8. Saving your Analyzed Image

   a. Click “Save As” -> .jpeg

   b. Add “_ANALZYED” to the end of the image and save as .jpeg

   c. Save Analyzed image in the “Analyzed” folder for the given subject.

APPENDIX D

ULTRASOUND IMAGE ANALYSES PROTOCOL – PENNATION ANGLE

ULTRASOUND IMAGE ANALYSES PROTOCOL
Pennation Angle of the Quadriceps

Supplies Needed / Used	Item Number
iMac	Apple
NIH Image J	https://imagej.nih.gov/ij/index.html
Fixed Angle Line Tool	https://imagej.nih.gov/ij/macros/tools/FixedAngleLineTool.txt

1. Open ImageJ with photo.
    a. Drag image file onto ImageJ icon on Dashboard
2. Process -> Sharpen
    a. Up to 2 times, depending on clearness of fascicles
3. Image Navigation
    a. Zoom In = “Command” plus “+”
    b. Zoom Out= “Command” plus “-“
4. Tracing the Deep Aponeurosis
    a. Using the Straight Line tool, draw a line on the superficial border of the deep aponeurosis, spanning approximately 2 inches over the left and right side of the field of view.
    b. Click ‘Enter’, then ‘M’
    c. This will save a yellow line on the image
5. Tracing Pennation Angles
    a. Using the Angle Tool, click on the superficial portion of a visible fascicle, move cursor to the yellow line along the deep aponeurosis and click again.
        i. It is crucial to plot the second point exactly on the yellow line of the deep aponeurosis (zoom in if needed).
        ii. There are now 2 points plotted along a fascicle to the deep aponeurosis.
    b. Next, move cursor along the yellow line, to the right and click. This completes your angle.
        c. Click ‘T’; “ROI Manager” window will appear.
        d. In the “ROI Manager” window, press “M” to measure the angle of drawn lines; “Angle” values will appear in “Results” window.
6. Trace Pennation Angles NOT Touching Deep Aponeurosis
    a. Right click on Fixed Angle Line Tool, and enter the same degree of the line drawn on the deep aponeurosis.
        i. Any new line drawn should be parallel with deep aponeurosis.

b. Draw new line at the base of fascicles that are not touching deep aponeurosis.
    i. Click ‘Enter’, line is now saved on image
c. Using the Angle Tool, repeat the steps in #5

7. Close the “ROI Manager” window and select “Save as Overlay”. Then, save the image as “image title_ANALYZED.jpg”

APPENDIX E

S ULTRASOUND IMAGE ANALYSES PROTOCOL – ECHOGENICITY

ULTRASOUND IMAGE ANALYSES PROTOCOL
Echogenicity of the Quadriceps

Supplies Needed / Used	Item Number
iMac	Apple
NIH Image J	https://imagej.nih.gov/ij/index.html
Optical Density Calibration Tool	https://imagej.nih.gov/ij/docs/examples/calibration/index.html

1. Calibrate ImageJ for Optical Density
    a. Calibrate ImageJ Optical Density (OD) by opening the "ImageJ OD Calibration Tablet" in ImageJ
    b. Open the brightness/contrast control (Image → Adjust → Brightness/Contrast)
    c. Starting with the left most white panel, draw a vertical panel that fills most of each shaded panel.
        i. Press "T" after each rectangle to save ROI for later measurement.
    d. Draw a rectangle in the first 19 panels, starting from left to right. Adjust the contrast/brightness to better visualize the panels following the 8th rectangle.
    e. In the "ROI Manager" window, select "Measure" after drawing all 19 rectangle. Results window should show 19 measurements.
    f. Open Calibration control ((Analyze → Calibrate). All 19 measurements should automatically populate left panel in window.
        i. From the "Function" drop down menu, select "Rodbard"
        ii. Enter "O.D." in the "Unit" option
        iii. Check the "Global Calibration" box
        iv. Copy and paste the 19 "ImageJ O.D. Calibration Values" from the desktop into the right panel in window

2. Measurement of Echogenicity
    a. Prior to analysis, confirm ultrasound image settings are constant:
        i. Image being directly compared over time (i.e. Pre to Post):
            1. Images of a particular site (i.e. Right L1) across time (i.e. Pre - Post) have identical Gain (Gn), Dynamic Range (DR), and # of Focal Zones (pink stars)
        ii. Image being compared to other sites/individuals (i.e. ultrasound study)
            1. Images between individuals must have identical Gain (Gn), Dynamic Range (DR), and # of Focal Zones (pink stars)
    b. Using the "Polygon Selections" tool, draw a shape that fills most of the subcutaneous fat, superficial muscle (vastus lateralis or rectus femoris), and deep muscle (vastus intermedius).

i. Make sure to avoid including skin, aponeurosis, and bone in the drawn polygon. Press “T” following the drawing of each polygon. Then in the “ROI Manager” window, press “M” once all polygons have been drawn to obtain measurements.

1. Record the “Mean” value in the spreadsheet under the appropriate heading

c. Close the “ROI Manger” window and select “Save as Overlay”. Then save the image as “image title_ANALYZED

APPENDIX F

SKELETAL MUSCLE RNA ISOLATION

SKELETAL MUSCLE RNA ISOATION

Supplies Needed / Used	Item Number
PRO200 Bio-Gen Motor Assembly	Pro Scientific: PRO-01-01200
Multi-Gen Adaptor	Pro Scientific: PRO-07-07200
7XL Multigen Generator	Pro Scientific: PRO-07-070MGXL-12
2.0 ml Tubes	USA Scientific: 1620-2700
1.5 ml Tubes	USA Scientific: 1615-5500
500 µl Tubes	USA Scientific: 1405-8100
PIPETMAN G P200G	Gilson: F144058MG
PIPETMAN G P1000G	Gilson: F144059MG
200 µl Pipette Tips	USA Scientific: 1120-8810
1000 µl Pipette Tips	USA Scientific: 1182-1830
TriReagent	Molecular Research Center: TR118
Chloroform	Alfa Aeser: 43685
100% Isopropanol	Fisher: A464-1
75% Ethanol	Fisher: BP28184
RNAse Free Water	Fisher: BP5611
General Lab Equipment	
Vortex	Fisher: 02-215-365
Refrigerated Centrifuge	Fisher: 13-100-676

1. Keep tissue cold if not frozen during this process.

2. Prepare centrifuge tubes by pipetting 1 ml (50-100 mg sample) TriReagent (MRC# TR 118) into 2ml tube (USA Scientific Cat # 1620-2700).

3. Pipet 4ul polyacryl carrier (MRC) if little RNA in sample (not necessary very often).

4. Weight out muscle (~15-30 mg) and homogenize for 1-2 minutes with hand held homogenizer (Pro Scientific)

5. Let samples sit at RT for 5 minutes.

6. Add 0.2 ml Chloroform per 1ml TriReagent. Shake vigorously/Vortex for 15sec.

7. Allow samples to incubate at RT for 15 minutes then centrifuge at 12,200 rpm for 15 min at 4 C.

8. Remove upper phase while being careful not to pipette interphase. Put into fresh tube. Volume of upper phase is generally about 60% of initial TriReagent. It is advisable to leave a small later of upper phase to reduce risk of pipetting interphase. Use 200ul pipette.

- Place into 1.5 ml tube (USA Scientific Cat# 1615-5500)

9. Pipette 0.5 ml 100% Isopropanol per 1 ml TriReagent into RNA phase. Mix by pipetting up and down. Allow the samples to incubate at RT for 10 min.

10. Precipitate by centrifuging at 12.200 rpm for 8 min at 4 C. Gel-like pellet should form at bottom.

11. Pour off isopropanol. Wash pellet with 1 ml 75% Ethanol. Disrupt pellet by vortexing. Centrifuge sample at 9,600 rpm for 5 min at 4 C.

12. Remove ethanol by inverting. Remove excess ethanol with 10 ul pipette. Let air dry for 3-5 min. Do not completely dry pellet.

13. Dissolve the pellet in 1.5 ul of RNAse free water (Fisher BP5611) by pipetting up and down and vortexing. Place RNA into fresh 500 ul tube (USA Scientific Cat# 1405-8100).

14. Label tube as RNA

APPENDIX G

DETERMINATION OF RNA CONCENTRATION – BIOTEK TAKE 3 PLATE

DETERMINATION OF RNA CONCENTRATION – BIOTEK TAKE 3 PLATE

Supplies Needed / Used	Item Number
BioTek H1 Synergy Plate Reader	BioTek: 43685
BioTek Take3 Microplate	Fisher: 11-120-571
PIPETMAN G P10G	Gilson: F144055MG
10 µl Pipette Tips	USA Scientific: 1121-3810
General Lab Equipment	
Dry Bath	Fisher: 11-718-4Q
Dry Block	Fisher: 11-718-23Q
Dry Block	Fisher: 11-718-9Q
Thermometer	Fisher: 13-201-644

1. Turn on heat block to 70 °C
2. Thaw RNA samples on ice
3. Power on Gen5 plate reader software
4. Selected Read Now and specify sample type as RNA
5. Specify the number of samples on the microplate setup
6. Blank microspots by pipetting 2 ul of nuclease free water onto microspots
    a. Close lid of microplate and place into plate reader
    b. Read plate and approve blank read
7. Heat RNA samples for 2 minutes, allow samples to cool on tube rack for 1 minute
8. Pipette 2 ul of RNA sample onto microspots, close microspot lid, place into plate reader
9. Microsoft Excel will open after read and will display RNA concentration results

APPENDIX H

DNASE TREATMENT OF ISOLATED RNA

DNASE TREATMENT OF ISOLATED RNA

Supplies Needed / Used	Item Number
DNA-Free Kit	Ambion: AM1906
500 µl Tubes	USA Scientific: 1405-8100
PIPETMAN G P2G	Gilson: F144054MG
PIPETMAN G P20G	Gilson: F144056MG
2 µl Pipette Tips	USA Scientific: 1121-3810
20 µl Pipette Tips	USA Scientific: 1120-1810
General Lab Equipment	
Centrifuge	Fisher: 13-100-676
Oven or Incubator	

1. NOTE: For use with Applied Biosystems DNA-free kit; AM1906
2. Use up to 5 ug (when using 1ul rDNase 1) of RNA and put into new 500 ul tube (USA Scientific Cat# 1405-8100)
3. Pipet 0.1 volume of DNase 1 Buffer and 1 ul rDNase 1 into each sample. Mix gently.
    a. Note: This is good for up to 50 ul reaction
4. Incubate at 37 C for 25 minutes.
5. Add 2 ul (or 0.1 volume, which ever is greater) of DNase inactivating reagent. Mix well by pipetting up and down and flicking.
6. Incubate at RT for 2 min. Mix occasionally (2-3x)
7. Centrifuge at 10,000 rpm for 2min. Pipet off RNA to fresh 500 ul tube (USA Scientific Cat# 1405-8100).
8. Label tube as DNASE

APPENDIX I
cDNA SYNTHESIS

cDNA SYNTHESIS

Supplies Needed / Used	Item Number
Bioline SensiFast cDNA Synthesis Kit	Bioline: BIO-65053
Nuclease Free H_2O	Fisher: BP5611
Low Profile 8 tube strip	BioRad: TLS0801
Low Profile 8 tube cap	BioRad: TCS0803
PIPETMAN G P2G	Gilson: F144054MG
PIPETMAN G P10G	Gilson: F144055MG
PIPETMAN G P20G	Gilson: F144056MG
Pipette Tips	USA Scientific: 1121-3810
Pipette Tips	USA Scientific: 1120-1810
General Lab Equipment	
Thermocycler (CFX Connect)	BioRad: 1855201

1. NOTE: For use with Bioline SensiFast cDNA Synthesis Kit
2. Turn on CFX connect to warm-up
3. Set up Reaction Protocol on CFX connect. Listed as “iScript cDNA Synthesis Protocol JMD
    a. No plate reads will occur
4. Determine volume of DNASE treated RNA to add, equivalent to 1 ug total RNA
5. Determine amount of nuclease-free water to add (ul H_2O = 20 ul - x ul RNA - 4 ul TransAmp Buffer - 1 ul reverse transcriptase). Add to 500 ul reaction tube
    a. BioRad TLS0801 (8 tube strip)
    b. BioRad TCS0803 (8 tube cap)
6. Add 4 ul of 5X TransAmp Buffer
    a. For several samples, may want to create master mix with TransAmp Buffer (4 ul per sample) + reverse transcriptase (1 ul per sample). Use appropriate sized RNAse free tube
7. Add RNA template
8. Add Reverse Transcriptase (1 ul)

9. Label tube as cDNA

10. For human cDNA dilute cDNA 1:8 with nuclease-free water by adding 6 ul of cDNA to 42 ul nuclease-free water. Label tube as cDNA 1:8. Diluted cDNA is used for PCR reactions

5 X TransAmp Buffer	4 ul
Reverse Transcriptase	1 ul
Nuclease-free Water	x ul
RNA template	x ul
Total volume	20 ul

Temperature Protocol

25 C	10 min
42 C	15 min
85 C	5 min
4 C	Hold (optional)

APPENDIX J

PRIMER DESIGN

PRIMER DESIGN AND DILUTION

Supplies Needed / Used	Item Number
1X TE Buffer	Invitrogen: 12090015
PIPETMAN G P200G	Gilson: F144058MG
200 µl Pipette Tips	USA Scientific: 1120-8810
General Lab Equipment	
Mini Centrifuge	Fisher: 12-006-901
Vortex	Fisher: 02-215-365

1. Go to Pubmed home
2. Type in name of the gene/protein and species (Rrbp1 mouse; Naf-1 homo sapien) and select Gene on the drop down menu
3. Click on gene name
4. Scroll down to “mRNA and Protein(s)” heading
5. Click on appropriate accession number (NM_xxxxxxx) – can double check against TAQMAN probes on life technologies website
6. Scroll down to CDS (coding sequence) and click it
7. Click Pick Primers from right hand menu
8. Set amplicon length to 70-120
9. Melting Temperature 60 d (57-63) or 55d (52-58)
10. Highlight and change that primers to span an exon-exon junction
11. Make sure organism is “homo sapiens” should be 9606
12. Also can allow primers to amplify mRNA splice variants at the bottom of the page
13. Get Primers!

NOTES:

- Primer should be 18-22 bp
- Melt temp <65d, 60 or 55 ideal, depends on selection
- 40-60% GC Content
- Product close to 100bp ideal
- Product with least potential overlaps should be chosen

PRIMER ORDERING

- Invitrogen (Life Technologies) website (lifetechnologies.com):
    - Go to “Custom DNA Oligos”
    - Researcher Name:
    - Oligo Name: gene name Fwd or Rev
    - Oligo sequence: cut and paste appropriate sequence
    - Synthesis Scale: 25 nmol
    - Purification: desalted

DILUTION

- Upon arrival, spin down primer tubes for 1 minute
- Dilute primers with 1X TE buffer
    - 10 x nmol concentration- look on data sheet
    - e.g. 10 x 16.0 nmol = 160 ul 1X TE buffer
- Vortex and spin down

APPENDIX K

PRIMER TESTING AND OPTIMIZATION

PRIMER TESTING AND OPTIMIZATION

Supplies Needed / Used	Item Number
Thermocycler (CFX Connect)	BioRad: 1855201
PIPETMAN G P10G	Gilson: F144055MG
PIPETMAN G P20G	Gilson: F144056MG
PIPETMAN G P100G	Gilson: F144057MG
PIPETMAN G P1000G	Gilson: F144059MG
10 µl Pipette Tips	USA Scientific: 1121-3810
20 µl Pipette Tips	USA Scientific: 1120-1810
100 µl Pipette Tips	USA Scientific: 1120-1840
1000 µl Pipette Tips	USA Scientific: 1182-1830
1.5 ml Tubes	USA Scientific: 1615-5500
200 µl Colored Tubes	USA Scientific: 1402-8108
Low Profile 96 Well Plate (unskirted)	BioRad: MLL9601
96 Well Plate Adhesive Seals	BioRad: MSB1001
Plate Sealer (Scraper)	Option, BioRad: MSR0001
General Lab Equipment	
Vortex	Fisher: 02-215-365
Mini Centrifuge	Fisher: 12-006-901
Centrifuge	Beckman Coulter: Allegra 64R
Centrifuge Rotor	Beckman Coulter: S2096

SERIAL DILUTION PCR RUN TO DETERMINE PRIMER EFFICIENCY

1. Create 6 point 1:2 decreasing dilution series of cDNA
    a. Pipette 15 ul of nuclease free water into 6 500 ul clear tubes
        i. Label tubes 1 – 6
        ii. cDNA concentration of dilution series ranges from 1:2 to 1:64
    b. Pipette 15 ul of cDNA into tube #1
        i. Vortex and spin down
    c. Pipette 15 ul of tube #1 into tube #2
        i. Vortex and spin down
    d. Repeat step “c” for tubes 3, 4, 5, 6
2. Determine how many samples and gene targets you plan to analyze (6 samples x primers being tested)
3. Record samples/genes on blank 96-well plate template
4. Label 1 clear 1.5 ml tube with the name of each primer. This is your master mix tube
5. Label colored 500ul tubes with name of sample and primer
    a. (Hint: multiply the number of samples you have by the number of targets you plan to analyze and this equal the number of colored tubes to label)
6. Follow the ‘SYBR RT PCR Pipetting Spreadsheet’ formula for creating your master mix for each target gene. Make sure to vortex and spin-down each tube prior to adding to master mix
    a. Determine the number of reactions (samples x 2 duplicates per sample)
    b. Add x ul of nuclease free water (9.5 ul per reaction)
    c. Add x ul Sybr Green Supermix (12.5 ul per reaction)
    d. Add x ul of forward and reverse primers (0.5 ul per reaction)
7. Vortex and spin-down master mix tubes
8. Aliquot 48.2ul of each master mix into the colored 500ul reaction tubes for that target
9. Vortex and spin-down cDNA tubes
10. Add 4.28ul of cDNA from each sample into the appropriate reaction tubes. You should now have 52.48ul total volume in each colored tube (master mix + cDNA)
11. Vortex and spin-down completed reaction tubes
12. Pipette in duplicate, 25ul from reaction tube into assigned wells on plate (use template). Duplicates should be horizontal (i.e. A1 and A2) and should be pipetted using the same tip
13. Seal plate with adhesive seal and white scraper
14. Spin-down plate in large centrifuge at 1000 rpm for 2 min. Rotor#: 2096

15. Place plate in thermocycler with A1 in back left corner. Wipe top of plate with kimwipe

SETTING UP THE THERMOCYCLER SOFTWARE

1. Open ‘Bio-Rad CFX Manager’ on desktop
2. Click OK at login window
3. Click ‘User Defined’ at Startup Window
4. Select the appropriate protocol in the ‘Express Load’ dropdown window
    a. All SYBR protocols are titled “CFX_2StepAmp+Melt --d SYBR”
        i. The correct run temperature (--d) will be based on primer testing results
5. Click the Plate tab
6. Select the appropriate plate in the ‘Express Load’ dropdown window
    a. All SYBR PCR’s will use plate titled “Bio-Rad_96 wells_SYBR-pltd”
7. Click ‘Edit Selected’. Highlight all well and click ‘Clear Wells’
8. Under ‘Editing Tools’, click ‘Setup Wizard’
    a. Assign ‘Target names’ and ‘Sample names’ to their respective wells and click OK
9. Highlight all wells and assign ‘Sample Type’ as ‘Standard’
    a. Next, highlight wells and input ‘Replicate Series’. Replicate size will always be 2
    b. Next, highlight wells and input ‘Dilution Series’. Dilution factor = 2, Decreasing
10. If you are running a RT-qPCR, highlight all wells and assign ‘Sample Type’ as ‘Unknown’
11. Click OK, and YES to save plate
12. Click the Start Run tab
13. Under ‘Notes’ input date, target genes, samples
14. Visually inspect Melt Curve Analysis
    a. Ensure each dilution series results in a single melt peak (variation in melt temperature up to 1.0 degrees between 6 points acceptable)
15. Visually inspect Efficiency, R^2, and Ct range of standard curve
    a. Efficiency should be between 95% and 110%
    b. R^2 should be above 0.995
    c. Ct range should be greater than 20 while not exceeding 35

APPENDIX L

AGAROSE GEL – PRIMER DESIGN TESTING

AGAROSE GEL – PRIMER DESIGN TESTING

Supplies Needed / Used	Item Number
Agarose	BioRad; 161-3101
10X TBE	BioRad; 161-0733
Ethidium Bromide	BioRad; 161-0433
EZ Load 20bp Molecular Ruler	BioRad; 170-8351
PIPETMAN G P2G	Gilson: F144054MG
PIPETMAN G P10G	Gilson: F144055MG
2 µl Pipette Tips	USA Scientific: 1121-3810
10 µl Pipette Tips	USA Scientific: 1121-3810
Power Supply Unit	BioRad: 1645050
Mini Sub Cell GT	BioRad: 1704466
General Lab Equipment	
25 mL Flask	
Microwave	
Petri Dish	

1. Dilute 15ml 10X TBE (BioRad; 161-0733) to 0.5X in 285ml Millipore H_2O
2. Cast Agarose Gel (2.5%) in Mini Sub Cell GT (BioRad; 170-4487):
    a. Suspend 625mg Agarose (BioRad; 161-3101) in 25ml 0.5X TBE
    b. Microwave for 1min, spinning flask every 10-15 sec
        i. After microwaving, place pietri dish over flask to reduce evaporation
    c. Add 1 ul of Ethidium Bromide (10mg/ml; BioRad; 161-0433) after Agarose is cooled (1-2 min). Twirl flask to mix
    d. Add appropriate comb into gel
    e. Slowly pour into Mini Sub Cell GT (avoid air bubbles). Pop with pipette tip if present
3. Allow gel to polymerize for 30 min
4. Cover gel with 0.5X TBE until wells are covered (1-2 cm)

5. Remove comb from gel
6. Load Molecular Ladder (5 ul; BioRad EZ Load 20bp Molecular Ruler; 170-8351)
7. Prepare samples:
    a. Mix 4ul DNA product and 1ul 5X Loading Buffer (BioRad; 161-0767)
    b. Load on gel
8. Fill Mini Sub Cell GT with remaining 0.5X TBE
9. Power Unit: 75V for 60min (Black → Red electrode direction)
10. Each lane should have a single band at the targeted bp for the expected product.

IMAGE DNA AGAROSE GEL

1. Open Image Lab software
2. Select New Protocol
3. Select Single Channel
4. Under Application, select Ethidium Bromide
5. Position gel onto UV tray, image gel
6. Visually inspect gel image to ensure each sample results in a single band at appropriate product size

APPENDIX M

PCR ANALYSIS PROTOCOL

PCR ANALYSIS PROTOCOL

Supplies Needed / Used	Item Number
Thermocycler (CFX Connect)	BioRad: 1855201
PIPETMAN G P10G	Gilson: F144055MG
PIPETMAN G P20G	Gilson: F144056MG
PIPETMAN G P100G	Gilson: F144057MG
PIPETMAN G P1000G	Gilson: F144059MG
10 µl Pipette Tips	USA Scientific: 1121-3810
20 µl Pipette Tips	USA Scientific: 1120-1810
100 µl Pipette Tips	USA Scientific: 1120-1840
1000 µl Pipette Tips	USA Scientific: 1182-1830
1.5 ml Tubes	USA Scientific: 1615-5500
200 µl Colored Tubes	USA Scientific: 1402-8108
Low Profile 96 Well Plate (unskirted)	BioRad: MLL9601
96 Well Plate Adhesive Seals	BioRad: MSB1001
Plate Sealer (Scraper)	Option, BioRad: MSR0001
iTaq Universal Sybr Green Supermix	BioRad: 1725120
Nuclease Free H_2O	Fisher: BP5611
General Lab Equipment	
Vortex	Fisher: 02-215-365
Mini Centrifuge	Fisher: 12-006-901
Centrifuge	Beckman Coulter: Allegra 64R
Centrifuge Rotor	Beckman Coulter: S2096

1. Determine how many samples and gene targets you plan to analyze
2. Record samples/genes on blank 96-well plate template

3. Label 1 clear 1.5 ml tube with the name of each target gene. This is your master mix tube

4. Label colored 500ul tubes with name of sample and target gene.
    a. (Hint: multiply the number of samples you have by the number of targets you plan to analyze and this equal the number of colored tubes to label)

5. Follow the 'SYBR RT PCR Pipetting Spreadsheet' formula for creating your master mix for each target gene. Make sure to vortex and spin-down each tube prior to adding to master mix
    a. Determine the number of reactions (samples x 2 duplicates per sample)
    b. Add x ul of nuclease free water (9.5 ul per reaction)
    c. Add x ul Sybr Green Supermix (12.5 ul per reaction)
    d. Add x ul of forward and reverse primers (0.5 ul per reaction)

6. Vortex and spin-down master mix tubes

7. Aliquot 48.2ul of each master mix into the colored 500ul reaction tubes for that target

8. Vortex and spin-down cDNA tubes

9. Add 4.28ul of cDNA from each sample into the appropriate reaction tubes. You should now have 52.48ul total volume in each colored tube (master mix + cDNA)

10. Vortex and spin-down completed reaction tubes

11. Pipette in duplicate, 25ul from reaction tube into assigned wells on plate (use template). Duplicates should be horizontal (i.e. A1 and A2) and should be pipetted using the same tip

12. Seal plate with adhesive seal and white scraper

13. Spin-down plate in large centrifuge at 1000 rpm for 2 min. Rotor#: 2096

14. Place plate in thermocycler with A1 in back left corner. Wipe top of plate with kimwipe

SETTING UP THE THERMOCYCLER SOFTWARE

1. Open 'Bio-Rad CFX Manager' on desktop

2. Click OK at login window

3. Click 'User Defined' at Startup Window

4. Select the appropriate protocol in the 'Express Load' dropdown window
    a. All SYBR protocols are titled "CFX_2StepAmp+Melt --d SYBR"
        i. The correct run temperature (--d) will be based on primer testing results

5. Click the Plate tab

6. Select the appropriate plate in the 'Express Load' dropdown window
    a. All SYBR PCR's will use plate titled "Bio-Rad_96 wells_SYBR-pltd"

7. Click ‘Edit Selected’. Highlight all well and click ‘Clear Wells’
8. Under ‘Editing Tools’, click ‘Setup Wizard’
    a. Assign ‘Target names’ and ‘Sample names’ to their respective wells and click OK
9. If you are testing primers, highlight all wells and assign ‘Sample Type’ as ‘Standard’
    a. Next, highlight wells and input ‘Replicate Series’. Replicate size will always be 2
    b. Next, highlight wells and input ‘Dilution Series’. Dilution factor = 2, Decreasing
10. If you are running a RT-qPCR, highlight all wells and assign ‘Sample Type’ as ‘Unknown’
11. Click OK, and YES to save plate
12. Click the Start Run tab
13. Under ‘Notes’ input date, target genes, samples
14. Start Run

APPENDIX N

SKELETAL MUSCLE IMMUNOHISTOCHEMICAL ANALYSES – CSA AND FIBER TYPE

SKELETAL MUSCLE IMMUNOHISTOCHEMICAL ANALYSES
CSA and Fiber Type
MHC I, MHC IIa, Laminin, DAPI in frozen muscle

Supplies Needed / Used	Item Number
Superfrost Plus Microscope Slides	Fisher: 12-550-15
Cover Glasses Rectangle No.1	Fisher: 12-545F
Hydrophobic Pen	Vector: H-4000
Normal Goat Serum (NGS)	Fisher: 31872
1X PBS	Recipe
Vectashield Antifade Mounting Medium	Vector #H-1000
10% Normal Goat Serum	Fisher: 31872
Mouse anti-MHCI IgG2b	DSHB: BAD5 Mouse IgG2b, supernatant
Mouse anti-MHCIIa IgG1	DSHB: SC71 Mouse IgG1, supernatant
Rabbit anti-Laminin IgG	Sigma: L9393 (Rabbit IgG)
2º antibody: Goat anti mouse IgG2b AF488 (MHC I)	Invitrogen: A21141
2º antibody: Goat anti mouse IgG1 AF 546 (MHC IIa)	Invitrogen: A21123
2º antibody: Goat anti rabbit IgG AF633 (Laminin)	Invitrogen: A21071
DAPI	Invitrogen: D3571
General Lab Equipment	
PIPETMAN G P100G	Gilson: F144057MG
100 µl Pipette Tips	USA Scientific: 1120-1840
Cryostat	Leica: CM1950

DSHB, Developmental Studies Hybridoma Bank

Note: This stain requires approximately 5 hours

1. Air dry sections for 30 mins at RT

2. Encircle sections with hydrophobic pen

3. Rehydrate sections in 1X PBS for 3 mins
4. Wash in 1X PBS (2x2min)
5. Block with 10% NGS for 60mins
6. Wash in 1X PBS (pipette rinse)
7. Incubate in 1^{o} antibody for 90min at RT
    a. MHCI: BAD5 Mouse IgG2b (1:10; DSHB, supernatant)
        - *Note:* All antibodies diluted in 1X PBS
    b. MHCIIa: SC71 Mouse IgG1 (1:10; DSHB, supernatant)
    c. Laminin Rabbit IgG (1:50; Sigma, L9393)
8. Wash in 1X PBS (4x5min)
9. Apply 2^{o} antibody for 60min at RT
    a. MHCI: Goat anti mouse IgG2b AF488 (1:300; Invitrogen, A21141)
        - *Note:* All antibodies diluted in 1X PBS
    b. MHCIIa: Goat anti mouse IgG1 AF 546 (1:300; Invitrogen, A21123)
    c. Laminin: Goat anti rabbit IgG AF633 (1:300; Invitrogen, A21071)
10. Wash in 1X PBS (3x5min)
11. Incubate in DAPI (1:10,000) in 1X PBS for 5min
12. Wash in 1X PBS (3x5min)
13. Dry excess liquid on slide
14. Air dry for 2mins
15. Mount coverslip with Vectashield
16. Image slide at 100X magnification

Phosphate Buffered Saline (10X) – Dilute to 1X

Chemical	Vendor	Amount for 10X
1. NaCl	(Fisher: S271-500)	80g
2. KCl	(Fisher: P217-500)	2g
3. Na_2HPO_4	(Sigma: 255793)	14.4g
4. KH_2PO_4	(MP Biomedicals: MP021954531)	2.4g

APPENDIX O

SKELETAL MUSCLE IMMUNOHISTOCHEMICAL ANALYSES – SATELLITE CELLS AND MYONUCLEI

SKELETAL MUSCLE IMMUNOHISTOCHEMICAL ANALYSES
Satellite Cells and Myonuclei
Pax7, Type 1, Laminin IHC Protocol for frozen rat skeletal muscle

Supplies Needed / Used	Item Number
Superfrost Plus Microscope Slides	Fisher: 12-550-15
Cover Glasses Rectangle No.1	Fisher: 12-545F
Hydrophobic Pen	Vector: H-4000
Vectashield Antifade Mounting Medium	Vector #H-1000
4% PFA	Recipe
1X PBS	Recipe
30% H_2O_2 in PBS	Fisher: H325
TSA Kit (Alexa fluor 555 tyramide)	Invitrogen: T-30955
PAX-7 (Concentrate)	DSHB
Mouse anti-MHCI IgG2b	DSHB: BAD5 Mouse IgG2b, supernatant
Laminin	Sigma: L9393 (Rabbit IgG)
Biotin-SP-AffiniPure Goat Anti-Mouse IgG, Fcγ Subclass 1 Specific	Jackson Immuno Research Cat #115-065-205
2º antibody: Goat anti-Rabbit AF488	Invitrogen: A-11034
2º antibody: Gt anti-Ms IgG2B AF647	Invitrogen: A-21242
DAPI	Invitrogen: D3571
General Lab Equipment	
PIPETMAN G P100G	Gilson: F144057MG
100 µl Pipette Tips	USA Scientific: 1120-1840
Water Bath	
Cryostat	Leica: CM1950

Day 1

1. Cut 7µm thin sections & air dry for 1hr at RT.

2. Fix sections with 4%PFA for 7min.

3. Wash 3x3min in PBS

4. Perform AntiRetrival step*(see below) with Na.citrate (10mM, P^H 6.5) at 92ºC water bath for 20min. Then cool slides to RT.

5. Wash 3x3min in PBS.

6. Block endogenous peroxidases with 3% H_2O_2 in PBS for 7min.

7. Wash 3x3min in PBS.

8. Block 1hr in 1% blocking reagent (came with Invitrogen TSA kit – item D, or use BSA).

9. Incubate in 1ºAb for 1hr at RT then overnight at 4ºC in 1% blocking reagent: Ms IgG1 Pax7 (1:500) (DSHB); Type 1 BA.D5 Ms IgG2b (1:500) (BA.D5 –C, from DHSB Iowa); Rb laminin (1:500) (Sigma cat #L9393) in 2.5% NHS at 4ºC.

Day 2

10. Wash 4x5min in PBS.

11. Incubate 70min in 2ºAb in 1% blocking reagent: Gt α Ms Biotinylated 2ºAb (1:1000), 2ºAb Gt anti-Ms IgG2b, AF647 (1:500) (Invitrogen, Cat # A-21242), Gt anti Rb IgG AF488 (1:500) (Invitrogen, Cat # A-11034).

12. Wash 3x3 min in PBS.

13. Incubate 1hr in SA-HRP (1:500, blue top) in PBS (came with Invitrogen TSA kit – item C).

14. Wash 3x3min in PBS.

15. Incubate 15-20 min in Alexa flour 488 (1:500) in amplification diluents (came with Invitrogen TSA kit – item E).

16. Wash 3x3min in PBS.

17. Incubate 10min in DAPI. (From Invitrogen, Cat# D35471) at RT
    a. (Dilute (100µM) DAPI stock, 1:10,000 in PBS)

18. Wash 2x3 min in PBS

19. Mount slides with vector shield fluorescent mounting media.

20. Image slide at 10-20X magnification

***Antigen Retrival:** add slides to Na.citrate in glass coplin jar or glass beaker & preheat water bath to 65ºC, then place beaker/coplin jar containing slides and NA Citrate in water bath and raise the temperature to 92 ºC. Water bath temperature will slowly raise to 92ºC (it will take 7-10 min to reach temp from 65ºC to 92ºC, then keep the slides at 92ºC for an additional 10 min)

Phosphate Buffered Saline (10X) – Dilute to 1X

Chemical	Vendor	Amount for 10X
NaCl	(Fisher: S271-500)	80g
KCl	(Fisher: P217-500)	2g
Na_2HPO_4	(Sigma: 255793)	14.4g
KH_2PO_4	(MPBiomedicals: MP021954531)	2.4g

4% Paraformaldehyde (PFA)

Chemical	Vendor	Amount for 1L
PFA	(Sigma: P6148)	40g
1X PBS	Recipe	1000 ml

a. Slowly dissolve PFA in 1X PBS over low heat until solution clear. Pass through filter, then use immediately or aliquote and store at -20C

APPENDIX P

SKELETAL MUSCLE IMMUNOHISTOCHEMICAL ANALYSES – CAPILLARY DENSITY

SKELETAL MUSCLE IMMUNOHISTOCHEMICAL ANALYSES
Capillary Density
IHC-Fr: Capillary CD31, and WGA on frozen rat muscle

Supplies Needed / Used	Item Number
Superfrost Plus Microscope Slides	Fisher: 12-550-15
Cover Glasses Rectangle No.1	Fisher: 12-545F
Hydrophobic Pen	Vector: H-4000
Mouse anti- CD31/PECAM IgG1	BD Biosciences: 550300
Goat anti-mouse IgG1 AF555	Invitrogen: A-21127
Goat anti-mouse AF488 conjugated WGA	Invitrogen: W11261
DAPI	Invitrogen: D3571
Normal Horse Serum (NHS)	Vector: S-2012
1X PBS	Recipe
Acetone	Fisher: A18P-4
Vectashield Antifade Mounting Medium	Vector: #H-1000
General Lab Equipment	
PIPETMAN G P100G	Gilson: F144057MG
100 µl Pipette Tips	USA Scientific: 1120-1840
Cryostat	Leica: CM1950

Day 1

1. Cut 7µm thin sections & air dry them.
2. Fix sections 10min in acetone at -20°C.
3. Wash 3x3 min in 1X PBS.
4. Block 1hr in 2.5% NHS blocking solution at RT (Vector #S-2012)

5. Incubate overnight in 1ºAb, Ms IgG1 CD31/PECAM (1:50) (BD Biosciences cat #550300) in 2.5% NHS at 4ºC.

Day 2

6. Wash 3x3 min in 1X PBS.

7. Incubate 1hr in 2ºAb Gt anti Ms IgG1 AF555 (1:500) (Invitrogen, Cat #A-21127); AF488 conjugated WGA (Invitrogen, Cat #W11261) in 1X PBS at RT

8. Wash 3x3 min in 1X PBS.

9. Incubate 10min in DAPI (Invitrogen, cat#D3571); dilute (100µm) stock (1:10,000 in PBS) at RT.

10. Wash 2x3min in 1X PBS.

11. Mount slides with vector shield mounting media. Drain excess mounting media before storing slides at 4°C.

12. Image slide at 10X magnification

Phosphate Buffered Saline (10X) – Dilute to 1X

Chemical	Vendor	Amount for 10X
5. NaCl	(Fisher: S271-500)	80g
6. KCl	(Fisher: P217-500)	2g
7. Na_2HPO_4	(Sigma: 255793)	14.4g
8. KH_2PO_4	(MP Biomedicals: MP021954531)	2.4g